CHEMICAL STUDIES OF SOME LIFE PROCESSES

A thesis submitted in partial fulfilment of
the requirements for the degree of
Doctor of Philosophy in Chemistry
in the University of Canterbury,
Christchurch, New Zealand

by

ONG CHIN CHOON

1984

To

my family especially my parents,

Madam LEE MOOI and

the late Mr. ONG TAY PHONG

ACKNOWLEDGEMENTS

I would like to express my sincere appreciation to my Supervisor, Dr. G.A. Rodley, for his considerate supervision, patience, enthusiasm, help, advice and encouragement throughout the course of this work. I am grateful to Dr. V. McKee for her assistance in the X-ray structural work and Dr. C. Tomblin of the Physics Department for work on Resonance Raman as well as Circularly Polarised Light. I am also indebted to Dr. C. Winterbourn of the Clinical School, Christchurch Hospital, and Miss C. Miles of the Physics Department for their helpful discussions. Thanks are also due to Miss Cheah Siew Hoong and Miss Jan Elizabeth Gregor for proof-reading this thesis. I am also grateful to my family for their financial and moral support throughout the years. The awards of a Teaching Fellowship and Charles Cook, Warwick House Scholarship are also appreciated.

CONTENTS

LIST OF FIGURES

LIST OF TABLES

ABBREVIATIONS

AMP	adenine monophosphate
Bchl	bacteriochlorophyll
CD	circular dichroism
Chl	chlorophyll
CM	carboxymethylcellulose
DCDP(DME)	dichlorodeuteroporphyrin dimethyl ester
DNA	deoxyribonucleic acid
DNDP(DME)	dinitrodeuteroporphyrin dimethyl ester
DP(DME)	deuteroporphyrin dimethyl ester
DSPE(MME)	desoxophylloerythrin monomethyl ester
EDTA	ethylene diamine tetraacetic acid
EP	etioporphyrin
EtO_2POS	diethylphosphorothioato
HAl-t-Bu	tertiary-butyliminoalane
Hb	apohemoglobin ($\alpha_2\beta_2$)
H_2TMpyP-4	tetrakis(4-N-methylpyridyl)porphyrin
IR	infra-red
L	ligand
Mb	apomyoglobin
MeIm	methylimidazole
MP(DCE)	mesoporphyrin dicholesteryl ester
MP(DME)	mesoporphyrin dimethyl ester
NMR	nuclear magnetic resonance
N_3-fluorenone	2,4,7-trinitro-9-fluorenone
OEP	octaethylporphyrin
ORD	optical rotatory dispersion
Pc	phthalocyanine
pic	picoline
pip	piperidine

PMB	ρ-hydroxymercuribenzoate
PP(DME)	protoporphyrin dimethyl ester
py	pyridine
TBAP	tetrabutylammonium perchlorate
THF	tetrahydrofuran
TMEDA	N,N,N',N'-tetramethylethylenediamine
TPP	5,10,15,20-tetraphenylporphyrin

ABSTRACT

This thesis is primarily concerned with model complexes of some living systems. The two areas of biological interest are photosynthetic systems and chemical interaction between living cells. In both cases the chemical properties are very complex and generally not well understood.

Mg porphyrin was used as a model for chlorophyll. The chemical properties of Mg porphyrin were determined by physical techniques using (1) different axial ligands and (2) protein environment models. Equilibrium studies indicate that the Mg centre is preferentially five-coordinated but under high ligand concentration and low temperature, six-coordination is observed. The spectrum of the six-coordinate Mg porphyrin species is red-shifted in the same manner as also observed for chlorophyll molecules *in vivo*. X-ray studies show that the six-coordinate Mg porphyrin species have long axial bonds with the Mg atom situated in the plane of the porphyrin ring. The shorter the axial bond lengths, the larger the red-shifts.

The interactions of Mg porphyrin with protein environments have been studied by electronic circular dichroism and optical rotatory dispersion spectroscopy. In all cases, the spectra of Mg porphyrin-apomyoglobin are more complex and more red-shifted than those of Mg porphyrin-apohemoglobin analogues. These effects may arise directly from differences in protein interactions with porphyrin side chains or indirectly through water coordination to the Mg atom. The latter appears to be facilitated by features of the apomyoglobin heme pocket but inhibited in

apohemoglobin. X-ray studies suggest that the key feature may be hydrogen bonding of the water molecule to the distal histidine group of apomyoglobin. This hydrogen bonding also enhances the displacement of the Mg atom out of the plane of the porphyrin ring. This could be crucial for the charge separation required for the first step in photosynthesis.

The induced Cotton effects for the Mg porphyrin-protein complexes are different from those observed for Mg porphyrin in chiral amino acid solutions. For Mg porphyrin-protein complexes, these effects are interpreted in terms of the coupled oscillator mechanism between the transitions of Mg porphyrin and protein, while for Mg porphyrin in chiral amino acids, these effects are explained in terms of the formation of six-coordinate (Mg porphyrin)(amino acid)$_2$ complexes. Mg porphyrin-protein complexes are more stable to light than Mg porphyrin in amino acid solutions. This stability is explained in terms of the smaller accessibility of the heme pocket and the effects of the coordinated imidazole group, which protects the porphyrin ring from decomposition. The observations of different photodecomposition patterns for Mg porphyrin-apomyoglobin and Mg porphyrin-apohemoglobin are then correlated with the different protein conformations.

The coupling of oscillating chemical reactions in a two reactor cell system was used as a model for the interaction between living cells. The degree of interaction was measured by a coupling constant. Generally, two coupling constants were observed depending upon the time of coupling. The coupling constant for starting oscillating reactor cells is smaller than that for organised oscillating reactor cells.

This shows that starting oscillating reactor cells are more likely to be entrained or influenced by external factors. The small differences in the coupling constants for different kinds of apparatus are interpreted in terms of the effect of apparatus design.

Finally, the medical and technological significance of all these results are highlighted.

CHAPTER 1

OUTLINE OF STUDIES

1.1 INTRODUCTION

Chemical processes in living systems are difficult to understand because of their complicated and diverse nature. In this work, two different chemical aspects of living systems were investigated using simplified models:

(A) The coordination behaviour of magnesium in chlorophyll systems.

(B) Oscillating processes and the interaction of such ordered states in biological systems.

Natural photosynthetic systems are very complex and they contain a variety of chlorophyll-protein entities [1]. Generally, the chlorophyll molecule consists of a Mg ion coordinated to a tetrapyrrole ring, a five-membered cyclopentanone ring and a phytyl group on ring IV (Figure 1.1). Besides the tetrapyrrole ring, other groups especially water and protein amino acid residues, can coordinate to Mg in the axial positions [2-7]. This axial coordination is of considerable interest as chemical reactions like the splitting of water possibly occur at such sites. The bulk of this thesis will concentrate on the chemical and coordination properties of Mg porphyrin systems, especially as they relate to photosynthesis.

Several cases of oscillating chemical behaviour are known for living systems. Such oscillations between two or more different states indicate the presence of chemical ordering. This kind of behaviour has been observed in

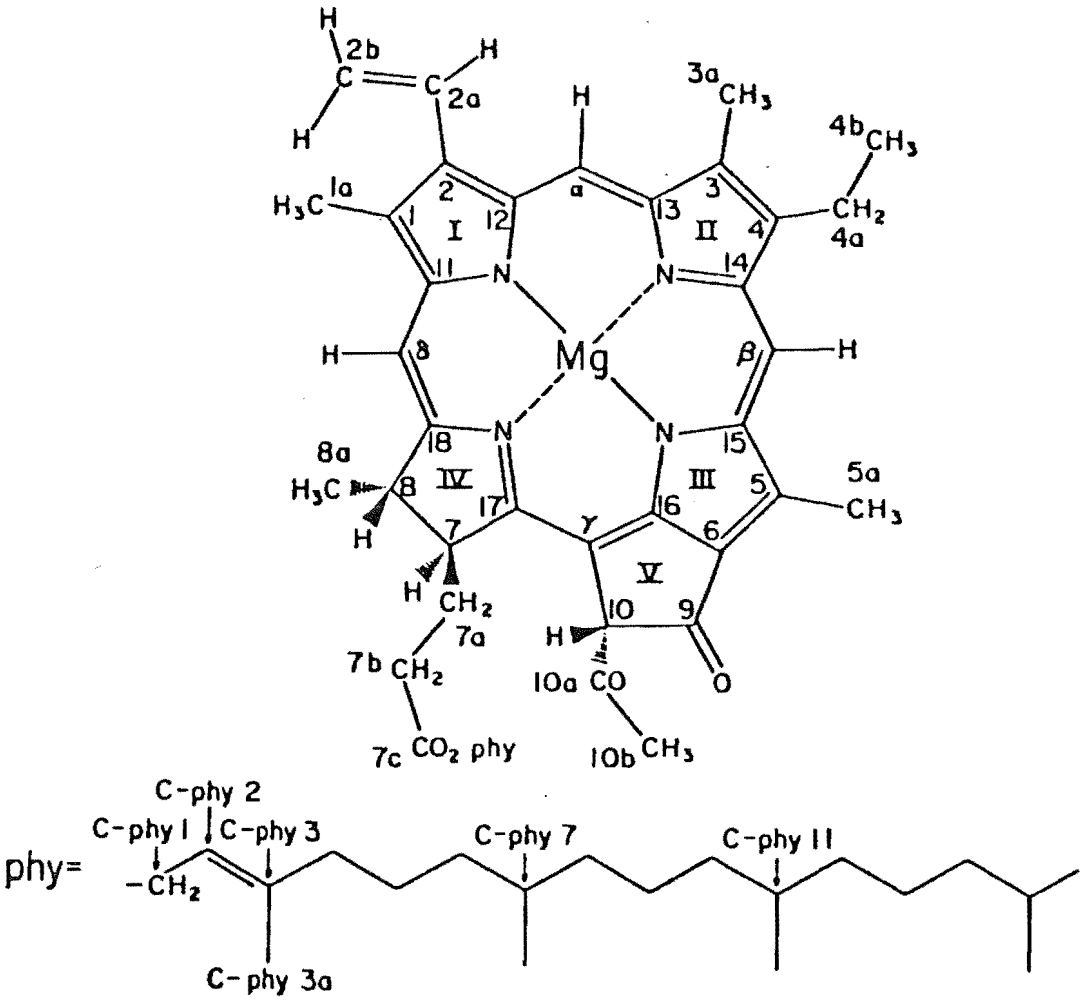

Figure 1.1 : Structural formula of chlorophyll a

photosynthesis where short periodic bursts of oxygen are liberated [8], slime mould aggregation [9-10], and other biochemical pathways, particularly the glycolytic one [11]. In view of the generality of this behaviour, model studies of oscillating reactions are important for a greater understanding of the biochemical properties in living systems.

1.2 STUDIES RELATED TO CHLOROPHYLL SYSTEMS

Several methods of modelling chlorophyll *in vivo* have been reported [12-18]. In this work, the approach has been to use:-

(A) Simple molecular models of Mg porphyrin interacting with different ligands.

(B) Protein environment models having Mg porphyrin incorporated into apomyoglobin and apohemoglobin.

For both models, two coordination numbers, 5 and 6, for Mg were observed. The important factors which influence the coordination number are steric and environmental effects. Steric interaction between the ligand and porphyrin favours five-coordination, while protein environment can stabilise six-coordination by localising a second axial ligand via hydrogen bonding. Overall, the preferred coordination number for Mg is five. The geometry is square pyramidal with the Mg atom displaced out of the porphyrin ring towards the ligand (Figure 1.2). Six-coordinate Mg porphyrin systems are octahedral with the Mg atom situated at the centre of the porphyrin ring (Figure 1.3). Both coordination numbers are likely to be important in chlorophyll systems.

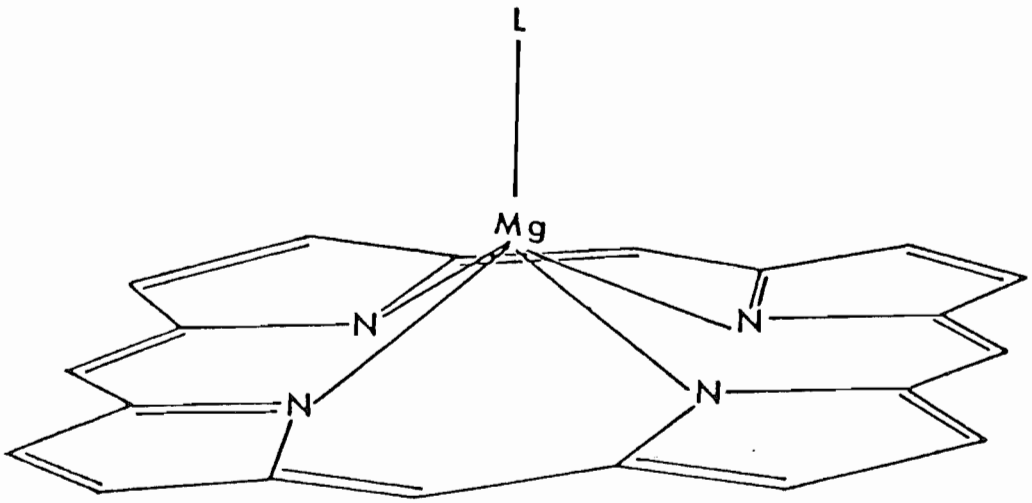

Figure 1.2 : Square pyramidal five-coordinate Mg porphyrin(L)

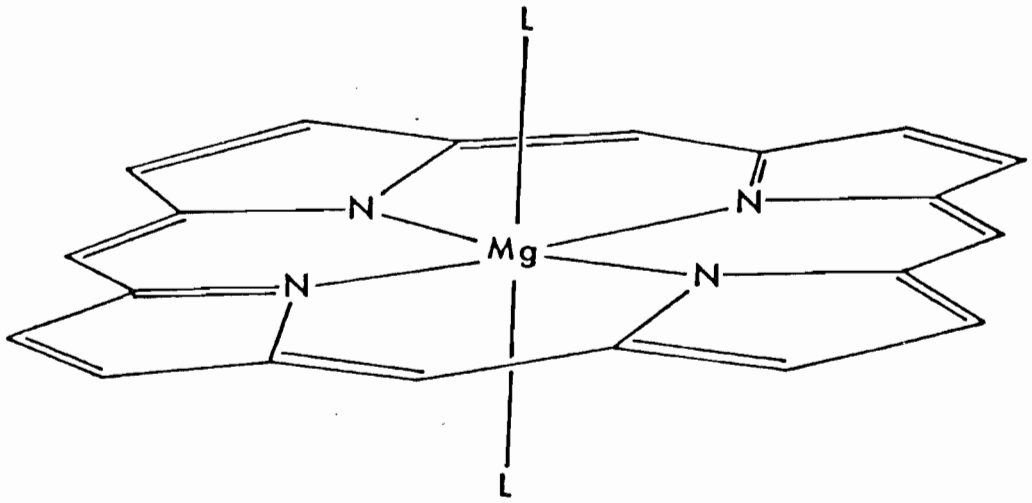

Figure 1.3 : Octahedral six-coordinate Mg porphyrin$(L)_2$

The protein model studies also enable specific Mg porphyrin-protein interactions to be assessed in detail. These are significantly different from those found for Mg porphyrin in organic solvents and are likely to be more closely related to features existing in natural chlorophyll-protein complexes.

For successful modelling of natural systems, an understanding of the key features in the system is essential. In photosynthesising organisms, the primary events are performed by chlorophyll molecules. Most of the chlorophyll molecules serve as antennae for collecting light quanta and transferring this energy very efficiently to a few special chlorophyll molecules constituting the photoreaction center [19]. In plants, the antenna chlorophyll absorb light near 680 nm. However, in polar solvents, the absorption maximum of the chlorophyll is blue-shifted to 662-665 nm [20]. Similarly, antenna bacteriochlorophyll *in vivo* has an absorption maximum at 865 nm but in diethyl ether, this is blue-shifted to 770 nm. These differences are likely to be due to the different environments of antenna chlorophyll *in vivo* and *in vitro*. An insight into the molecular organisation of antenna chlorophyll *in vivo* is therefore important for a thorough understanding of the way in which light energy is transferred among the light-harvesting components and photoinduced charge separation in the photoreaction center occurs.

Various mechanisms have been suggested to account for the nature of the antenna chlorophyll and bacterio-chlorophyll interactions *in vivo* which purport to explain the red-shifts of the absorption maxima. The two main mechanisms that have been proposed are:-

(1) Interaction between chlorophyll molecules and proteins

The most direct evidence for this mechanism is related to X-ray crystal structure analyses of bacteriochlorophyll-protein complex from *Prosthecochloris aestuarii* [3-7]. These studies show 7 bacteriochlorophyll molecules contained within a protein matrix. Theoretical exciton calculations based on the overall interactions of the 7 bacteriochlorophyll molecules are unable to account for the red-shift from 770 nm to 809 nm. It was therefore suggested that the protein matrix can perturb the electronic transition of the bacteriochlorophyll either by providing a general hydrophobic environment or by specific protein-bacteriochlorophyll interaction.

Reconstitution of chlorophyllide with apomyoglobin produced spectra that were significantly red-shifted [12-17]. Complementary results were obtained when chlorophyll-protein complexes from cauliflower were extracted [21]. Separation of the chlorophyll from the protein resulted in a blue-shift of the absorption maximum of the chlorophyll to that found in organic solvents. When the chlorophyll was recombined with the apoprotein, a red-shift to the original absorption maximum was observed. Other studies like disk gel analysis and addition of mild detergents also indicate that chlorophyll is closely associated with protein residues in natural systems [22].

(2) Aggregation of chlorophyll molecules into dimers and oligomers.

In vitro studies of model systems indicate that chlorophyll molecules tend to aggregate into dimers and oligomers [23]. The absorption maxima of these complexes

are similar to those observed in antenna chlorophyll. Theoretical calculations for such a complex, ethyl chlorophyllide.$2H_2O$ [24] where the chlorophyll molecules are parallel and close together, indicate that chlorophyll-chlorophyll interactions can produce a large red-shift.

In oligomeric chlorophyll species, both five- and six-coordinate Mg are present [23]. Equilibrium studies show that the absorption maxima of six-coordinate chlorophyll species are red-shifted [25,26]. Consequently, it is possible that the red-shift for chlorophyll *in vivo* is at least in part due to Mg being six-coordinated.

It is possible that both mechanisms (1) and (2) could be important but research is still in progress to determine the actual contribution of each mechanism to the red-shift in *in vivo* antenna chlorophyll.

In this work, the effects of protein environment and the coordination state of Mg porphyrin were studied by physical techniques in order to gain further insight into the environments of metalloporphyrin and chlorophyll *in vivo*. Induced Cotton effects were studied for Mg porphyrin in proteins and for Mg porphyrin-chiral amino acid complexes and related to *in vivo* chlorophyll-protein interactions. The effects of different light sources on these species were investigated and the influence of protein environment assessed in relation to the photodecomposition of *in vivo* chlorophyll. X-ray analyses of a number of Mg porphyrin complexes were also determined.

1.3 STUDIES OF OSCILLATING REACTIONS

Oscillating reactions are part of a more general phenomenon of nonlinear systems. Under non-equilibrium

conditions, coupling between reactants can lead to the formation of what are called spatiotemporal dissipative structures [27,28]. These structures include periodic oscillations and spatial ordering. Periodic oscillations occur in stirred systems and they are a result of regular changes in concentrations with time. These changes can be monitored by gas evolution, colour or redox potential. Spatial ordering appears in non-stirred systems as travelling bands of oxidation which can be found in one-, two-, or three-dimension(s). A number of chemical systems which exhibit these properties have now been identified and studied. In this work, interest has centred on the "coupling" of two chemical oscillators of the same type. This is carried out by bringing the oscillators into limited chemical contact with each other. The study reported here provides an insight into intrinsic coupling between chemical oscillators and possibly provides a model for interaction of ordered systems like living cells in higher organisms.

Generally, three different types of coupling are distinguished:-

(i) coupling by diffusion or by passive forms of exchange of matter [29,30],

(ii) chemical coupling where the decay product from one oscillator is the initial product of the chemical mechanism involved in the second oscillator [31], and

(iii) coupling between individual oscillators and external stimuli [32].

The Belousov-Zhabotinskii (B-Z) reaction was used to investigate the intrinsic coupling which is a combination of diffusion and coupling with an external stimulus. The B-Z

reaction requires four reactants - bromate, malonic acid, sulphuric acid and a catalyst which can be ferroin, manganese or cerium. This oscillating system involves as many as 11 different reactions and possibly more [33-38]. The overall reaction rate is dependent upon the amount of oxygen present [39], different light intensities [40] and other environmental factors [41], as also found for living systems.

In higher organisms, diffusion of matter can occur through structures connecting the cells and mutual entrainment of the cells is observed [42,43]. For chemical oscillators, the degree of interaction is dependent upon the matter exchanged and the frequencies of the oscillators [44]. The magnitude of this interaction can be calculated from the expression, $C = \frac{2\pi N}{\Delta W}$ where C is the coupling constant, N is the number of holes and ΔW is the difference between the natural limit cycle frequencies. Exchange of chemicals under specific oscillatory-type conditions may control, among other processes, the mechanism of cellular replication [29]. In turn, this could be important for an understanding of the growth of cancer cells [45,46].

In relation to model systems of living cells, the most common and simple interaction to model is the two reactor cell system [47]. This system is important because it models the circadian [48,49], neural [50] and other coupled natural oscillators [51,52] well.

The first model of a two reactor cell system using the B-Z reaction was reported by Marek and Stuchl [30]. They observed:-

(i) synchronisation of oscillators by entrainment at a common or multiple of a common frequency between reactor cells,

(ii) rhythm splitting, where the period of the slower oscillator is split into two parts by the action of the faster oscillator during non-synchronisation, and

(iii) amplitude amplification.

Fujii and Sawada extrapolated this idea further by having two reactor cells which were connected by holes on the walls of these reactor cells [44]. The two reactor cells were allowed to oscillate at different frequencies with the holes closed. Then the holes were opened and the degree of coupling estimated in terms of the coupling constant. The two reactor cells were found to couple when the coupling constant was greater than 6 hours. Recent results show that this coupling constant was indeed dependent upon the difference between the natural frequencies of the two cells. Irregular synchronisation can also be obtained [53,54].

In this work, the determination of this constant in relation to the influence of one reactor cell on the starting of another, was carried out. Effects of apparatus design and geometry were also studied. The results indicate that the starting reactor cell is more sensitive than an established one to coupling and also, that the coupling constant is dependent on features of the apparatus.

1.4 OUTLINE OF THESIS PRESENTATION

In Chapter 2, equilibrium constant studies for the six-coordination of (magnesium porphyrin)(pyridine)$_2$ complex in an hydrophobic solvent are reported [55]. This work provides some indication of the preferred coordination number for isolated magnesium porphyrin entities. The

constant is small compared to that for five-coordination and lowering the temperature enhances its magnitude. In addition, a comparison of these results with those for Zn and Fe analogues, provides some understanding as to why Mg is the preferred metal ion for chlorophyll.

The preparation and spectral properties of the myoglobin and hemoglobin complexes, MgPP-Mb, MgMP-Mb, MgDP-Mb, MgPP-Hb, MgMP-Hb and MgDP-Hb are reported in Chapter 3 [56-58]. These studies provide information on the influence of protein environment on magnesium porphyrin groups. The Mg porphyrin-Mb complexes show prominent splittings and red-shifts of the visible absorption bands, with respect to those for the Mg porphyrin-Hb analogues. Different reasons for these observations are considered. A comparison is also made with other heme protein systems that display similar spectral features. The larger magnitudes of the red-shift observed for MgPP compared with MgDP and MgMP is specifically associated with the presence of an interaction between the protein and the vinyl groups of protoporphyrin.

The observations of induced Cotton effects for magnesium porphyrin in certain chiral amino acid solutions are discussed in Chapter 4 [55,59]. The electronic band positions indicate the species which produce these effects are six-coordinate (Mg porphyrin)(amino acid)$_2$ entities, where the asymmetry of the amino acid is coupled to the magnesium porphyrin electronic transitions. The five-coordinate (Mg porphyrin)(amino acid) species which are the major components of these mixtures do not produce Cotton effects. Various reasons for the particular stereochemical coordination of amino acids are suggested.

These results are then compared with those of the corresponding protein complexes and the influence of the amino acids on the optical activity of hemoproteins highlighted.

In Chapter 5, results for the photochemical reactions of MgPP-Mb, MgMP-Mb, MgDP-Mb, MgPP-Hb and MgMP-Hb are reported. Changes in electronic spectra were monitored for irradiation in the ultra-violet, visible and infra-red regions. The protein species are less susceptible to photodecomposition than the corresponding uncomplexed magnesium porphyrins. In addition, the photodecomposition patterns of myoglobin and hemoglobin pairs of derivatives show significant differences. These are interpreted in terms of different protein conformations. The identification of optical activity in(Mg porphyrin) (chiral amino acid)$_2$ also provided the basis of a preliminary circularly polarised light irradiation study.

Analyses of the crystal structures of six-coordinate MgTPP(1-MeIm)$_2$, MgTPP(4-pic)$_2$ and MgTPP(pip)$_2$ complexes are reported in Chapter 6. MgTPP(4-pic)$_2$ and MgTPP(pip)$_2$ are isomorphous and crystallise in a triclinic space group, while MgTPP(1-MeIm)$_2$ crystallises in a tetragonal space group. Although these complexes are isostructural with those of iron analogues, they show significantly longer axial bond lengths. The close structural similarities observed for complexes of a non-transition metal ion, Mg(II), and a transition metal ion, Fe(II), enable steric effects of the ligands and the influence of the filled d orbitals in Fe(II) to be assessed in detail. In addition, comparison of the axial bond lengths with corresponding

electronic spectra data provides an insight into the influence of axial ligands on the chemical properties of Mg porphyrin.

In Chapter 7, the crystal structure of five-coordinate $MgTPP(H_2O)(2\text{-pic})_2$, which crystallises in a triclinic space group, is reported and discussed. The water molecule coordinated to Mg is hydrogen bonded to nitrogen atoms of two 2-picoline groups. These interactions localise the coordinated water molecule, as considered to be likely for Mg porphyrin-Mb complexes (Chapter 3). The Mg atom in the aquo 2-picoline complex is displaced 0.416Å out of the plane of the four chelating nitrogen atoms of the porphyrin ring, compared with a corresponding value of 0.273Å for $MgTPP(H_2O)$ [60]. The importance of this enchanced displacement of Mg for chlorophyll molecules *in vivo* is discussed in some detail.

Chapter 8 is concerned with the coupling effects of oscillating chemical reactions in a two reactor cell system. A comparison of the coupling constants under various conditions indicates that a starting reactor cell is about 4 to 6 times more sensitive to coupling than an established one. The geometry of the apparatus design influences the coupling constant by a small but measurable amount. The relevance of this work to living systems is also discussed.

Chapter 9 highlights the importance of chemical studies on Mg porphyrin complexes and coupled oscillators for a broader understanding of biological and technological systems.

CHAPTER 2

EQUILIBRIUM STUDIES OF MAGNESIUM PROTOPORPHYRIN – PYRIDINE COMPLEXES

2.1 INTRODUCTION

The determination of the coordination state of Mg in bacteriochlorophyll and chlorophyll is of considerable importance because it has been suggested that the nature of the coordination sphere around Mg could account for the red-shift in absorption of chlorophyll *in vivo* [61]. IR [62-65] and NMR [23,66-70] studies of chlorophyll *in vitro* indicate that the four-coordinate Mg centre is coordinatively unsaturated, and that five-coordination is the preferred coordination state. However, equilibrium studies using pyridine [25,26,71] and etherate [71] suggest that under certain conditions, six-coordination can be obtained.

It is generally accepted that the Mg atom in bacteriochlorophyll [25,71], chlorophyll [26,72-75] and porphyrin [55,76-83] has a high affinity for coordinating nitrogenous bases like pyridine. Increasing the pyridine concentration increases the red-shift in the absorption bands and the equilibrium constants may be determined from the changes in the visible absorption spectra [78]. This technique gives accurate results [84] which are also important in the characterisation of the coordination state of metal ions in biological systems like microsomes [85-87], cytochromes [88] and hemoproteins [89].

In this chapter, detailed studies of the equilibrium constant for the reaction $MgPP(py) + py \rightleftharpoons MgPP(py)_2$ are

reported using pyridine/benzene mixtures. The magnitude of this equilibrium constant is dependent on the polarity of the solvent environment [83]. Benzene, being non-polar, mimics the hydrophobic environments of bacteriochlorophyll and chlorophyll [90]. Pyridine, which is polar and has a nitrogen atom for coordination, is similar to histidine. X-ray studies on *Prosthecochloris aestuarii* show that most of the Mg atoms in bacteriochlorophyll are coordinated to histidine groups [3-7].

2.2 EXPERIMENTAL

PPDME was prepared from whole blood by the procedure of Grinstein [91]. Hydrolysis of PPDME by 1% KOH in methanol gave the desired PP and the purity was checked by the extinction coefficients [92]. MgPP was prepared from PP and magnesium perchlorate [93,94] and the purified MgPP had the same optical absorption spectrum as that reported by Falk [92]. It is possible that during the preparation of MgPP, a water molecule could still be coordinated to the Mg to form aquo magnesium protoporphyrin [60]. Consequently, the sample was placed in an oven at 160°C for 2 hours before each spectrophotometric measurement. All the determinations were made in duplicate and the results were reproducible.

Analytical grade pyridine and benzene were purchased from British Drug Houses Ltd and stored in the dark at 0°C over 4 Å molecular sieves under nitrogen. Electronic absorption spectra were recorded using water-jacketed quartz cells on a Varian Superscan 3 UV-visible spectrophotometer. Water at the required temperature from a

waterbath was circulated through the water-jacketed cells and the temperature of the water was measured using a thermometer. All spectra were then run at least twice at 10 minute intervals to ensure temperature equilibration.

2.3 RESULTS

When pyridine is added to MgPP in benzene, the spectral changes are negligible for concentrations of pyridine to MgPP up to 10:1 [79,80]. Hence the equilibrium constant for MgPP + py$\rightleftharpoons$MgPP(py) cannot be determined accurately by electronic absorption spectroscopy. Further increase in the concentration of pyridine shifts the bands towards the red region (Figure 2.1). The isosbestic points confirm previous assumptions of an equilibrium which depends on the concentration of pyridine that was present, MgPP(py) + py $\rightleftharpoons$ $MgPP(py)_2$. The intensity of the Q_1 transition at 552-556 nm was relatively constant but the intensity of the Q_o transition at 591-598 nm was reduced significantly. Consequently, it was possible to use the Q_o transition at 591 nm to determine the equilibrium constant by plotting $^1/x$ against $^1/B$ where x is the difference in absorbance between an equilibrium mixture at some given MgPP concentration and at zero complexing, and B is the concentration of pyridine (Figure 2.2, Tables 2.1, 2.2, 2.3 and 2.4).

The equilibrium constants were found to be 1.400, 1.081 and 0.859 at 20.9°C, 32.0°C and 42.4°C respectively by least square calculations. The correlation coefficients between $^1/x$ and $^1/B$ were over 0.997 for all three temperatures.

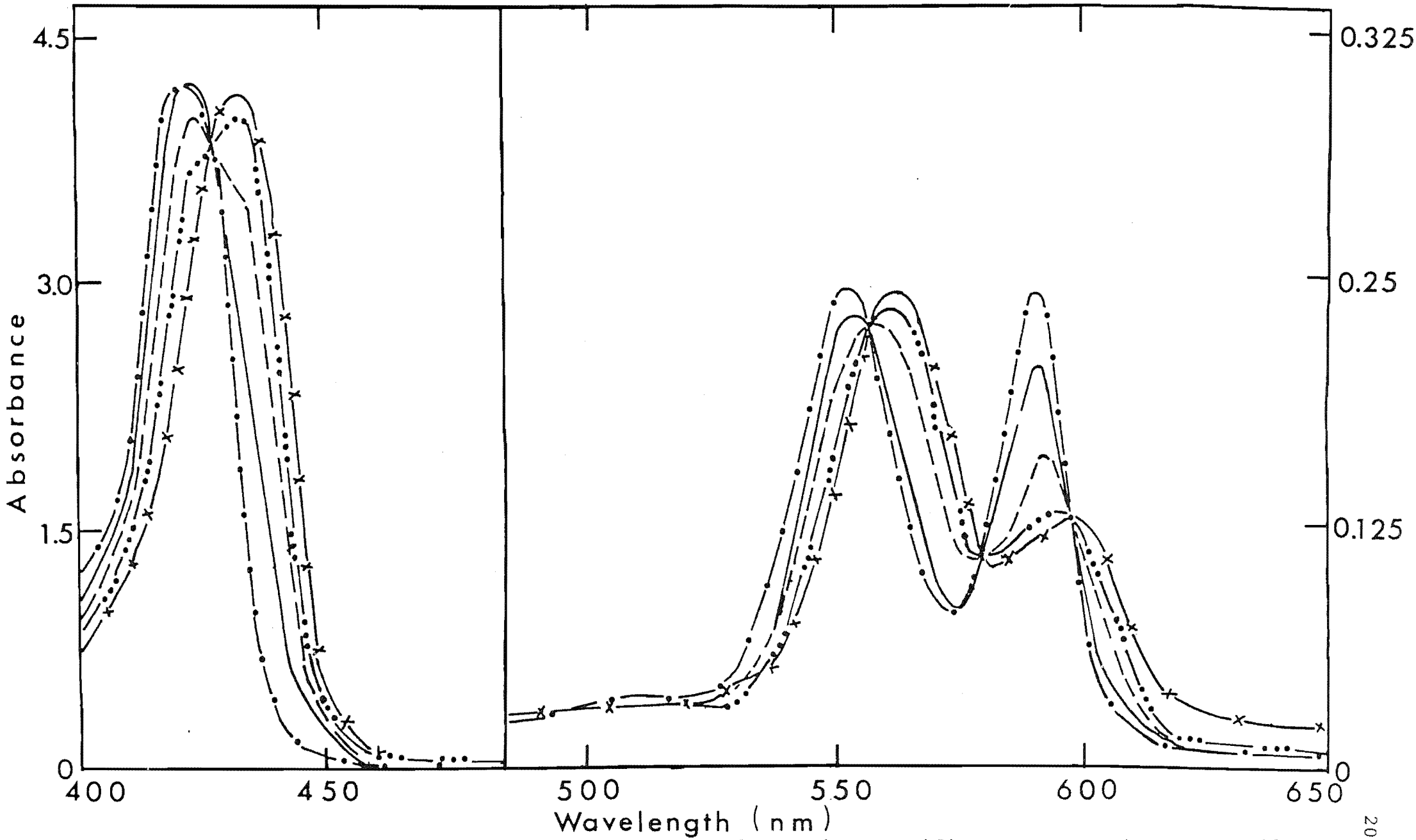

Figure 2.1 : Electronic absorption spectra of MgPP under various pyridine concentrations at 20.9°C to determine the equilibrium constant: MgPP(pyridine)+pyridine $\rightleftharpoons$ MgPP(pyridine)$_2$

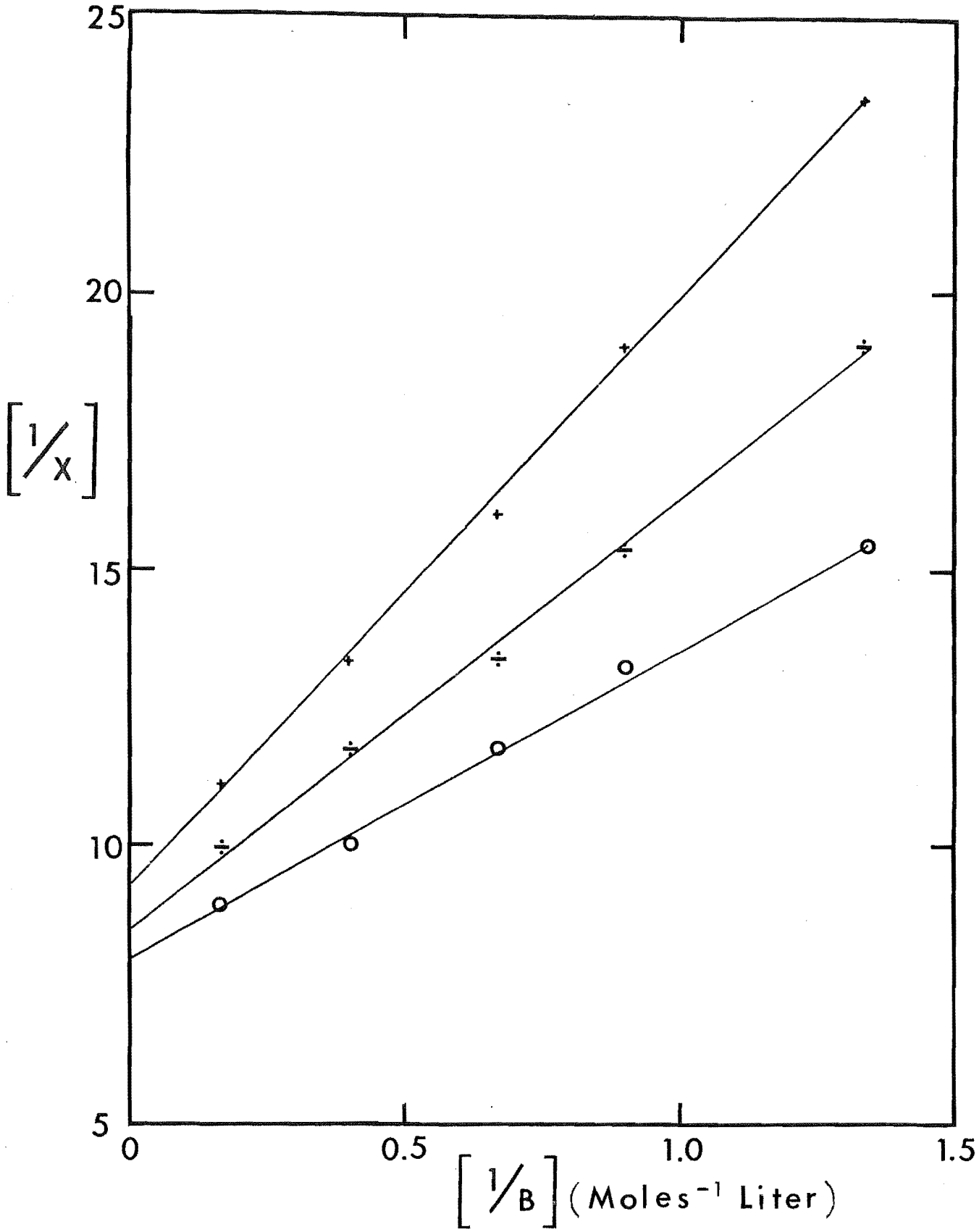

Figure 2.2 : Determination of the equilibrium constant for MgPP(pyridine)+pyridine⇌MgPP(pyridine)$_2$ at 20.9°C [o], 32.0°C [÷], and at 42.4°C [+].

Table 2.1

Spectral properties of MgPP in pyridine at 20.9°C

Concentration of pyridine (moles liter^{-1})	Concentration of MgPP in benzene (μM)	Wavelength (nm)		
		Q_1	Q_o	Soret
12.3500	12.1	565	599	435
11.7000	12.1	565	598	435
6.2000	12.1	564	595	433
2.4800	12.1	560	593	423, 433 broad, strong
1.4890	12.1	559	593	423.5**
1.1170	12.1	556	592.5	423.5**
0.7445	12.1	556	592.5	423.5*
0.6204	12.1	556	592	423*
0.4963	12.1	555.5	592	423
0.3722	12.1	555.5	592	423
0.3102	12.1	555	592	423
0.2482	12.1	555	592	423
0.1861	12.1	555	592	423
0.1241	12.1	555	592	423
0.0000	12.1	552	591	420

**band has distinct shoulder

*band has shoulder

Table 2.2

Determination of equilibrium constant for $MgPP(py)+py \rightleftharpoons MgPP(py)_2$

Temperature = 20.9 ± 0.1°C Total MgPP concentration = 12.1×10^{-6} moles liter^{-1}

Initial pyridine concentration, B_o (moles liter^{-1})	Observed Absorbance at 591 nm	X $A_u - A_c$	Equilibrium pyridine concentration, B (moles liter^{-1})	$1/X$	$1/B$
0.0000	0.2400 (A_u)	0.0000	0.0000		
0.2747	0.2050 (A_c)	0.0350	0.2747	28.57	3.64
0.4963	0.1950	0.0450	0.4963	27.22	2.01
0.7445	0.1750	0.0650	0.7445	15.38	1.34
1.1170	0.1650	0.0750	1.1170	13.33	0.90
1.4890	0.1550	0.0850	1.4890	11.76	0.67
2.4820	0.1400	0.1000	2.4820	10.00	0.43
6.2000	0.1275	0.1125	6.2000	8.89	0.16

Intercept = 7.935, Slope = 5.669, K = 1.400, ℓn K = 0.336, Correlation = 0.997

Table 2.3

Determination of equilibrium constant for $MgPP(py) + py \rightleftharpoons MgPP(py)_2$

Temperature = 32.0 ± 0.1°C Total MgPP concentration = 12.1×10^{-6} moles liter^{-1}

Initial pyridine concentration, B_o (moles liter^{-1})	Observed Absorbance at 591 nm	X $A_u - A_c$	Equilibrium pyridine concentration, B (moles liter^{-1})	$1/X$	$1/B$
0.0000	0.2400 (A_u)	0.0000			
0.7445	0.1875 (A_c)	0.0525	0.7445	19.05	2.01
1.1170	0.1750	0.0650	1.1170	15.38	0.90
1.4890	0.1650	0.0750	1.4890	13.33	0.67
2.4820	0.1550	0.0850	2.4820	11.76	0.40
6.2000	0.1395	0.1005	6.2000	9.95	0.16

Intercept = 8.44, Slope = 7.801, K = 1.081, ℓn K = 0.078, Correlation = 0.998

Table 2.4

Determination of equilibrium constant for $MgPP(py)+py \rightleftharpoons MgPP(py)_2$

Temperature = 42.4 ± 0.1°C. Total MgPP concentration = 12.1×10^{-6} moles liter^{-1}

Initial pyridine concentration, B_o (moles liter^{-1})	Observed Absorbance at 591 nm	X $A_u - A_c$	Equilibrium pyridine concentration, B (moles liter^{-1})	$1/X$	$1/B$
0.0000	0.2400 (A_u)	0.0000	0.0000		
0.7445	0.1975 (A_c)	0.0425	0.7445	23.53	2.01
1.1170	0.1875	0.0525	1.1170	19.05	0.90
1.4890	0.1775	0.0625	1.4890	16.00	0.67
2.4820	0.1650	0.0750	2.4820	13.33	0.40
6.2000	0.1500	0.0900	6.2000	11.11	0.16

Intercept = 9.179, Slope = 10.686, K = 0.859, ℓn K = -0.152, Correlation = 0.999

ΔH and ΔS for this equilibrium were -4.17 kcal mol^{-1} and -13.49 cal mol^{-1} respectively (Figure 2.3).

2.4 DISCUSSION

2.4.1 General Discussion

Magnesium porphyrin has a high affinity for nitrogenous bases like pyridine to form five-coordinate species and the equilibrium constant for MgPP + py $\rightleftharpoons$ MgPP(py) is so high that accurate measurements cannot be obtained. Only the equilibrium constant for the second axial pyridine is measurable. From the intensities of the Soret bands, Storm and co-workers [81] obtained a value of 0.242 for this equilibrium constant in 2,6-lutidine. A corresponding value of 1.400 in benzene was determined by using the Q_o band in the visible region. The increase in equilibrium constant by about 5.8 times is due mainly to differences in the solvent. This result agrees well with the ratio value of 5.02, for the equilibrium constants of MgPP(DME) in benzene and 2,6-lutidine [81]. Thus, either the Soret or the Q_o band may be used for equilibrium constant measurement.

The main contributing factor to this change in equilibrium constant is the entropy term and not the enthalpy term which is constant for both benzene and 2,6-lutidine [81,83]. This entropy term highlights the importance of solvent-solute interactions. These interactions are a result of the different solvation energies of MgPP(py), pyridine and $MgPP(py)_2$. MgPP(py) and pyridine are more polar to the solvent molecules than

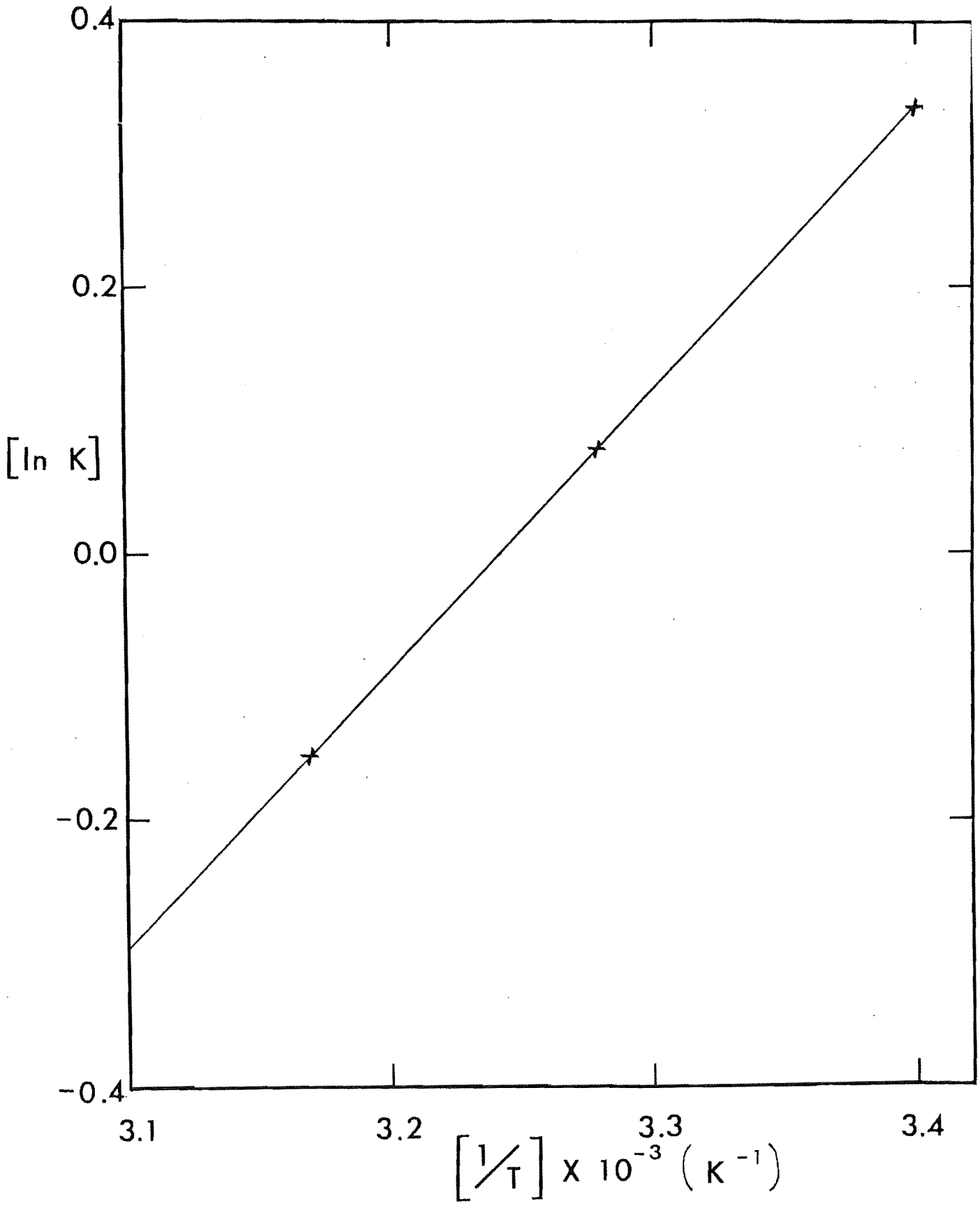

Figure 2.3 : Determination of ΔH and ΔS for the reaction
MgPP(pyridine)+pyridine⇌MgPP(pyridine)$_2$

$MgPP(py)_2$ which has only the backside of the pyridine ring and the periphery of the porphyrin ring exposed to the solvent. Consequently, in polar solvent, MgPP(py) and pyridine are more solvated than $MgPP(py)_2$ and more energy is then required to disrupt the solvent shell. This leads to lowering of the equilibrium constant. Conversely, in benzene, $MgPP(py)_2$ is more solvated than the other two species and the equilibrium constant is therefore higher.

While five-coordinate Mg is the dominant form in these systems, six-coordinate Mg can be favoured by lowering the temperature and increasing the concentration of the polar ligands. Lowering the temperature results in an increase in the intensity of the longer wavelength band and a decrease in the intensity of the shorter wavelength band suggesting increased formation of $MgPP(py)_2$. The red-shift from five- to six-coordination indicates that the ground and excited state energies have been brought closer together [95].

All of these solution properties of MgPP are also observed for other Mg porphyrin [55,81-83], bacteriochlorophyll [25,71] and chlorophyll [72-75,96] systems (Table 2.5). The second equilibrium constant is generally small except for the complex, $MgTPP(2\text{-methylimidazole})_2$, and independent of the porphyrin basicity [77]. In the case of 2-methylimidazole, the second equilibrium constant is about 10^5 times higher than that of 1-methylimidazole [82]. The pKa values of 2-methylimidazole and 1-methylimidazole are 7.56 and 7.33 respectively which indicate that ligand basicity does not contribute significantly to this constant.

Table 2.5

Comparison of the equilibrium constants for various Mg porphyrins, bchl and chl

Compound (M)	Ligand (L)	Solvent	Equilibrium constant		Reference
			$M + L \rightleftharpoons ML$	$ML + L \rightleftharpoons ML_2$	
MgPP	py	benzene		1.400	55
MgPP(DME)	py	2,6-lutidine		0.242	81
MgPP(DME)	N_3-fluorenone	$CHCl_3$	2320		83
MgMP(DME)	py	2,6-lutidine		0.070	81
MgMP(DCE)	py	2,6-lutidine		0.142	81
MgDP(DME)	py	2,6-lutidine		0.228	81
MgDP(DME)	4-methylpy	2,6-lutidine		0.163	81
MgDP(DME)	4-ethylpy	2,6-lutidine		0.152	81
MgDP(DME)	4-vinylpy	2,6-lutidine		0.091	81
MgDP(DME)	4-methoxyl-carbonylpy	2,6-lutidine		0.362	81
MgDSPE(MME)	py	2,6-lutidine		0.074	81
MgTPP	py	2,6-lutidine		0.161	81
MgTPP	py	benzene	2000(estimated)	0.577	78
MgTPP	py	TBAP/CH_2Cl_2	15488	0.141	82
MgTPP	3,5-dichloropy	TBAP/CH_2Cl_2	76	0.724	82
MgTPP	3-cyanopy	TBAP/CH_2Cl_2	158	1.148	82
MgTPP	4-cyanopy	TBAP/CH_2Cl_2	214	0.955	82

(cont...)

Table 2.5 continued

Compound (M)	Ligand (L)	Solvent	Equilibrium constant		Reference
			$M + L \rightleftharpoons ML$	$ML + L \rightleftharpoons ML_2$	
MgTPP	3-chloropy	TBAP/CH_2Cl_2	309	0.794	82
MgTPP	3-bromopy	TBAP/CH_2Cl_2	427	0.437	82
MgTPP	3-acetylpy	TBAP/CH_2Cl_2	1820	0.603	82
MgTPP	4-acetylpy	TBAP/CH_2Cl_2	2399	0.603	82
MgTPP	3-methylpy	TBAP/CH_2Cl_2	4266	0.186	82
MgTPP	4-methylpy	TBAP/CH_2Cl_2	16218	0.158	82
MgTPP	3,4-lutidine	TBAP/CH_2Cl_2	16982	0.129	82
MgTPP	1-methylimidazole	TBAP/CH_2Cl_2	251188	0.110	82
MgTPP	piperidine	TBAP/CH_2Cl_2	21380	0.302	82
MgTPP	2-methylpy	TBAP/CH_2Cl_2	295	0.631	82
MgTPP	2-methylimidazole	TBAP/CH_2Cl_2	575440	14125	82
MgTPP	imidazole	TBAP/CH_2Cl_2	95500	1.622	82
MgTPP	4-(N,N-dimethylamino)py	TBAP/CH_2Cl_2	30903	1.950	82
MgTPP	2-aminopy	TBAP/CH_2Cl_2	1122	0.692	82
bchl b	py	n-propylbenzene		10	71
bchl b	py	toluene		11	25
chl a	4-ethylpy	nitromethane		19	73
chl a	4-ethylpy	acetonitrile		34.5	73
chl a	4-ethylpy	t-butanol	3.5	0.35	73
chl a	ethanol	acetone	1.86	0.31	73
chl a	py	ethanol	8.2	0.055	73
chl a	py	ethanol	4.85	0.243	72

Although the magnitude of the second equilibrium constant for 2-methylimidazole is large, the expected trend where the first equilibrium constant is greater than the second equilibrium constant, is still observed.

These results confirm other reports which show that the Mg centres in bacteriochlorophyll and chlorophyll are either five- or six-coordinate. In addition, the results also help to characterise the coordination state of Mg^{2+} in Mg porphyrin-Mb and Mg porphyrin-Hb (Chapter 3). Detailed crystal structures of such six-coordinate (Mg porphyrin)(nitrogenous base)$_2$ complexes will be discussed in Chapter 6.

2.4.2 Comparison of the Coordination Behaviours of Mg(II), Zn(II) and Fe(II) Porphyrin

The equilibrium constants for metalloporphyrins of Cu(II) [97], Zn(II) [78,98-104], Cd(II) [78], Hg(II) [78], Ni(II) [105], VO(II) [106], Fe(II) [108-109] and Fe(III) [110,111] in nitrogenous bases have also been reported. A comparison of the equilibrium constants of Zn(II), Mg(II) and Fe(II) porphyrin should therefore enable the role of Mg(II) ions in metalloporphyrins and other biological systems to be elucidated.

Although Mg(II) and Zn(II) ions are both closed shell diamagnetic ions [112], equilibrium studies show that the coordination behaviours of Mg(II) and Zn(II) porphyrin are different. When a small amount of pyridine is added, the positions of the three electronic bands of Mg porphyrin remain the same, but the relative intensities of the Q_o and Q_1 bands change [78,82]. Further addition of excess pyridine produces a red-shift in the positions of the

electronic bands. This result suggests a sequential 5 → 6 coordination change. By contrast, the electronic bands of Zn porphyrin are red-shifted for all pyridine concentrations indicating the formation of a five-coordinate species only [78,98-104]. The magnitude of this equilibrium constant is compatible with the first equilibrium constant for Mg porphyrin and it is dependent on solvent-solute interactions. This result suggests that the coordination behaviours of Mg(II) and Zn(II) porphyrin towards a fifth ligand are similar.

However, if the maximum coordination number of Zn(II) porphyrin is five, Zn^{2+} may only be able to mimic the behaviour of Mg^{2+} to a certain extent in biological systems like chlorophyll [113,114]. This difference in the coordination number is likely to be a result of the different ionic sizes of Mg^{2+} (0.66Å) and Zn^{2+} (0.74Å) [115]. X-ray studies show that the Mg^{2+} is displaced by a smaller value out of the plane of the porphyrin ring [60] than Zn^{2+} [116]. Consequently, the Mg^{2+} is likely to experience the effect of the second axial ligand and show six-coordination.

Recent results suggest that the capability of Mg^{2+} to show six-coordination behaviour is important in photosynthesis, especially for the formation of an adduct of basic composition, chlorophyll-ligand-chlorophyll [18]. Such an adduct may be found in the photosynthetic reaction centre which absorbs light maximally at 680 nm.

It has been accepted that in the common biosynthetic pathway between plants and animals, the last member is protoporphyrin [117]. Insertion of iron leads to the prosthetic groups of cytochromes, myoglobin, hemoglobin

and the heme enzymes, while insertion of Mg leads to the porphyrin ring being used for chlorophyll formation [118, 119] (Figure 2.4). Consequently, it is interesting to compare the equilibrium constants of Mg(II) and Fe(II) porphyrin.

The equilibrium constants of Fe(II) porphyrin have been extensively studied because of their importance to the understanding of the coordination behaviour of iron in hemoproteins. Similarly as for Mg(II), the coordination number of Fe(II) porphyrin is dependent on the ligand and the environment. Hydrophobic environments [120] and ligands with steric interaction like 2-methylimidazole [121], tend to favour five-coordination. In addition, the magnitudes of the formation constants for six-coordinate complexes of both Mg(II) and Fe(II) porphyrins increase as the ligand basicity decreases [99].

By contrast to Mg(II), the equilibrium constant for the second ligand of Fe(II) porphyrin is usually higher than the first equilibrium constant [122,123]. This higher equilibrium constant is a result of a change in spin state. Five-coordinate (Fe(II) porphyrin)(py) is high spin. With the addition of another pyridine, the low-spin state is readily obtained for the six-coordinate octahedral conformation [124]. It is probably the high crystal field stabilisation energy associated with the low-spin t_{2g}^{6} configuration, which contributes to the additional stability of the six-coordinate state for Fe(II) [125]. This effect is absent for Mg(II).

Another difference between Mg(II) and Fe(II) porphyrin is that increasing the Fe(II) porphyrin basicity

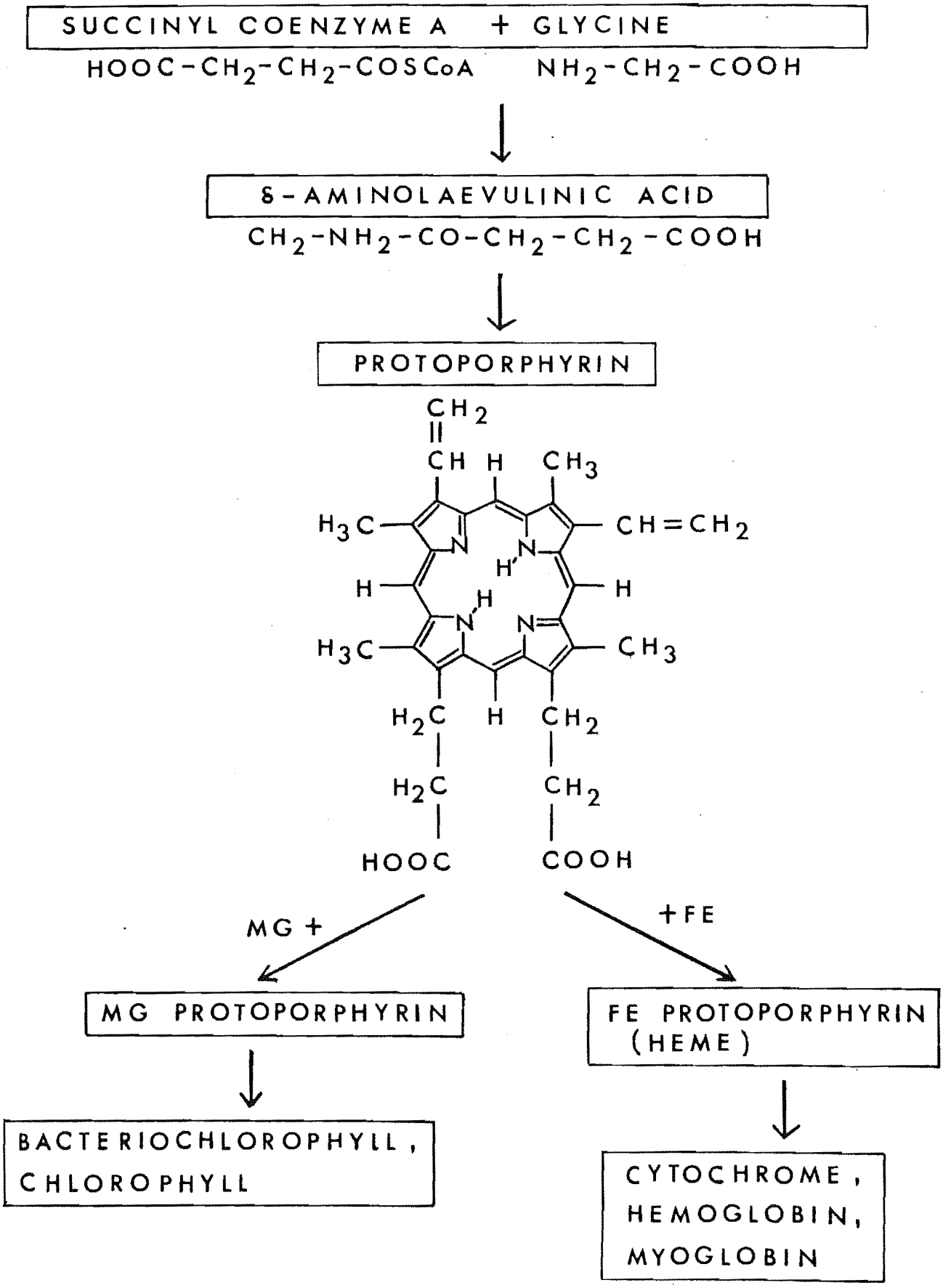

Figure 2.4 : Common biosynthetic pathway between heme and chlorophyll compounds.

increases the magnitude of the equilibrium constants [85]. The result suggests that π-bonding between Fe(II) and axial ligands can occur [86,87] and favours six-coordination. Overall, six-coordinate Fe(II) porphyrin is the dominant species while Mg(II) porphyrin is usually five-coordinate or in equilibrium with six-coordination.

CHAPTER 3

PREPARATION AND SPECTRAL STUDIES OF MAGNESIUM PORPHYRIN-APOMYOGLOBIN AND -APOHEMOGLOBIN COMPLEXES

3.1 INTRODUCTION

The isolation of photochemically active chlorophyll-protein complexes with absorption maxima similar to those of antenna chlorophyll, suggests that chlorophyll molecules *in vivo* are closely associated with proteins [127-134]. Most of these natural chlorophyll-containing proteins have tetrameric structures [135,136], but monomeric and trimeric structural proteins have also been isolated [3,137]. Their molecular weights range from 9,000 to 110,000 daltons [138,139] and they are especially hydrophobic in the reaction centre regions [140,141]. They are generally globular in shape [142].

Although these chlorophyll-protein complexes show different chemical and physical properties from chlorophylls *in vitro* [143], the influence of the protein is generally not well understood [131]. X-ray studies on such a bacteriochlorophyll-protein from the green bacterium, *Prosthecochloris aestuarii* show that most of the bacteriochlorophyll molecules are coordinated to histidine groups [3-7] (Figure 3.1). Consequently, apomyoglobin and apohemoglobin have been considered as useful protein models for studying chlorophyll-protein interactions because of the favourable positioning of an imidazole group for the same kind of coordination to Mg [144,145]. Until recently, experimental results were interpreted using the exciton

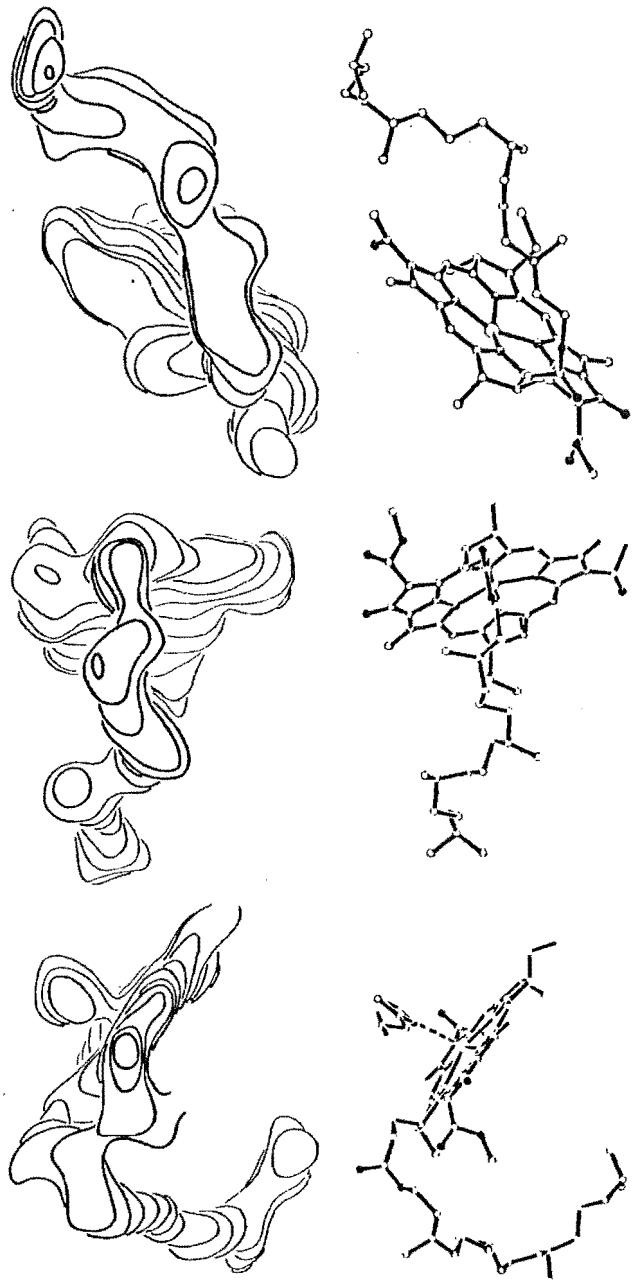

Figure 3.1 : Electron density (left) and molecular shape (right) of bacteriochlorophylls in the bacteriochlorophyll-protein of *Prosthecochloris aestuarii* (from ref. 3)

theory based on chlorophyll-chlorophyll interactions [146, 147]. The maximum distance for this interaction is assumed to be about 20Å or less in chlorophyll [95] and 12Å to 15Å in bacteriochlorophyll [148]. For chlorophyll molecules incorporated into the heme pockets of the globular proteins, apomyoglobin or apohemoglobin which have crystal distance of 25Å to 35Å, such chlorophyll-chlorophyll interaction is excluded, thus enabling chlorophyll-protein interactions to be independently studied [144,145]. It has been suggested that the chlorophyll-protein interactions produce the red-shift for chlorophyll *in vivo* [149], as compared with chlorophyll dissolved in organic solvents [96]. Recent studies of substituted chlorophyllin-, chlorophyllide- and bacteriochlorophyllide-apomyoglobin complexes appear to support the importance of chlorophyll-protein interactions [12-17].

A possible region for chlorophyll-protein interactions and also for metalloporphyrin-protein interactions, is between the peripheral substituents of the metallochlorin or metalloporphyrin ring and the amino acid side chains of the proteins [150-155]. An effective way of probing this interaction in porphyrin is by modifying the structure of the heme peripheral substituent and then relating these modifications to alterations in the functional properties of the protein reconstituted with these porphyrins [156]. Previous studies of this type of substitution effect for iron hemoglobin, where the vinyl groups of the heme periphery were replaced by other functional groups, have produced interesting results which suggest that steric effects [156,157], inductive effects [158,159], and protein-heme interactions play an important role in the binding

properties of hemoglobin [160,161]. It has been suggested that in native hemoglobin, Valine FG 5 (93) is in close contact with the vinyl groups and the absence of the vinyl groups in deuteroporphyrin provides an explanation for its reduced cooperativity [162]. Quantitative calculations of the energetics of heme-protein interactions in hemoglobin also indicate the importance of this interaction between the vinyl group and the protein [153].

In this chapter, the preparation and spectral results for MgPP-Mb, MgPP-Hb, MgMP-Mb, MgMP-Hb, MgDP-Mb and MgDP-Hb are reported (Figure 3.2). Some solution nmr and single crystal electronic spectral data have previously been reported for MgPP-Mb [12,13,15]. The results obtained for the species, where the vinyl groups are absent from the porphyrin rings, when compared with related MgMP and MgPP complexes enable, in particular, the role of the vinyl groups to be assessed in some detail. The spectral results also enable the coordination characteristics of the magnesium centre in two closely related proteins having small but well-defined differences in amino acid sequence and conformation to be elucidated. These results indicate significant differences in the coordination environment of magnesium for the hemoglobin and myoglobin derivatives. Other heme proteins provide useful information on the possible reasons for the changes because of similarities with, in particular, results for the magnesium myoglobin species. These are the nitrogenous base compounds of iron myoglobin [163], the carbon monoxide complex of a ruthenium (II) myoglobin derivative [164,165], and the carbon monoxide complexes of iron hemoglobin and myoglobin [166]. A detailed comparison of the spectral

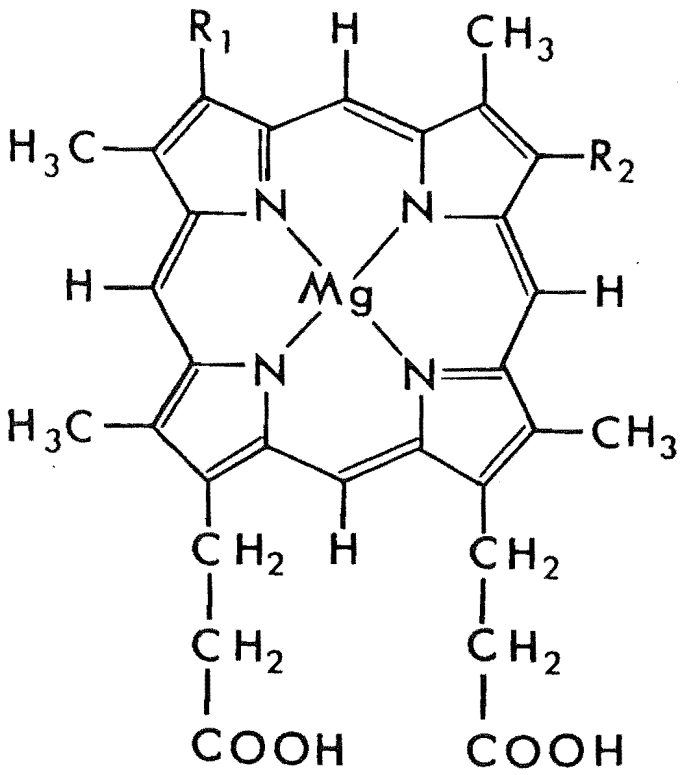

Compound	R_1	R_2
Mg Protoporphyrin	$CH=CH_2$	$CH=CH_2$
Mg Mesoporphyrin	CH_2-CH_3	CH_2-CH_3
Mg Deuteroporphyrin	H	H

Figure 3.2 : Structure and nomenclature for Mg porphyrins

properties of the carbon monoxide complexes of iron hemoglobin and myoglobin will also be made with corresponding data for the Mg complexes.

Using these comparisons with other related systems it has been possible to deduce the likely nature of the coordination changes about Mg for the hemoglobin and myoglobin systems. This study aims at elucidating in more detail the role of the protein environment and illustrates the importance of using metal substituted derivatives of a protein system such as the heme one, for which a very wide range of spectral and structural information is available, in order to gain further insight into the coordination behaviour of a biologically important centre like Mg. Furthermore, Mg porphyrin can be considered to be a suitable model for chlorophyll as it is the first metabolic precursor committed to the biosynthesis of chlorophyll and it is also a photosensitizer [167].

3.2 EXPERIMENTAL

Protohemin was prepared from whole blood by standard procedures [168,169]. DPDME was prepared from protohemin according to the methods of Walter [170] and Chu and Chu [171] with minor modifications. 1 gm of protohemin was thoroughly mixed with 5 gm of resorcinol and fused in an oil bath at 180°-190° C for 30 minutes. The reaction mixture was then dissolved in 98-100% formic acid and 0.5 gm of reduced iron powder was added in small batches over 10 minutes. The greenish solution turned deep violet and a sample of the solution showed no absorption band at 545 nm in pyridine-hydrazine hydrate solution [172]. Further preparative work was similar to that of Chu and Chu

[171] except that purification of DPDME was carried out by using a column of Grade IV alumina. The Grade IV alumina was prepared by standing alumina in distilled water for 2 hours and dried overnight at 28°C. The DPDME was developed with analytical grade chloroform-benzene (1:10 v/v) and the DPDME was eluted as a clean violet band. The volume of the solvent was then reduced by boiling and on cooling, long red glittering needles appeared. The purity of the DPDME was checked by the extinction coefficients [92] and ^{1}H nmr [173]. The shifts and intensities of the ^{1}H nmr spectrum using $CDCl_3$ as solvent and trimethylsilane as the standard reference show peaks at 9.92 (multiplet, 4H), 9.00 (singlet, 2H), 4.33 (triplet, 4H), 3.50 to 3.70 (multiplet, 12H), 3.23 (triplet, 6H) and -4.00 (singlet, 2H). The melting point of 225°C, agrees well with the reported values of 223°C [171] and 224.5°C [172].

MgDPDME was prepared from DPDME and magnesium perchlorate [93,94] and the reaction was completed when a sample of the solution showed no absorption band at 621 nm in ether solution. Base hydrolysis by NaOH gave the desired MgDP [174]. MgPP was prepared according to the method described in Chapter 2. MPDME was purchased from Sigma chemical company. MgMPDME was obtained by the same procedure [93,94] and base hydrolysis by NaOH gave MgMP [174]. The identities of the magnesium porphyrins were verified by thin layer chromatography and electronic extinction coefficients [81].

Sperm-whale metmyoglobin was purchased from Koch-Light Laboratories Ltd. Mb was prepared by removing the heme group of metmyoglobin using 2-butanone [175]. Hb was prepared

from sheep and ox hemoglobin [176-178] and used within 10 days of preparation. Separation of α_2 and β_2 chains of Hb using PMB was based on the methods of Bucci and Fronticelli [179] and Waterman and Yonetani [180]. A fresh solution of hemoglobin was prepared from whole blood. Sodium dithionite was added to this hemoglobin solution and any excess sodium dithionite was removed by passage through a Sephadex G-25 column. CO was bubbled through the solution until the characteristic peaks at 540, 569 and 419 nm were observed (Figure 3.3). Then PMB was added to the CO-FePP-Hb solution and the pH immediately adjusted to 6. PMB was prepared from p-tolylmercuric chloride and potassium permanganate [181], and purified using the method of Boyer [182]. The resulting solution was left overnight and then dialysed exhaustively against a pH = 6 buffer for 12 hours. The chains were separated using a 3 x 10 cm CM32 column by a pH gradient. Each fraction of the elution from the column was determined spectroscopically at 540 nm and two main fractions, α_2 and β_2 chains were obtained (Figure 3.4). The -SH groups were regenerated by adding 300 times molar excess of β-mercaptoethanol [183] or 50 times molar excess of cysteine. After cooling for three hours in an ice bath, the mixture was loaded onto a CM32 column equilibrated with a pH = 7 buffer. The protein band was concentrated and dialysed several times against distilled water. The apo-β_2 and apo-α_2 chains were prepared by the same method as for Mb. The yield for the apo-β_2 chains was very low because of substantial denaturation. The yield for the apo-α_2 chains was slightly better but generally a high phosphate concentration causes rapid denaturation.

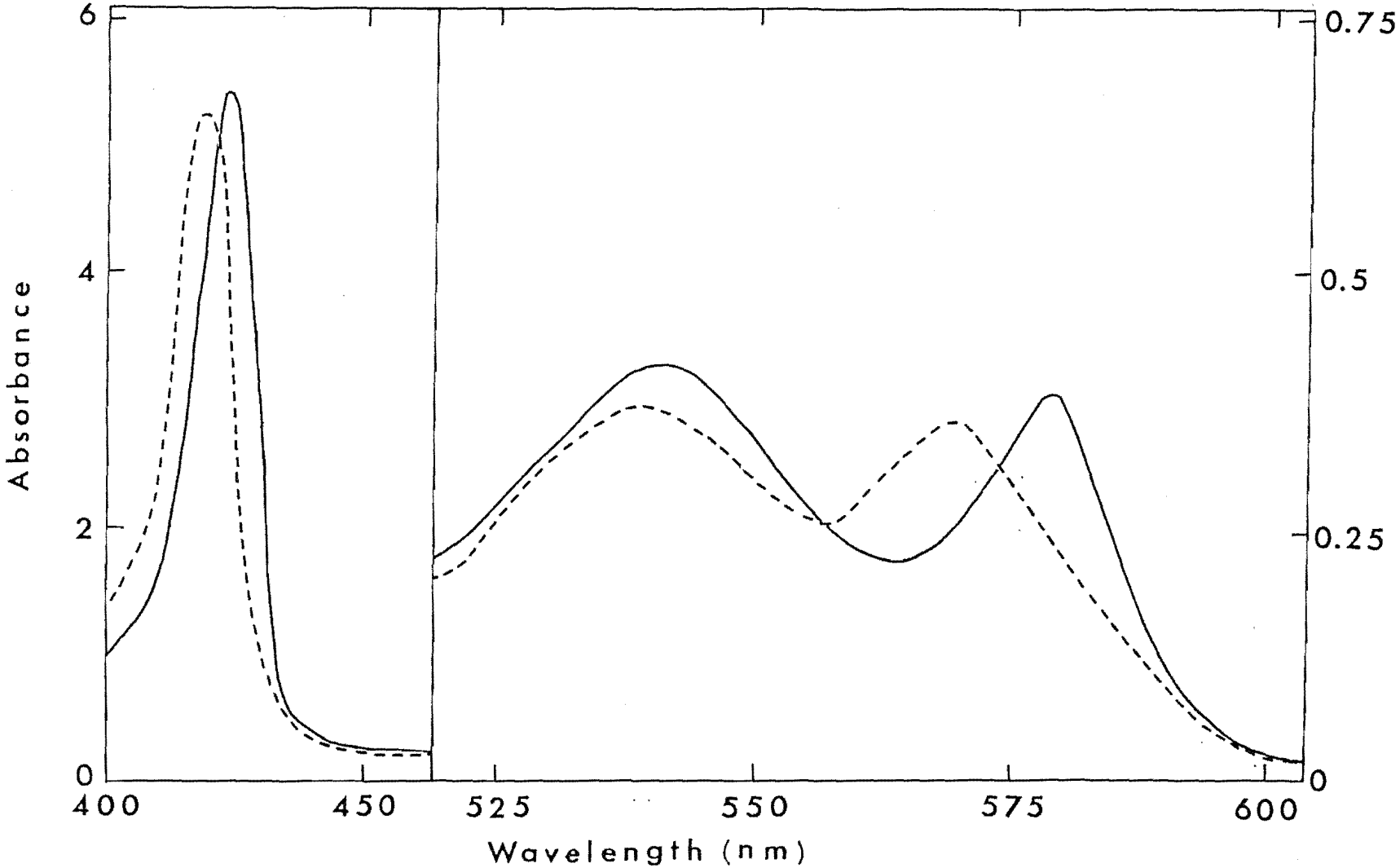

Figure 3.3 : Electronic absorption spectra of CO-FePP-Hb [---] and CO-FePP-Mb [____] in 10 mM phosphate buffer of pH = 7.0

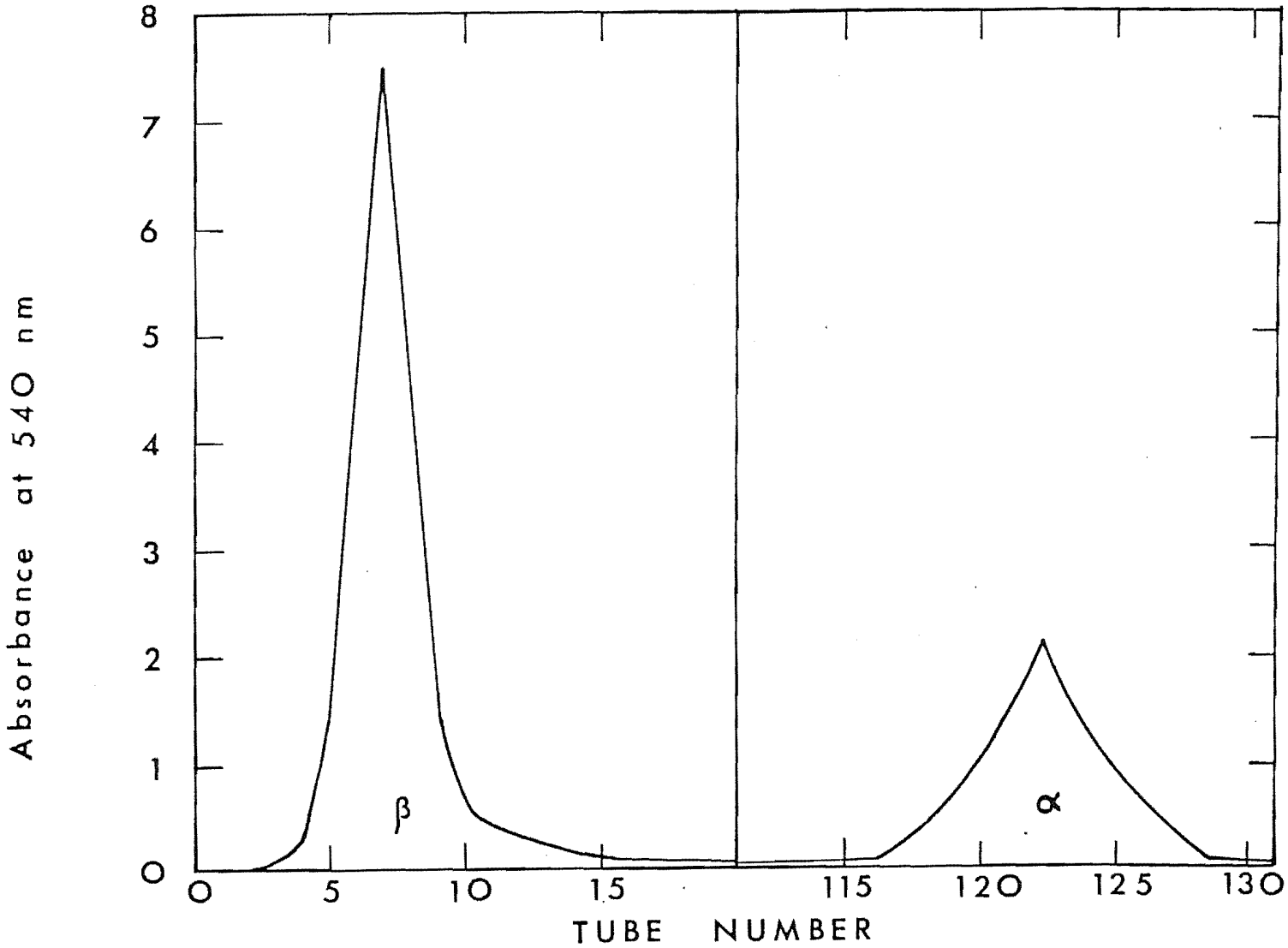

Figure 3.4 : Separation of α_2 and β_2 hemoglobin strands using pH gradient elution

An alternative method of obtaining α_2 and β_2 chains of Hb using urea and a phosphate gradient was also attempted. The globin was prepared by adding 20 times excess 1% HCl in acetone and 0.2 ml/100 ml of mercaptomethanol to the hemoglobin solution. The mixture was then centrifuged at 3,000 rpm and the liquid was carefully decanted. The globin was washed twice with acetone-mercaptomethanol solution and dried by blowing nitrogen across it. The elutant was prepared by adding 4 ml of mercaptomethanol to 480 g ℓ^{-1} of urea (8M). Then 0.665 g and 1.34 g of $Na_2HPO_4.2H_2O$ were added to 750 ml and 250 ml of the urea-mercaptomethanol solution respectively. The pH of both urea-mercaptomethanol solutions were then adjusted to 6.86 by adding phosphoric acid. The globin was placed on a 1.5 x 16 cm CM32 column of pH = 7 and separated by the phosphate gradient. Two main bands were observed in the column and the maximum amount of Hb for each separation was 100 mg. The main bands were dialysed exhaustively in 10 mM phosphate solution. However, this procedure was not used for further preparations of α_2 and β_2 chains of Hb because urea produces more denaturation than PMB [184].

The purified MgMP, MgDP and MgPP were dissolved in 0.05 M pyridine-water. The pyridine prevents the loss of Mg from the porphyrin ring and disaggregates the Mg porphyrin.

Standard solutions of MgPP in 0.05 M pyridine-water were titrated against standard Mb and Hb at 424 nm and 420 nm respectively in order to determine the stoichiometry of the combination of these species (Figures 3.5 and 3.6). The concentrations of apoprotein used were between 4 and 10μM. The same ratios of MgPP to apoprotein were obtained

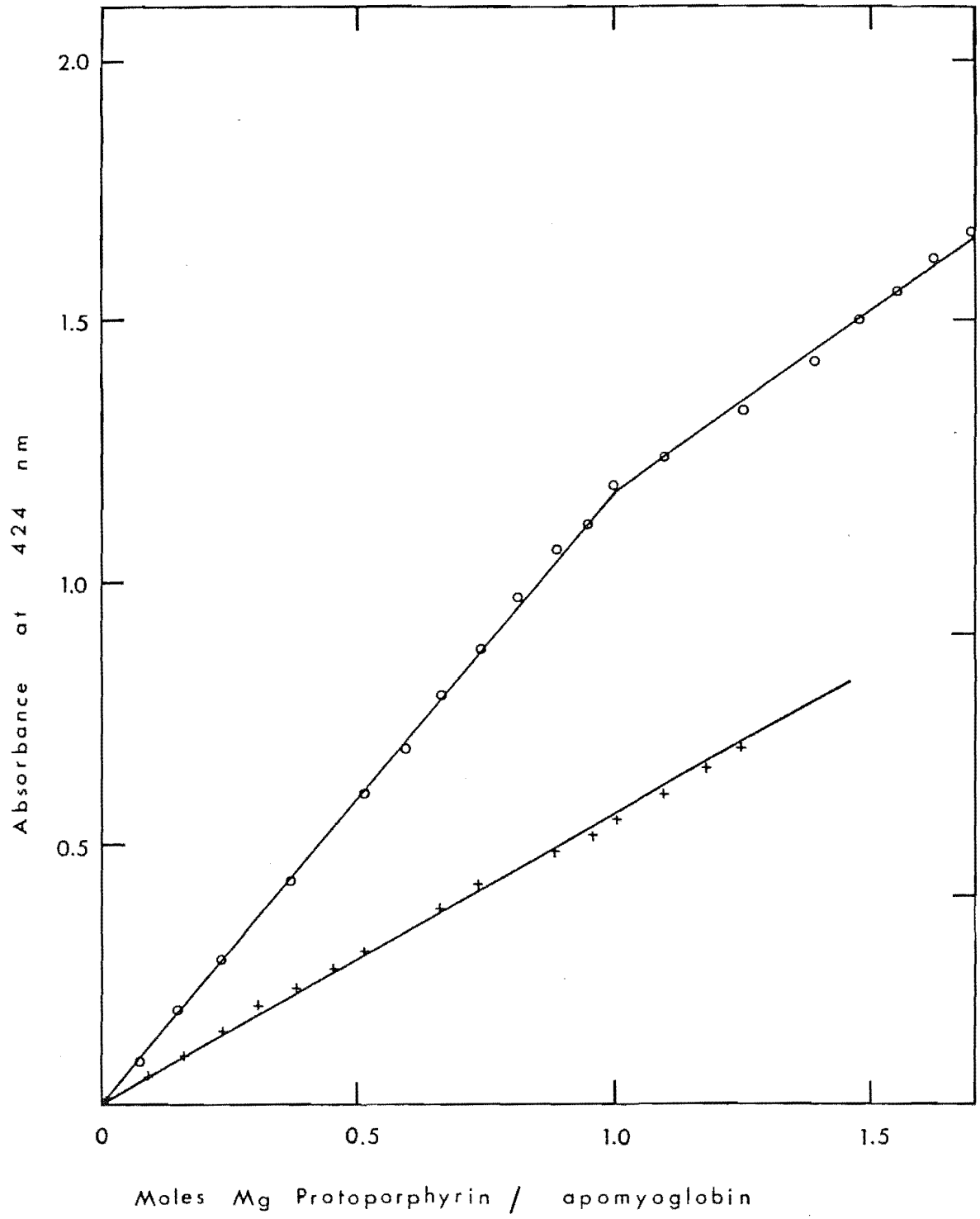

Figure 3.5 : Spectrophotometric titration of apomyoglobin with magnesium protoporphyrin in 0.1 M phosphate buffer of pH = 7.0 (with (o) and without (+) apomyoglobin)

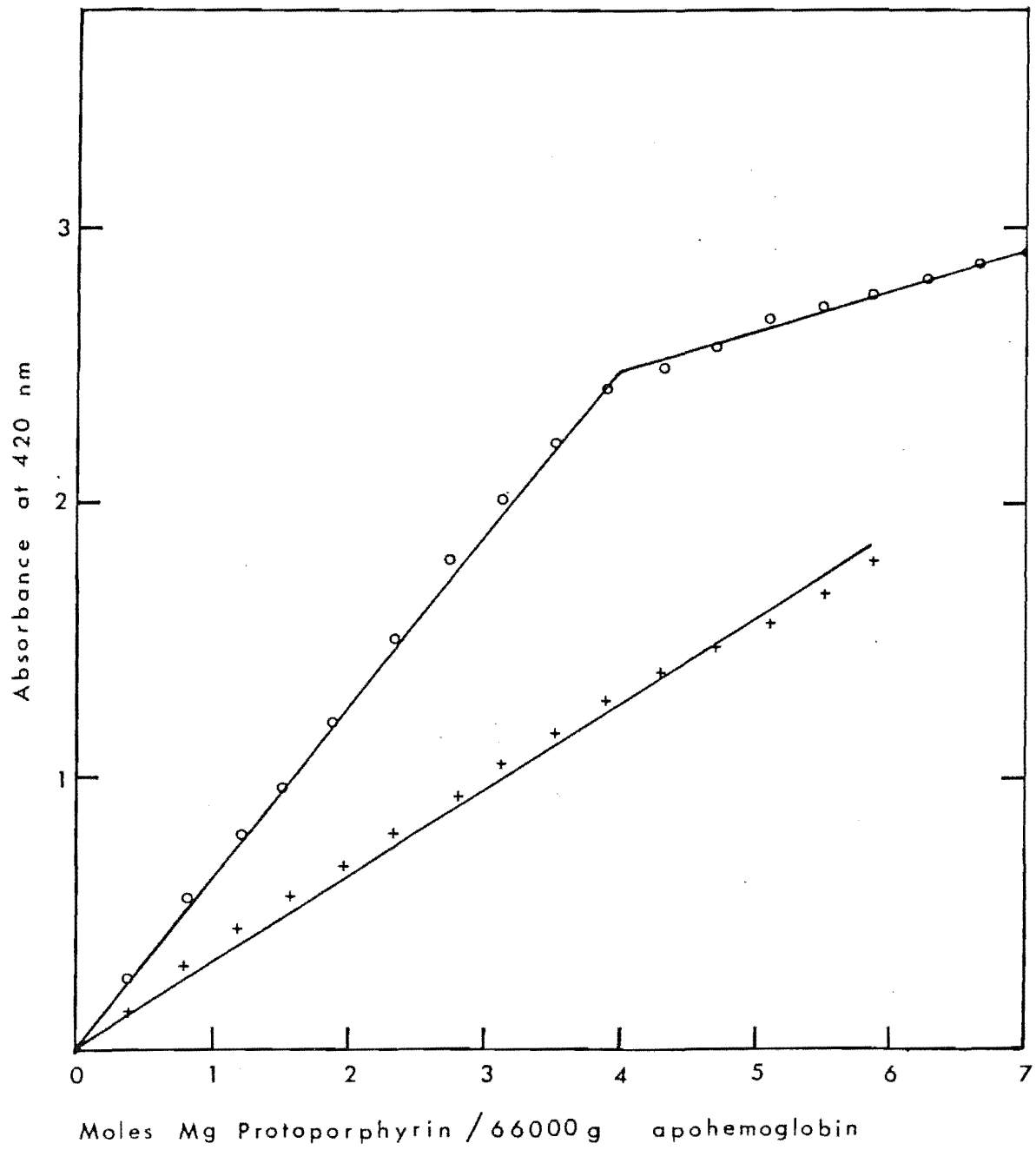

Figure 3.6 : Spectrophotometric titration of apohemoglobin with magnesium protoporphyrin in 0.1 M phosphate buffer of pH = 7.0 (with (o) and without (+) apohemoglobin)

when equal volumes of the apoprotein were added to equal volumes of increasing MgPP concentrations. This second method has no dilution effect and all the absorbance values lie on straight lines.

Reconstitution of Mg porphyrin and apoprotein was carried out by two different methods:-

(a) Mg porphyrin dissolved in methanol-water, was passed through a Sephadex G-25 column which was equilibrated with a buffer of pH = 7. The column was then washed with the buffer until the effluent was free from methanol. The presence of methanol in the effluent can be easily detected by gas chromatography. Usually the amount of buffer solution required to wash the column free of methanol is 15 times the volume of methanol used. A solution of the apoprotein was then passed through the column to give reconstitution as the apoprotein flowed over the Mg porphyrin. The reconstituted complex was then further purified as described for method (b).

(b) The concentrations of Hb and Mb were determined by the extinction coefficients of 16.2 mM cm^{-1} [180] and 15.8 mM cm^{-1} [185] at 280 nm respectively. A two-fold excess of standard Mg porphyrin in 0.05 M pyridine-water was added to apoprotein with gentle stirring. Within half an hour, the mixture was placed on a 15 x 2.5 cm Sephadex G-25 column, which was previously equilibrated with 10 mM phosphate solution, to remove the pyridine and excess Mg porphyrin. The reconstituted complex was then passed through a CM32 column of pH = 7 to remove any Mg porphyrin that was loosely bound to the surface of the protein. The Mg porphyrin-globin complex was eluted as a clean pink band

with 20 mM phosphate solution. The reconstituted material was further dialysed against 10 mM phosphate (pH = 6.86). In order to be sure that Mg porphyrin was bound in the heme pocket, ether was added to the solution of reconstituted complex and shaken. Mg porphyrin dissolves preferentially in the ether layer of an ether-water mixture. For the reconstituted complex, the pink colour remained entirely in the aqueous layer. The formation of the tetramer unit was checked by the flow rate method [186]. Sephadex G-(50-80) and Sephadex G-(75-120) were used for purification of the reconstituted MgDP-Mb and MgDP-Hb respectively. Using Sephadex G-(75-120) for MgDP-Hb which has the capability to exclude proteins of molecular weight greater than 50,000 daltons, it was not necessary to check the formation of the tetramer unit by the flow rate method. Further evidence that only one reconstituted product is obtained in all cases, has been obtained by using the procedure of Srivastava [164]. The Mg porphyrin-globin complex was passed through a long Sephadex G-25 column followed by a long CM32 column. Each fraction was identified by absorption spectroscopy which strongly suggests the formation of only one protein complex. All precipitate formed was removed either by filtering or centrifuging.

Pc was purchased from Tokyo Chemical Industry. MgPc was prepared by heating Mg perchlorate and Pc in pyridine [93,94]. However attempts to reconstitute MgPc with Mb and Hb were unsuccessful.

Electronic absorption spectra were recorded on a Varian Superscan 3 UV-visible spectrophotometer. Analytical grade pyridine and benzene were purchased from British Drug

Houses Ltd and stored in the dark at 0°C over 4Å molecular sieves under nitrogen. Other reagents used were of analytical grade.

ORD and CD measurements were recorded on a Jasco ORD UV-5 spectrophotometer. Reagents were kept away from strong light and all apparatus was covered by aluminium foil. All the preparative work was carried out at temperatures between 0°C and 4°C.

Detection of dioxygen was by Varian Aerograph 90 D-3 thermal conductivity detector using helium as carrier gas, molecular sieve 5Å as column, pressure of 96 psi, injector, detector and oven temperatures of 193°C, 240°C and 72°C respectively, filament current attenuator of 16, recorder range 1 mV, recorder speed 300 mm hr^{-1} and sample size of 50 µℓ.

All measurements were recorded at room temperature, unless mentioned otherwise.

The PMB obtained had a melting point over 300°C and not 273°C as reported in the earlier literature [187]. It is very corrosive and should not come into contact with the skin.

3.3 RESULTS

3.3.1 Electronic Spectra of MgPP-Mb, MgPP-Hb, MgMP-Mb, MgMP-Hb, MgDP-Mb and MgDP-Hb Species

The absorption maxima wavelengths of the α_2, β_2 and $\alpha_2\beta_2$ chains of MgPP-Hb were similar to those of MgPP in organic solvents like ether except for the Soret band which is red-shifted by 3 nm (Figure 3.7). The relative intensities of the Q_o and Q_1 transitions are also changed (Table 3.1).

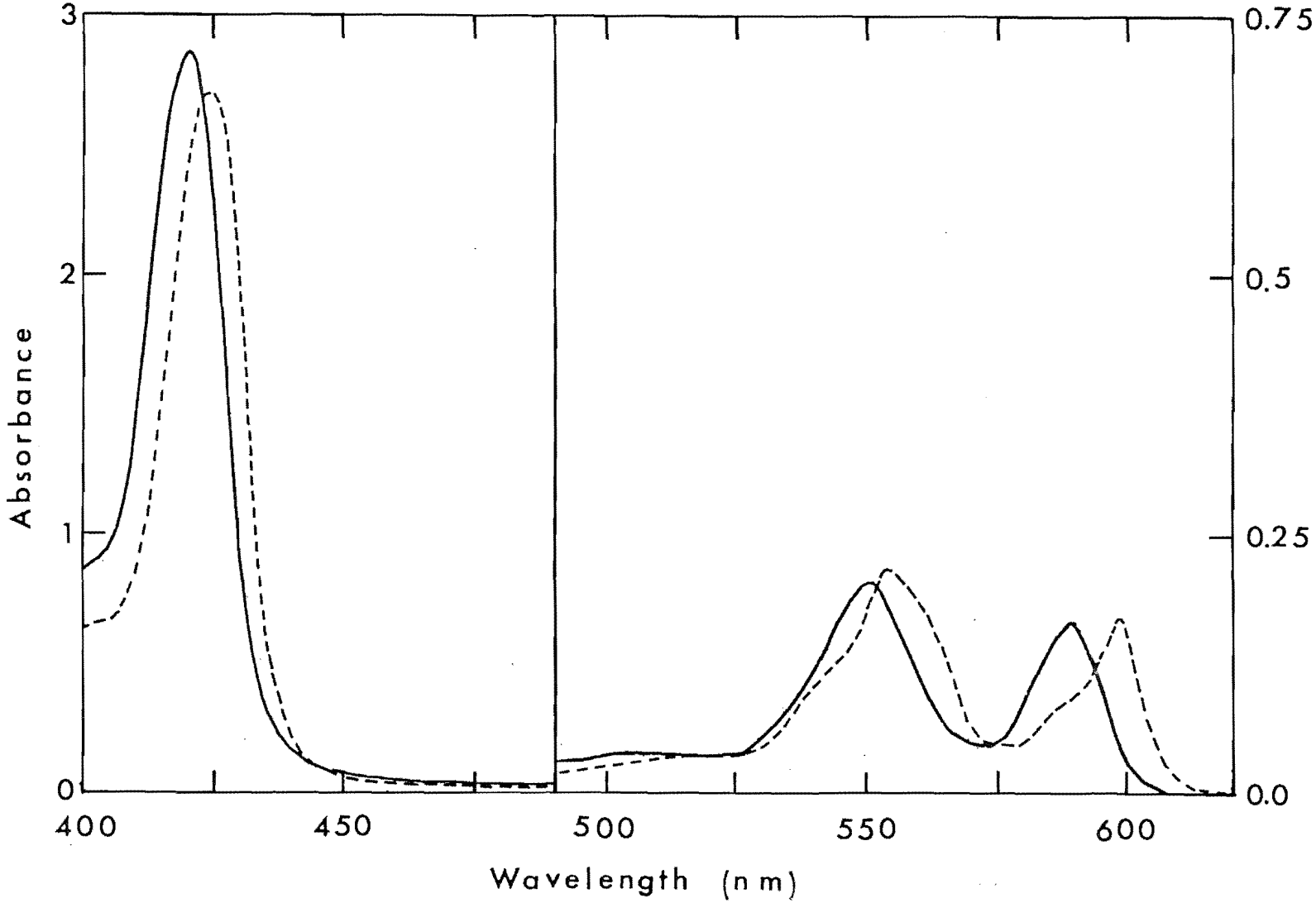

Figure 3.7 : Electronic absorption spectra of MgPP-Hb [——] and MgPP-Mb [---] in 0.02 M phosphate buffer of pH = 7.0

Table 3.1 Comparison of the Electronic and Circular Dichroism Data for the Various Metal Porphyrin Complexes

	Electronic Bands (nm)						Circular Dichroism Bands (nm)		
	Soret		Q_1		Q_o		Soret	Q_1	Q_o
Compound	λ max	A[a]	λ max	A	λ max	A	λ max	λ max	λ max
MgPP in ether	417	1.000	550	0.060	589	0.060			
MgPP - Hb	420	1.000	550	0.070	589	0.060	425	548,558	589
MgPP - Mb	424	1.000	553 560(sh) 545(sh)	0.080 0.064 0.044	598[b] 590(sh)	0.065 0.039	420	538-552,560	600
MgMP in ether	409	1.000	544	0.041	581	0.041			
MgMP - Hb	408	1.000	543	0.053	580.5	0.040	412	542,549	576
MgMP - Mb	409	1.000	542 549(sh) 533(sh)	0.063 0.050 0.029	585[b] 574	0.040 0.025	408	542,550	574,585
MgDP in ether	405	1.000	542	0.040	578.5	0.03			
MgDP - Hb	406	1.000	541.5	0.049	578	0.03	408	533,547	574
MgDP - Mb	408	1.000	542 548(sh) 533(sh)	0.061 0.049 0.040	582[b] 572(sh)	0.027 0.023	406	533,549	576
CO-FePP-Mb	423	1.000	542	0.074	579	0.067	420	527,552	575
CO-FePP-Hb	419	1.000	540	0.070	569	0.069	420	520,540	560,583

Table 3.1 cont...

Table 3.1 continued

	Electronic Bands (nm)						Circular Dichroism Bands (nm)		
	Soret		Q_1		Q_o		Soret	Q_1	Q_o
Compound	λ max	A[a]	λ max	A	λ max	A	λ max	λ max	λ max
CO-Ru(II)MP-Mb*	398.5		519(br)		554 546.5				
Nicotinate-FePP-Mb*	424		535 528		566 554				

a = absorbance data normalised to 1.000 relative to most intense transition

sh = shoulder

b = major component

br = broad.

* All data in Table recorded in this work except for CO-Ru(II)MP-Mb [164,165] and Nicotinate-FePP-Mb [163]. Values for CO-FePP-Mb and CO-FePP-Hb are similar to those reported by Bolard and Garnier [205] and Li and Johnson [206] respectively.

The spectrum of MgPP-Mb was shifted towards the red region relative to MgPP in ether and MgPP-Hb. The same magnitude of shift in the electronic spectrum for MgPP-Hb compared with MgPP-Mb is observed for CO-FePP-Hb and CO-FePP-Mb (Figure 3.3). Addition of pyridine, sodium dithionite, fluoride, azide, dinitrogen and dioxygen did not affect the spectrum. However, addition of a high concentration of NaCN shifted the spectrum to the shorter wavelength region and small bubbles of gas were observed (Figure 3.8). A small amount of gas was also liberated when freshly prepared MgPP-Mb was illuminated for a short period. Determination of dioxygen content of the gas using the thermal conductivity detector method showed very little increase in the height of the dioxygen peak (Figure 3.9).

The absorption maxima wavelengths of MgMP-Hb and MgDP-Hb are close to those of MgMP and MgDP in ether respectively. However, the relative intensities of the Q_1 and Q_o bands are higher in MgDP-Hb and MgMP-Hb. The Q_o transitions for MgDP-Mb and MgMP-Mb are split into bands of unequal intensities and the Q_1 transition is highly unsymmetrical (Figures 3.10 and 3.11) as observed for MgPP-Mb. The position of the major Q_o band of MgDP-Mb at 582 nm is red-shifted with respect to the Q_o band of MgDP-Hb at 578 nm; while the position of the major Q_o band of MgMP-Mb at 585 nm is red-shifted with respect to the Q_o band of MgMP-Hb at 580.5 nm. This red-shift of 4 nm is significantly smaller than the shift of 9 nm observed for MgPP-Mb relative to MgPP-Hb. The possibility that the extra band at 574 nm for MgMP-Mb arises from MP can be excluded as MP absorbs only at 567 nm and no Soret band was observed in the 395-401 nm region where MP absorbs [92]. Furthermore,

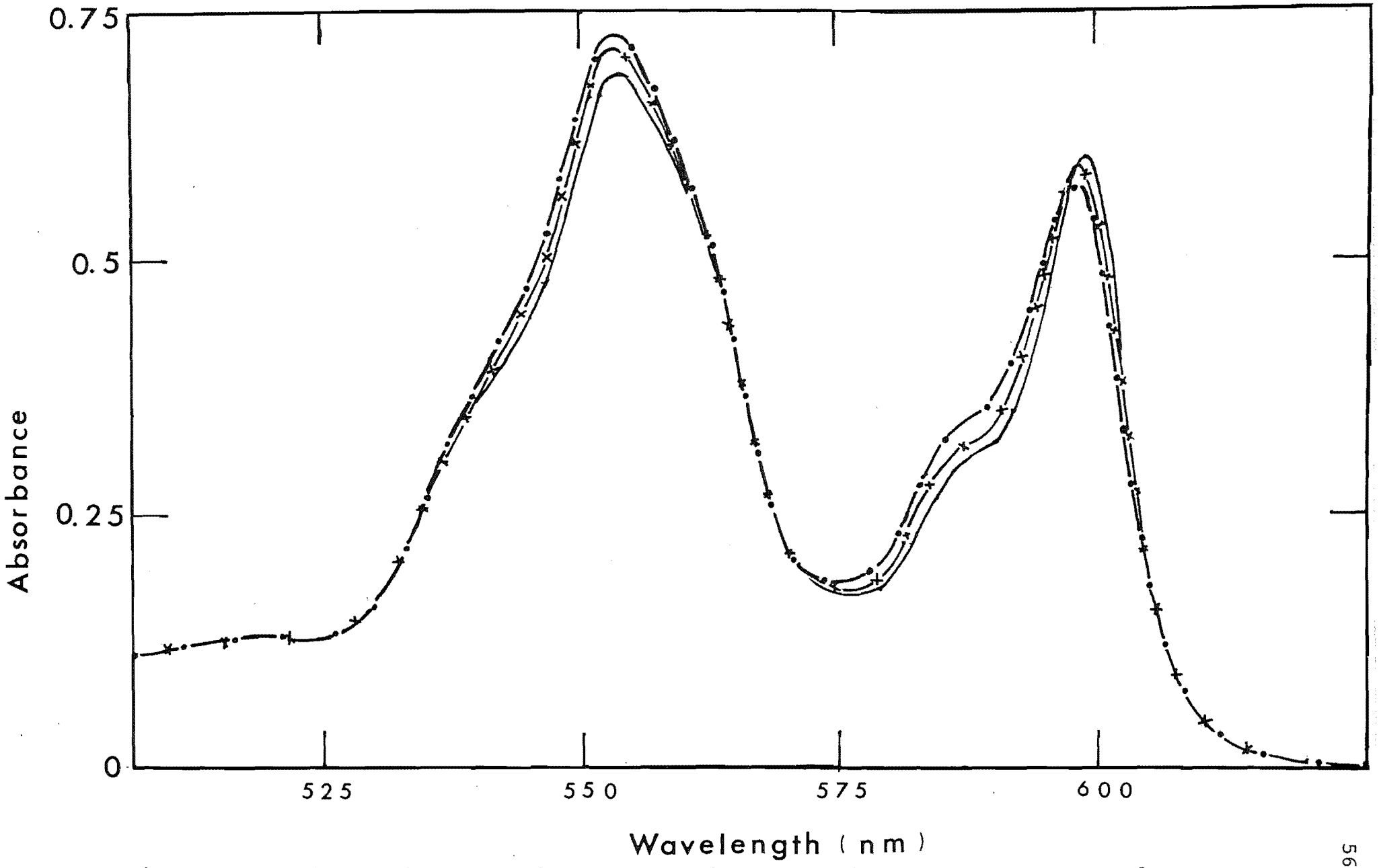

Figure 3.8 : Electronic absorption spectra of MgPP-Mb with NaCN: no NaCN [——]; 0.67 M NaCN [—x—]; 2.67 M NaCN [—·—]

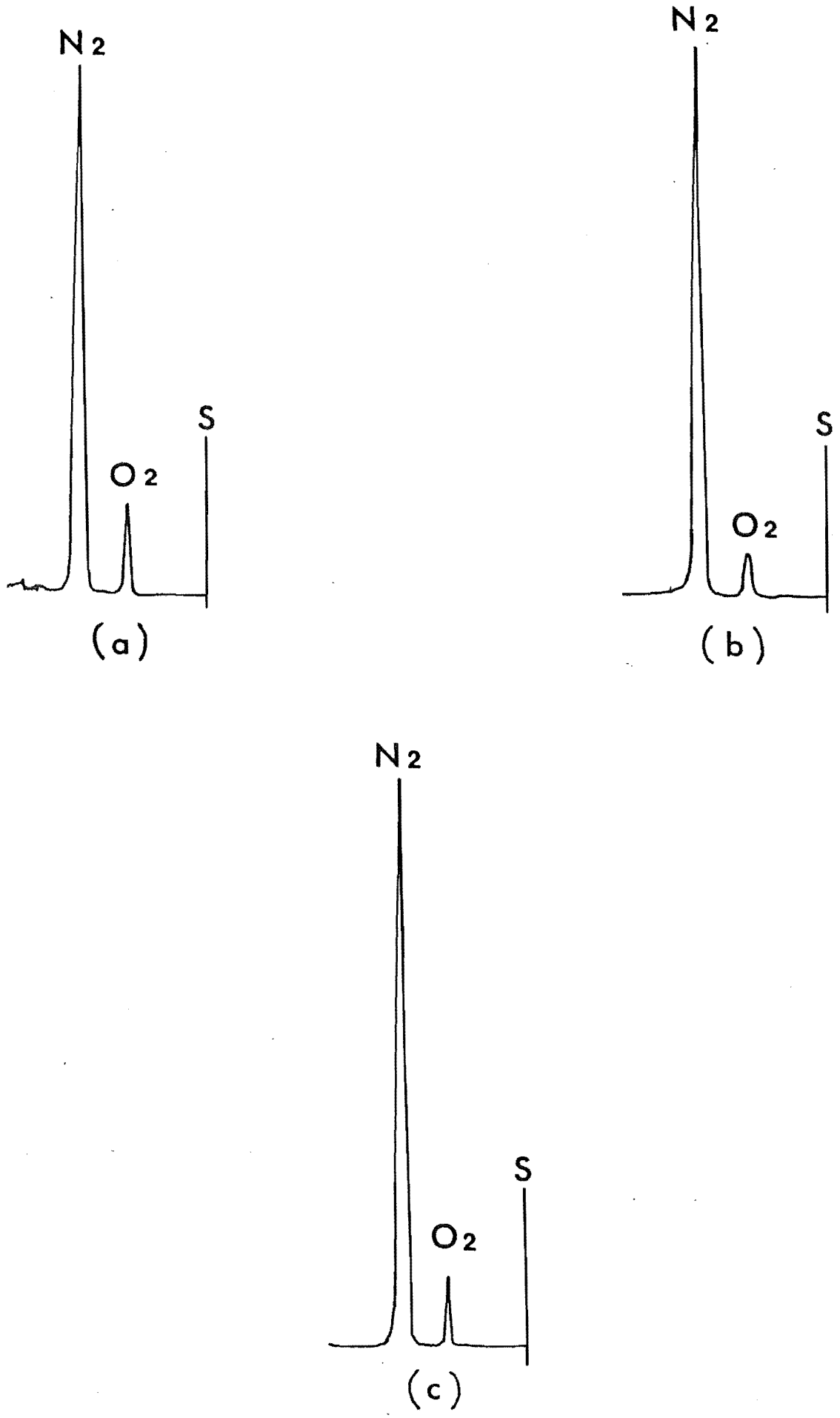

Figure 3.9 : Determination of dioxygen gas using gas chromatography. Intensities of (a) 80% nitrogen, 20% oxygen and (b) 95% nitrogen, 5% oxygen were used as standards. (c) The relative amount of dioxygen gas in a mixture of MgPP-Mb/NaCN

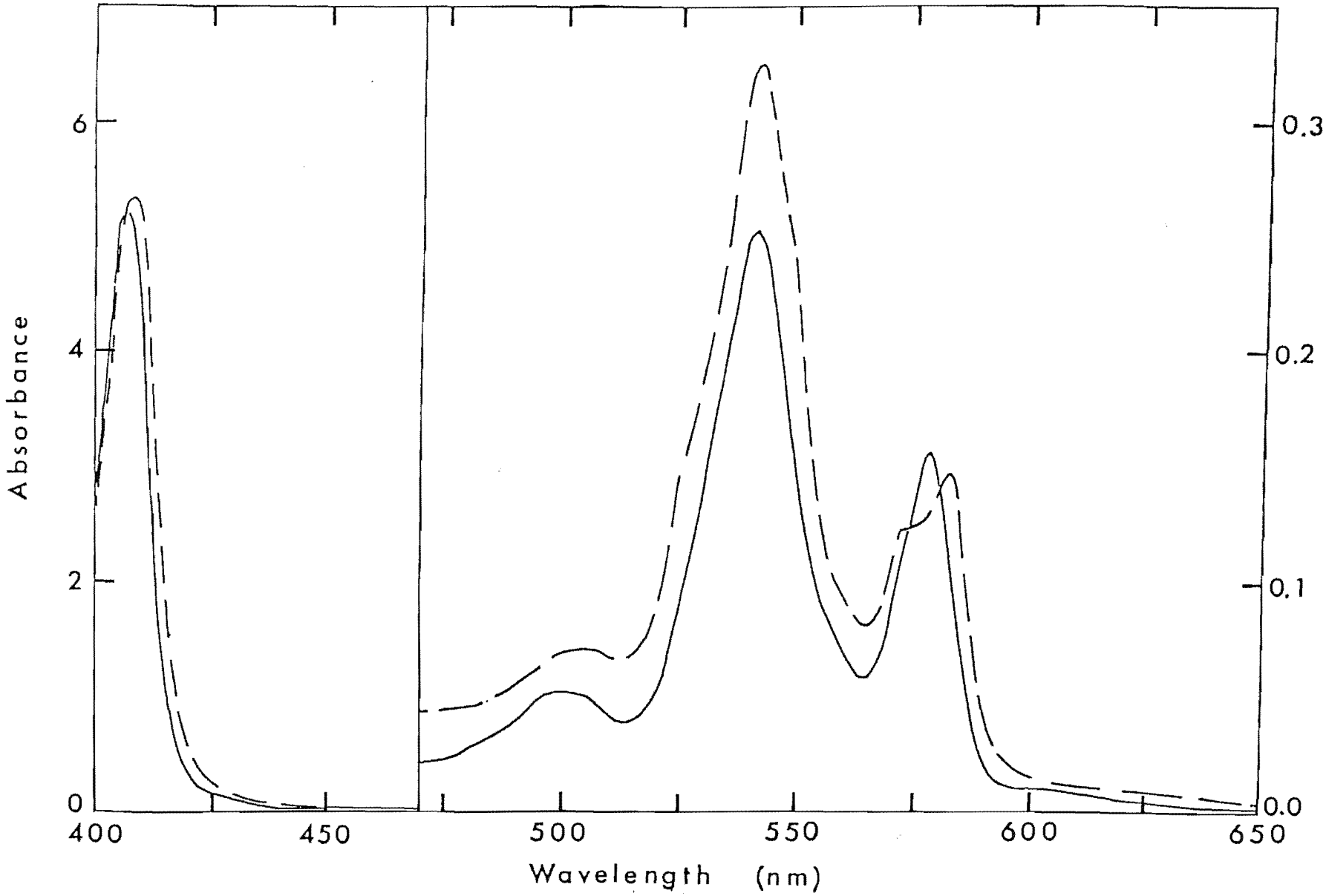

Figure 3.10 : Electronic absorption spectra of MgDP-Hb [——] and MgDP-Mb [---] in 0.02 M phosphate buffer of pH = 7.0

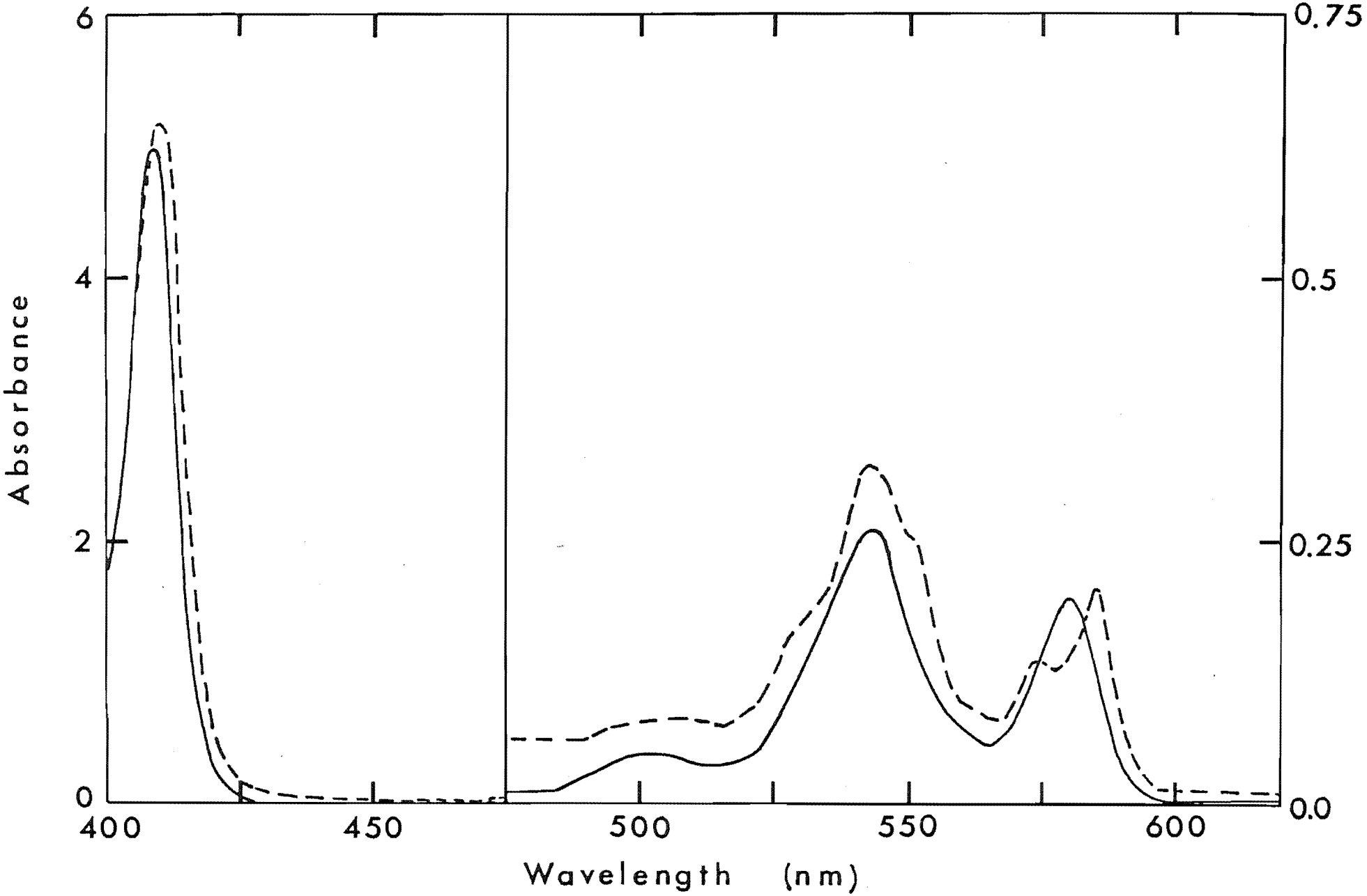

Figure 3.11 : Electronic absorption spectra of MgMP-Hb [——] and MgMP-Mb [---] in 0.02 M phosphate buffer of pH = 7.0

deliberate addition of MP to MgMP and reconstitution with Hb did not produce the 574 nm band. This extra band is likely to correspond to the shoulder observed for the Q_o transition of MgPP-Mb.

Temperature and pH effects were not studied in detail. However, it was noted that at about 5°C the intensities of the visible absorptions of the MgPP-Mb complex were increased slightly with respect to those at 28°C. For the same species an increase in pH shifted the Q_o band in particular to higher energy.

3.3.2 CD Spectra

MgPP, MgMP and MgDP do not show any definite CD spectra in pyridine, ether or benzene. However, the reconstituted products show dominant Cotton effects for all the absorption bands (Table 3.1).

The Q_o transitions of MgPP-Hb and MgDP-Hb have single bands while the Q_1 transitions are split into two bands (Figures 3.12 and 3.13). The Soret bands of MgPP-Hb and MgDP-Hb are split unsymmetrically into a dominant positive band and a small negative band. The Soret bands of MgPP-Hb and α_2, β_2 chains show small but significant differences in the positions of the maximum absorption of the positive peaks. The positions of these peaks for MgPP-Hb and α_2, β_2 chains are at 425 nm, 427 nm and 423 nm respectively. The Q_o and Q_1 transitions for MgPP-Mb are shifted by about 11 nm and 2 nm to the red region relative to those for MgPP-Hb respectively (Figure 3.14). However, the Soret band is shifted to the blue region and there is no negative region. The Q_o and Q_1 transitions (at about 548 nm) for MgDP-Mb are shifted by

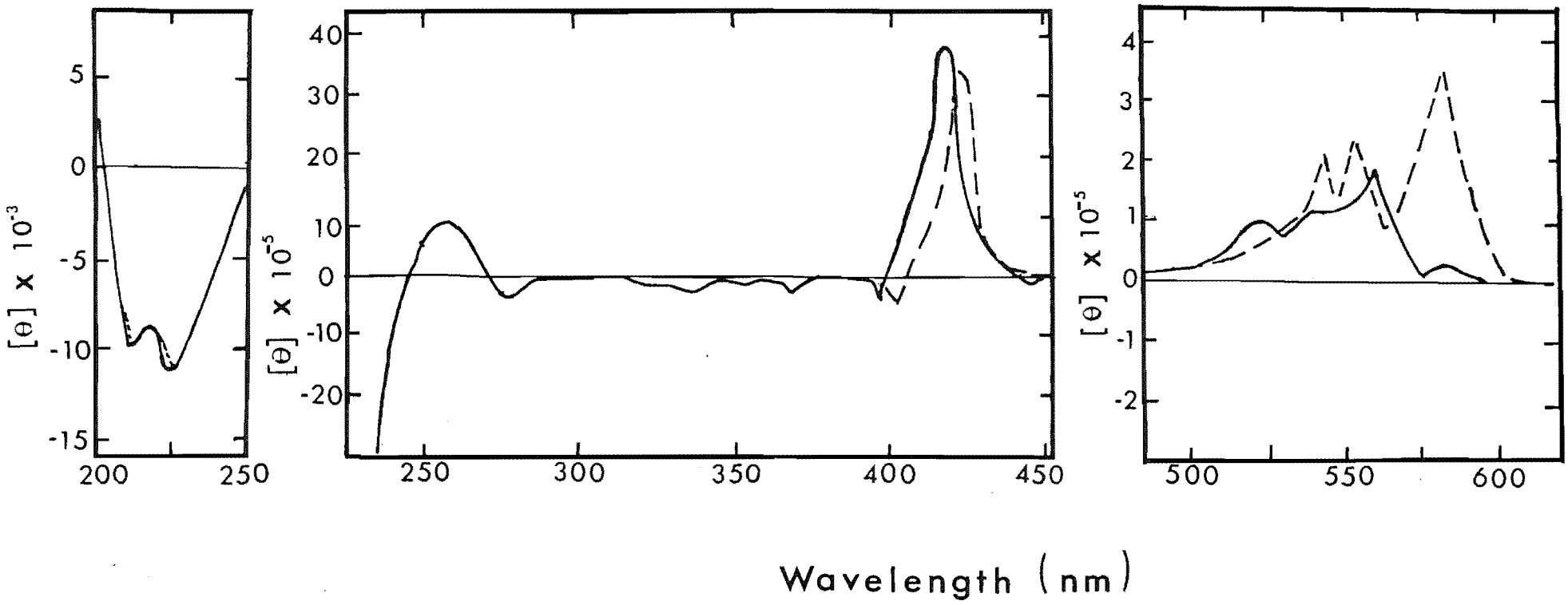

Figure 3.12 : Circular dichroism spectra of MgPP-Hb [---] and CO-FePP-Hb [——] under 10 mM phosphate buffer redrawn to show main bands. Solution for 500 to 200 nm was diluted 10 times relative to the region between 500 and 700 nm

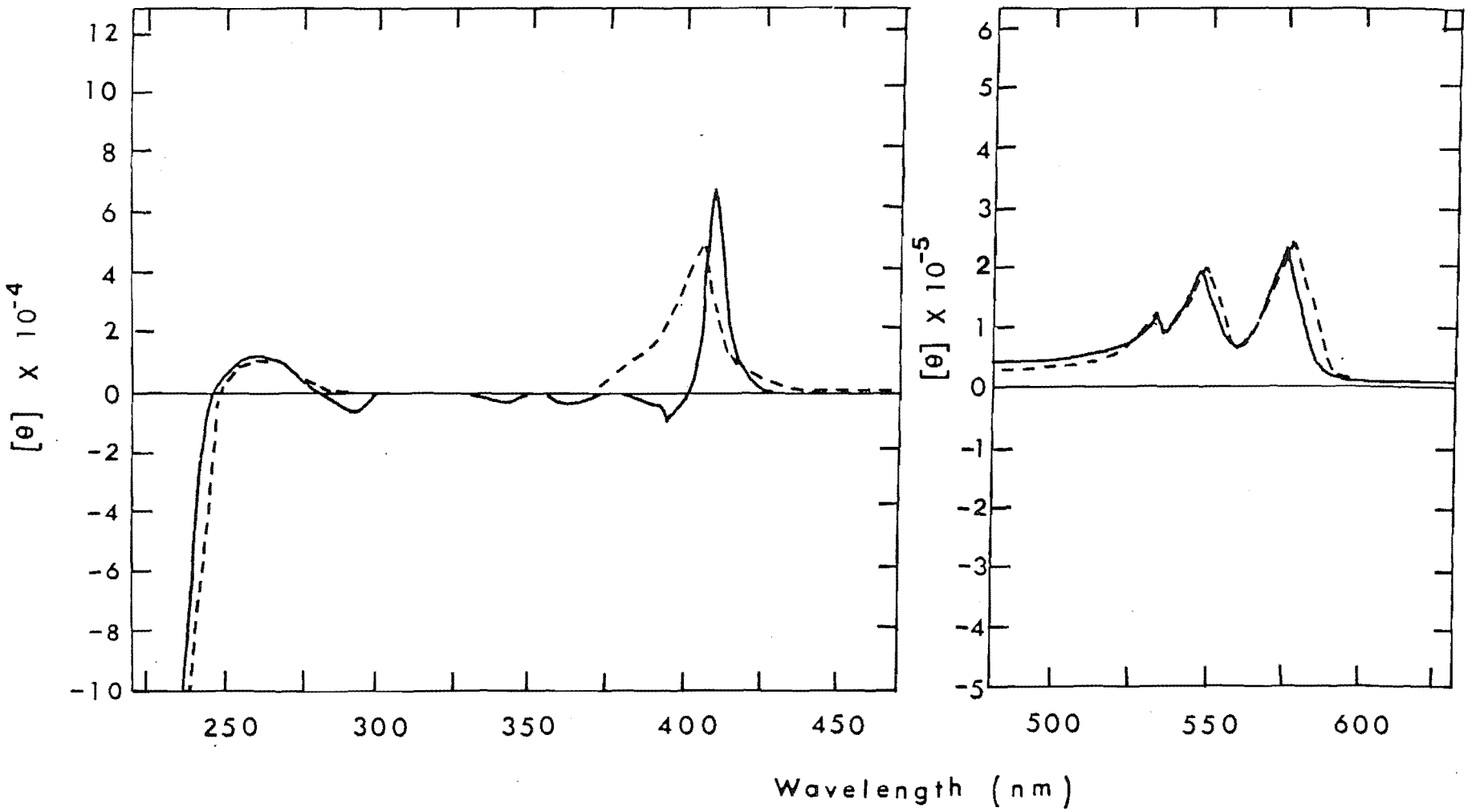

Figure 3.13 : Circular dichroism spectra of MgDP-Hb [——] and MgDP-Mb [---] under 10 mM phosphate buffer redrawn to show main bands. Solution for 450 to 250 nm was diluted 20 times relative to the region between 500 and 620 nm

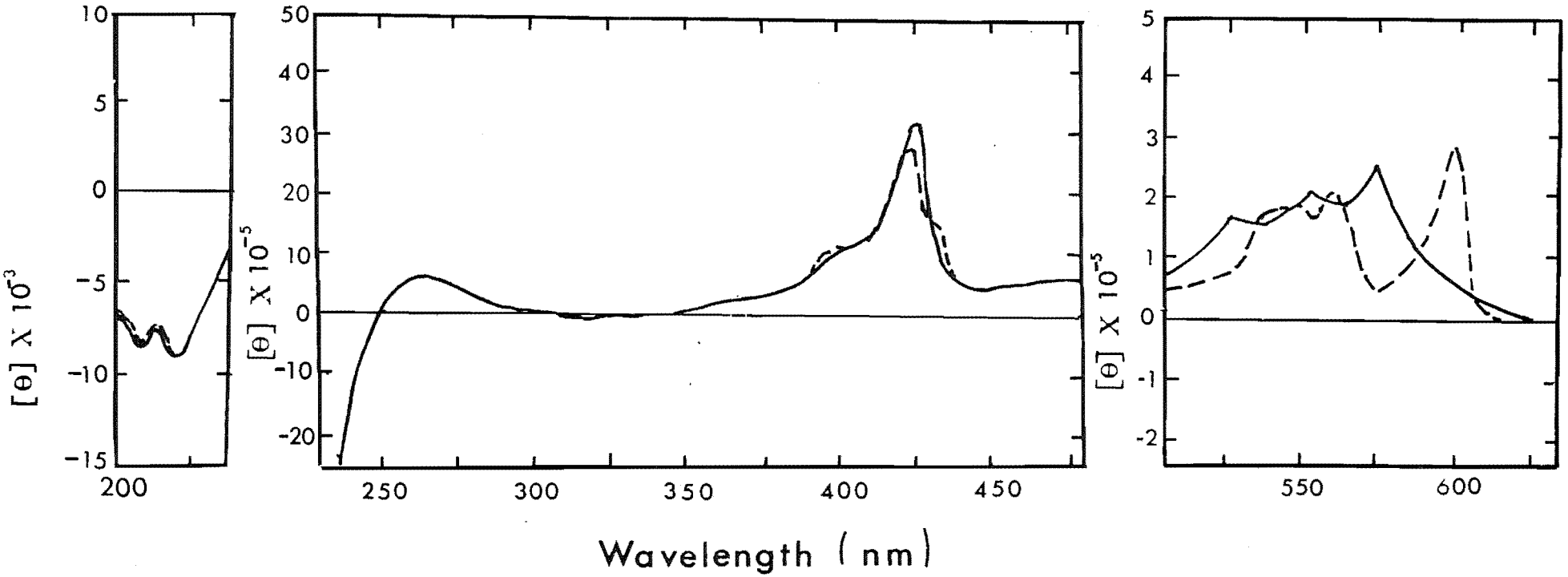

Figure 3.14 : Circular dichroism spectra of MgPP-Mb [---] and CO-FePP-Mb [——] under 10 mM phosphate buffer redrawn to show main bands. Solution for 500 to 200 nm was diluted 10 times relative to the region between 500 and 700 nm

about 2 nm to the red region for both transitions relative to those for MgDP-Hb (Figure 3.13). The band at 533 nm remains the same for both MgDP-Mb and MgDP-Hb. However, the Soret band for MgDP-Mb is blue-shifted by 2 nm and there is no negative region.

The CD spectra of CO-FePP-Mb and CO-FePP-Hb were also determined for comparison with corresponding spectra of MgPP species (Figures 3.12 and 3.14). The shapes of the bands of MgMP-Hb (Figure 3.15) are essentially the same as those of MgPP-Hb. The most significant difference between MgPP-Mb and MgMP-Mb is in the Q_o transition where the Q_o transition of MgMP-Mb exhibits two bands. The Soret band of MgMP-Mb is also shifted to the blue region relative to the Soret band of MgMP-Hb.

3.3.3 ORD Spectra

MgPP-Hb has a complex ORD curve with peaks at 600, 564, 552 and 430 nm and troughs at 580, 555, 544 and 420 nm. MgPP-Mb also has the same complex curve with peaks at 606, 567, 554 and 425 nm and troughs at 597, 558, 548 and 416 nm (Figure 3.16).

MgMP-Hb has peaks at 584, 553, 546 and 417 nm and troughs at 570, 549, 538 and 407 nm. MgMP-Mb has peaks at 590, 579, 556 and 412 nm. The troughs are at 582, 572, 544 and 404 nm (Figure 3.17).

MgDP-Hb has peaks at 582, 550, 413 and 396 nm and troughs at 576, 543, 533, 401 and 393 nm. MgDP-Mb has peaks at 586, 554, 534, 410 and troughs at 578, 544, 526 and 400 nm (Figure 3.18).

The maximum peaks of the CD spectra of all these

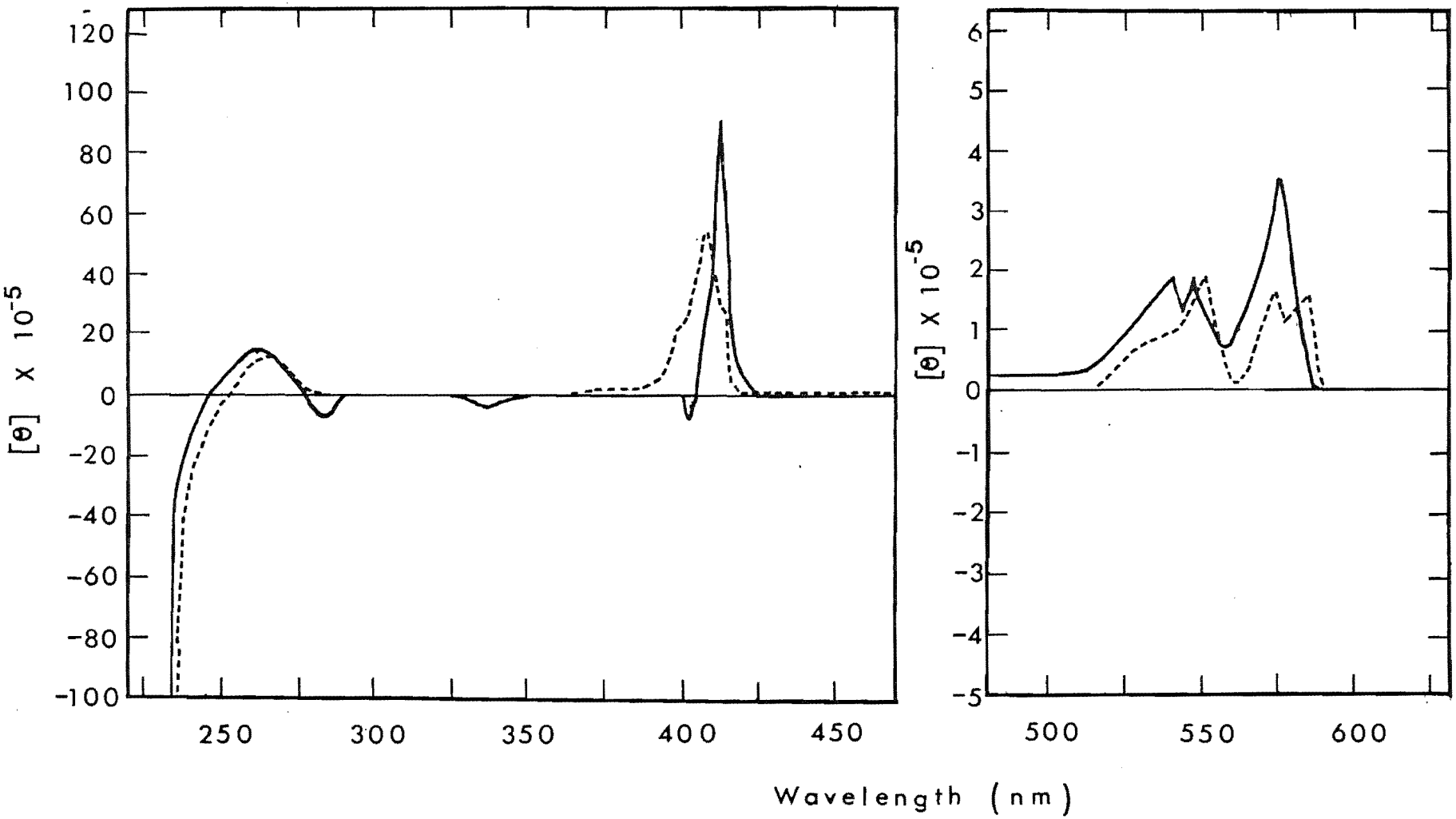

Figure 3.15 : Circular dichroism spectra of MgMP-Mb [---] and MgMP-Hb [——] under 10 mM phosphate buffer redrawn to show main bands. Solution for 500 to 250 nm was diluted 20 times relative to the region between 500 and 620 nm

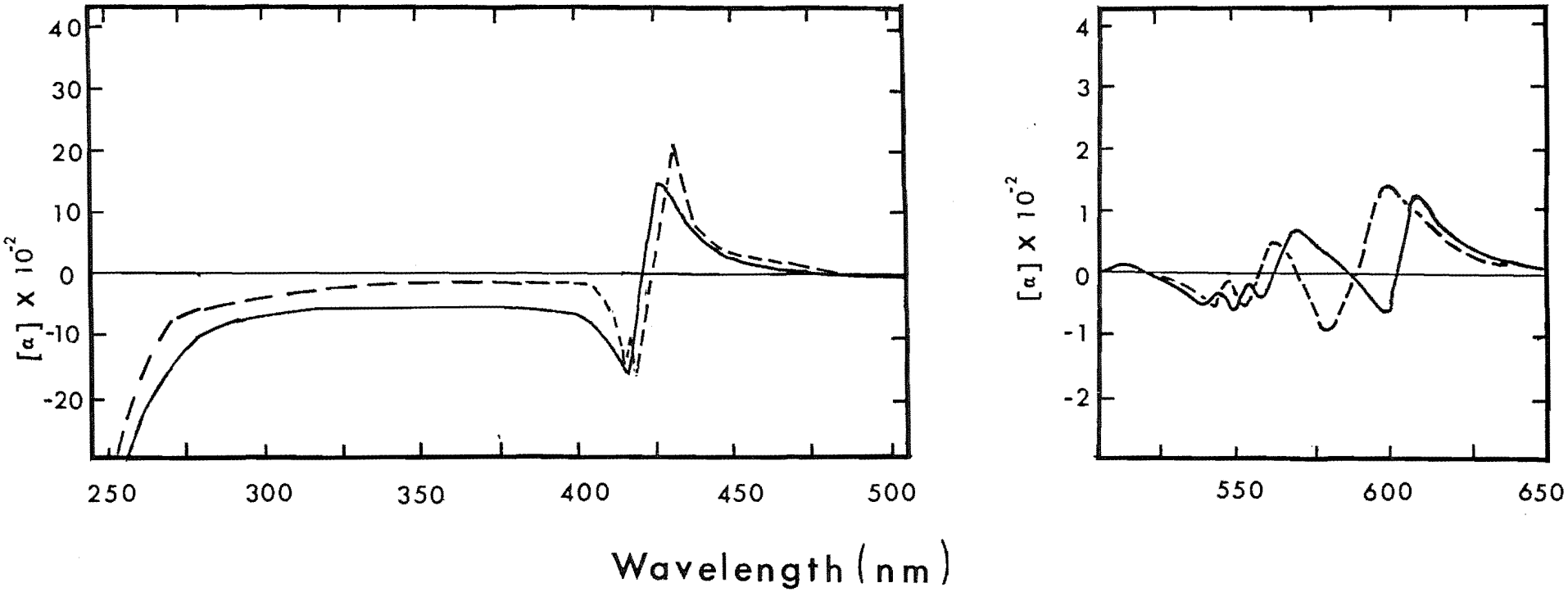

Figure 3.16 : Optical rotatory dispersion of MgPP-Mb [——] and MgPP-Hb [---] under pH = 7 redrawn to show main bands

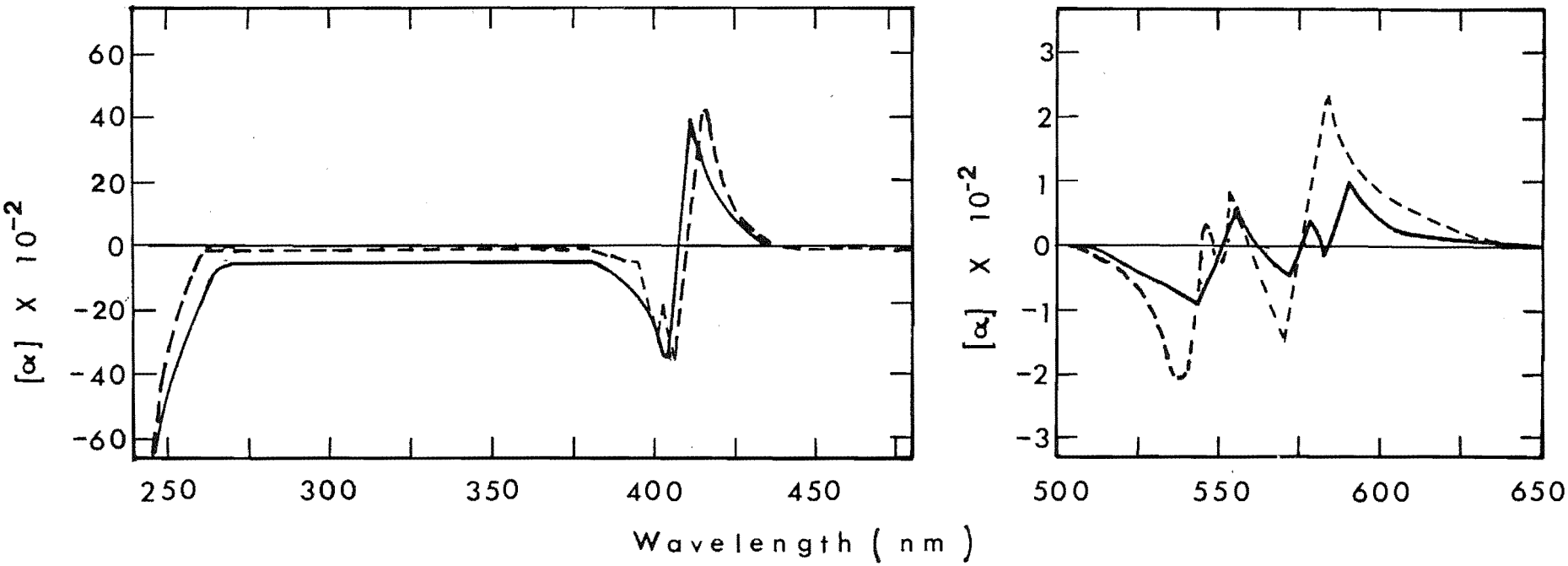

Figure 3.17 : Optical rotatory dispersion of MgMP-Mb [——] and MgMP-Hb [---] under pH = 7 redrawn to show main bands

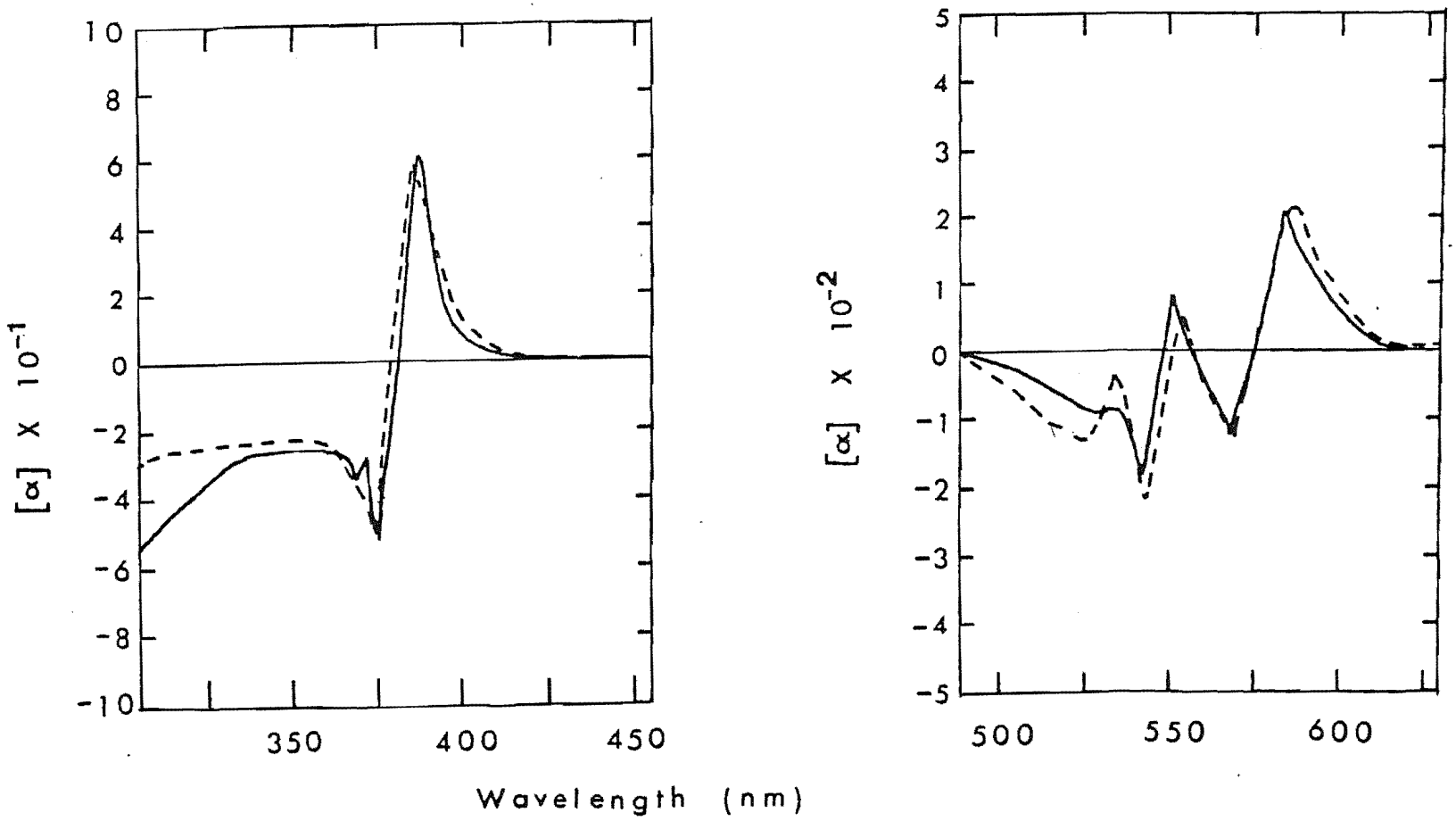

Figure 3.18 : Optical rotatory dispersion of MgDP-Mb [---] and MgDP-Hb [——] under pH = 7 redrawn to show main bands

species correspond very closely to the zero rotation in the corresponding ORD spectra.

3.4 DISCUSSION

3.4.1 General Discussion

The tendency of four-coordinate Mg porphyrin complexes to bind ligands at the axial positions has been highlighted in Chapter 2. Thus when Mg porphyrin is introduced into a protein environment, it is expected to readily form Mg porphyrin-globin complexes, especially as a result of the coordination to a nitrogen donating residue like histidine. The similarities between the general features of the electronic and CD spectra of MgPP-Mb MgMP-Mb and MgDP-Mb, as well as MgPP-Hb, MgMP-Hb and MgDP-Hb show that well-defined 1:1 and 1:4 protein complexes are formed in all cases. Reconstitution of Mg porphyrin with cytochrome also shows that a well-defined 1:1 complex is formed [188]. This contrasts with results for the chlorophyllide-apomyoglobin complexes where three different species with different electronic and CD spectra were obtained [17].

By contrast to the situation for the α_2 and β_2 chains of Fe porphyrin-Hb [189], the visible spectral bands of the isolated α_2 and β_2 chains are at similar positions to those for $\alpha_2\beta_2$ chains of MgPP-Hb. However, for Mg porphyrin-Mb complexes, the electronic spectra show distinctive red-shifts of bands with respect to those for MgPP-Hb. Such distinct red-shifts are also observed in photosynthetic systems when chlorophyll [190,191] or pheophytin [191] is constituted into the apoprotein of

chlorophyll. Consequently, a comparison of the two systems may provide some insight into the possible role of protein environment in producing bathochromic shifts of absorption bands in photosynthetic systems *in vivo*.

3.4.2 Influence of the Protein Environment on the Coordination State of Magnesium Porphyrin

The appearance of multiple band features for the visible Q_o and Q_1 transitions and the red-shift of these bands for both Mg porphyrin-Mb and -Hb is the central result of this section. These details of the visible spectra are remarkably similar to those observed for two other quite different types of heme protein complex; nitrogenous base compounds of iron myoglobin [163] (Figure 3.19) and the carbon monoxide complex of ruthenium (II) myoglobin [164,165] (Figure 3.20). In all three cases definite splitting of the Q_o bands occurs with the higher energy component being of lower intensity, while the Q_1 band varies from being generally broad in the case for Ru(II) complex, to split with a shoulder on the low energy side in the other two cases. The Mg complexes also have a shoulder on the high energy of the Q_1 band. This is not observed for the room temperature spectra of the Ru(II) and Fe-Mb complexes, although a shoulder of this type does appear at low temperatures for the myoglobin-nicotinate complex [163].

This 4-banded spectrum was observed only for myoglobin and not for hemoglobin [192]. The splitting of the transitions could arise from the formation of more than one species which was considered but rejected as a possibility for the myoglobin-nitrogenous base derivatives

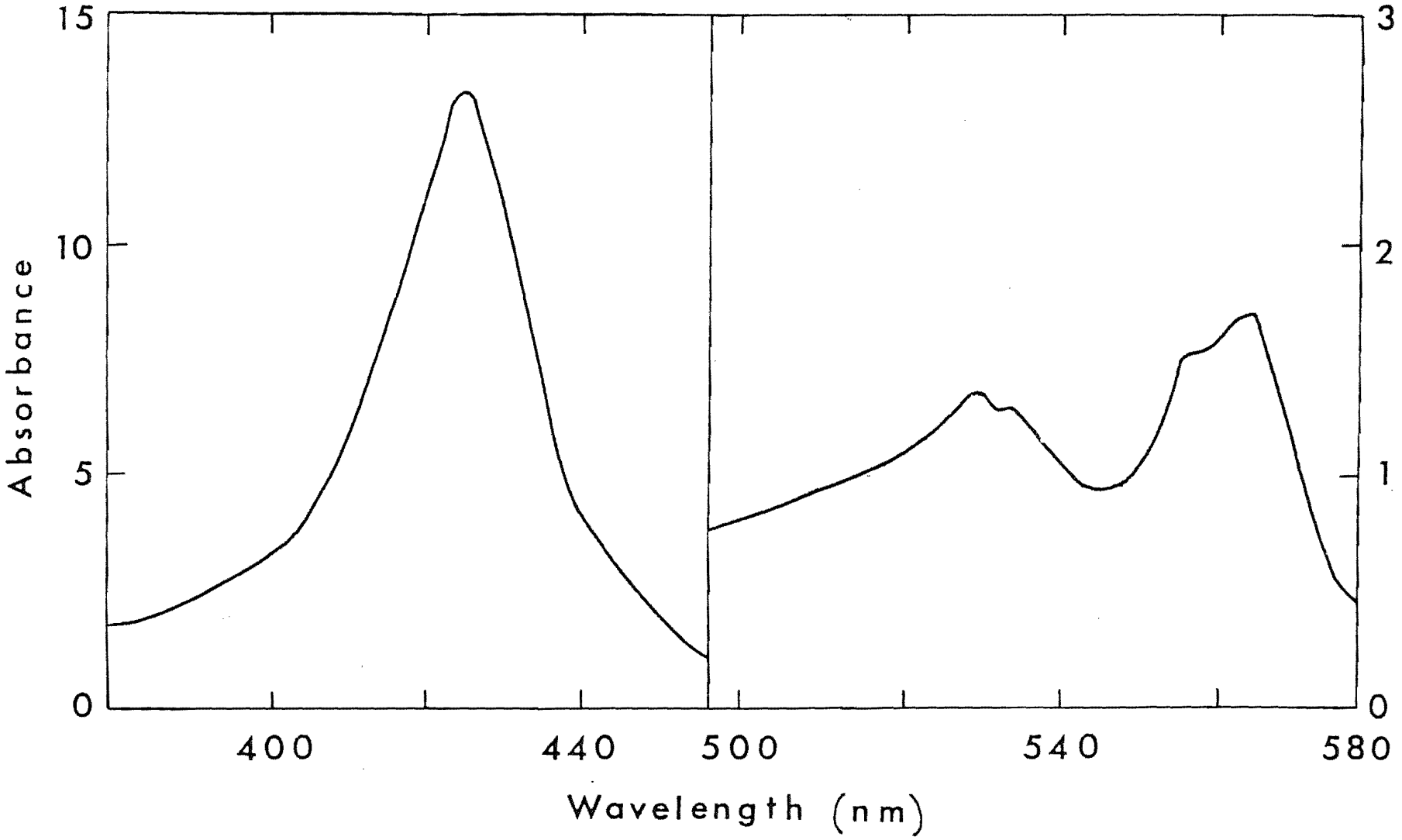

Figure 3.19 : Electronic spectrum of nicotine-myoglobin complex
(from ref. 163)

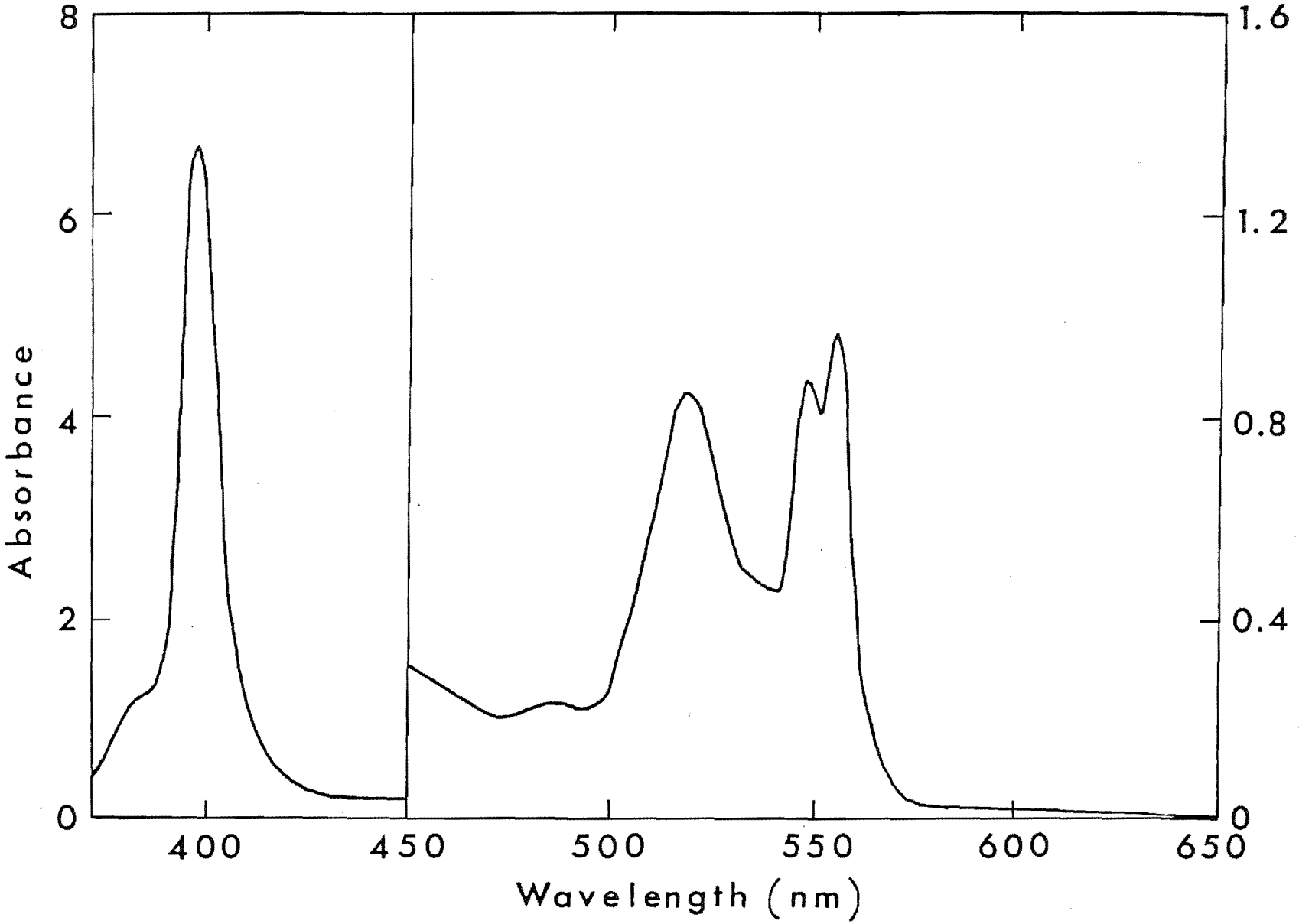

Figure 3.20 : Electronic spectrum of CO-Ru(II)MP-Mb in 0.05 M Bis-Tris acetate buffer of pH = 7.0 (from ref. 164)

[163], or from a marked lowering of the metal site symmetry for a single product, as postulated for the CO-RuMP-Mb complex [164,165]. It is unlikely that the additional bands for myoglobin products arise from free Mg porphyrin. Reconstituted products were carefully treated with CM32 column separation and no Soret bands appeared in likely positions for the free Mg porphyrins. Furthermore, the visible spectra of Mg porphyrin-Mb complexes are very similar to each other in general appearance, but have corresponding absorption bands at different positions (Table 3.1).

Multiple component features for myoglobin could arise from the formation of additional species having a different orientation of the porphyrin ring in the protein pocket [193] or from changes in the orientation of the proximal imidazole group. However the electronic spectra of various reconstituted FePP-Mb complexes show no difference from those of natural myoglobin derivatives [194]. In addition, CD results for the MgPP products, in particular, indicate that replacement of Mg for Fe in both hemoglobin and myoglobin complexes does not produce any significant orientation changes. From the shapes of the CD Soret peaks of Mg porphyrin-Hb species which have small negative regions, the angle between the transition dipole and the line joining the two opposing nitrogens was calculated to be 75° using the method of Hsu and Woody [195,196]. This is comparable to the corresponding angle of 70° for FePP-Hb oxy and deoxy derivatives, and 80° for Co(III)PP-Hb [197]. The single positive Soret CD band for Mg porphyrin-Mb suggests that the polarization direction is along the bridging methine carbons, as also found for

FePP-Mb [195,196]. Thus the overall heme-protein conformations for the Mg complexes are similar to those found for hemoglobin and myoglobin and the spectra splitting effect observed for the Mg porphyrin-Mb complexes is unlikely to be due to conformational variations of this type.

Furthermore, neither the CD nor ORD spectra of Mg porphyrin-Mb and -Hb give any indication of significant differences in the influence of the protein environment (the source of the optical activity) on the general properties of Mg porphyrin (Figures 3.12-3.18). Essentially the same CD and ORD patterns are observed for all systems. However, the corresponding CD and ORD spectra for the MgMP-Mb and MgMP-Hb species do show differences but these are likely to be due either to the coordination changes about Mg or steric effects having a greater influence for MP than for PP. Consequently the general spectral differences observed for Mg porphyrin-Mb and -Hb species are not directly related to the differences in the amino acid sequences that exist in the protein environment of Mb and Hb. Thus features of the more immediate coordination environment of the magnesium centre may be the origin of the observed spectral differences.

The main possibility to consider is the formation of six-coordinate magnesium species for the myoglobin complexes. This could either produce an equilibrium five-coordinate:six-coordinate mixture or a single six-coordinate component having marked asymmetry about the Mg centre. In both cases splitting of visible bands could result. While the equilibrium constant for six-coordination between

Mg porphyrin and pyridine in benzene is low [55], mixed ligations to Mg have been found to be favourable, especially for Mg in chlorophyll [73]. The Mg porphyrin-Hb complexes show insignificant changes in the visible band positions with respect to those for the five-coordinate (Mg porphyrin) (py) species (Table 3.1). By contrast, the Mg porphyrin-Mb complexes show a red-shift typical of a 5 → 6 coordination change (Chapter 2).

Under the preparative conditions used, the only possible additional ligands that could bind to the vacant sixth coordination site would appear to be O_2 or H_2O. The possibility of pyridine being coordinated can be excluded as the same products were obtained from method (1) where pyridine was absent. The lack of change in the electronic spectrum of MgPP-Mb on the addition of sodium dithionite appears to preclude the O_2 possibility.

Further evidence for six-coordination for the myoglobin products comes from results for the treatment of MgPP-Mb with CN^-. As shown in Figure 3.8, there are distinctive but only small spectral changes. For a five-coordinate MgPP-Mb species larger spectral changes might have been expected for the supposed production of a six-coordinate derivative. On the other hand, for CN^- replacement of the sixth ligand, already present, only relatively small changes of the type observed would be expected. Both components of the Q_o band are affected by CN^-, indicating the presence of a single six-coordinate complex rather than a five-coordinate:six-coordinate equilibrium mixture. For the latter case either the presumably higher energy five-coordinate component should

remain unaffected or it should move to the position of the six-coordinate component through the addition of CN^-, to displace the equilibrium completely to the six-coordinate entity. It is possible that the observed spectral changes arise from the effect of added NaCN on the myoglobin-protein conformation.

A six-coordinate formulation is also implied from the close similarity of the Mg porphyrin-Mb visible spectra with those of the well-established six-coordinate heme species; the CO-RuMP-Mb complex [164,165] and the nitrogenous base derivatives of FePP-Mb [163]. Moreover, the existence of similar and specific spectral features for three quite different heme protein systems indicates the formation of a special kind of asymmetric six-coordinate centre, as suggested by Srivastava [164]. A maximum of four visible bands can arise if the symmetry is lowered to a sufficient extent. This could occur in these systems if steric hindrance at the sixth ligand site forced the metal-ligating atom bond to be displaced from the normal position of a regular octahedron as observed for the carbon atom in the carbon monoxide derivative of myoglobin [198]. Presumably, the generality of this asymmetry effect is related to particular features of the myoglobin-protein environment of the sixth coordination site that are distinctly different from those in hemoglobin. For the Mg porphyrin-Mb complexes, a favourable hydrogen bonding interaction with the distal imidazole group, of the type recently described for oxymyoglobin [199,200] and carbon monoxide derivative of hemoproteins [201], may be a key additional factor stabilizing the binding of a water molecule to Mg in the myoglobin species.

As noted above, the Mg porphyrin-Mb complexes show a fifth absorption as a shoulder on the high energy side of the Q_1 band. This could be an additional vibrational transition and such an extra band appears at this position at low temperatures for the FePP-Mb nicotinate complex. Alternatively, it could be considered to arise from the splitting of a weak band generally observed at about 500 nm for Mg porphyrins [81]. Thus the weak band observed for Mg porphyrin-Hb near 500 nm may be envisaged to have split into two new weak bands, as for Q_o and Q_1, and also to have red-shifted in Mg porphyrin-Mb (one of which appears as a shoulder on the Q_1 band).

While the visible bands for the Mg porphyrin-Mb complexes are split, no similar splitting of the Soret bands was observed, as also reported for the six-coordinate CO-RuMP-Mb [164,165], and nitrogenous base FePP-Mb complexes [163]. Some definite splitting of the Soret bands would have been expected to accompany the visible band splitting if the products contained multiple species. Furthermore, the high-field ^1H nmr spectrum of MgPP-Mb shows no obvious splitting of the diagnostic ring current (peak I) resonance at approximately -3.5 ppm [13]. In other systems studied, splitting of this resonance does occur [13], indicating multiple conformer formation in those cases. However interconversion between multiple conformers can be too rapid to be detected by nmr spectroscopy, as reported for some carbon monoxide myoglobin and hemoglobin species [202-204].

While the carbon monoxide complexes of hemoglobin and myoglobin are both six-coordinate, results for these complexes may be usefully compared with those for the Mg

porphyrin-Hb and -Mb species (Figure 3.3). The CD spectral patterns for the CO species [205,206] are similar to each other (Figures 3.13 and 3.14), again indicating that the 10 nm red-shift (Table 3.1) is not directly due to differences in protein environment but more directly associated with coordination effects on the metal centre. Here direct evidence for such an effect comes from infrared results. The ν(C-O) frequencies are significantly different at 1944 and 1951 cm^{-1} for CO-FePP-Mb and CO-FePP-Hb, respectively. Maxwell and Caughey have commented that the constancy of the 1951 cm^{-1} band for a range of different species suggests something special about the structure of CO-FePP-Hb [207]. The 1944 cm^{-1} value is used for CO-FePP-Mb on the basis of a recent analysis [208] that assigns the other ν(C-O) bands to metmyoglobin and deoxy-myoglobin conformers. These values suggest that the Fe-C bond is stronger for myoglobin because of a weaker C-O bond, and these differences in the strength of the Fe-C bonds may, in turn, be the origin of the differences in the visible spectral band positions (Table 3.1). In myoglobin and hemoglobin, steric hindrance about the sixth co-ordination site prevents CO from binding in the normal manner [198]. Thus differences in the strength of CO binding for myoglobin and hemoglobin are probably being amplified by the hindered binding of CO to the iron atom. It may be noted that for the dioxygen derivatives of myoglobin and hemoglobin, differences in the ν(O-O) frequencies are much less than for ν(C-O) frequencies [209,210]. Also, unlike the CO derivatives, there is a significantly smaller change in the positions of the visible spectral bands for the dioxygen derivatives. Thus it may be

concluded that in the carbon monoxide derivatives of myoglobin and hemoglobin, the spectral red-shift may be correlated with an increase in the strength of the bonding at the sixth coordination site.

Consequently, part of the red-shifts observed for the Mg porphyrin-Mb complexes can be considered to be primarily due to the increased bonding at the sixth coordination site. There is a change from five-coordination in the hemoglobin derivatives to full six-coordination for the myoglobin entities. By contrast, Zn porphyrin-Mb and -Hb give essentially the same electronic spectra [211-213]. This may be due to the lower tendency of zinc to form six-coordinate species of this type. Addition of nitrogenous bases of myoglobin which produces a five-coordinate to six-coordinate change within the same protein system (Figure 3.19), also shows red-shifts and overall spectral changes that are very similar to those reported here for the changes from Mg porphyrin-Hb to Mg porphyrin-Mb. Thus there is no particular need to invoke other factors such as changes in the polarity of the heme environment for hemoglobin and myoglobin [214] for the red-shifts observed for all the Mg porphyrin-Mb complexes. However, such effects, especially different interactions between hemes and amino acid [215], may increase the magnitude of the red-shift and influence band positions to some extent.

Overall, the changes in the more immediate environment of the magnesium centre can be considered to be the most likely explanation of both the splitting of visible bands and part of the red-shifts observed for Mg porphyrin-Mb complexes. The results strongly indicate the formation

of six-coordinate species, probably through the binding of a water molecule at the sixth ligand site.

3.4.3 Magnesium Porphyrin-Protein Interaction

The absorption maxima of the transitions of MgPP in ether are red-shifted with respect to those of MgDP and MgMP (Table 3.1). Thus the peripheral substituents of the Mg porphyrin generally affect the electronic transitions.

Reconstitution of these 2,4 disubstituted Mg porphyrins into Mb also shows significant differences in the magnitude of the red-shifts. The magnitudes of the red-shift for the Q_o transitions of MgDP-Mb with respect to MgDP-Hb, and MgMP-Mb with respect to MgMP-Hb are only 4 and 4.5 nm respectively compared to 9 nm in the case of MgPP-Mb and -Hb. Thus, differences between the coordination state of Mg in MgPP-Mb and MgPP-Hb, alone, is insufficient to account for all of the red-shift (Section 3.4.2). The order of the red-shift is MgPP > MgDP = MgMP which is similar to that observed in iron [216-218] and cobalt [186] complexes. The magnitudes of these red-shifts for the oxy protein complexes of FePP, FeDP and FeMP are 4, 1 and 1 nm respectively [216-218]. Similar magnitudes of red-shifts are also observed for the iron protein complexes of isospirographis, spirographis and 2,4-diformyl [219] (Figure 3.21). For oxy CoPP-protein complexes, this red-shift is about 6 nm. This type of red-shift is very different from the red-shift in stacked double Mg porphyrin [220]. In stacked double Mg porphyrin, the electronic Soret band is blue-shifted with respect to the single Mg porphyrin, while the electronic Soret bands of Mg porphyrin-Mb remain red-shifted.

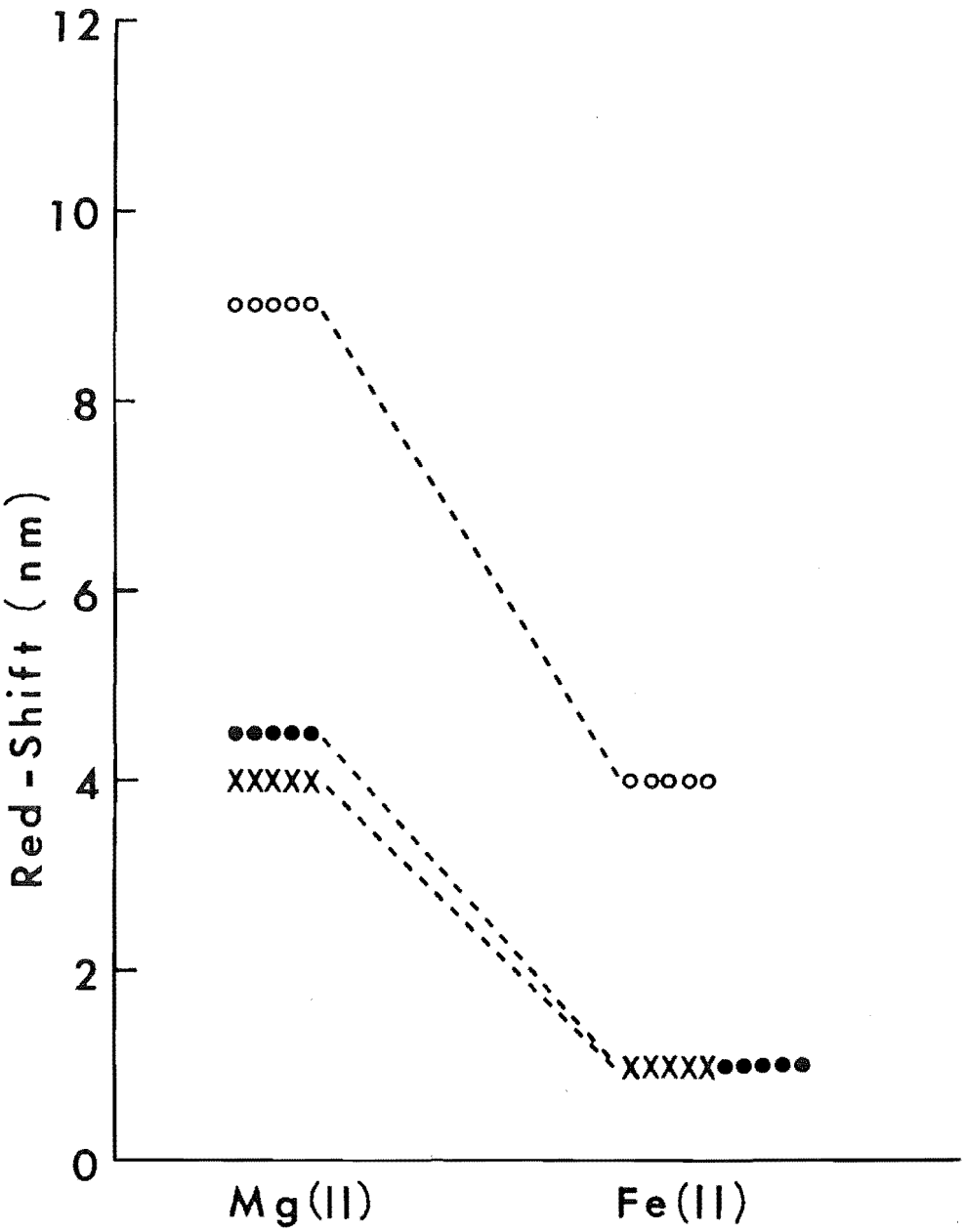

Figure 3.21 : Relative red-shifts of Mg(II) and Fe(II) porphyrin-Mb with respect to the corresponding Mg(II) and Fe(II) porphyrin-Hb. Protoporphyrin [o o o], Mesoporphyrin [• • •] and Deuteroporphyrin [x x x]

Various factors can possibly contribute to the Q_o red-shift. The first factor involves deprotonation of the proximal imidazole. Mincey and Traylor have shown that different imidazolate axial ligands red-shift the absorption bands by different magnitudes [221]. However, in the case of MgPP-Mb, this factor does not appear to contribute significantly to the red-shift. Since all the experiments were performed at pH 7, the degree of deprotonation of the proximal imidazole of Mb should remain the same for MgDP-Mb, MgMP-Mb and MgPP-Mb. Consequently, any red-shift associated with this effect should be approximately the same for all three complexes.

The second factor involves changes in the polarity of the heme environments for hemoglobin and myoglobin [222]. Romberg and Kassner, using model heme complexes in a variety of solvents, have shown that the red-shift correlates with the polarity of the solvents [214]. The change in the polarity of the heme environment from MgPP-Hb to MgPP-Mb is likely to be similar to that from MgDP-Hb to MgDP-Mb and MgMP-Hb to MgMP-Mb. But only small red-shifts were observed when the electronic spectra of MgDP-Mb and -Hb, and MgMP-Mb and -Hb were compared. Thus, this factor is unlikely to contribute to the red-shift in MgPP-Mb.

The third factor involves conformational changes of the protein. However, the similarities between the shapes of the CD spectra of MgPP-Mb and MgDP-Mb suggest that there is no difference in the orientation between MgPP-Mb and MgDP-Mb. Similar results were observed for the iron myoglobin analogues [223]. Furthermore, the Soret bands of MgDP-Mb and MgPP-Mb suggest that the polarisation direction is the same and occurs along the bridging methine

carbons in both protein complexes [195,196]. In addition, Perutz and coworkers have shown that changes in the T → R states of six-coordinate iron complexes change the electronic spectra by only 0.5 nm to 2 nm [224]. Thus, this factor cannot be considered to contribute significantly to the red-shift.

The fourth factor is different interactions between the 2,4 disubstituents and the protein environment of hemoglobin and myoglobin. X-ray studies have shown that these 2,4 disubstituents are intimately involved in hydrophobic contacts with the protein [144,145] and that the heme pocket of myoglobin is more rigid than in hemoglobin [215] and leghemoglobin [225,226]. Thus, the peripheral substituents of Mg porphyrin are more likely to interact with the side chains of the amino acid groups in myoglobin than in hemoglobin. Evidence for the importance of interaction between the protein and peripheral substituents has been obtained by Sono and Asakura [219], where the oxy protein complexes of the two isomers, spirographis and isospirographis, show different absorption spectra. In addition, reconstitution of MgPc with Hb did not produce any definite complex. Pc is different from MP, DP and PP as it has no substituted groups on the ring. This suggests that interaction between the protein and porphyrin substituents is important.

Slight variations in the visible bands of MgMP-Mb compared with those of MgPP-Mb and MgDP-Mb may be due to differences in the binding of the sixth ligand that arise from corresponding differences in steric interactions with the ligand. Thus steric interaction between the ethyl

groups of MgMP and the protein may affect the nature of the six-coordination geometry. X-ray studies suggest that the π systems of the vinyl groups of protoporphyrin are parallel to the porphyrin ring [227] while the ethyl groups of mesoporphyrin are almost at right angles to the ring [228]. However, the similarities between the shapes of the CD spectra of MgDP-Mb and MgPP-Mb suggest that in MgPP-Mb, an electronic effect also determines the red-shift.

NMR studies using ^{13}CO and various 2,4 disubstituted iron myoglobins and hemoglobins support the idea that the electronic interactions between the 2,4 disubstituents and the two heme environments are different [229]. Experimental results from iron and cobalt protein analogues suggest that both steric [156,157] and electronic [158-161] interactions are important. The vinyl groups, being electron withdrawing, can transfer charge to the side chains of the amino acid groups either by direct charge transfer [230] or by hydrogen bonding [150,151]. Recent studies show that the positions of the electronic bands are indeed affected when there are electronic interactions between the vinyl groups and another charged species, e.g. Cu(I) [231]. Thus, the extra red-shift in MgPP-Mb is likely to be a result of electronic interaction between the vinyl groups and the proteins.

These results suggest that in photosynthetic systems, a red-shift can be observed for monomeric chlorophyll species if chlorophyll-protein interactions are significant, especially at the peripheral substituents. This kind of behaviour has also been observed in other biological systems, particularly retinal Schiff base-protein interactions in rhodopsin [151]. It is likely that during the evolution of photosynthesis, the sensitivity of the electronic

spectrum to the charges on the substituted groups of the ring becomes more highly developed in chlorophyll than in Mg porphyrin. Consequently, the red-shift in chlorophyll is larger. Direct evidence obtained by Davis and coworkers appears to support this suggestion [155]. Their results show that protonation of 3-dimethyl-3-(aminomethyl) chlorophyll produces a large difference of 4 nm in the absorption maxima. Furthermore, X-ray studies of bacteriochlorophyll-protein *in vivo* also show interaction between the oxygen atom of the cyclopentanone ring and the protein environment [7].

Overall, this approach shows that in addition to the coordinating properties of Mg, interaction between the peripheral substituents of the ring and the amino acids of a protein environment is also important in producing a red-shift of electronic bands. The magnitude of this interaction could be large and could even account for most of the red-shift observed in photosynthetic systems.

3.4.4 Optical Activity of Magnesium Porphyrin-Globin Complexes

A series of metalloporphyrins having different metal ion centres has been used to probe the immediate porphyrin environment. The metal ions that have been commonly substituted for iron in myoglobin and hemoglobin are lutetium [232], chromium [233,234], manganese [235-243], cobalt [186,244-249], nickel [250,251], copper [178,250], zinc [211-213], ruthenium [164,165,252], indium [253] and ytterbium [254]. Most of these metal ions in the substituted hemoproteins have d electrons whereas Mg(II)

ion has the electronic configuration $1s^2\ 2s^2\ 2p^6$ [115]. Consequently, the spectra of Mg porphyrin-globin complexes are of interest particularly for the elucidation of the direct effect of d electrons on the ORD/CD spectra of hemoproteins.

Substitution of Fe by Mg can be an important technique for studying this effect, e.g. in cytochrome C3 where it is still not known whether the splitting of the Soret CD spectrum is due to the coupling effect of d → d transitions or simply transition dipole interaction between two or more heme groups [255].

The strong Cotton effects observed for Mg porphyrin-globin complexes suggest that the Mg porphyrin is incorporated into the heme pocket, as Mg porphyrin itself has no asymmetric centre and is thus optically inactive. These Cotton effects have been generally used to probe the heme environment and changes in the structure of proteins [256]. Two types of Cotton effect have been proposed, namely intrinsic which gives the percentage of α-helix content of the protein and extrinsic which is the interaction of the heme with the protein.

Determination of the intrinsic Cotton effect by ORD gives results which are in good agreement with those observed from X-ray diffraction studies [144,145]. This shows that the α-helix content of hemoproteins does not change significantly either in the crystalline state or in solution [257]. Using this technique, Harrison and Blout showed that the small loss of α-helix content in Mb was restored when the heme was reconstituted [258]. Similar results were obtained by Breslow and coworkers [259].

The CD spectra of Mg porphyrin-globin and CO-FePP-globin in the 200-250 nm region show similar magnitudes of rotation which suggest that the α-helix contents are the same (Figures 3.12 and 3.14). Thus, as highlighted in Section 3.4.2, substitution of Fe by Mg does not affect the intrinsic Cotton effect. This suggests that the red-shift is not likely to be a result of α-helix content. By contrast, the α-helix content of other complexes like Fe-, Co- and Cu-tetrasulphonatedPc-globin, show considerable differences in their intrinsic Cotton effect [260,261].

The extrinsic Cotton effect observed for Mg porphyrin-globin can arise from several possible effects. The first possible effect is nonplanarity of the porphyrin ring which leads to an inherent dissymmetric chromophore [262]. Although this mechanism is observed in Vitamin B12 coenzyme, where the distortion of the corrin ring results in the induced Cotton effect [263], X-ray studies on hemoproteins show little puckering of the porphyrin ring [144,145]. Thus this effect is unlikely to be important.

The second effect is the influence of different ligands coordinated to the metalloporphyrin which presumably gives rise to chirality at the metal centre [264]. However, metal-free porphyrin-globin complexes still exhibit a similar magnitude of rotation to that of native hemoglobin [265,266] and this shows that the presence of a metal centre is not crucial for the development of optical activity.

A third effect is mixing of the heme π-π^* transition with d $\rightarrow$ d transition of the metal ions [267]. Studies using globin containing metal-free porphyrin and this work

[55,57] show that the presence of d electrons is not a necessary requirement for the development of induced Cotton effects.

The fourth effect is the coupled oscillator mechanism where the electronic transition of one chromophore couples with the transitions of other chromophores [268-270]. It has been generally accepted that in myoglobin and hemoglobin, this effect gives rise to the induced Cotton effect. Theoretical calculations by Hsu and Woody [195,196,271], show that the coupled oscillator interaction between the heme π-π^* transitions with π-π^* transitions of globin aromatic side chains could account for the magnitude and sign of the CD spectra in myoglobin and hemoglobin. Aromatic residues as far as 12Å can influence these transitions, but contributions from coupling between heme π-π^* transition with π-π^* and n-π^* transitions in the polypeptide backbone and the σ-σ^* transitions in allyl side chains were found to be negligible.

The effect of small differences in conformation is reflected in the Soret bands of α_2 and β_2 chains of MgPP-Hb. These α_2 and β_2 chains have different maximum absorption wavelengths and the Soret band of the $\alpha_2\beta_2$ chains is intermediate between them. This result is similar to that for α_2 and β_2 chains of FePP-Hb [272,273] and it shows that measurements by CD give better resolution and information than do electronic absorption spectra. The absence of splitting of the CD bands in the visible region of Mg porphyrin-globin into two components of opposite sign, strongly suggests that the dimerisation and exciton explanations [274] can be excluded.

It is unlikely that the CD spectrum of Mg porphyrin-Mb will alter significantly when sperm whale myoglobin is substituted by myoglobin from goat, lamb, beef and camel because the amino acid sequences in the heme pockets are similar [275]. Although no negative CD peaks were observed in the visible region, it is possible that in a protein environment, the CD spectra of Mg porphyrin and chlorophyll can show the characteristics of an exciton effect. Harrington and coworkers [276] have already obtained both positive and negative CD spectra from the hemoglobins of earthworms. Their results show that the multichain heme proteins of *Lumbricus terrestris* and the four-chain heme proteins of human both gave positive CD bands, while the single-chain protein of *Glycera dibranchiata* gave the reverse CD bands. Boxer and Wright observed an inversion of the CD peaks of Mg pyrochlorophyllide in dichloromethane with respect to those of Mb [12,13]. In plants, the ability to synthesise heme proteins that show negative CD is clearly defined in studies of leghemoglobin from the root nodules of soybean [277,278]. The observed negative CD spectra compared to those of corresponding myoglobin complexes, show that the protein side chains interacting with the hemes are different for leghemoglobin and myoglobin.

These results show that in chlorophyll-protein complexes, the coupled oscillator mechanism which gives rise to the induced Cotton effect, is strongly influenced by the particular nature of the protein side chains. Consequently, the effect of protein should also be taken into consideration when the CD spectra of chlorophyll systems are interpreted.

CHAPTER 4

OBSERVATION OF INDUCED COTTON EFFECTS FOR MAGNESIUM PORPHYRIN-(CHIRAL AMINO ACID) SPECIES

4.1 INTRODUCTION

The induced Cotton effect in hemoprotein is an interesting aspect of the optical activity of heme transitions because metalloporphyrin, being planar, is optically inactive. Possible factors which can give rise to this effect have been discussed in Chapter 3. Theoretical calculations for hemoproteins support the coupled oscillator mechanism which involves the coupling of heme π-π^* transitions with the π-π^* transitions of globin aromatic side chains [195,196]. Other couplings between heme π-π^* with the π-π^* and n-π^* transitions in the polypeptide backbone and the σ-σ^* transitions in allyl side chains were found to be negligible. Several attempts to model this induced Cotton effect using a variety of chiral amino acids and polymers have been unsuccessful [279].

In this chapter, the induced Cotton effects and spectral results are reported for protein-free Mg porphyrin entities coordinated to various chiral amino acids (D- and L-proline, L-histidine, L-tryptophan, L-threonine and L-serine (Figure 4.1)). The induced Cotton effects observed are different from those of Mg porphyrin-globin species which have been shown to be similar to their iron analogues (Chapter 3). The positions of the electronic and CD/ORD bands indicate that six-coordinate (Mg porphyrin) $(\text{amino acid})_2$ species produce these effects. The major

Nomenclature	Structure
Cysteine	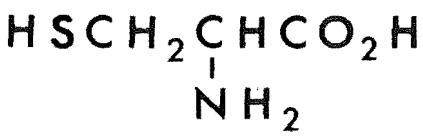
Glutamic acid	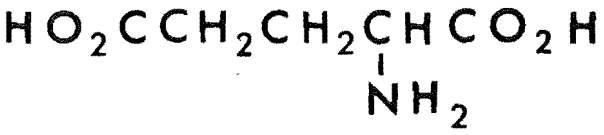
Histidine	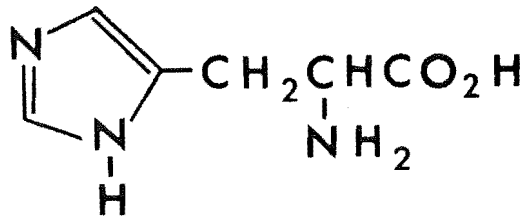
Leucine	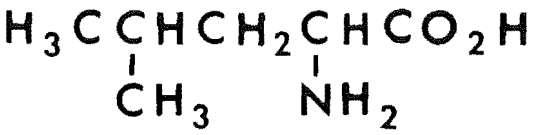
Malic acid	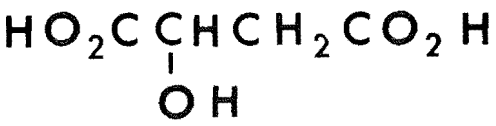
Mandelic acid	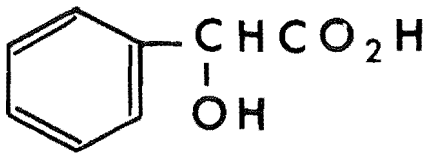
2-Methyl-1-butanol	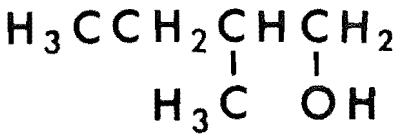
Nicotine	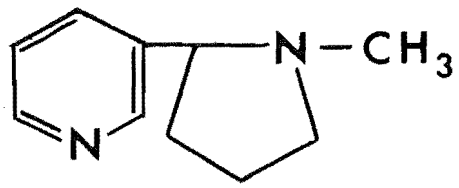
Proline	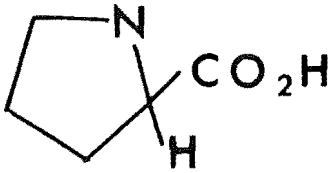

Figure 4.1 : Nomenclature and structure of chiral compounds discussed in text

Nomenclature	Structure
Serine	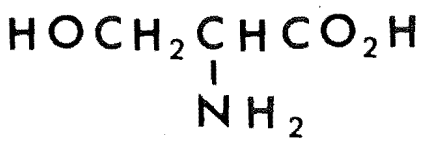
Tartaric acid	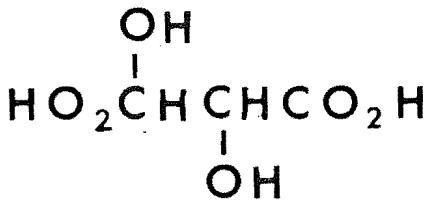
Threonine	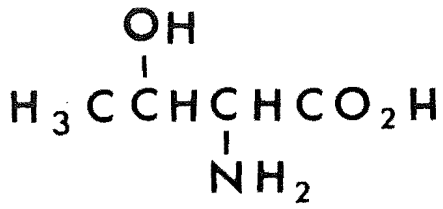
Tryptophan	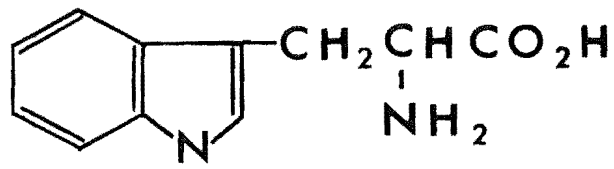

(Figure 4.1 continued)

five-coordinate components of the solutions, (Mg porphyrin)(amino acid), do not produce Cotton effects. Results of this type may be of value in elucidating the structural and functional relationships between metalloporphyrin and the amino acid residues in biological systems [280-282].

4.2 EXPERIMENTAL

MgMP, MgDP and MgPP which were basic because of the presence of residual NaOH, were prepared according to methods described in Chapter 3. MnMPDME was prepared according to the procedure by Taylor [283]. Hemin, L-histidine, L-proline, L-tartaric acid, L-threonine, L-serine, L-cysteine, L-leucine, L-nicotine, L-tryptophan, L-glutamic acid, L-malic acid and D-proline were purchased from Sigma Chemical Company and British Drug Houses Ltd. D-mandelic acid and S(-)-2-methyl-1-butanol were obtained from Fluka.

The samples were generally prepared by adding solid magnesium porphyrin to neat S(-)-2-methyl-1-butanol and to concentrated solutions of the various chiral amino acids. Then the solutions were filtered before recording the spectra. This method appears to produce more intense spectra than that whereby the magnesium porphyrin is completely dissolved before being added to the amino acid solution. In concentrated solutions of magnesium porphyrin, a red precipitate forms after about one hour and in dilute solutions, the pink colour turned orange and then yellow. Consequently, all spectral measurements must be completed before these changes occur. It was observed that visible light rapidly causes these changes.

Electronic absorption spectra were recorded on a Varian Superscan 3 UV-visible spectrophotometer. All

reagents used were of analytical or chromatographically homogeneous grade. ORD and CD measurements were recorded on a Jasco ORD UV-5 spectrophotometer. Reagents were kept away from strong light and all apparatus were covered with aluminium foil.

4.3 RESULTS

4.3.1 Electronic Spectra

The electronic spectra of MgMP and MgPP in D-proline, L-proline, L-histidine, L-serine and L-threonine all show distinct shoulder at 433 nm which is diagnostic of six-coordinate species as indicated in Chapter 2 (Figure 4.2, Table 4.1). These spectra are significantly different from that of Mg porphyrin-Hb (Figure 4.3). The electronic spectra of MgMP in L-tartaric acid, L-malic acid, D-mandelic acid, L-cysteine, L-leucine and L-glutamic acid show distinct red-shifts in their bands, but no band at 433 nm is observed. Furthermore, the relative intensity of the Q_o band to the Q_1 band is reduced significantly. MgMP in neat S(-)-2-methyl-1-butanol or L-nicotine is also red-shifted but the relative intensity of the Q_o band to the Q_1 band is reduced only marginally. MgDP in the various chiral amino acids did not show any band at 433 nm and the spectra are slightly red-shifted.

The electronic spectra of hemin in L-proline and L-histidine show the characteristic bands of iron in oxidation state 3 [92].

When the electronic spectra of MgMP and MgDP in the chiral amino acids were measured after one hour, the spectra had the characteristic features of MP and DP [92].

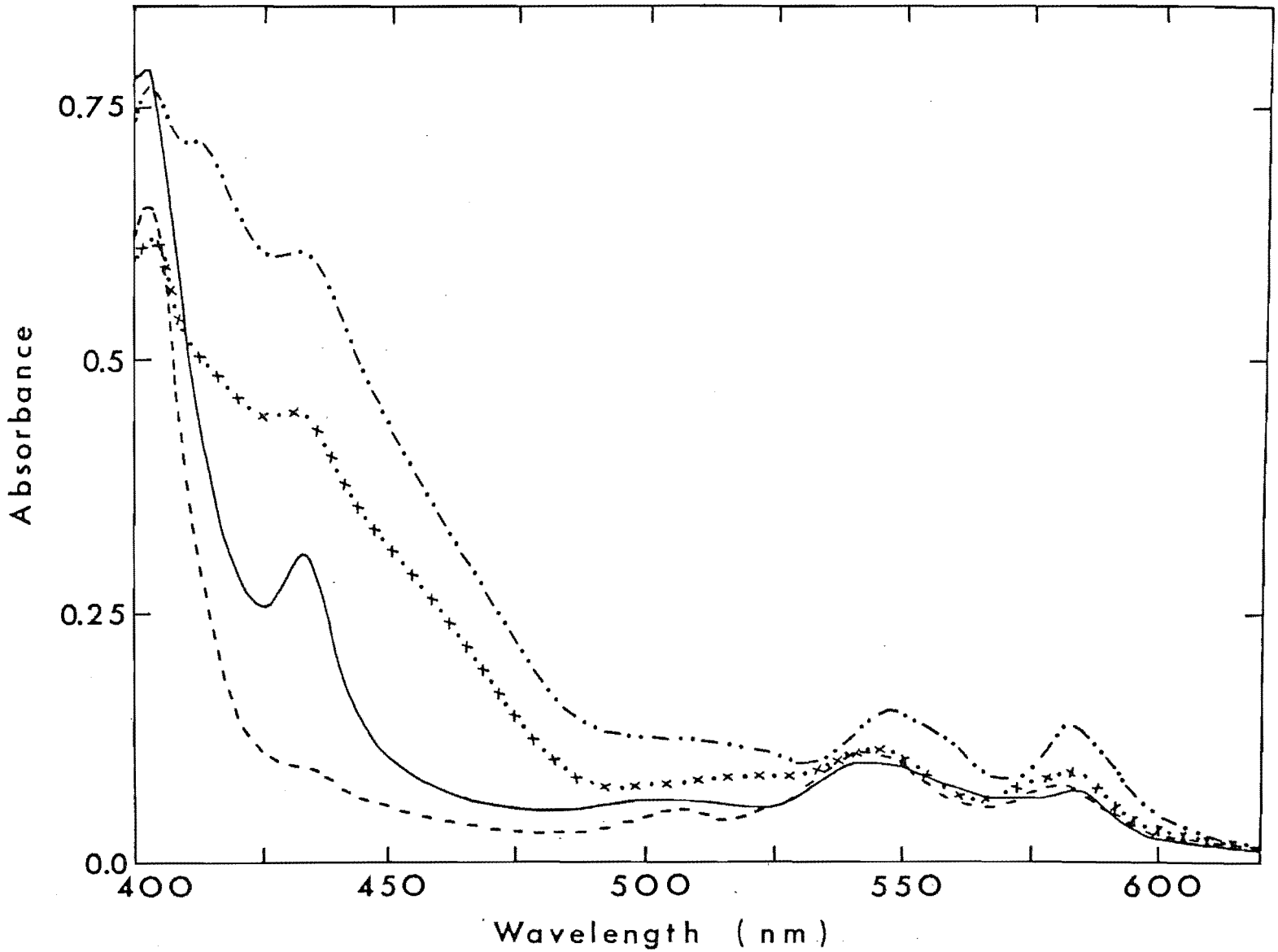

Figure 4.2 : Electronic spectra of MgMP in L-histidine [____], in L-serine [-·-·-], L-threonine [x·x] and in L-proline [---].

Table 4.1 : Comparison of electronic bands of Mg porphyrin in chiral amino acids

Chiral compounds	MgMP			MgPP		
	Q_o	Q_1	Soret	Q_o	Q_1	Soret
L-proline/D-proline	581	543	403 433(sh)	594	557	414 433(sh)
L-histidine	584	544	403 433	594	556	416 433
L-serine	583	547	403 413(sh) 433(sh)			
L-threonine	583	546	403 433(sh)			
L-tryptophan	582	545	403 433(sh)			
D-mandelic acid/L-tartaric acid	592	549	401			
S(-)-2-methyl-1-butanol	580	543	406			

sh = shoulder

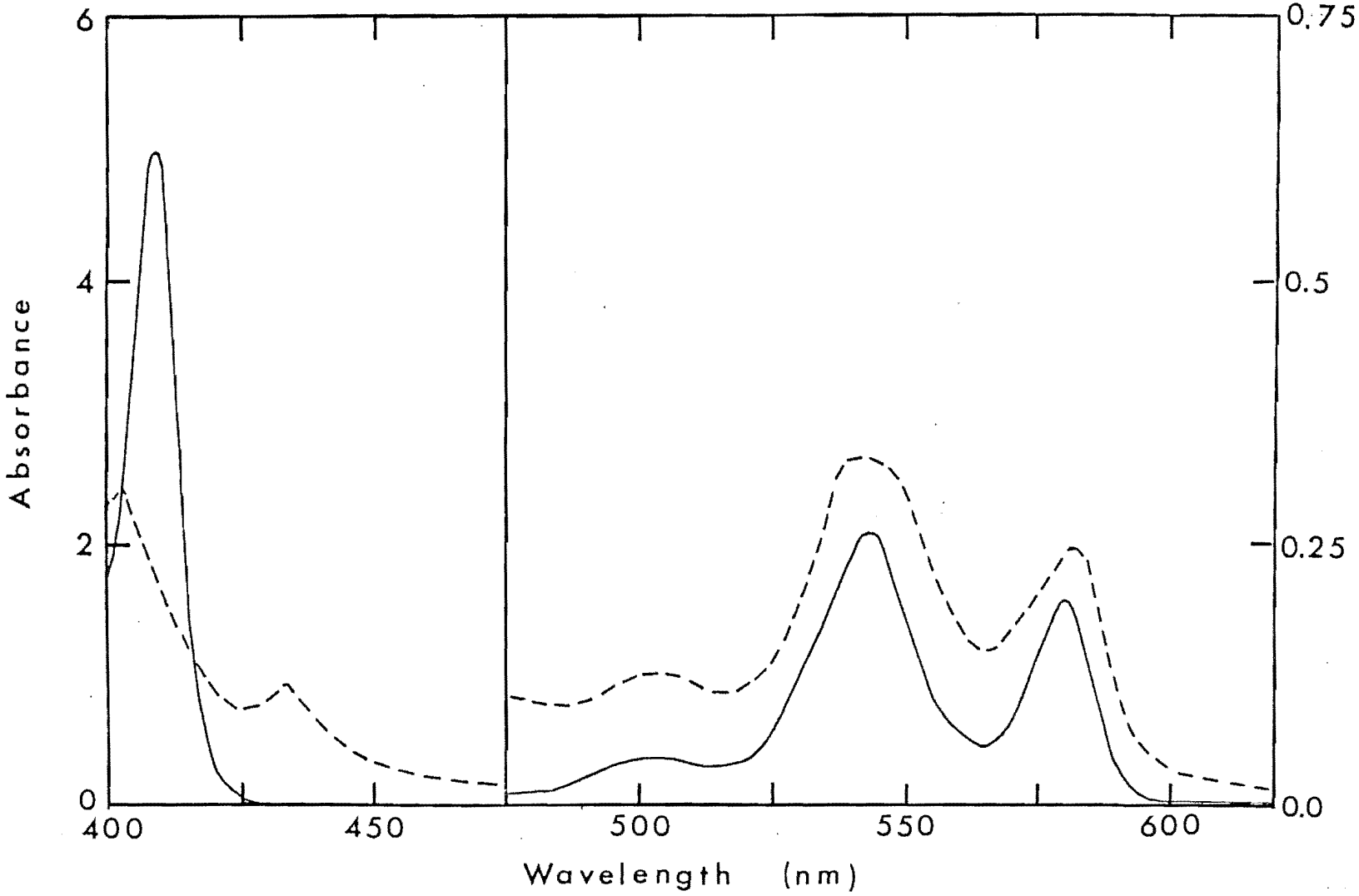

Figure 4.3 : Electronic spectra of MgMP in 0.1 M L-histidine [---] and MgMP-Hb [——]

This suggests that decomposition of Mg porphyrin is a result of Mg^{2+} being removed from the porphyrin ring.

4.3.2 CD Spectra

MgMP, MgDP and MgPP are optically inactive, while the chiral amino acids and alcohol used in these experiments have no significant CD features in the visible region [115]. In solvents like ether, benzene and pyridine, MgMP, MgDP and MgPP do not produce optical rotation, although the electronic spectra of MgPP in L-histidine and pyridine are similar (Figure 4.4). However, freshly prepared solutions of MgMP and MgPP in L-proline, L-serine, L-threonine, D-proline and L-histidine show distinct CD bands in the visible region (Table 4.2). MgMP in L-tryptophan shows very weak CD bands. The two well-formed bands between 500 nm and 600 nm (Figures 4.5, 4.6 and 4.7) are likely to correspond to the Q_1 and Q_o bands observed in the electronic spectra (Figures 4.2, 4.3 and 4.4). Increasing the concentration of L-histidine from 0.05 M to 0.2 M does not appear to vary the positions of these two bands significantly (Figure 4.5). Of all the samples of MgPP and MgMP studied, one preparation of MgPP gave CD spectra of opposite rotation to that obtained in all other cases, for L-histidine and L-threonine. By contrast, L-proline did not give any change for the particular MgPP sample. The signs of the bands of MgPP and MgMP in L-proline are opposite to those observed for most of the solutions of MgMP and MgPP in L-histidine respectively (Figure 4.6). Increasing the concentration of L-proline from 0.05 M to 1 M did not change the positions and signs of the bands of MgMP in L-proline. The only difference is that at higher

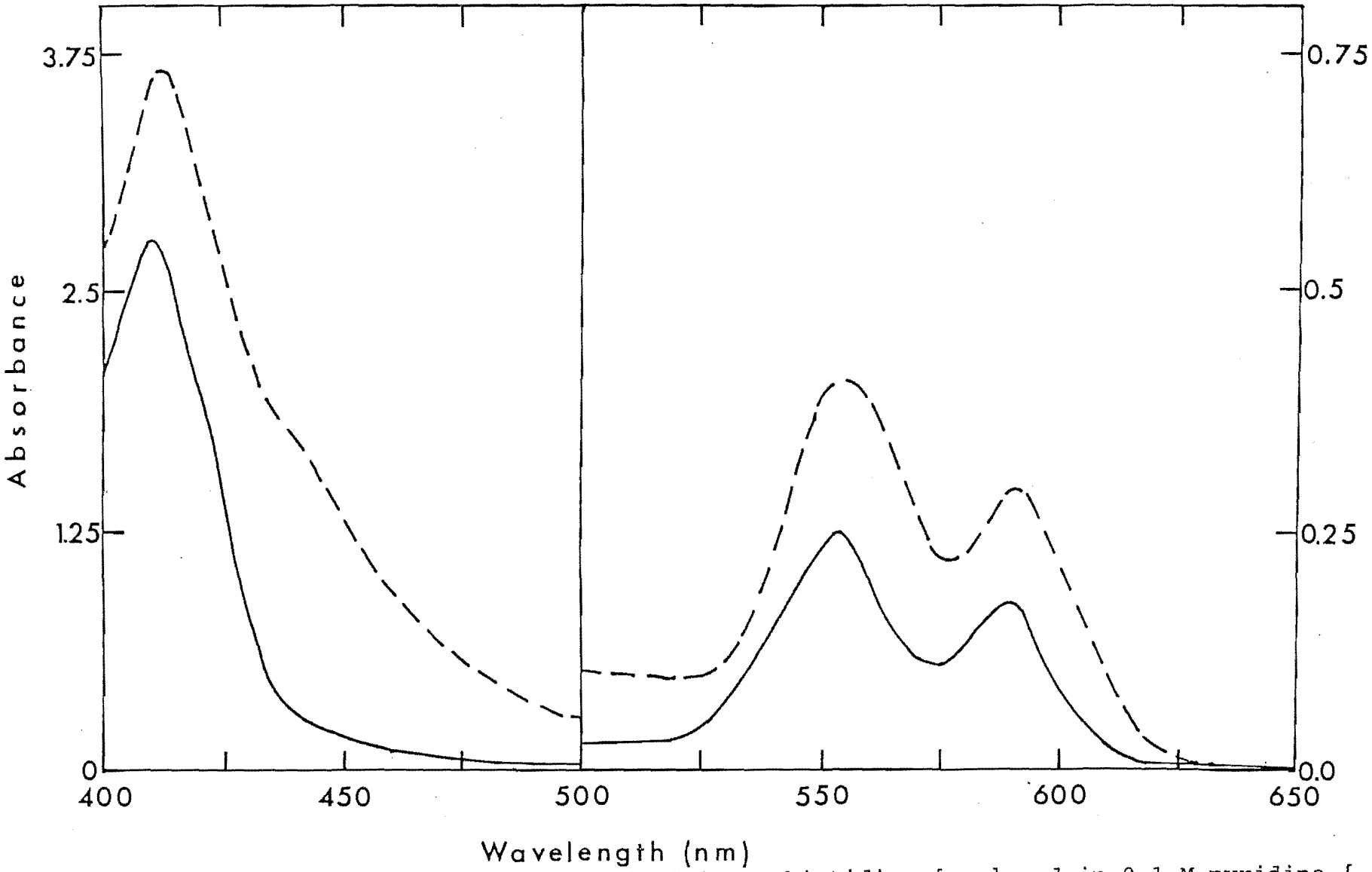

Figure 4.4 : Electronic spectra of MgPP in 0.1 M L-histidine [---] and in 0.1 M pyridine [___]

Table 4.2 : Comparison of circular dichroism bands of Mg porphyrin in chiral amino acids

Chiral compounds	MgMP			MgPP		
	Q_o	Q_1	Soret	Q_o	Q_1	Soret
L-proline	586	552	435 (negative) 425 (positive) 430 (cross-over point)	603	564	446 (negative) 429 (positive) 438 (cross-over point)
D-proline	586	552	425 (negative) 435 (positive) 430 (cross-over point)	603	564	429 (negative) 446 (positive) 438 (cross-over point)
L-histidine	589	556	425 (negative) 445 (positive) 435 (cross-over point)	604	568	425 (negative) 445 (positive) 435 (cross-over point)
L-serine	589	559	420 (negative) 448 (positive) 434 (cross-over point)			
L-threonine	586	558	421 (negative) 435 (positive) 428 (cross-over point)			
L-tryptophan*	589	554	421 (negative) 435 (positive) 438 (cross-over point)			

* very weak signal

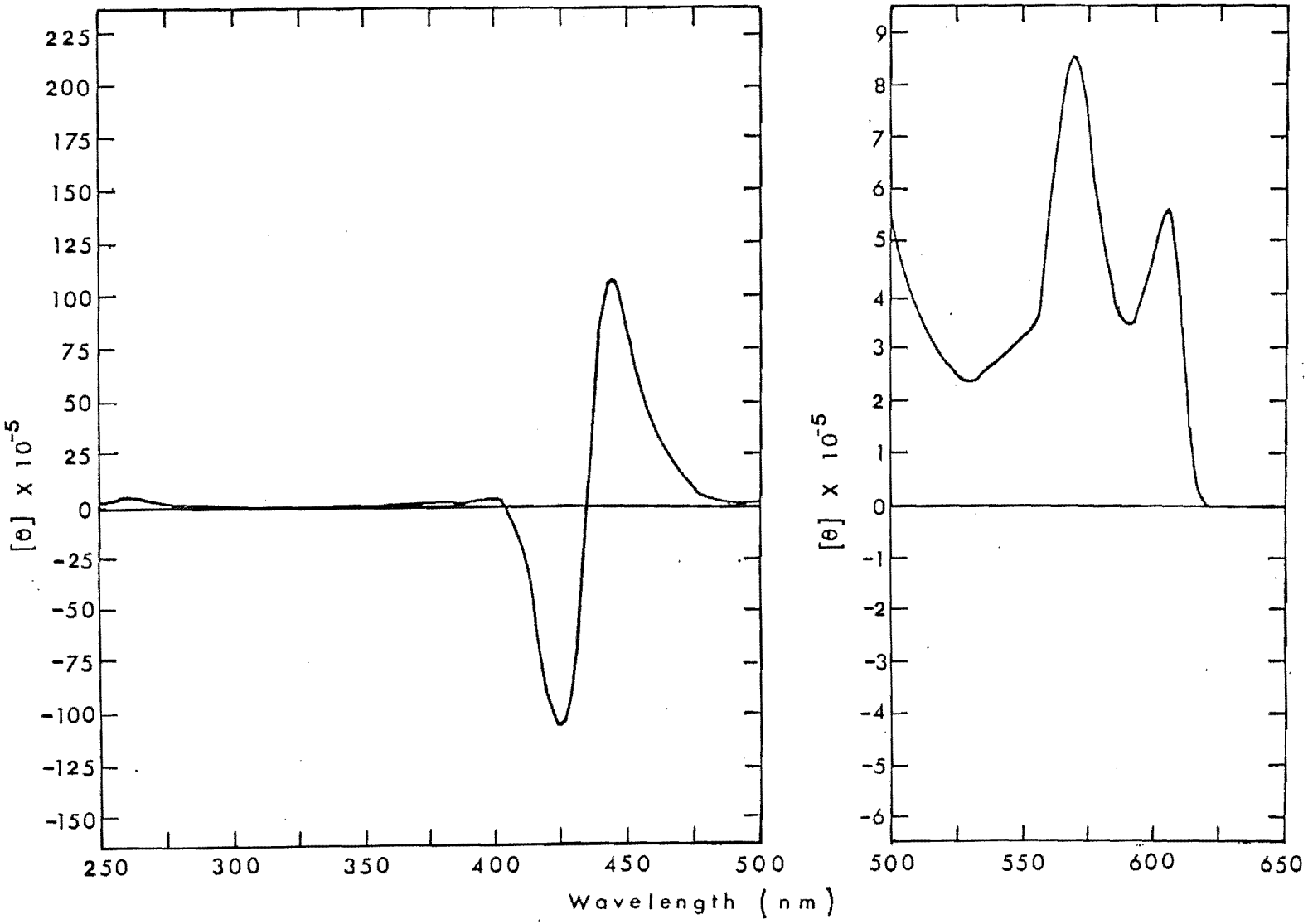

Figure 4.5 : Circular dichroism spectrum of MgPP in 0.1 M L-histidine redrawn to show main bands

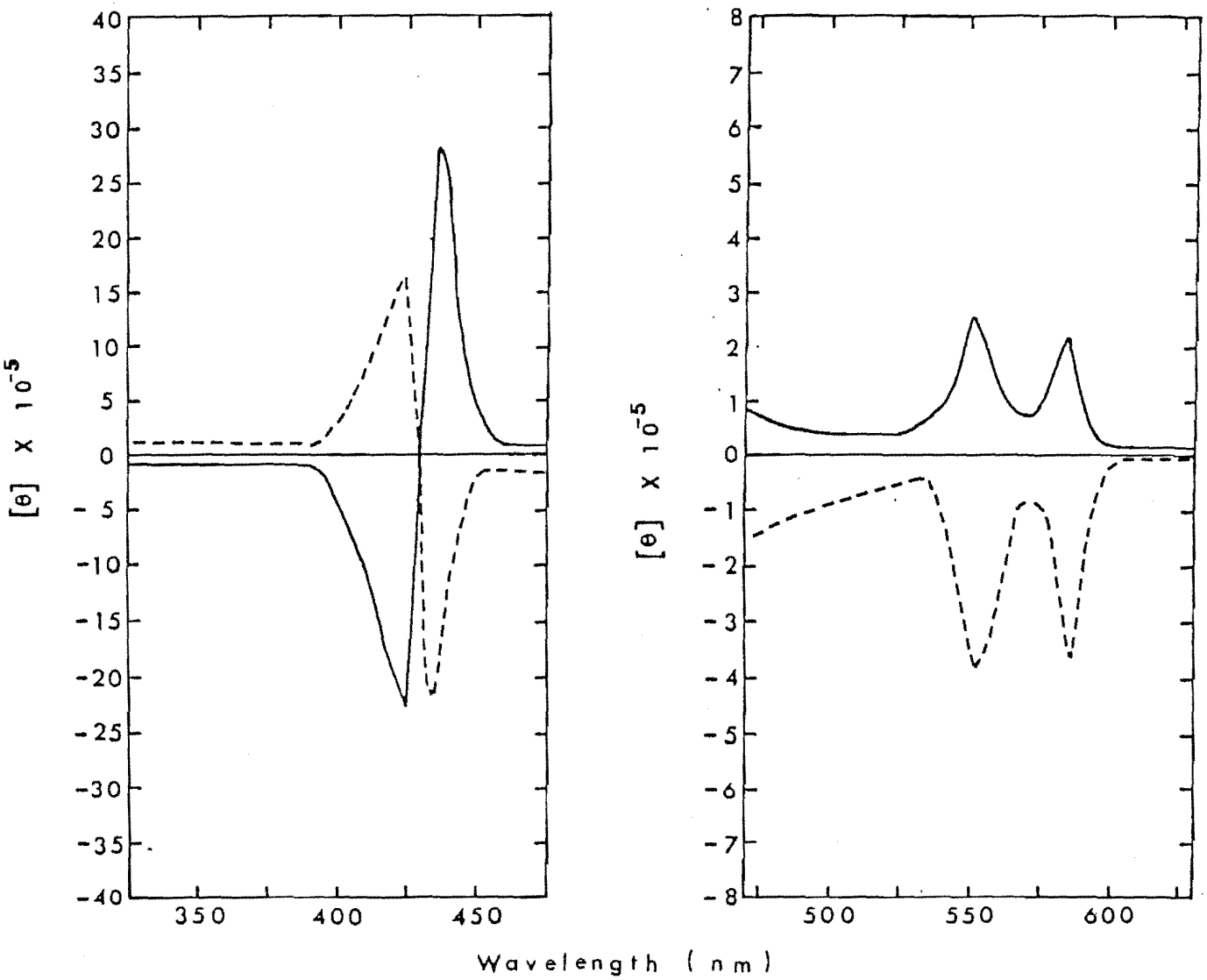

Figure 4.6 : Circular dichroism spectra of MgMP in 0.1 M L-proline [---] and in 0.1 M D-proline [——] redrawn to show main bands

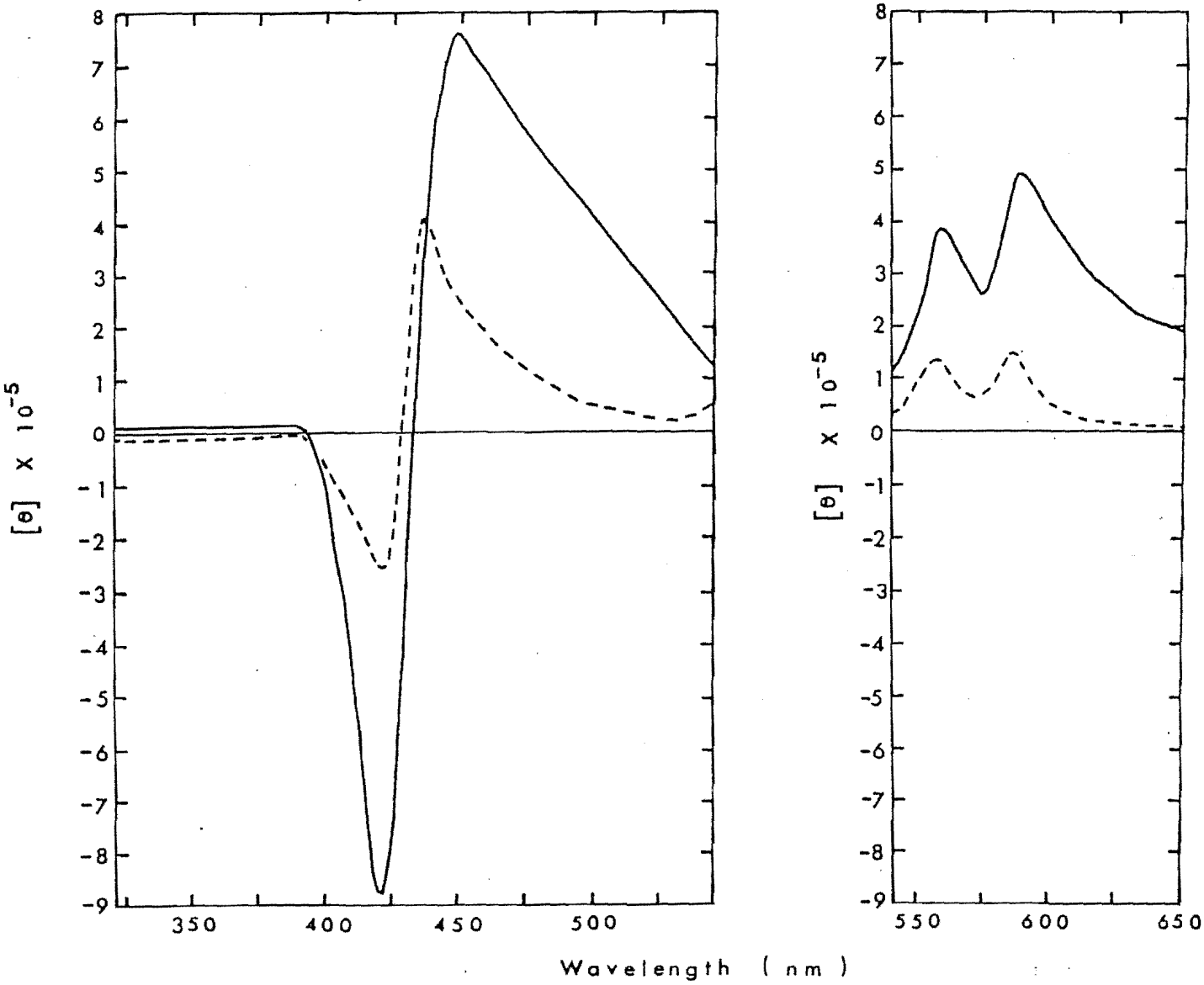

Figure 4.7 : Circular dichroism spectra of MgMP in 0.1 M L-serine [——] in 0.1 M L-threonine [---] redrawn to show main bands

concentrations of L-proline, these CD bands are more intense. Nonetheless, decomposition of MgMP still persists after one hour. The CD spectrum in D-proline is the opposite to that of the corresponding L-proline sample, as expected (Figure 4.6).

The Soret band is split into two equal and opposite bands. For both MgMP and MgPP in L-histidine, the positions of these two bands appeared to be the same and the cross-over point is at 435 nm. However, for MgMP and MgPP in chiral proline, the cross-over point is slightly different (Table 4.2).

No significant CD spectrum was observed for MgMP dissolved in L-tartaric acid, L-glutamic acid, L-cysteine, D-mandelic acid, L-malic acid, L-leucine, L-nicotine solutions and also in S(-)-2-methyl-1-butanol.

A variety of studies using MgDP under various conditions including different pH values did not produce any CD with chiral amino acids.

As for hemin in L-histidine, no significant CD spectrum was obtained for hemin dissolved in a solution of L-proline. Mn(III)MPDME in L-histidine did not yield any CD rotation.

4.3.3 ORD Spectra

MgMP and MgPP did not show any optical rotation, while all the amino acids and the chiral alcohol show rotational properties [115]. However, extra features are observed in the visible region when Mg porphyrin is dissolved in solutions of L-serine, L-threonine, D-proline, L-proline and L-histidine (Figures 4.8, 4.9 and 4.10, Table 4.3). Some variations in the features of the ORD

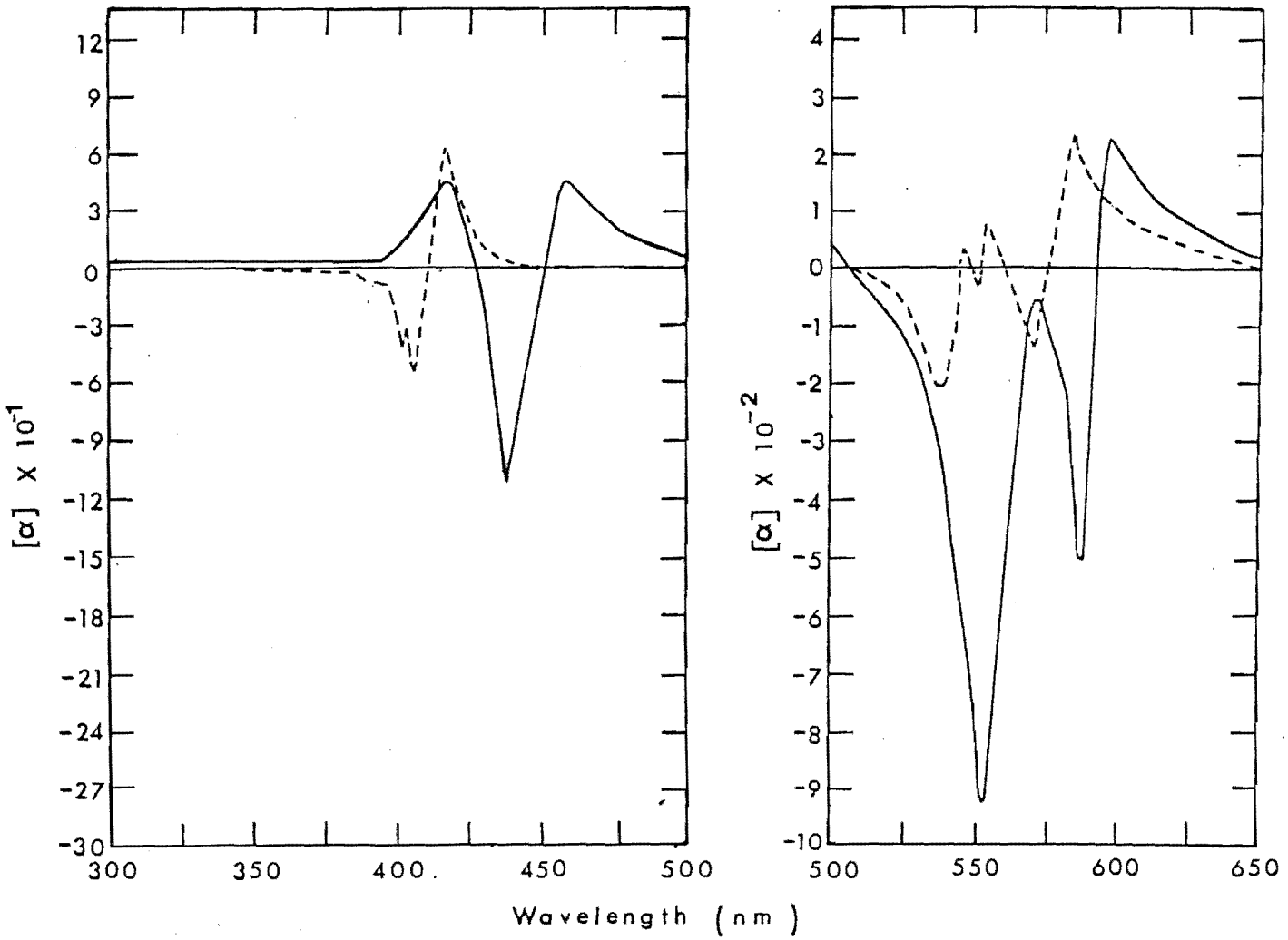

Figure 4.8 : Optical rotatory dispersion of MgMP in 0.1 M L-histidine [——] and MgMP-Hb [---] redrawn to show main bands

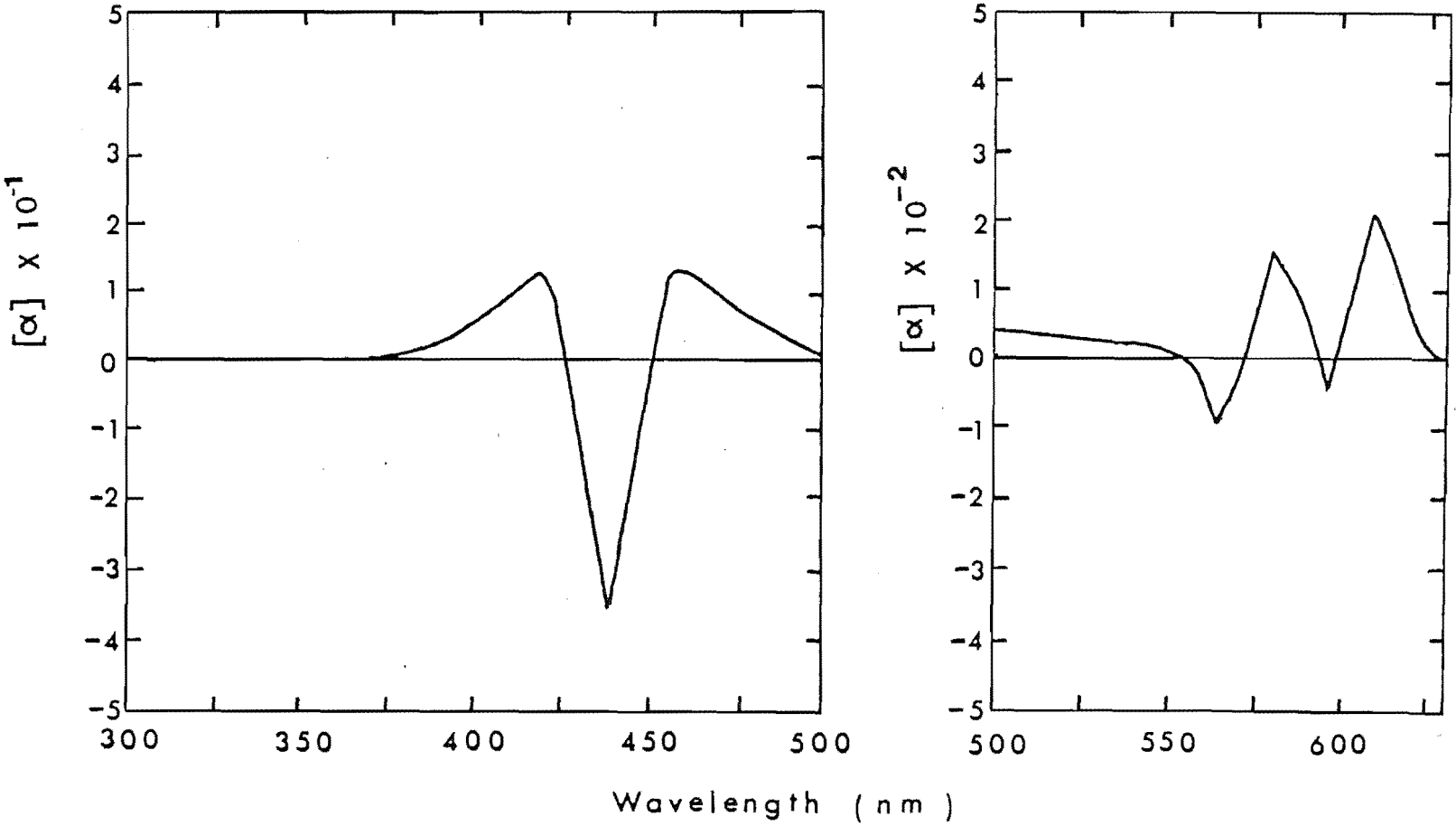

Figure 4.9 : Optical rotatory dispersion of MgPP in 0.1 M L-histidine redrawn to show main bands.

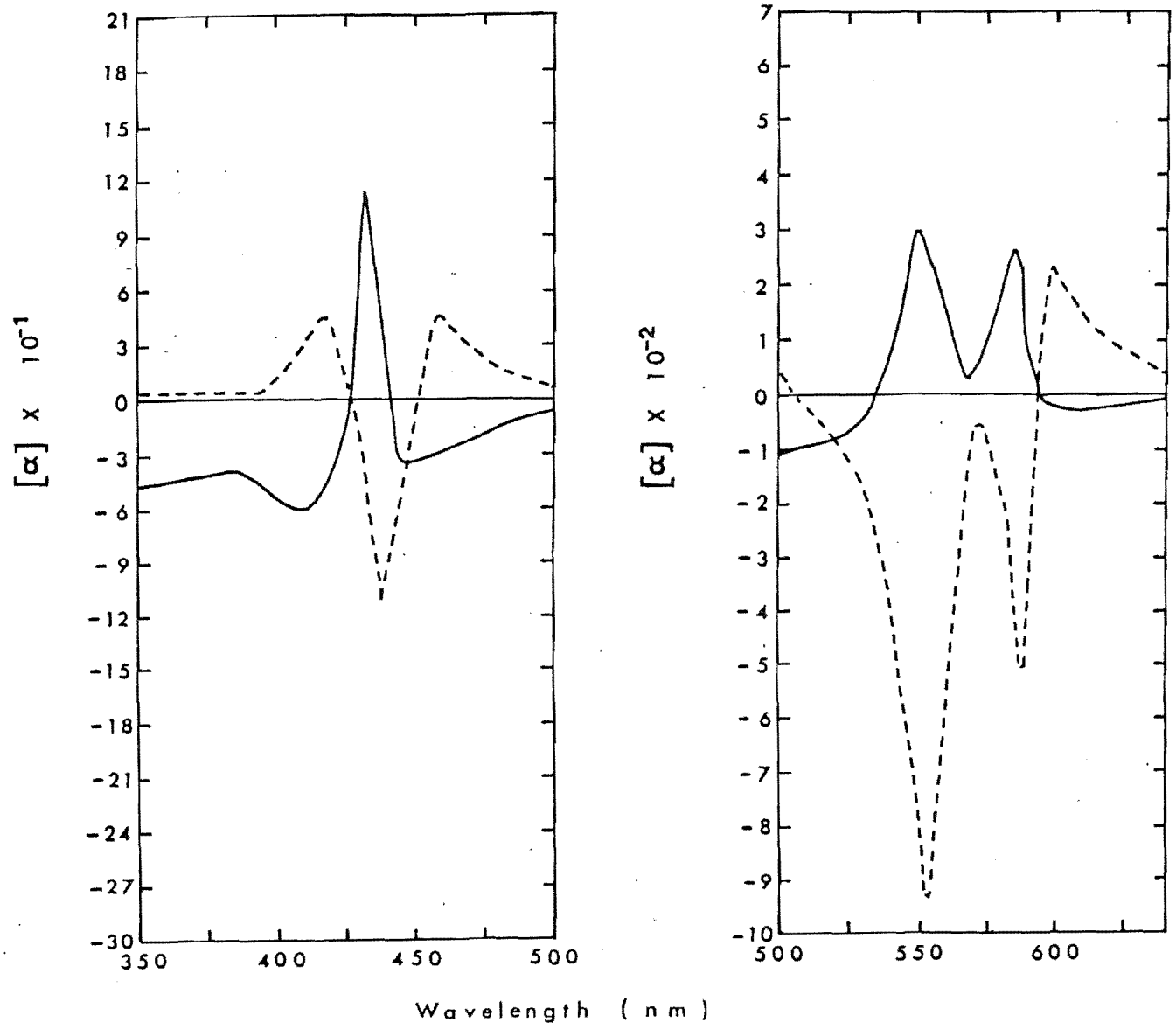

Figure 4.10 : Optical rotatory dispersion of MgMP in 0.1 M L-histidine [---] and in 0.1 M L-proline [——] redrawn to show main bands

Table 4.3 : Comparison of optical rotatory dispersion of Mg porphyrin in chiral amino acids

Chiral compounds		MgMP	MgPP
L-proline	(peaks)	584, 548, 431	601, 568, 438
	(troughs)	598, 568, 447, 412	626, 588, 445, 431
D-proline	(peaks)	598, 568, 447, 412	
	(troughs)	584, 548, 431	
L-histidine	(peaks)	597, 570, 447, 412	607, 578, 445
	(troughs)	588, 553, 435	598, 562, 435
L-serine	(peaks)	599, 566, 450, 410	
	(troughs)	586, 550, 434	
L-threonine	(peaks)	604, 564, 448, 412	
	(troughs)	580, 544, 428	

spectra of the proline solutions were observed in the visible region.

No significant extra ORD features were obtained for MgMP dissolved in solutions of L-tartaric acid, L-glutamic acid, L-cysteine, D-mandelic acid, L-malic acid, L-leucine, L-nicotine and in S(-)-2-methyl-1-butanol. MgDP in the various chiral amino acids did not produce any extra ORD features. Similarly, no extra ORD features were obtained for hemin dissolved in a solution of L-proline and L-histidine.

4.4 DISCUSSION

4.4.1 General Discussion

The multiple features observed in the Soret region of the electronic spectra indicate that the interaction of amino acids with MgMP/PP produces a variety of molecular species. Although the visible bands are generally not well resolved, the Soret peaks show the formation of a five-coordinate:six-coordinate equilibrium mixture of complexes for Mg porphyrin with amino acids. From equilibrium studies (Chapter 2), it is apparent that the lower energy band at ~433 nm is diagnostic of six-coordinate bis axial ligand magnesium porphyrin complexes. The high energy bands at ~403 nm and ~415 nm are probably diagnostic of five-coordinate MgMP/PP (nitrogenous base) species, while the third band at ~413 nm for L-serine with MgMP may indicate the formation of a six-coordinate MgMP(nitrogenous base) (H_2O) species.

All of the Mg porphyrin-amino acid complexes decompose over a period of an hour by loss of Mg to give the free porphyrin. It is likely that axial coordination, particularly

the formation of the five-coordinate (Mg porphyrin)(amino acid) complex, facilitates removal of Mg from the porphyrin rings.

Although the equilibrium constants for six-coordinate (Mg porphyrin)(nitrogenous base)$_2$ complexes are generally small [55,82], it can be seen from the CD spectra that the cross-over positions of the Soret peaks at 435 nm correspond closely to the 433 nm peak positions in the electronic spectra. Therefore, the induced Cotton effects observed may be interpreted in terms of six-coordinate (Mg porphyrin)(nitrogenous base)$_2$ entities.

Theoretical calculations for hemoproteins suggest that a fifth ligand, histidine (93, 8F) alone, does not contribute significantly to the observed induced Cotton effects [195,196]. The imidazole ring of this amino acid group is coordinated in a symmetrical manner with respect to the porphyrin ring in hemoproteins and the coordination behaviour by other amino acids in five-coordinate Mg porphyrin complexes is likely to be the same. The observation of no induced Cotton effects for (Mg porphyrin)(nitrogenous base) is therefore in agreement with this theory [195,196]. Such symmetrical bonding is also observed for comparable zinc and cobalt complexes [284].

Theoretical considerations of induced circular dichroism have identified two possible situations - one where there is a fixed mutual orientation of the chiral and achiral molecules [285-288] and another where the molecules are randomly orientated [289,290]. The large magnitude of the Cotton effects observed here suggests that the former case exists for the (Mg porphyrin)(nitrogenous base)$_2$ complexes. It may also be necessary for the two

amino acid ligands trans to each other to be bound with a particular mutual orientation for optical rotation to occur. Furthermore, it is possible that there is interaction between the side chains of the porphyrin and the amino acid. For the porphyrin, interactions can occur at the carboxylate group and at the 2,4 disubstituents. The absence of Cotton effects for MgMP dissolved in S(-)-2-methyl-1-butanol supports the suggestion that these amino acids may be bound to the carboxylate group of Mg porphyrin in a stereospecific manner because there is no additional hydrogen bonding group in S(-)-2-methyl-1-butanol. In addition, the observation that MgDP(nitrogenous base)$_2$ complexes do not produce any Cotton effects indicates that interaction between the 2,4 disubstituents of porphyrin and the amino acid is important. The overall structures of six-coordinate (Mg porphyrin) (nitrogenous base)$_2$ of this type would be comparable to that of cis-Co(en)$_2$Cl$_2^+$ [291].

By construction of 1Å = 2 cm molecular models based on unrefined bond angles and distances, it was found that for both L-serine and L-threonine, the -OH and -NH$_2$ groups have the appropriate stereochemical locations for simultaneous binding of -NH$_2$ to the metal and hydrogen bonding of the -OH to the carboxylate (-COO$^-$) sidechains of the magnesium porphyrin entities (Figure 4.11). Coordination through -NH$_2$ is preferred as it would be a stronger donor than -OH to metal ions. L-threonine has an additional chiral carbon centre arising from the substitution of CH$_3$ for H when compared with L-serine. This centre is further away from the porphyrin ring and its effect on CD/ORD spectra is expected to be small. However, the results show that this carbon centre does influence the

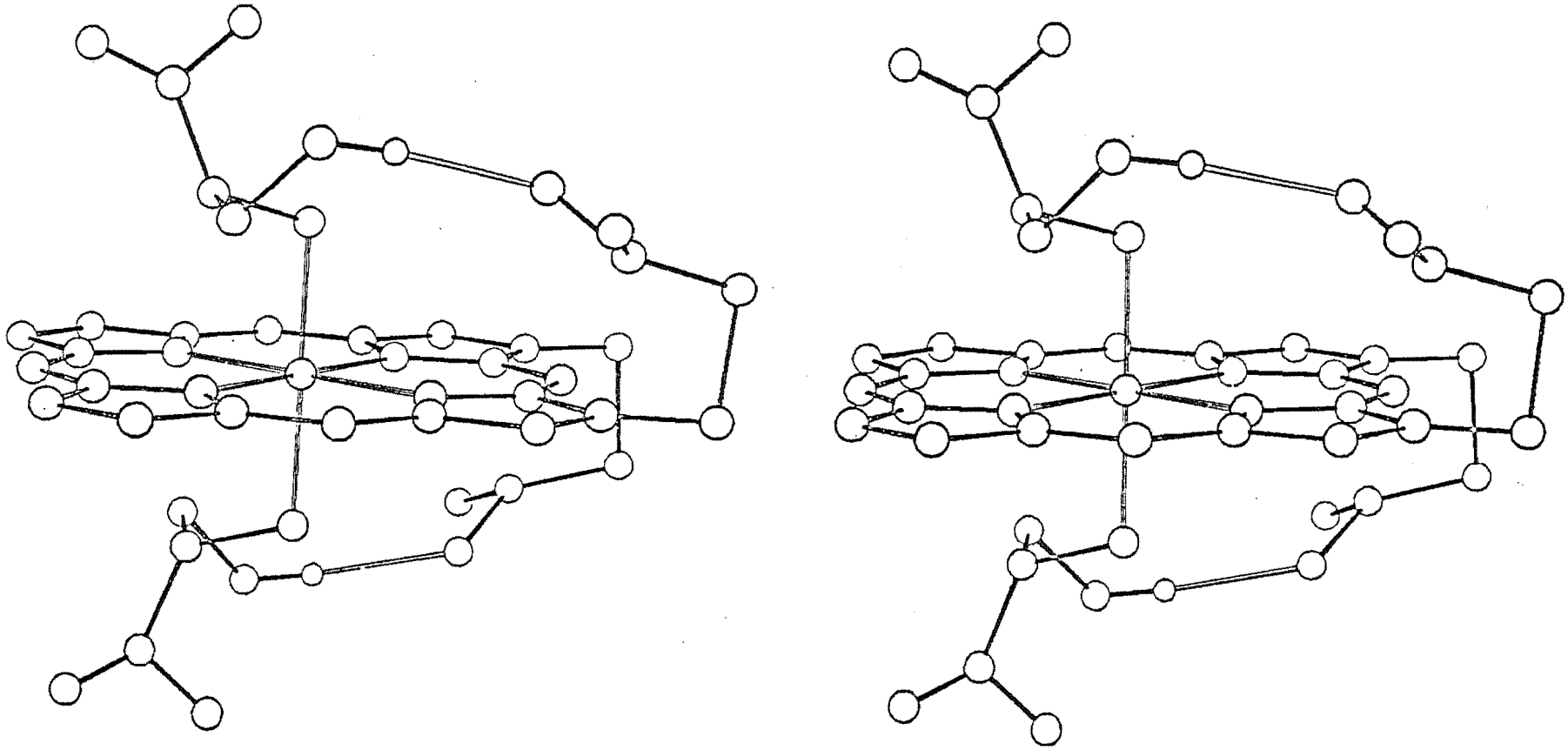

Figure 4.11 : MgMP(L-serine)$_2$ to show the effect of hydrogen bonding of the amino acid -OH group to the $-COO^-$ porphyrin side chain in locating the coordinated amino acid groups (Stereoscopic view)

Cotton effects to some extent (Figure 4.7). It is possible that coordination occurs at the $-COO^-$ group, rather than $-NH_2$, because of the basic conditions used. In order to check this possibility, studies were made of the interaction of D-mandelic acid and L-malic acid. However, no significant Cotton effects were observed, although this does not conclusively eliminate the carboxylate coordination possibility as an additional interaction for fixing the positions of the ligands.

L-proline, an important biological neurotransmitter [292] and catalyst for induction of asymmetry [293], is unique as it is the only amino acid for which a new asymmetric centre is formed when it is coordinated to a metal ion. Molecular models show that the opposite chirality is produced to that existing at the asymmetric carbon centre, already present in the five-membered ring, because of steric interactions between the COO^- group and the porphyrin ring (Figures 4.12, 4.13, 4.14 and 4.15). There were no distinct changes in the CD bands for different preparations of Mg porphyrin. When the chirality of the carbon centre is altered, the ORD and CD spectra invert as expected. It is of interest that the induced Cotton effect for proline coordinated to Cu^{2+} is also inverted with respect to that observed for other amino acids of the same chirality [294-296]. An analogous explanation has also been proposed for the Cu^{2+} compounds [297-300]. However, for Mg porphyrin, monodentate coordination in the axial position is expected rather than the bidentate type considered for Cu^{2+}. The results for proline appear to be interpretable only in terms of binding through the nitrogen atoms. The new chiral nitrogen centres are close

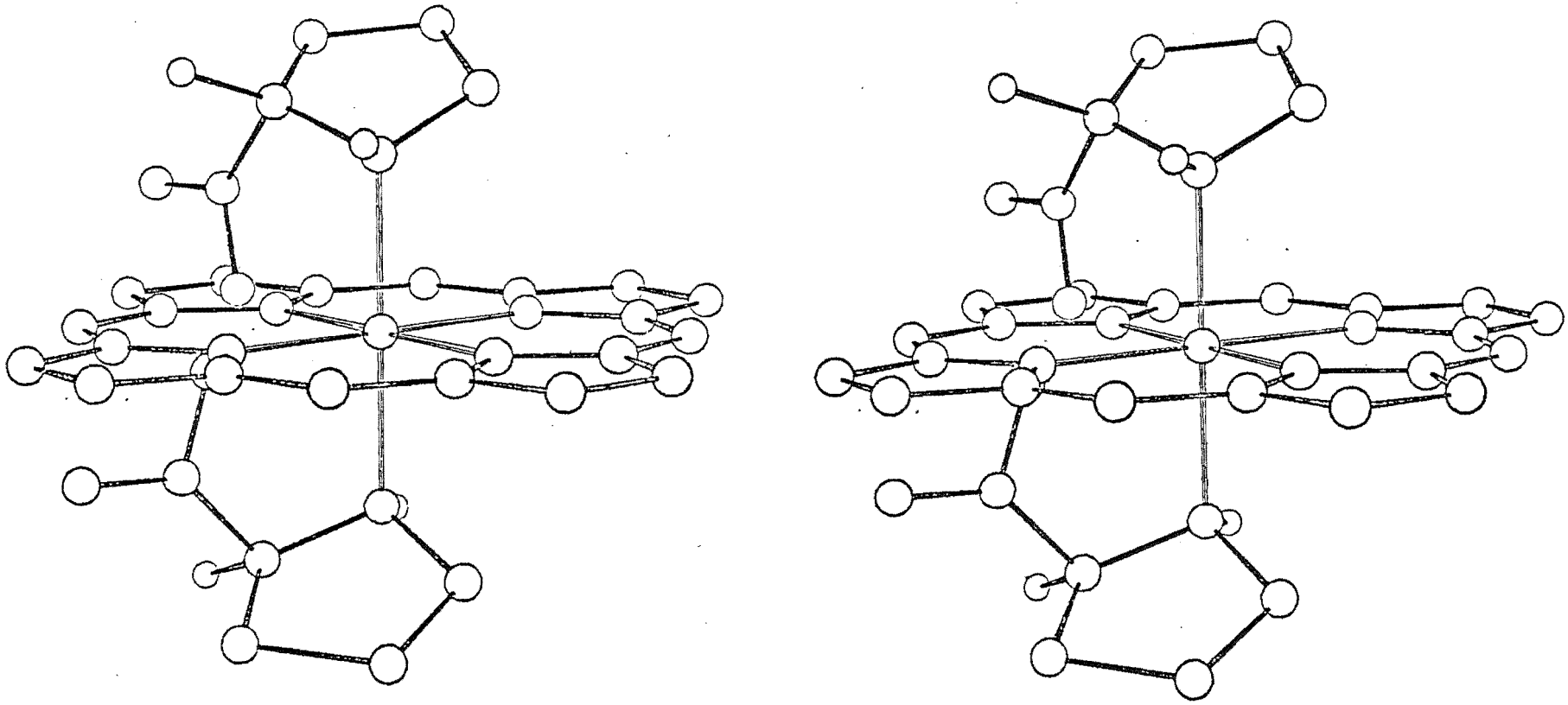

Figure 4.12 : Stereoscopic view of a model of MgMP(L-proline)$_2$ to show that steric interactions prevent the formation of nitrogen coordination with L-chirality at that atom

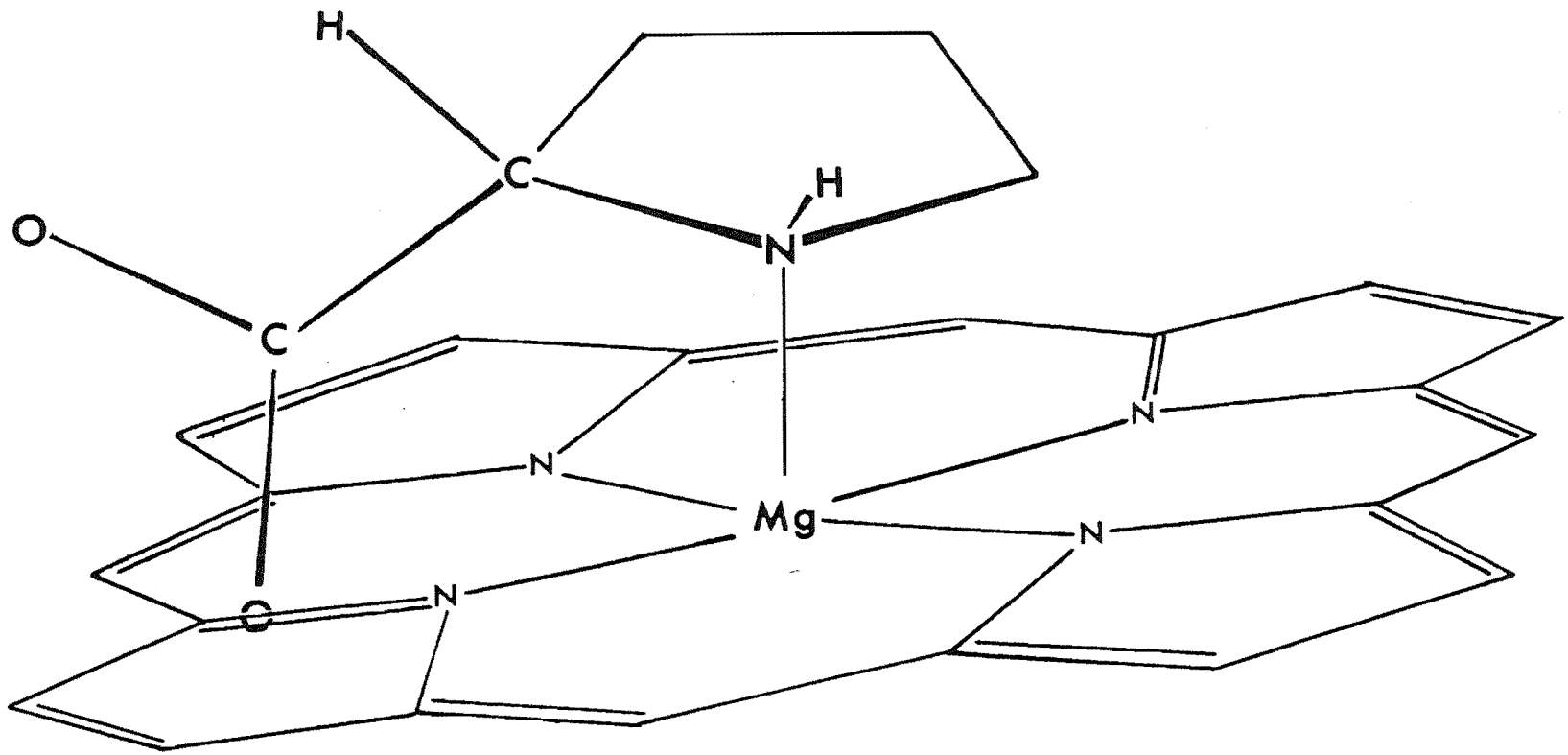

Figure 4.13 : Diagram illustrating steric interactions which prevent the formation of nitrogen with L-chirality at that atom

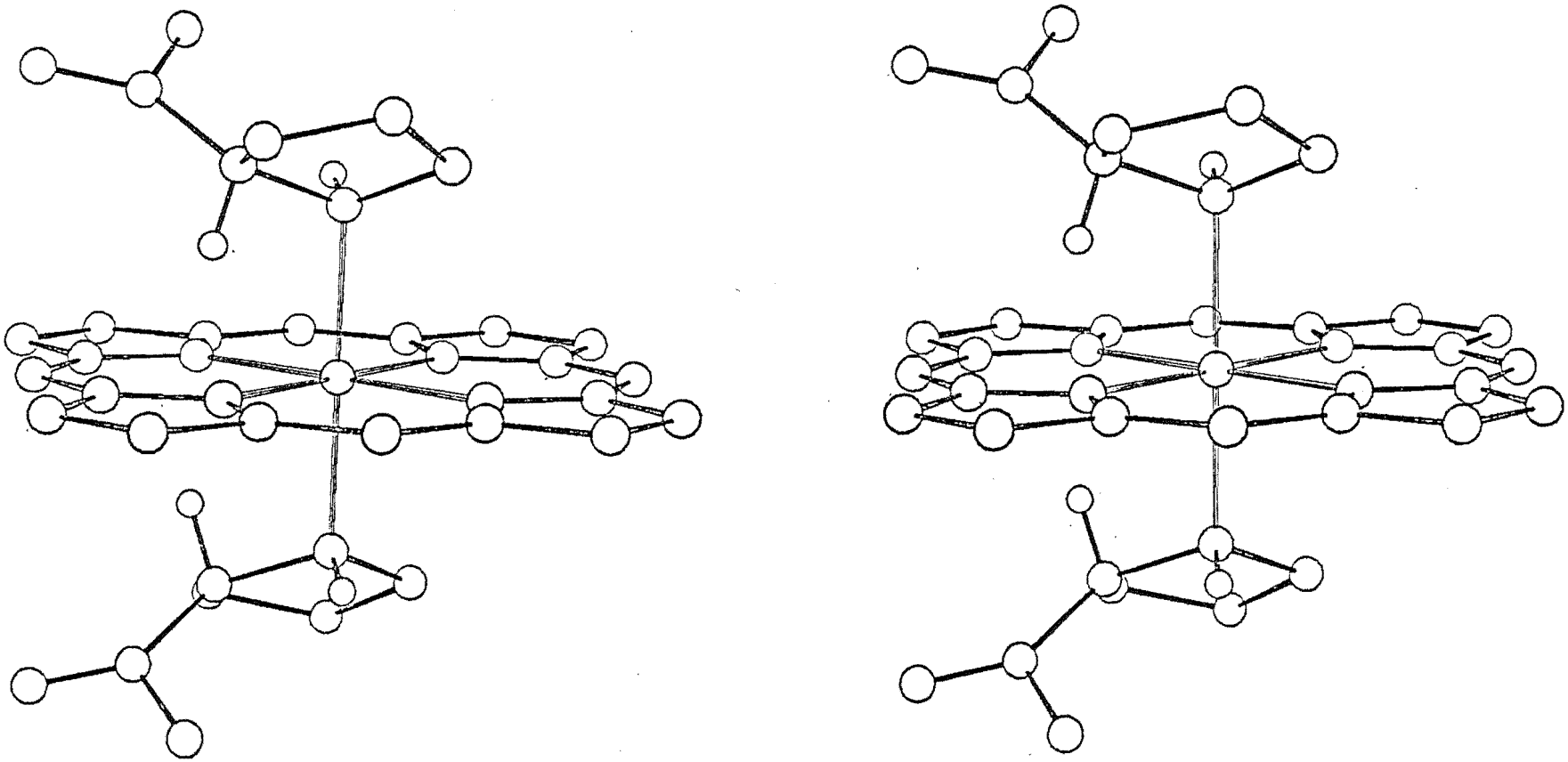

Figure 4.14 : Stereoscopic view of a model of MgMP(L-proline)$_2$ to show formation of D-chirality at the coordinated nitrogen atom for a stereochemically acceptable structure

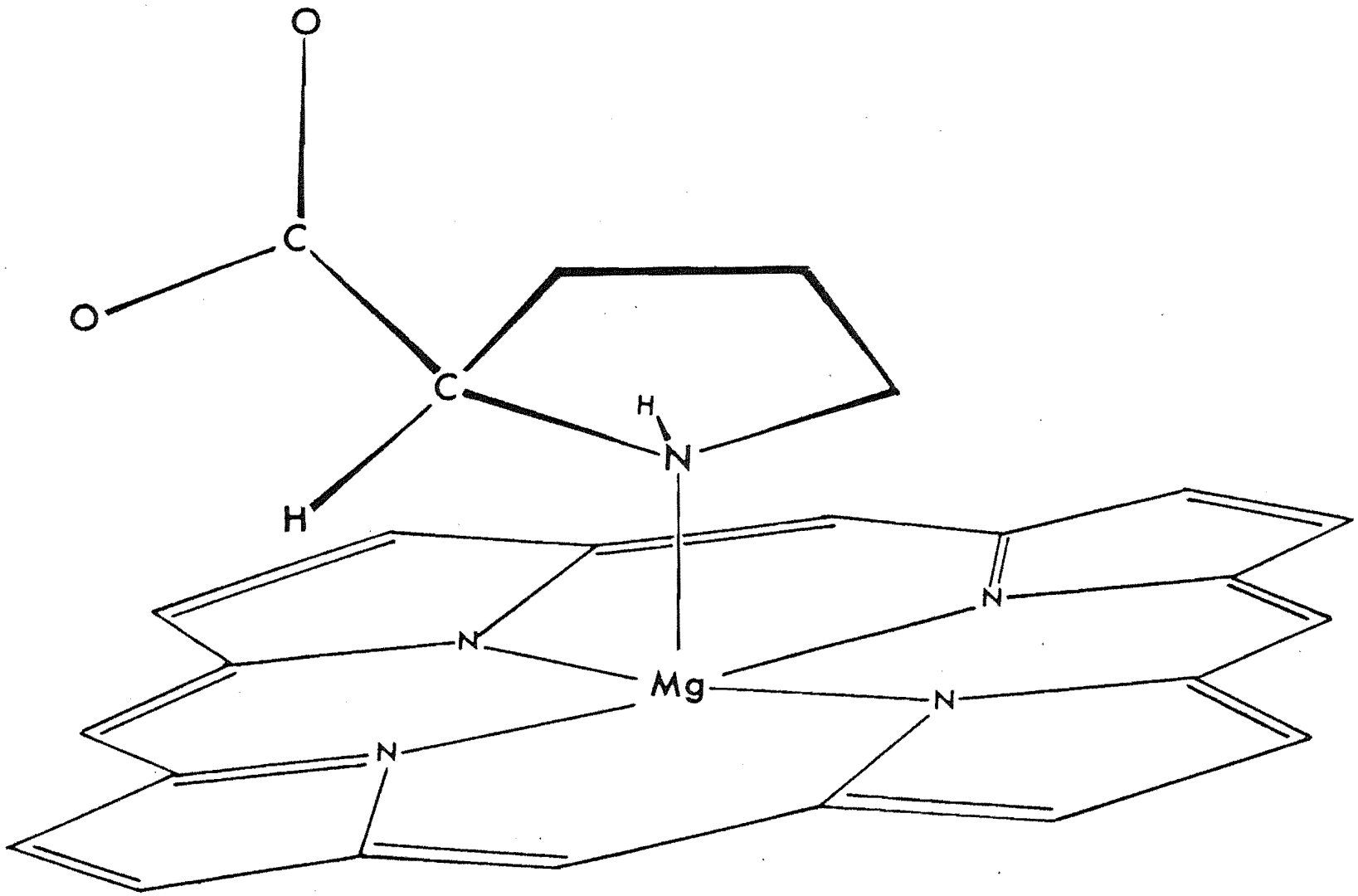

Figure 4.15 : Diagram illustrating the formation of D-chirality at the coordinated nitrogen atom for a stereochemically acceptable structure

to the Mg porphyrin and can interact with the π electrons of the ring. It is not clear how this electronic interaction occurs but the empty 3d orbitals of Mg may be important. Recent NMR results show that there is electronic interaction between the amino acid and the 2,4 disubstituents of porphyrin [301].

In the case of L-tryptophan, where a weaker Cotton effect is observed, stacking interactions can possibly provide a localising effect. A molecular model study showed that there is a favoured 3.4Å stacking distance between the indole and the porphyrin groups, for $-NH_2$ binding to the metal atom.

For L-histidine, X-ray studies of six-coordinate (Mg porphyrin)(1-methylimidazole)$_2$ indicate that there is mutual orientation of the ligands (Chapter 6). This orientating effect is likely to be the major localising factor and other secondary factors like hydrogen bonding between L-histidine and the carboxylate groups of the porphyrin could also be important. The absence of comparable Cotton effects for corresponding solutions of ferric, ferrous and manganic porphyrin may be due to some advantage that a magnesium (II) d^o configuration has over an ion having d electrons. Thus, the orientating interactions are possibly between the histidine ring and the empty 3d orbitals of Mg.

The reversal of the signs for the Cotton effects of (Mg porphyrin)(L-histidine)$_2$ and (Mg porphyrin)(L-threonine)$_2$ may be a result of crystallisation. During the crystallisation of Mg porphyrin, different forms of crystals can be formed. The crystal packing will then influence the orientation of the carboxylate groups with respect to the

porphyrin ring. When these crystals are dissolved in the amino acid solutions, hydrogen bonding between the amino acid and the carboxylate group ($-COO^-$) of the porphyrin is possible. This bonding could give rise to optical isomers (like those for cis $Co(en)_2Cl_2^+$) which show opposite Cotton effects, depending on the preferred orientation of the carboxylate groups. For (Mg porphyrin)(L-proline)$_2$ complex which has no such hydrogen bonding, the observation of only one type of Cotton effect is consistent with this interpretation.

It was observed that the ease with which Mg is removed from the porphyrin ring is related to the photosensitive nature of the solutions and these results are reported in Chapter 5. Furthermore, the observation that the intensities of the ORD and CD transitions are markedly reduced at elevated temperature shows that these Cotton effects are indeed a result of six-coordinate Mg porphyrin species where a lower temperature favours the second equilibrium constant (Chapter 2). X-ray studies of such six-coordinate (Mg porphyrin)(nitrogenous base)$_2$ complexes support the suggestion that the nitrogen atoms are coordinated to Mg (Chapter 6). Although these complexes are of limited stability, the existence of marked Cotton effects enables detailed studies of six-coordinate Mg porphyrin complexes to be selectively carried out. This kind of study could be extended to other asymmetric ligands which bind to axial positions in an equilibrium mixture of five- and six-coordinate complexes.

4.4.2 Comparison of Induced Cotton Effects in Mg Porphyrin-globin and (Mg Porphyrin)(L-histidine)$_2$ Complexes

The observation of induced Cotton effects for corresponding protein and non-protein systems of Mg porphyrin complexes enables a detailed comparison to be made between the two systems (Figure 4.16). In both cases, the CD/ORD rotation may be understood in terms of the coupled oscillator mechanism, but significant differences are observed in the Soret region. These results support earlier studies which showed that L-histidine containing peptide complexes do not model apomyoglobin well [302].

For the non-protein Mg porphyrin complex, it has been suggested that localised L-histidine ligands give rise to the observed Cotton effects (Section 4.4.1). Similarly, for the naturally occurring hemoproteins, the location of comparable asymmetric entities trans to the bound histidine (such as the distal histidine in myoglobin and hemoglobin) may be important for the production of coupled rotational effects. Theoretical calculations by Hsu and Woody appear to support this suggestion [195,196]. The magnitude of the rotation in the Soret region for (Mg porphyrin)(L-histidine)$_2$ complex, is at least three times greater than that for the corresponding hemoproteins. This is possibly due to the second asymmetric entity being significantly closer to the metal ions in the former case.

The protein and non-protein species also differ from each other with respect to the details of molecular asymmetry. For the protein case, coupling is likely to occur between the heme π-π^* transitions and the amino acids that are asymmetrically oriented with respect to the heme group. In the non-protein six-coordinate complexes, the two

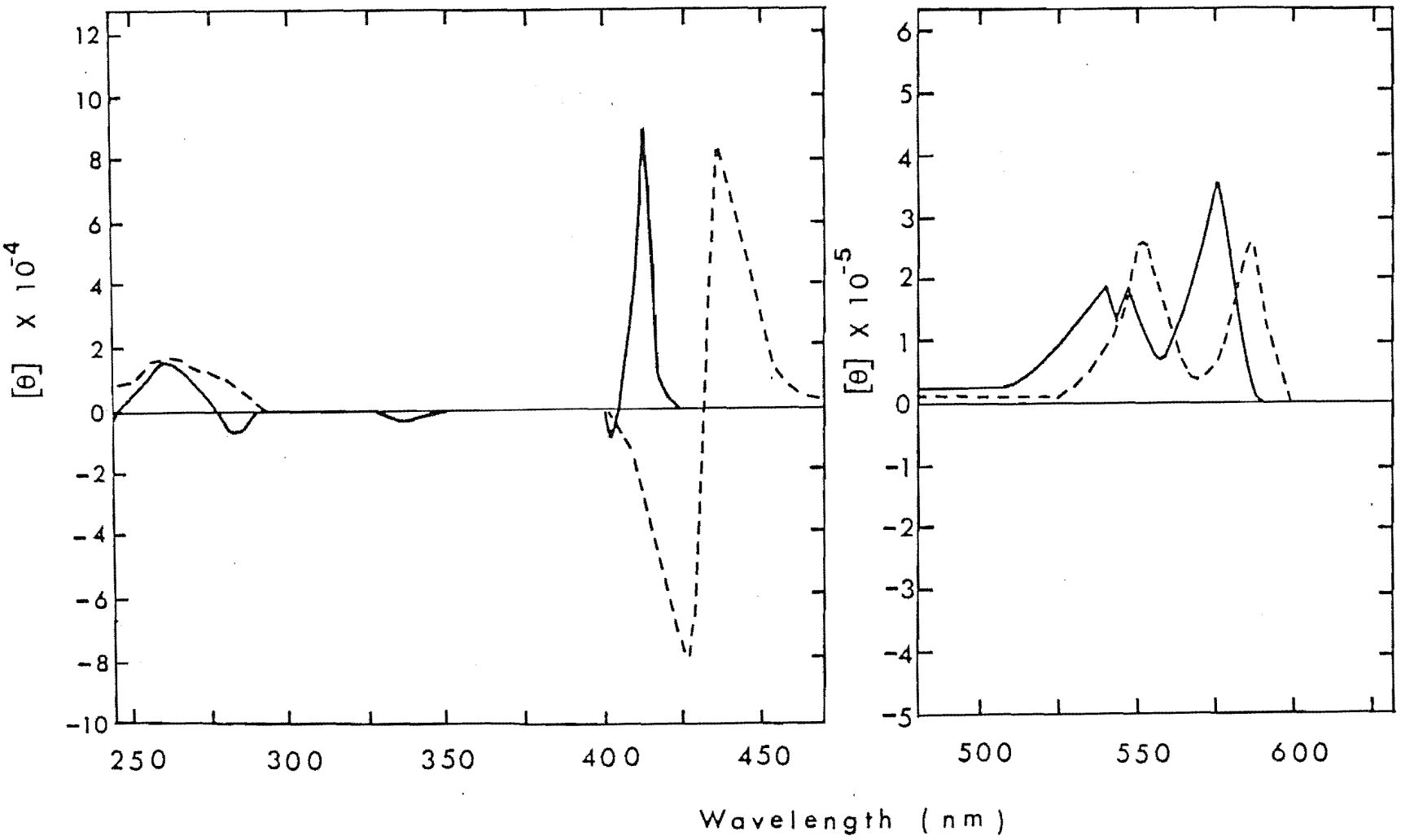

Figure 4.16 : Circular dichroism spectra of MgMP in 0.2 M L-histidine [---] and MgMP-Hb [——] redrawn to show main bands

histidine ligands, while being asymmetric, will be bound in equivalent positions trans to each other. This is possibly the reason for the more symmetrical nature of the CD bands observed in the Soret region for these non-protein complexes, compared to the corresponding bands of the magnesium porphyrin-globin complexes.

The asymmetrical "couplet" form of the ORD spectrum in the Soret region of (Mg porphyrin)(L-histidine)$_2$ complex, is characteristic of entities having degenerate or near degenerate electronic transitions (Figure 4.9) [270]. Neglecting the sidechains, the porphyrin ring is symmetrical and the Soret band is doubly degenerate [195,196]. The resolution of this degeneracy is probably greater for the protein species where the local metal site symmetry is likely to be lower than for the non-protein complexes. This is substantiated by the more complex ORD spectra of the protein species.

Thus this comparison shows that the Cotton effects observed are dependent on the details of the coordination sphere around Mg porphyrin including the relative positions and orientations of the amino acids to Mg porphyrin.

4.4.3 Comparison of CD Spectra of (Mg Porphyrin)(Amino Acid)$_2$ Species and Model Compounds of Chlorophyll-protein Complexes

The CD spectra of model compounds of chlorophyll-protein complexes have been of particular interest because they help to elucidate the effects of protein environment (see Section 3.4.4).

Pearlstein and coworkers have reconstituted chlorophyllide with apomyoglobin and they observed three different

complexes [17]. Two of these complexes display red-shift, non-conservative and intense CD spectra which are different from those observed in hemoglobin and myoglobin. These complexes have more than one mole of chlorophyll per mole of apomyoglobin and their spectra were similar to those in the photoreaction centre from purple photosynthetic bacteria. Pearlstein and coworkers suggested that this CD effect was due to aggregated chlorophyll molecules with six-coordinate Mg centres [17]. The red-shifted and intense CD bands observed for (Mg porphyrin)(amino acid)$_2$ appear to support this suggestion. It shows that six-coordination red-shifts the spectra significantly and the coupling of a second amino acid or chlorophyll is essential for the production of intense CD bands (Section 4.4.2).

Boxer and coworkers have observed that the triplet lifetime of pyrochlorophyllide-Mb complexes lies between the values of five- and six-coordinate pyrochlorophyllide [14]. They suggest that a water molecule or the distal histidine can possibly form a weak bond to the Mg centre of pyrochlorophyllide. The results for (Mg porphyrin)(L-histidine)$_2$ suggest that if the pyrochlorophyll interacts with the distal histidine, intense and red-shifted CD bands can be observed. However, these effects were not present for the pyrochlorophyllide-Mb complexes, indicating axial coordination of two chiral histidine groups is therefore unlikely. Consequently, weak interaction by a water molecule appears to be the more favourable possibility, as also suggested in Chapter 3.

It is possible that in the photosynthetic system, amino acid residues could form π-complexes with the

chlorophyll molecules [303]. The weak CD spectrum observed for the MgPP(L-tryptophan)$_2$ complex, which has been suggested to be due to stacking arrangement, indicates that the formation of π-complexes does produce a very weak CD spectrum. However, this formation can still affect the overall transitions of the chlorophyll molecules. This result is consistent with the theoretical calculations which showed that amino acids as far as 12Å can couple to the transitions of the heme [195,196] but the effect may be small.

The observation of six-coordinate (Mg porphyrin) (amino acid)$_2$ complexes suggests that the Mg ion can be coordinated at both axial positions. Equilibrium studies show that this effect is also found in chlorophyll molecules *in vitro* (Chapter 2). This effect is absent in Zn complexes of porphyrin and chlorophyll because the maximum coordination state for such complexes is five (Section 2.4.2).

The overall results indicate that in Mg porphyrin systems, the formation of six-coordinate Mg centres having two ligated chiral amino acids produces significant red-shift and intense CD spectra. The same type of mechanism may be important for photosynthetic systems.

CHAPTER 5

PHOTOCHEMISTRY OF MAGNESIUM PORPHYRIN-GLOBIN AND MAGNESIUM PORPHYRIN-AMINO ACID SPECIES

5.1 INTRODUCTION

The effect of light on porphyrins and their metal complexes has been of general interest because of its relevance to the photochemistry of biological systems [304, 305] and because of the photosensitizing properties of these complexes [306-310]. Recent studies show that some metalloporphyrins are efficient photosensitizers for the cleavage of water to produce hydrogen in the presence of light [311,312]. One of these metalloporphyrins, MgPP, has been of considerable interest because it is also the first metabolic precursor committed to the biosynthesis of chlorophyll [313]. Most of the photochemistry of MgPP has been studied in hydrophobic solvents to biomimic the hydrophobic environments in cell membranes of plants interacting with MgPP [305,314]. These studies have shown that in the presence of light, photo-oxidised products were formed rapidly [315-317]. Other possible models for the natural hydrophobic environments are the heme proteins.

Mb and Hb proteins can be considered to be ideal models for hydrophobic environments as X-ray studies and amino acid sequence determinations show that the heme pockets of both proteins consist of a large number of hydrophobic groups [88,144,145]. In addition, X-ray studies on *Prosthecochloris aestuarii* show that most of the Mg atoms in bacteriochlorophylls are coordinated to

histidine groups [3-7], as established for Mb and Hb. Thirdly, both proteins do not absorb in the visible region and they occur naturally in biological systems.

The distinct differences in the shapes and absorption maxima of the bands of Mg porphyrin-Mb and Mg porphyrin-Hb have been highlighted in Chapter 3 and it was suggested that the Mg porphyrin environments in the two proteins were different. In this chapter, the effects of various light sources on Mg porphyrin-Mb, Mg porphyrin-Hb and (Mg porphyrin)(amino acid)$_2$ species are reported. Distinct differences in the photodecomposition patterns for all three species were observed. These highlight the role of environmental effects on the photochemistry of Mg porphyrin. The differences in photochemistry between Mg porphyrin-Mb and Mg porphyrin-Hb are then correlated with corresponding spectral differences of the non-irradiated complexes in an attempt to elucidate the reasons for the observed differences.

The possibility of selective photodecomposition of Mg porphyrin-racemic amino acid mixtures, using circularly polarised light is also discussed.

5.2 EXPERIMENTAL

MgPP-Mb, MgMP-Mb, MgDP-Mb, MgPP-Hb, and MgMP-Hb were freshly prepared according to methods described in Chapter 3. Fresh solutions of basic MgMP and MgPP in various chiral amino acids were also prepared according to procedures reported in Chapter 4. Photolyses were carried out by placing either (1) an ultra-violet or (2) an ordinary projector lamp or (3) a Philips infra-red source two metres away from the Mg porphyrin-globin species

which were kept at 0°C to 4°C. The changes in pH were carried out by dialysing the Mg porphyrin-globin species against the required pH which was determined by a pH meter.

The photochemical decomposition of magnesium porphyrin-racemic amino acid species using laser circularly polarised light was studied using the set-up shown in Figure 5.1 The racemic amino acids used were DL-histidine and DL-threonine, and each sample was irradiated for a different period of time. After irradiation, the sample was filtered and examined for any CD/ORD rotation using a Jasco ORD UV-5 spectrophotometer. A 1.0 Watt continuous wave argon ion laser source (λ=457.9 nm) was used for this photolysis study.

All the electronic absorption spectra were recorded on a Varian Superscan 3 UV-visible spectrophotometer. Before the photolysis experiments were performed, all apparatus and reagents were kept away from strong light and covered by aluminium foil. DL-histidine and DL-threonine were purchased from EGA-CHEMIE.

5.3 RESULTS

Irradiation of MgPP-Mb and MgPP-Hb for over 50 hours under infra-red light showed no extra bands in the electronic spectra. Ultra-violet light photodecomposed Mg porphyrin-Mb and Mg porphyrin-Hb rapidly and the products showed a band at 630 nm. No isosbestic points were observed. By contrast, ordinary projector light affected the spectra of Mg porphyrin-Mb and Mg porphyrin-Hb only after a long period of irradiation. Under similar conditions, ordinary light rapidly photodecomposed a solution of five-coordinate (Mg porphyrin)(pyridine) in

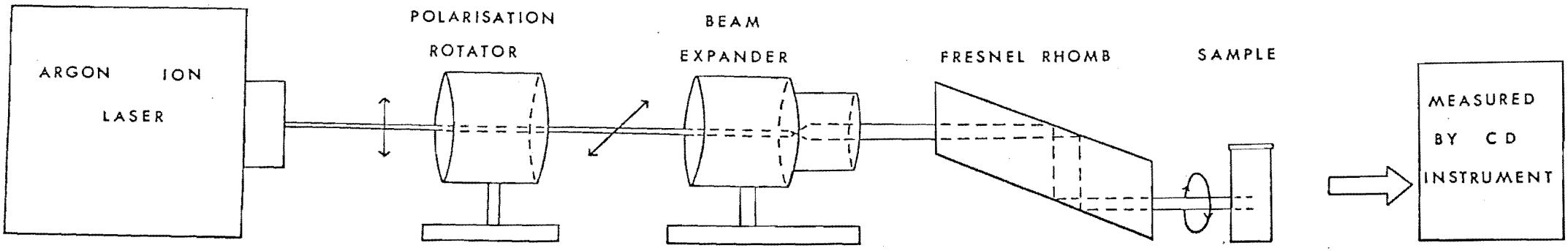

Figure 5.1 : Experimental set-up for irradiation studies with circularly polarised light

benzene. However, the rate was still slower than that of Mg porphyrin in benzene.

Visible light blue-shifted the Q_o band of Mg porphyrin-Mb species with concomitant photodecomposition (Table 5.1).

Table 5.1

Spectral properties of the Q_o band for the various Mg porphyrin complexes

Complex	Position of the Q_o band	
	Before irradiation	After irradiation
MgPP-Mb	598,590 (sh)	590
MgMP-Mb	585,574	578
MgDP-Mb	582,572 (sh)	578

sh = shoulder

Figure 5.2 shows the more complex photodecomposition pattern observed for the Mg porphyrin-Mb species. At pH 11 or higher, the Q_o band changes faster than at pH 7. For Mg porphyrin-Hb species, the photodecomposition pattern is less complex with no shift in the Q_o band being observed (Figure 5.3).

Irradiated Mg porphyrin-Mb and Mg porphyrin-Hb species, kept in the dark at 0°C and monitored over a month, did not produce by a reverse reaction, the original positions of the non-irradiated bands.

Mg porphyrin-racemic amino acid species show no rotation in their spectra. The photodecomposed products

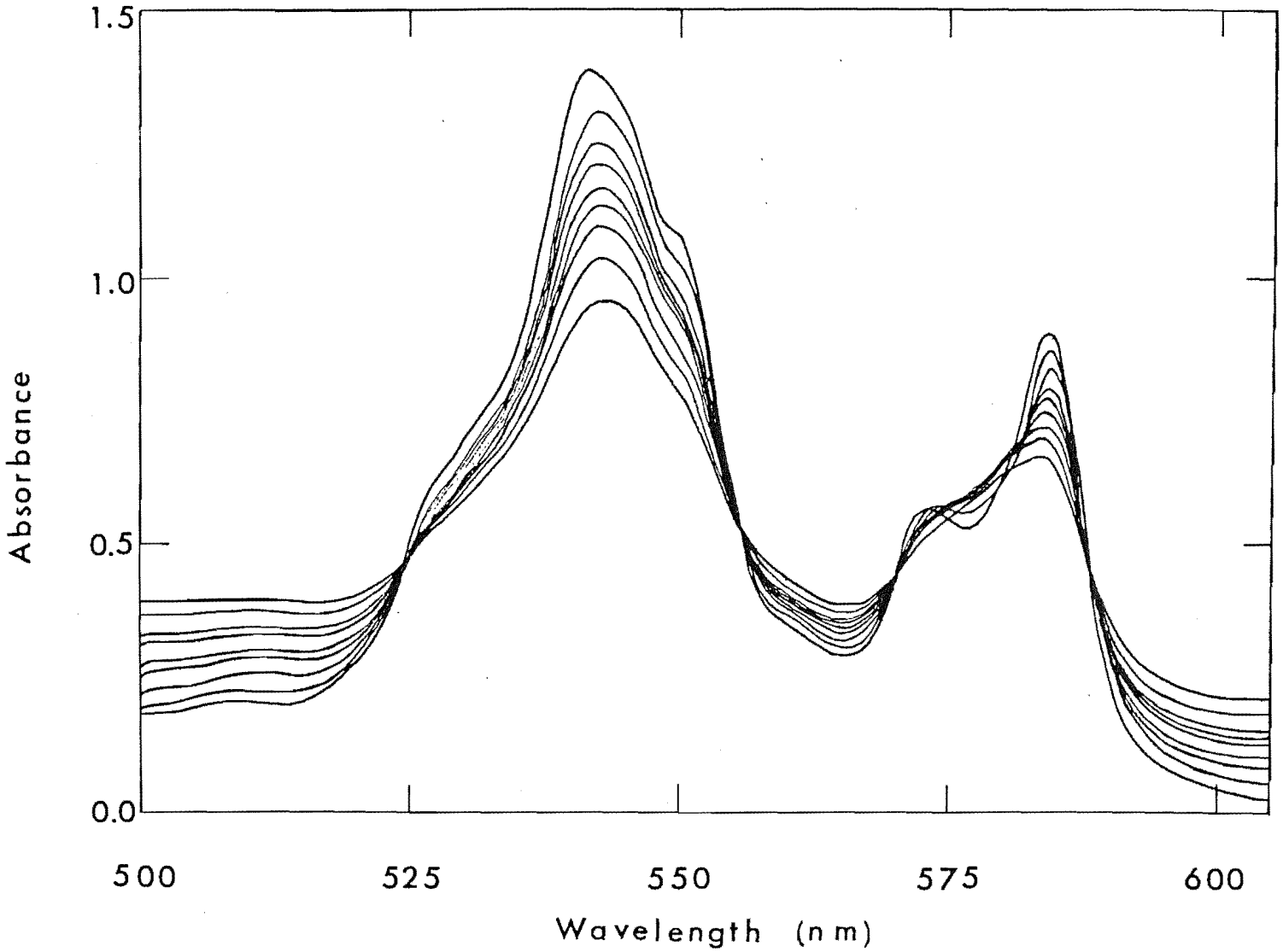

Figure 5.2 : Photodecomposition of the visible bands of MgMP-Mb at pH = 7.0

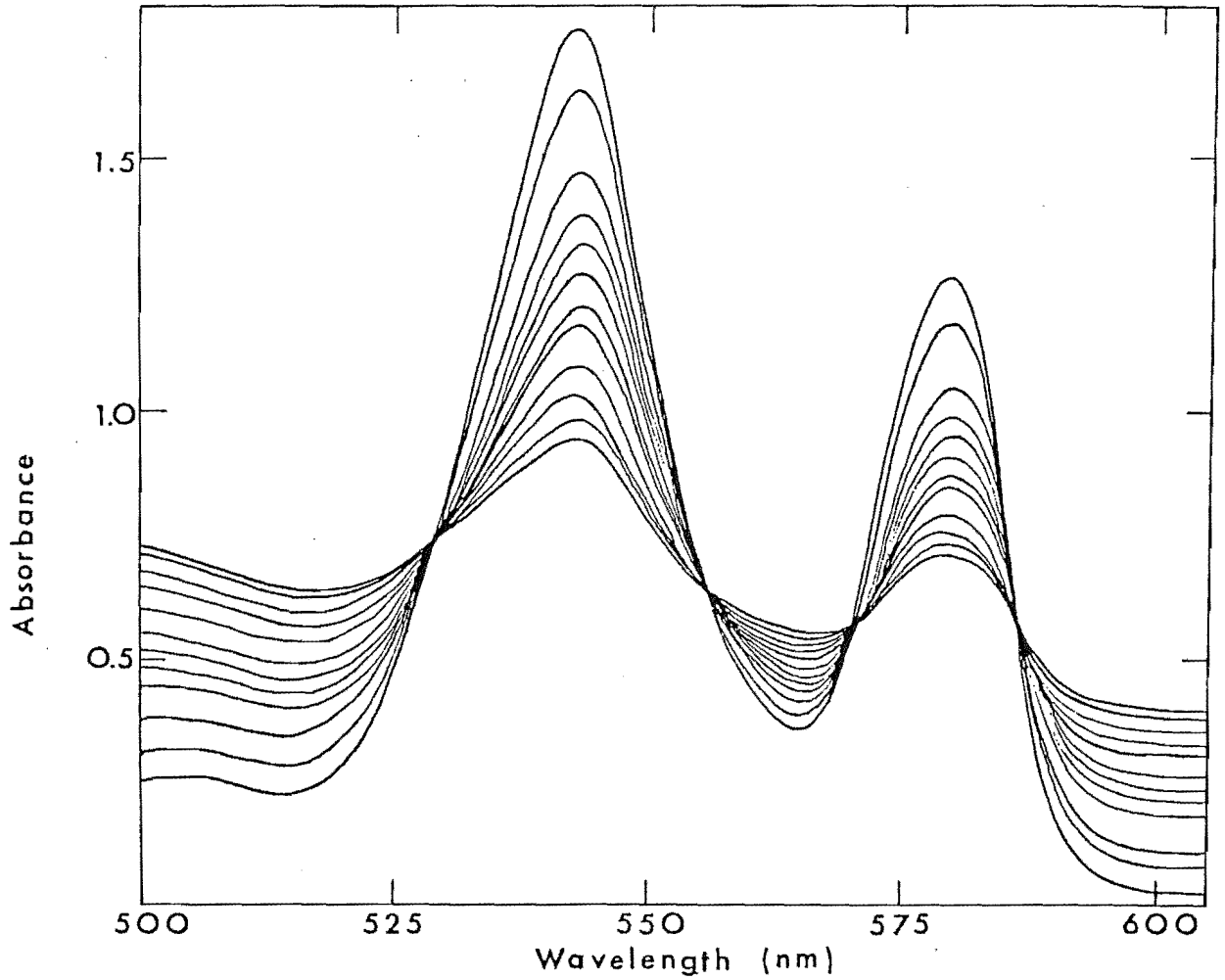

Figure 5.3 : Photodecomposition of the visible bands of MgMP-Hb at pH = 7.0

also showed little rotation except for two samples of Mg porphyrin-DL-histidine where CD rotation was observed around 400 nm (Figure 5.4). Longer periods of irradiation rapidly diminished the CD rotation effect.

5.4 DISCUSSION

5.4.1 Photochemical Reactions of Mg Porphyrin-globin and Mg Porphyrin-(L-amino acid) species

It has been suggested that the photochemical activity of chlorophyllin and chlorophyll are enhanced when they are bound to higher molecular weight polymers [318]. Addition of such a polymer, polyvinylpyrrolidone, to chlorophyllin (also called Mg chlorin e_6) in the dark, indeed showed an extra band at 688 nm and its formation was further enhanced when irradiated with red light [319]. It was then suggested that this band was a result of the formation of dimeric chlorophyllin species, as observed in concentrated alcoholic solutions [320]. However, recent studies of chlorophyllin-Mb species also showed this band after irradiation with red light [16]. It was then suggested that this band was due to a specific chlorophyllin-protein interaction, but similar spectral changes were observed during the photolysis of protein-free chlorophyllin in methanol [12]. This band was postulated to arise from the formation of a photodecomposed product [12]. The absence of this band when Mg porphyrin-globin species are irradiated with different sources of light, suggests that the photochemical properties of Mg porphyrin are different from those of chlorophyllin.

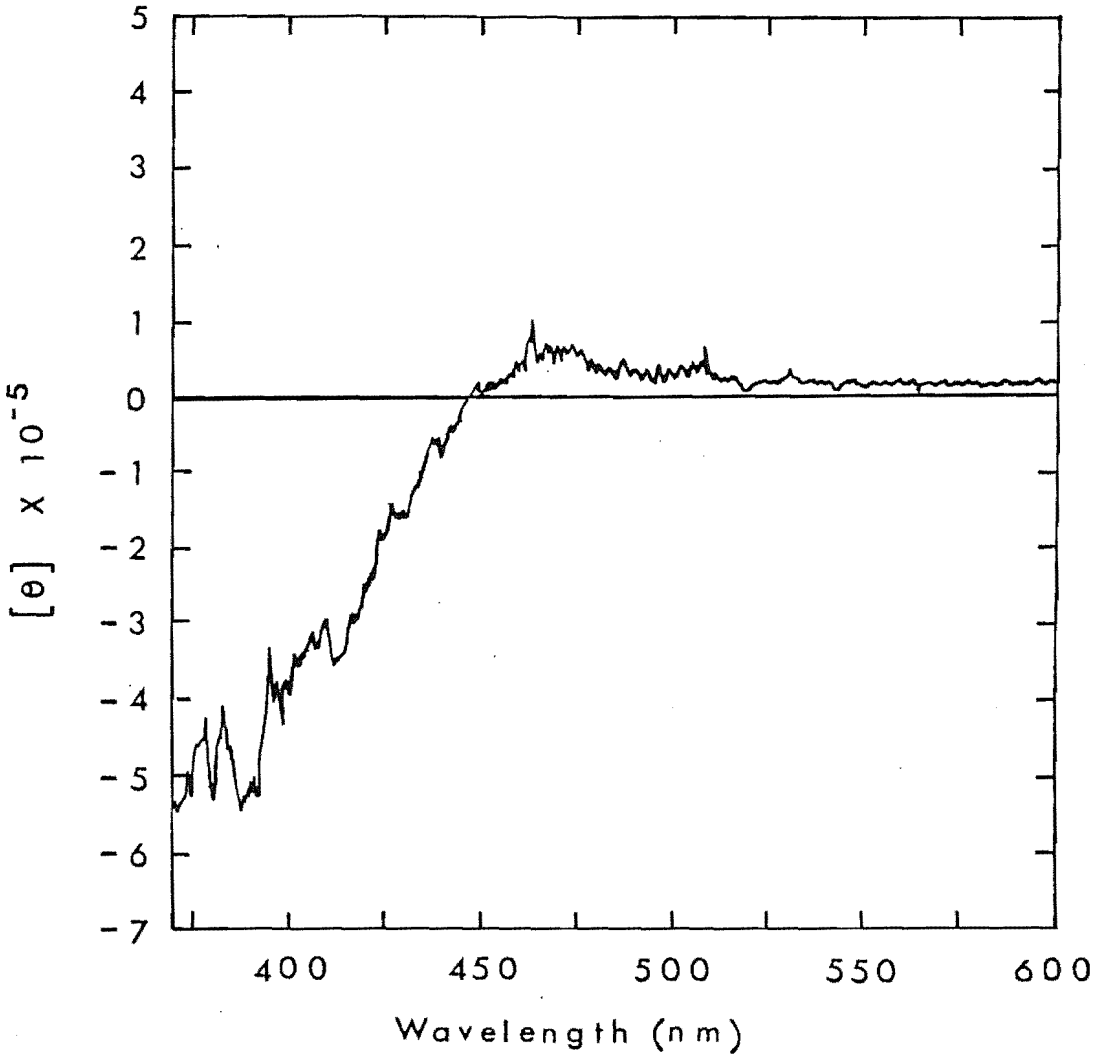

Figure 5.4 : Circular dichroism spectra of magnesium porphyrin-DL-histidine solution after irradiation with circularly polarised light

A comparison of the photodecomposition patterns of Mg porphyrin-globin and (Mg porphyrin)(amino acid)$_2$ species strongly supports previous spectral studies showing that Mg porphyrin is fully incorporated into the heme pocket and not loosely bound to the exterior of the protein (Chapter 3).

The photolysis decomposition pattern of Mg porphyrin-Mb is complex, indicating the decomposition is possibly sequential, A→B→C. The main band of the Q_o transition appears to go initially to a single band and the position of this band is similar to that of five-coordinate Mg porphyrin-Hb (A→B). The observation of a single initial A→B photoreaction implies that A is a single species in spite of the multiple band character of its absorption spectrum. For Mg porphyrin-Hb, there appeared to be one single reaction, B→C. These results correlate well with previous spectral studies which showed that the environments around Mg porphyrin in Mb and Hb are different.

Two possible reasons may be cited for the initial A→B reaction of Mg porphyrin-Mb species: (1) conformational change in the protein and (2) change in the coordination state of Mg. It has been shown that the heme pocket of myoglobin is more hydrophobic that of hemoglobin [88,144,145]. Light energy absorbed by Mg porphyrin could be transmitted through the proximal imidazole group to the polypeptide chain, thereby producing some conformational changes. These could lead to a decrease in the hydrophobicity of the Mg porphyrin environment and thus produce the spectral changes [222].

The second possibility is that Mg porphyrin-Mb is six-coordinated, having a water molecule bound in the sixth

position (as considered in Chapter 3). Light absorbed by this species could dissociate the sixth ligand from the Mg atom, in a similar manner to that observed for MbCO [248] to produce a five-coordinate Mg porphyrin species which is blue-shifted.

The second possibility appears to be more likely. The bands after irradiation correspond to the positions of five-coordinate Mg porphyrin and show no splitting, whereas the bands before irradiation show splitting characteristic of related six-coordinate entities (Chapter 3). Furthermore, equilibrium studies show that six-coordination is obtained only in suitable conditions (Chapter 2). Under the influence of light, it is possible for Mg porphyrin to photodissociate to the more stable five-coordinate state. This type of blue-shift is also observed during the photo-oxidation of antenna bacteriochlorophyll from mutant *Rhodopseudomonas sphaeroides* and it is irreversible [321]. This shift has been suggested to be a result of the conversion of the dimeric to monomeric bacteriochlorophyll. However, Mg porphyrin-Mb species do not exist as dimers and the changes in the bacteriochlorophyll of *Rhodopseudomonas sphaeroides* may not therefore be due to dimer-monomer changes.

The irreversible photo-oxidation of Mg porphyrin-globin species suggests that the proteins are denatured at the end of the photochemical reactions, B→C. It is possible that the proximal histidine is affected and the greater photo-oxidation rate of magnesium complexes compared to hemin suggests that a shorter irradiation time is required for such photochemical studies [322-324]. Consequently, Mg porphyrin could be considered to be another substitute for protoporphyrin as a photosensitizing probe of the active sites of hemoproteins [325,326].

5.4.2 Comparison of Photochemical Reaction of Mg Porphyrin in Hydrophobic Solvent and Mg Porphyrin-globin species

Photochemical studies of Mg porphyrin in hydrophobic solvents show that the porphyrin is photo-oxidized to bile pigments [314]. This process is likely to be an important biological pathway in some genera of algae [327]. The pigments then form covalent bonds to proteins to become biliproteins which serve as light harvester, light sensory pigments and photoregulator of plant growth [328]. The reverse order of reaction, incorporation of Mg porphyrin to proteins and then photodecomposition appears to be unlikely because of the slow photo-oxidation of Mg porphyrin-globin species.

The two possible factors which stabilise Mg porphyrin-globin against photodecomposition are (1) protein environment and (2) coordination of the imidazole ring to Mg. X-ray studies have shown that the heme is in close contact with the amino acids and the heme crevice has limited accessibility for environmental factors [144,145]. This limited access prevents oxidation of the porphyrin ring and can therefore be an important contributing factor for the stability of Mg porphyrin-globin species.

The formation of metalloporphyrin-nitrogenous base complexes which stabilises the porphyrin against oxidation has been clearly illustrated by studies of pyridine with MgPP [314] and chlorophyll [72]. The possible stabilising effects for Mg porphyrin-nitrogenous base complexes are described in Chapter 6.

The photolysis results suggest that the main reason for the stability of Mg porphyrin-globin against photo-oxidation is likely to be the protein environment rather

than the electron donating properties of the imidazole ring because (Mg porphyrin)(pyridine) in benzene still shows a faster rate of photodecomposition. However, coordination of pyridine and possibly imidazole can slow down the photo-oxidation to some extent. It is likely that in photo-synthetic bacteria, the protein environment and coordination of imidazole also inhibit the photo-oxidation of bacterio-chlorophyll. Synthetic chlorophyllide-Mb and bacterio-chlorophyll-Mb have indeed been shown to be photostable [12,13].

5.4.3 Photoresolution of Racemic Amino Acid by Photo-decomposition of Magnesium Porphyrin

The origin of molecular asymmetry has been of considerable interest because living systems are made up of asymmetric molecules [329]. Many possible reasons for the origin of asymmetry have been suggested [330,331] and the four common ones are:-

(1) A random event that depended on the chirality of the first molecule that was formed [332-334].

(2) Both D and L forms were developed but later, one form has an advantage of survival over the other [335-336].

(3) Nuclear asymmetry or parity non-conservation. These effects are generally small and chemical amplification processes are necessary [337-340].

(4) External asymmetry from circularly polarised light [341-343], magnetic field [344], surface catalyst [345], metal complexes [346,347] and other possible effects [348-350].

Asymmetric induction using circularly polarised light was initiated by the pioneering work of Van't Hoff in 1894

[351]. Subsequent studies, particularly the conversion of diethyl fumarate to (+)-tartaric acid by oxidation with hydrogen peroxide under the influence of right-handed polarised light, supported this idea [352]. The three different mechanistic principles that have been considered for asymmetric induction with circularly polarised light are (1) asymmetric synthesis [353,354], (2) photoinversion [355-357] and (3) asymmetric destruction [341,358].

The photoresolution of amino acids is of particular importance for an understanding of the occurrence of only L-amino acids in nature [359]. Recent results have shown that under the influence of right circularly polarised light in the ultra-violet region, photoresolution of amino acids can occur [341].

The observation of circular dichroism for two samples of Mg porphyrin-racemic histidine species suggests that either small particles could be scattering the light or absorption of visible circularly polarised light by Mg porphyrin can catalyse the asymmetric destruction of a racemic amino acid.

Scattering by particles appears to be unlikely as the two solutions were filtered and centrifuged several times. Thus some type of selective photoexcitation may have occurred in a similar manner to that observed for trans 1,2-diarylethylene [360,361]. The porphyrin itself could be photodecomposed [308] or the amino acid could be oxidised as has been observed in a related amine, N,N-dimethyl-piperazine, coordinated to porphyrin [362].

This observation of the possible photoresolution of a Mg porphyrin-racemic histidine solution suggests that in nature, both D and L mixtures were formed but under the

influence of external asymmetry (in this case it is circularly polarised light) only one form survived. Overall, the results agree reasonably well with that reported for the photoresolution of amino acids using circularly polarised light in the ultra-violet region [341].

CHAPTER 6

CRYSTAL STRUCTURES AND SPECTRAL PROPERTIES OF RELATED OCTAHEDRAL MAGNESIUM TETRAPHENYLPORPHYRIN COMPLEXES

6.1 INTRODUCTION

The crystal and molecular structures of metalloporphyrins have been of general importance because they provide an insight into the function and structure of hemoproteins [363]. Most of these metalloporphyrin structures consist of metals of the first transition series, especially iron [364,365]. However, the structures of magnesium porphyrins are also of interest because of their relevance to chlorophyll molecules, as highlighted in a recent report [366].

The majority of the X-ray structural studies of magnesium tetrapyrrole complexes are those of five-coordinate Mg centres. In these complexes the magnesium atom is displaced out of the mean plane of the four nitrogen atoms of the macrocyclic ring towards the axial ligands, by values ranging from 0.273Å to 0.496Å [24,60,366-370]. Physical studies of Mg porphyrins also indicate that five-coordination is the preferred coordination state of Mg [78,81]. However, equilibrium studies show that six-coordinate Mg porphyrin can be obtained under suitable conditions (Chapter 2).

Although the first attempt to determine six-coordinate (Mg etioporphyrin)(pyridine)$_2$ was limited by a high degree of disorder, the structure still reveals the presence of long Mg-N(axial) ligand bonds [284,371,372]. More recently, a complete structure determination of six-coordinate

(Mg octaethylporphyrin)(pyridine)$_2$ confirmed this result [373]. Such six-coordinate Mg centres may be important to photosynthetic systems because it has been suggested that their reaction centres consist of five- and six-coordinate chlorophyll, which are ligated by bifunctional ligands [18].

In this chapter, the crystal structures and spectral properties of three octahedral magnesium tetraphenylporphyrin complexes are reported. Two of these complexes, MgTPP(1-MeIm)$_2$ and MgTPP(pip)$_2$ are isostructural with those reported for the low spin iron (II) analogues [374,375], while MgTPP(pip)$_2$ and MgTPP(4-pic)$_2$ are isostructural with each other. The spectral properties of these complexes indicate that six-coordinate Mg centres can indeed red-shift the positions of the electronic bands but by different magnitudes. Detailed X-ray results show that the Mg-N(axial) ligand distances affect the magnitude of the red-shift. Such an effect is considered to be important for the red-shift of chlorophyll molecules *in vitro* [18]. Consequently, these six-coordinate Mg porphyrin complexes may be of particular relevance to an understanding of chlorophyll molecules.

6.2 EXPERIMENTAL

(TPP)H_2 was prepared by the condensation of pyrrole and benzaldehyde [376] and purified by a procedure adapted from Barnett and coworkers [377]. Mg (II) was inserted into (TPP)H_2 using $MgCl_2.6H_2O$ to produce the aquo complex, MgTPP(H_2O) [378]. Shiny, red-purple, hexagonal-shaped crystals of MgTPP(1-MeIm)$_2$ were obtained by heating

$MgTPP(H_2O)$ in pure 1-methylimidazole and then crystallising in an acetone-1-methylimidazole solution. The crystals were assigned to the tetragonal system after examination by precession photography, using Mo K_α radiation. A similar technique was used to obtain $MgTPP(pip)_2$ and $MgTPP(4\text{-pic})_2$. Long needle-like crystals were obtained from a solution of chloroform and the nitrogenous ligand.

The crystals chosen for data collection were mounted on a computer-controlled Nicolet R3m diffractometer. The cell constants and orientation matrices were determined from a least squares fit of at least 20 reflections. Important crystal data are summarized in Table 6.1.

Data were collected at room temperature using graphite monochromated Mo K_α radiation and the θ-2θ scan technique ($3° < 2\theta < 45°$ ($MgTPP(1\text{-MeIm})_2$), $50°$ ($MgTPP(4\text{-pic})_2$), $50°$ ($MgTPP(pip)_2$)). Crystal stabilities were monitored by recording three standard reflections for every 100 reflections and no significant variations were observed. Intensities were corrected for Lorentz-polarisation effects and empirical absorption corrections were applied based on ψ-scan data. Only those reflections for which $I_o \geqslant 3\sigma(I_o)$ were used in the subsequent structural analyses.

The structure of $MgTPP(1\text{-MeIm})_2$ was solved by direct methods, using the programme SOLV which revealed the positions of all the non-hydrogen atoms. For both $MgTPP(4\text{-pic})_2$ and $MgTPP(pip)_2$ crystal symmetry defined the position of the Mg atom (0, 0, 0 in each case) and the remaining non-hydrogen atoms were located from difference Fourier maps. The structures were refined by blocked cascade least squares refinement and hydrogen atoms were included at calculated positions (C-H = 0.96Å) with thermal

Table 6.1 Crystal data

Compound	MgTPP(1-MeIm)$_2$	MgTPP(4-pic)$_2$	MgTPP(pip)$_2$
Empirical Formula	$C_{52}H_{40}N_8Mg$	$C_{56}H_{42}N_6Mg$	$C_{54}H_{50}N_6Mg$
Molecular Weight	801.3	823.3	806.9
Crystal System	Tetragonal	Triclinic	Triclinic
Space Group	$P4_2/n$	$P\bar{1}$	$P\bar{1}$
Cell dimensions, a (Å)	20.764(4)	10.146(2)	9.944(3)
b (Å)		11.210(2)	11.463(3)
c (Å)	9.659(3)	11.643(3)	11.914(3)
α		65.63(2)°	101.78(2)°
β		76.32(2)°	104.59(2)°
γ		67.42(1)°	115.60(2)°
Volume	4164.3	1108.9	1103.7
Dm	1.28	1.25	1.23
Dc	1.28	1.23	1.21
Z	4	1	1
F(000)	1679.6	431.91	425.91
μ(cm^{-1})	0.85	0.81	0.79
Crystal dimensions(mm)	0.22x0.2x0.2	0.43x0.19x0.21	0.56x0.75x0.28
Mosaicity	0.31	0.25	0.22
Radiation	Mo K_α	Mo K_α	Mo K_α
2θ range	3-45	3-50	3-50
Total independent reflections	2741	3927	3907
Reflections used in refinements for which Io $\geq$ 3 σ(Io)	1132	2059	2144
R	0.074	0.0449	0.0591
Rw	0.057	0.045	0.0579
g	-0.00	-0.000109	-0.000262

parameters equal to 1.2 x U of their carrier atoms. All the programmes used for data reduction and structure solution are included in the SHELXTL (version 3.0) package [379]. Mg scattering factors were obtained from Cromer and Mann [380] and the anomalous dispersion corrections from Cromer and Liberman [381].

$MgTPP(1\text{-}MeIm)_2$ was refined to R = 0.074, R_w = 0.057 with all atoms isotropic except the Mg, the coordinated nitrogen atoms and the 1-MeIm group. A final difference map showed no features greater than ±0.3 $e^- Å^{-3}$. The 1-MeIm group shows two-fold disorder about the Mg-N(3) axis; thus the 1-Me group was found to have site occupancy of 0.68 (C44) and 0.32 (C44') in the two related orientations.

$MgTPP(4\text{-}pic)_2$ was refined with all the non-hydrogen atoms anisotropic and converged with R = 0.0499 and R_W = 0.045 and the final difference map showed no features greater than ± 0.26 $e^- Å^{-3}$. For $MgTPP(pip)_2$, the Mg, coordinated nitrogen atoms, phenyl groups and axial ligand were refined anisotropically to give R = 0.0591 and R_w = 0.0579 with no features greater than ± 0.24 $e^- Å^{-3}$ in the final difference map.

In all three cases the function minimised was $\Sigma w(|F_o|-|F_c|)^2$ with $w = [\sigma^2(F_o) + gF_o^2]^{-1}$. Atomic coordinates and associated thermal parameters are listed in Tables 6.2 to 6.10; selected interatomic distances and angles are given in Tables 6.11 to 6.16.

The electronic spectra of these complexes were recorded on a Cary spectrophotometer by grinding the crystals with KBr to form a disc and using another KBr disc as standard. The electronic spectra of these complexes in Nujol solution were also recorded on a Varian Superscan

Table 6.2 Atom coordinates ($x10^4$) and temperature factors ($Å^2 x10^3$) of $MgTPP(1\text{-}MeIm)_2$

Atom	x	y	z	U
Mg	5000	0	0	31(1)*
N(2)	4100(3)	-332(3)	-603(6)	28(3)*
C(50)	2820(4)	951(3)	-298(8)	29(2)
C(5)	3485(4)	674(4)	-308(8)	32(2)
C(9)	6043(4)	951(4)	982(8)	30(2)
C(6)	3545(4)	20(4)	-690(8)	29(2)
C(4)	3989(3)	1085(3)	114(9)	25(2)
N(1)	4609(3)	908(3)	359(7)	34(3)*
C(30)	5912(4)	2128(4)	1235(8)	30(2)
C(1)	4958(4)	1449(4)	628(8)	33(2)
C(10)	5615(4)	1478(4)	957(8)	28(2)
C(51)	2532(4)	1116(4)	951(9)	56(3)
N(3)	5246(4)	299(4)	-2228(8)	47(3)*
C(2)	4528(4)	2001(4)	576(8)	38(2)
C(55)	2481(4)	1046(4)	-1498(9)	45(3)
C(8)	3281(4)	-990(4)	-1383(7)	31(2)
C(32)	6038(4)	3086(4)	2635(10)	50(3)
C(34)	6690(4)	2954(4)	618(9)	56(3)
C(33)	6510(4)	3297(4)	1763(9)	49(3)
C(3)	3937(4)	1770(4)	263(8)	39(2)
C(35)	6379(3)	2364(4)	347(9)	41(2)
C(54)	1861(4)	1317(4)	-1455(9)	56(3)
C(31)	5740(4)	2494(4)	2374(8)	37(2)
N(4)	5642(5)	396(5)	-4333(9)	79(5)*
C(7)	3043(4)	-392(4)	-1178(7)	33(2)
C(52)	1918(4)	1400(4)	970(10)	67(3)
C(53)	1600(4)	1497(4)	-239(10)	59(3)
C(43)	5036(5)	840(5)	-2911(11)	63(5)*
C(41)	5630(5)	22(5)	-3129(11)	67(5)*
C(44)	6024(6)	266(6)	-5507(13)	60(5)
C(42)	5273(5)	886(5)	-4180(11)	68(5)*
C(44')	5300(13)	1202(12)	-5306(28)	50(10)

* Equivalent isotropic U defined as one third of the trace of the orthogonalised U_{ij} tensor

Table 6.3 Atom coordinates ($x10^4$) and temperature factors ($Å^2 x10^3$) of $MgTPP(4\text{-pic})_2$

Atom	x	y	z	U
Mg	0	0	0	46(1)*
N(1)	1253(3)	1026(3)	116(2)	44(1)*
N(2)	-1175(3)	119(2)	1686(2)	43(1)*
C(6)	-1084(3)	880(3)	2324(3)	41(2)*
C(9)	-2342(3)	-319(3)	2262(3)	41(2)*
C(1)	-2329(3)	-1413(3)	760(3)	44(2)*
C(21)	-4067(3)	-1556(3)	2663(3)	45(2)*
C(31)	-250(3)	2410(3)	2802(3)	43(2)*
C(2)	-2763(4)	-2306(3)	416(3)	53(2)*
C(3)	1935(3)	2465(3)	631(3)	53(2)*
C(4)	976(3)	1673(3)	973(3)	44(2)*
C(8)	-2989(3)	166(3)	3305(3)	49(2)*
C(36)	-1062(4)	3790(3)	2435(3)	64(2)*
C(7)	-2226(3)	893(3)	3343(3)	47(2)*
C(34)	-697(4)	3925(4)	4323(3)	62(2)*
C(5)	-85(3)	1588(3)	1999(3)	43(2)*
C(32)	352(4)	1803(4)	3937(3)	59(2)*
C(22)	-3859(4)	-2576(3)	3852(3)	56(2)*
C(33)	117(4)	2562(4)	4699(3)	67(2)*
C(10)	-2860(3)	-1062(3)	1850(3)	43(2)*
C(24)	-6259(4)	-2595(4)	4133(4)	89(3)*
C(35)	-1287(4)	4546(4)	3192(4)	70(2)*
C(23)	-4945(4)	-3111(4)	4570(4)	77(2)*
N(5)	-1633(3)	2233(3)	-1000(2)	55(2)*
C(51)	-3038(4)	2575(4)	-669(4)	69(2)*
C(55)	-1181(4)	3293(4)	-1765(4)	79(2)*
C(25)	-6507(4)	-1561(4)	2986(4)	85(3)*
C(26)	-5417(3)	-1044(4)	2243(3)	66(2)*
C(52)	-3969(4)	3910(4)	-1065(4)	78(2)*
C(53)	-3473(4)	4997(4)	-1830(3)	66(2)*
C(54)	-2045(5)	4649(4)	-2181(4)	85(2)*
C(56)	-4444(5)	6475(4)	-2246(4)	103(3)*

* Equivalent isotropic U defined as one third of the trace of the orthogonalised U_{ij} tensor.

Table 6.4 Atom coordinates ($x10^4$) and temperature factors ($Å^2 x10^3$) of $MgTPP(pip)_2$

Atom	x	y	z	U
Mg	0	0	0	49(1)*
N(2)	2251(3)	1010(3)	-88(2)	42(2)*
N(1)	-1044(3)	159(3)	-1661(2)	42(2)*
C(7)	4337(4)	2410(4)	-573(3)	48(1)
C(9)	3696(4)	1371(3)	783(3)	41(1)
C(8)	5003(4)	2240(3)	472(3)	48(1)
C(3)	-1356(4)	999(4)	-3238(3)	48(1)
N(5)	426(4)	2226(3)	1126(3)	58(2)*
C(6)	2606(4)	1645(3)	-927(3)	40(1)
C(4)	-225(4)	929(3)	-2263(3)	42(1)
C(24)	8762(5)	2523(4)	4257(4)	67(3)*
C(2)	-2824(4)	287(4)	-3220(3)	51(1)
C(53)	1290(6)	5168(5)	1848(4)	86(3)*
C(23)	8075(5)	1490(4)	3124(4)	66(3)*
C(10)	3897(4)	1009(3)	1855(3)	40(1)
C(55)	2108(5)	3378(4)	1737(5)	89(3)*
C(54)	2353(6)	4714(5)	2561(5)	102(3)*
C(25)	7857(5)	3029(4)	4625(4)	67(3)*
C(1)	2646(4)	249(3)	2226(3)	43(1)
C(22)	6503(4)	989(4)	2330(4)	57(2)*
C(21)	5582(4)	1501(4)	2695(3)	43(2)*
C(26)	6278(4)	2507(4)	3865(3)	56(2)*
C(51)	-613(5)	2688(4)	490(4)	74(3)*
C(52)	-427(5)	4004(4)	1297(4)	77(3)*
C(5)	1464(4)	1596(3)	-1942(3)	42(1)
C(31)	2102(4)	2380(4)	-2737(3)	45(2)*
C(34)	3248(4)	3856(4)	-4212(4)	63(2)*
C(32)	2077(5)	1727(4)	-3855(3)	59(2)*
C(36)	2722(5)	3801(4)	-2370(4)	69(3)*
C(33)	2658(5)	2467(4)	-4582(4)	67(3)*
C(35)	3284(5)	4522(4)	-3101(4)	78(3)*

* Equivalent isotropic U defined as one third of the trace of the orthogonalised U_{ij} tensor.

Table 6.5 Anisotropic temperature factors ($Å^2 x 10^3$) of $MgTPP(1\text{-}MeIm)_2$

Atom	U_{11}	U_{22}	U_{33}	U_{23}	U_{13}	U_{12}
Mg	23(3)	27(3)	43(3)	-2(2)	-4(2)	-3(2)
N(2)	26(4)	22(4)	37(5)	-7(4)	6(4)	-7(3)
N(1)	21(4)	24(4)	58(6)	1(4)	-2(4)	-7(3)
N(3)	49(6)	44(6)	47(6)	6(5)	-12(5)	-12(4)
N(4)	69(8)	136(11)	31(6)	-4(7)	4(6)	-47(7)
C(43)	53(8)	78(9)	59(9)	13(8)	-17(7)	-15(6)
C(41)	45(8)	86(9)	70(9)	1(8)	4(7)	-9(7)
C(42)	79(8)	97(10)	29(6)	20(7)	-2(6)	-38(7)

The anisotropic temperature factor exponent takes the form:

$-2\pi^2(h^2a^{*2}U_{11}+k^2b^{*2}U_{22}+ \ldots +2hka^*b^*U_{12})$

Table 6.6 Anisotropic temperature factors ($Å^2 x 10^3$) of MgTPP(4-pic)$_2$

Atom	U_{11}	U_{22}	U_{33}	U_{23}	U_{13}	U_{12}
Mg	54(1)	51(1)	43(1)	-23(1)	3(1)	-23(1)
N(1)	49(2)	49(2)	43(2)	-23(1)	2(1)	-21(1)
N(2)	52(2)	41(2)	42(1)	-19(1)	-1(1)	-19(1)
C(6)	50(2)	36(2)	37(2)	-16(2)	-4(2)	-9(2)
C(9)	44(2)	39(2)	41(2)	-17(2)	-1(2)	-15(2)
C(1)	46(2)	43(2)	45(2)	-17(2)	-5(2)	-16(2)
C(21)	46(2)	48(2)	48(2)	-25(2)	1(2)	-16(2)
C(31)	50(2)	40(2)	42(2)	-19(2)	-0(2)	-17(2)
C(2)	59(2)	59(2)	51(2)	-23(2)	1(2)	-29(2)
C(3)	62(2)	57(2)	53(2)	-25(2)	-5(2)	-28(2)
C(4)	53(2)	45(2)	43(2)	-22(2)	-6(2)	-16(2)
C(8)	48(2)	50(2)	46(2)	-22(2)	4(2)	-15(2)
C(36)	87(3)	49(2)	56(2)	-24(2)	-21(2)	-9(2)
C(7)	55(2)	46(2)	45(2)	-25(2)	-2(2)	-15(2)
C(34)	80(3)	65(3)	62(2)	-38(2)	4(2)	-34(2)
C(5)	50(2)	40(2)	41(2)	-16(2)	-6(2)	-13(2)
C(32)	76(3)	48(2)	55(2)	-23(2)	-17(2)	-10(2)
C(22)	64(2)	59(2)	49(2)	-22(2)	7(2)	-27(2)
C(33)	81(3)	78(3)	59(2)	-36(2)	-14(2)	-26(2)
C(10)	42(2)	40(2)	45(2)	-16(2)	-1(2)	-12(2)
C(24)	89(3)	117(4)	93(3)	-67(3)	42(3)	-65(3)
C(35)	94(3)	47(2)	72(3)	-30(2)	-10(2)	-15(2)
C(23)	106(3)	73(3)	61(2)	-27(2)	17(2)	-50(3)
N(5)	56(2)	53(2)	53(2)	-23(1)	-2(1)	-15(2)
C(51)	62(3)	59(3)	82(3)	-22(2)	-6(2)	-19(2)
C(55)	61(3)	61(3)	80(3)	-4(2)	7(2)	-15(2)
C(25)	50(2)	119(4)	106(3)	-62(3)	8(2)	-32(2)
C(26)	54(2)	74(3)	67(2)	-25(2)	-5(2)	-19(2)
C(52)	53(2)	79(3)	95(3)	-30(3)	-7(2)	-15(2)
C(53)	72(3)	55(2)	60(2)	-20(2)	-13(2)	-4(2)
C(54)	74(3)	54(3)	90(3)	-1(2)	-2(3)	-14(2)
C(56)	108(4)	72(3)	99(3)	-29(3)	-28(3)	10(3)

The anisotropic temperature factor exponent takes the form:

$-2\pi(h^2a^{*2}U_{11}+k^2b^{*2}U_{22}+ \ldots +2hka^*b^*U_{12})$

Table 6.7 Anisotropic temperature factors ($Å^2 x 10^3$) of $MgTPP(pip)_2$

Atom	U_{11}	U_{22}	U_{33}	U_{23}	U_{13}	U_{12}
Mg	41(1)	62(1)	44(1)	29(1)	17(1)	22(1)
N(2)	41(2)	51(2)	36(2)	23(1)	17(1)	22(1)
N(1)	39(2)	46(2)	42(2)	23(1)	18(1)	18(1)
N(5)	61(2)	64(2)	54(2)	24(2)	24(2)	34(2)
C(24)	47(2)	83(3)	68(3)	41(3)	14(2)	29(2)
C(53)	105(4)	74(3)	83(3)	31(3)	40(3)	48(3)
C(23)	61(3)	83(3)	83(3)	49(3)	39(2)	46(2)
C(55)	57(3)	70(3)	101(4)	-5(3)	1(3)	32(3)
C(54)	79(3)	87(4)	96(4)	-14(3)	-8(3)	50(3)
C(25)	62(3)	73(3)	46(2)	12(2)	3(2)	31(2)
C(22)	58(3)	60(3)	54(2)	20(2)	23(2)	30(2)
C(21)	42(2)	47(2)	42(2)	23(2)	16(2)	22(2)
C(26)	58(2)	65(3)	48(2)	19(2)	20(2)	34(2)
C(51)	64(3)	75(3)	75(3)	18(3)	12(2)	41(3)
C(52)	76(3)	77(3)	84(3)	32(3)	22(3)	48(3)
C(31)	40(2)	49(2)	39(2)	22(2)	15(2)	16(2)
C(34)	56(3)	68(3)	60(3)	41(2)	27(2)	20(2)
C(32)	74(3)	49(2)	53(2)	22(2)	32(2)	24(2)
C(36)	98(3)	51(3)	52(2)	23(2)	36(2)	28(2)
C(33)	76(3)	80(3)	53(2)	31(2)	39(2)	35(3)
C(35)	106(4)	47(3)	69(3)	32(3)	39(3)	21(3)

The anisotropic temperature factor exponent takes the form:

$$-2\pi(h^2a^{*2}U_{11}+k^2b^{*2}U_{22}+ \ldots +2hka^*b^*U_{12})$$

Table 6.8 Hydrogen coordinates ($x10^4$) and temperature factors ($Å^2 x10^3$) of $MgTPP(1\text{-}MeIm)_2$

Atom	x	y	z	U
H(51)	2754	1036	1805	61
H(2)	4641	2443	732	44
H(55)	2668	928	-2371	48
H(8)	3053	-1362	-1719	34
H(32)	5911	3342	3417	60
H(34)	7022	3111	14	71
H(33)	6722	3697	1960	59
H(3)	3551	2020	160	40
H(35)	6492	2123	-465	45
H(54)	1623	1374	-2298	66
H(31)	5414	2339	2994	44
H(7)	2605	-263	-1336	42
H(52)	1725	1524	1832	84
H(53)	1183	1696	-228	72
H(43)	4749	1151	-2511	75
H(41)	5864	-371	-2985	80
H(44a)	6251	-132	-5374	69
H(44b)	6328	609	-5636	69
H(44c)	5754	233	-6309	69
H(44a)	5031	1576	-5238	84
H(44b)	5152	935	-6054	84
H(44c)	5736	1331	-5477	84

Table 6.9 Hydrogen coordinates ($x10^4$) and temperature factors ($Å^2 x10^3$) of $MgTPP(4\text{-pic})_2$

Atom	x	y	z	U
H(2)	-3522	-2652	931	71
H(3)	1879	2969	1146	70
H(8)	-3815	-67	3806	61
H(36)	-1479	4235	1643	77
H(7)	-2301	1378	3881	59
H(34)	-856	4447	4850	87
H(32)	940	848	4203	74
H(22)	-2951	-2920	4186	95
H(33)	529	2123	5494	93
H(24)	-7010	-2961	4636	110
H(35)	-1858	5507	2923	84
H(23)	-4770	-3846	5378	94
H(51)	-3425	1848	-123	82
H(55)	-177	3095	-2046	83
H(25)	-7439	-1186	2688	76
H(26)	-5601	-324	1428	79
H(52)	-4975	4085	-804	84
H(54)	-1634	5357	-2727	102
H(56a)	-5410	6509	-1901	121
H(56b)	-4402	6860	-3154	121
H(56c)	-4139	7002	-1950	121

Table 6.10 Hydrogen coordinates ($x10^4$) and temperature factors ($Å^2 x10^3$) of $MgTPP(pip)_2$

Atom	x	y	z	U
H(7)	4906	2939	-1000	58
H(8)	6135	2626	926	58
H(3)	-1100	1473	-3800	57
H(5)	73	1989	1770	69
H(24)	9864	2889	4788	79
H(2)	-3812	155	-3767	61
H(53a)	1624	5404	1198	102
H(53b)	1385	5964	2403	102
H(23)	8688	1107	2875	82
H(55a)	2724	3084	2239	111
H(55b)	2507	3572	1102	111
H(54a)	2081	4565	3258	117
H(54b)	3465	5430	2853	117
H(25)	8329	3754	5419	81
H(22)	6051	287	1526	68
H(26)	5649	2845	4151	69
H(51a)	-354	2853	-208	89
H(51b)	-1718	1959	201	89
H(52a)	-778	3825	1956	91
H(52b)	-1086	4268	798	91
H(34)	3635	4365	-4720	75
H(32)	1650	742	-4137	71
H(36)	2761	4290	-1594	80
H(33)	2643	1991	-5353	80
H(35)	3706	5506	-2829	95

Table 6.11 Bond lengths (Å) of $MgTPP(1\text{-}MeIm)_2$

Atoms	Distance	Atoms	Distance
Mg-N(2)	2.074(6)	Mg-N(1)	2.082(6)
Mg-N(3)	2.297(8)	Mg-N(2a)	2.074(6)
Mg-N(1a)	2.082(6)	Mg-N(3a)	2.297(8)
N(2)-C(6)	1.368(10)	N(2)-C(9a)	1.370(10)
C(50)-C(5)	1.496(10)	C(50)-C(51)	1.390(12)
C(50)-C(55)	1.370(11)	C(5)-C(6)	1.412(11)
C(5)-C(4)	1.411(10)	C(9)-C(10)	1.409(11)
C(9)-N(2a)	1.370(10)	C(9)-C(8a)	1.459(10)
C(6)-C(7)	1.429(11)	C(4)-N(1)	1.360(9)
C(4)-C(3)	1.433(10)	N(1)-C(1)	1.361(10)
C(30)-C(35)	1.384(11)	C(30)-C(31)	1.384(11)
C(1)-C(10)	1.403(10)	C(1)-C(2)	1.454(11)
C(51)-C(52)	1.404(12)	N(3)-C(43)	1.373(14)
N(3)-C(41)	1.314(13)	C(2)-C(3)	1.352(11)
C(55)-C(54)	1.406(12)	C(8)-C(7)	1.352(10)
C(8)-C(9a)	1.460(10)	C(32)-C(33)	1.364(12)
C(32)-C(31)	1.399(11)	C(34)-C(33)	1.368(12)
C(34)-C(35)	1.409(11)	C(54)-C(53)	1.347(13)
N(4)-C(41)	1.399(14)	N(4)-C(44)	1.410(16)
N(4)-C(42)	1.282(15)	C(52)-C(53)	1.357(13)
C(43)-C(42)	1.324(15)	C(42)-C(44')	1.272(28)
N(2a)-C(9)	1.370(10)	C(9a)-C(8)	1.460(10)
N(3a)-Mg	2.297(8)	C(8a)-C(9)	1.460(10)

Table 6.12 Bond lengths (Å) of $MgTPP(4\text{-pic})_2$

Atoms	Distance	Atoms	Distance
Mg-N(1)	2.072(3)	Mg-N(2)	2.069(2)
Mg-N(5)	2.386(2)	Mg-N(1a)	2.072(3)
Mg-N(2a)	2.069(2)	Mg-N(5a)	2.386(2)
N(1)-C(4)	1.380(5)	N(1)-C(1a)	1.376(4)
N(2)-C(6)	1.380(5)	N(2)-C(9)	1.375(4)
C(6)-C(7)	1.450(4)	C(6)-C(5)	1.409(5)
C(9)-C(8)	1.448(5)	C(9)-C(10)	1.408(6)
C(1)-C(2)	1.452(6)	C(1)-C(10)	1.408(5)
C(1)-N(1a)	1.376(4)	C(21)-C(22)	1.384(4)
C(21)-C(10)	1.498(4)	C(21)-C(26)	1.388(5)
C(31)-C(36)	1.377(4)	C(31)-C(5)	1.508(6)
C(31)-C(32)	1.379(5)	C(2)-C(3a)	1.342(5)
C(3)-C(4)	1.444(6)	C(3)-C(2a)	1.342(5)
C(4)-C(5)	1.404(4)	C(8)-C(7)	1.340(6)
C(36)-C(35)	1.385(7)	C(34)-C(33)	1.363(5)
C(34)-C(35)	1.369(6)	C(32)-C(33)	1.391(7)
C(22)-C(23)	1.389(6)	C(24)-C(23)	1.362(6)
C(24)-C(25)	1.359(5)	N(5)-C(51)	1.330(5)
N(5)-C(55)	1.329(5)	C(51)-C(52)	1.377(5)
C(55)-C(54)	1.373(5)	C(25)-C(26)	1.390(5)
C(52)-C(53)	1.377(6)	C(53)-C(54)	1.355(6)
C(53)-C(56)	1.503(5)	N(1a)-C(1)	1.376(4)
C(1a)-N(1)	1.376(4)	C(1a)-C(2a)	1.452(6)
C(2a)-C(3)	1.342(5)	C(2a)-C(1a)	1.452(6)

Table 6.13 Bond lengths (Å) of $MgTPP(pip)_2$

Atoms	Distance	Atoms	Distance
Mg-N(2)	2.071(3)	Mg-N(1)	2.074(3)
Mg-N(5)	2.419(4)	Mg-N(2a)	2.071(3)
Mg-N(1a)	2.074(3)	Mg-N(5a)	2.419(4)
N(2)-C(9)	1.369(4)	N(2)-C(6)	1.379(5)
N(1)-C(4)	1.374(5)	N(1)-C(1a)	1.378(5)
C(7)-C(8)	1.349(6)	C(7)-C(6)	1.445(5)
C(9)-C(8)	1.446(5)	C(9)-C(10)	1.414(6)
C(3)-C(4)	1.441(6)	C(3)-C(2)	1.338(5)
N(5)-C(55)	1.467(4)	N(5)-C(51)	1.470(7)
C(6)-C(5)	1.408(5)	C(4)-C(5)	1.414(5)
C(24)-C(23)	1.368(5)	C(24)-C(25)	1.372(8)
C(2)-C(1a)	1.447(6)	C(53)-C(54)	1.521(9)
C(53)-C(52)	1.494(5)	C(23)-C(22)	1.387(6)
C(10)-C(1)	1.413(5)	C(10)-C(21)	1.496(5)
C(55)-C(54)	1.518(8)	C(25)-C(26)	1.376(6)
C(1)-N(1a)	1.378(5)	C(1)-C(2a)	1.447(6)
C(22)-C(21)	1.389(7)	C(21)-C(26)	1.385(4)
C(51)-C(52)	1.517(7)	C(5)-C(31)	1.503(6)
C(31)-C(32)	1.376(6)	C(31)-C(36)	1.385(6)
C(34)-C(33)	1.357(6)	C(34)-C(35)	1.369(7)
C(32)-C(33)	1.389(7)	C(36)-C(35)	1.375(7)
N(1a)-Mg	2.074(3)	N(1a)-C(1)	1.378(5)
C(2a)-C(1)	1.447(6)	C(1a)-C(2)	1.447(6)

Table 6.14 Bond angles (deg.) of MgTPP(1-MeIm)$_2$

Atoms	Angle	Atoms	Angle
N(2)-Mg-N(1)	89.8(2)	N(2)-Mg-N(3)	91.5(3)
N(1)-Mg-N(3)	89.9(3)	N(2)-Mg-N(2a)	180.0
N(1)-Mg-N(2a)	90.2(2)	N(3)-Mg-N(2a)	88.5(3)
N(2)-Mg-N(1a)	90.2(2)	N(1)-Mg-N(1a)	180.0
N(3)-Mg-N(1a)	90.1(3)	N(2a)-Mg-N(1a)	89.8(2)
N(2)-Mg-N(3a)	88.5(3)	N(1)-Mg-N(3a)	90.1(3)
N(3)-Mg-N(3a)	180.0	N(2a)-Mg-N(3a)	91.5(3)
N(1a)-Mg-N(3a)	89.9(3)	Mg-N(2)-C(6)	126.8(5)
Mg-N(2)-C(9a)	125.6(5)	C(6)-N(2)-C(9a)	107.6(6)
C(5)-C(50)-C(51)	119.9(7)	C(5)-C(50)-C(55)	121.6(7)
C(51)-C(50)-C(55)	118.5(7)	C(50)-C(5)-C(6)	116.9(6)
C(50)-C(5)-C(4)	116.8(6)	C(6)-C(5)-C(4)	126.3(7)
C(10)-C(9)-N(2a)	126.0(7)	C(10)-C(9)-C(8a)	124.6(7)
N(2a)-C(9)-C(8a)	109.4(6)	N(2)-C(6)-C(5)	124.9(7)
N(2)-C(6)-C(7)	108.4(6)	C(5)-C(6)-C(7)	126.7(7)
C(5)-C(4)-N(1)	126.1(6)	C(5)-C(4)-C(3)	125.0(7)
N(1)-C(4)-C(3)	108.8(6)	Mg-N(1)-C(4)	125.8(5)
Mg-N(1)-C(1)	124.9(5)	C(4)-N(1)-C(1)	108.2(6)
C(35)-C(30)-C(31)	118.6(7)	C(10)-C(1)-C(2)	124.8(7)
N(1)-C(1)-C(2)	108.5(6)	N(1)-C(1)-C(10)	126.6(7)
C(9)-C(10)-C(1)	125.7(7)	C(50)-C(51)-C(52)	120.4(8)
Mg-N(3)-C(43)	126.9(7)	Mg-N(3)-C(41)	129.6(7)
C(43)-N(3)-C(41)	103.4(8)	C(1)-C(2)-C(3)	106.5(7)
C(50)-C(55)-C(54)	120.2(8)	C(7)-C(8)-C(9a)	105.1(7)
C(33)-C(32)-C(31)	119.2(8)	C(33)-C(34)-C(35)	118.5(8)
C(32)-C(33)-C(34)	121.9(8)	C(4)-C(3)-C(2)	107.8(7)
C(30)-C(35)-C(34)	121.0(8)	C(55)-C(54)-C(53)	120.4(8)
C(30)-C(31)-C(32)	120.8(8)	C(41)-N(4)-C(44)	124.8(10)
C(41)-N(4)-C(42)	109.6(9)	C(44)-N(4)-C(42)	125.6(10)
C(6)-C(7)-C(8)	109.4(7)	C(51)-C(52)-C(53)	119.5(9)
C(54)-C(53)-C(52)	120.9(8)	N(3)-C(43)-C(42)	112.8(9)
N(3)-C(41)-N(4)	108.5(9)	N(4)-C(42)-C(43)	105.7(10)
N(4)-C(42)-C(44')	106.5(15)	C(43)-C(42)-C(44')	147.8(16)
Mg-N(2a)-C(9)	125.6(5)	N(2)-C(9a)-C(8)	109.4(6)

Table 6.15 Bond angles (deg.) of $MgTPP(4\text{-pic})_2$

Atoms	Angle	Atoms	Angle
N(1)-Mg-N(2)	90.9(1)	N(1)-Mg-N(5)	86.6(1)
N(2)-Mg-N(5)	86.3(1)	N(1)-Mg-N(1a)	180.0
N(2)-Mg-N(1a)	89.1(1)	N(5)-Mg-N(1a)	93.4(1)
N(1)-Mg-N(2a)	89.1(1)	N(2)-Mg-N(2a)	180.0
N(5)-Mg-N(2a)	93.7(1)	N(1a)-Mg-N(2a)	90.9(1)
N(1)-Mg-N(5a)	93.4(1)	N(2)-Mg-N(5a)	93.7(1)
N(5)-Mg-N(5a)	180.0	N(1a)-Mg-N(5a)	86.6(1)
N(2a)-Mg-N(5a)	86.3(1)	Mg-N(1)-C(4)	125.1(2)
Mg-N(1)-C(1a)	126.9(3)	C(4)-N(1)-C(1a)	107.0(3)
Mg-N(2)-C(6)	125.1(2)	Mg-N(2)-C(9)	127.4(3)
C(6)-N(2)-C(9)	106.6(3)	N(2)-C(6)-C(7)	109.0(3)
N(2)-C(6)-C(5)	125.5(3)	C(7)-C(6)-C(5)	125.5(4)
N(2)-C(9)-C(8)	109.4(3)	N(2)-C(9)-C(10)	124.8(3)
C(8)-C(9)-C(10)	125.8(3)	C(2)-C(1)-C(10)	125.8(3)
C(2)-C(1)-N(1a)	108.9(3)	C(10)-C(1)-N(1a)	125.2(4)
C(22)-C(21)-C(10)	120.8(3)	C(22)-C(21)-C(26)	117.6(3)
C(10)-C(21)-C(26)	121.6(2)	C(36)-C(31)-C(5)	120.1(3)
C(36)-C(31)-C(32)	118.2(4)	C(5)-C(31)-C(32)	121.6(3)
C(1)-C(2)-C(3a)	107.5(3)	C(4)-C(3)-C(2a)	107.6(4)
N(1)-C(4)-C(3)	109.1(3)	N(1)-C(4)-C(5)	125.3(4)
C(3)-C(4)-C(5)	125.7(4)	C(9)-C(8)-C(7)	107.3(3)
C(31)-C(36)-C(35)	121.0(3)	C(6)-C(7)-C(8)	107.6(3)
C(33)-C(34)-C(35)	119.8(4)	C(6)-C(5)-C(31)	115.6(3)
C(6)-C(5)-C(4)	127.2(4)	C(31)-C(5)-C(4)	117.2(3)
C(31)-C(32)-C(33)	120.7(3)	C(21)-C(22)-C(23)	121.0(3)
C(34)-C(33)-C(32)	120.3(4)	C(9)-C(10)-C(1)	126.2(3)
C(9)-C(10)-C(21)	117.1(3)	C(1)-C(10)-C(21)	116.6(4)
C(23)-C(24)-C(25)	120.0(4)	C(36)-C(35)-C(34)	120.1(3)
C(22)-C(23)-C(24)	120.2(3)	Mg-N(5)-C(51)	122.7(2)
Mg-N(5)-C(55)	121.7(2)	C(51)-N(5)-C(55)	114.6(3)
N(5)-C(51)-C(52)	123.7(4)	N(5)-C(55)-C(54)	124.7(4)
C(24)-C(25)-C(26)	120.3(4)	C(21)-C(26)-C(25)	120.8(3)
C(51)-C(52)-C(53)	120.8(4)	C(52)-C(53)-C(54)	115.5(3)
C(52)-C(53)-C(56)	122.5(4)	C(54)-C(53)-C(56)	122.0(4)
C(55)-C(54)-C(53)	120.7(4)	Mg-N(1a)-C(1)	126.9(3)
N(1)-C(1a)-C(2a)	108.9(3)	C(3)-C(2a)-C(1a)	107.5(3)

Table 6.16 Bond angles (deg.) of $MgTPP(pip)_2$

Atoms	Angle	Atoms	Angle
N(2)-Mg-N(1)	90.1(1)	N(2)-Mg-N(5)	89.3(1)
N(1)-Mg-N(5)	89.8(1)	N(2)-Mg-N(2a)	180.0
N(1)-Mg-N(2a)	89.9(1)	N(5)-Mg-N(2a)	90.7(1)
N(2)-Mg-N(1a)	89.9(1)	N(1)-Mg-N(1a)	180.0
N(5)-Mg-N(1a)	90.2(1)	N(2a)-Mg-N(1a)	90.1(1)
N(2)-Mg-N(5a)	90.7(1)	N(1)-Mg-N(5a)	90.2(1)
N(5)-Mg-N(5a)	180.0	N(2a)-Mg-N(5a)	89.3(1)
N(1a)-Mg-N(5a)	89.8(1)	Mg-N(2)-C(9)	126.4(3)
Mg-N(2)-C(6)	126.0(2)	C(9)-N(2)-C(6)	106.8(3)
Mg-N(1)-C(4)	125.8(2)	Mg-N(1)-C(1a)	126.1(3)
C(4)-N(1)-C(1a)	107.0(3)	C(8)-C(7)-C(6)	107.1(3)
N(2)-C(9)-C(8)	109.4(3)	N(2)-C(9)-C(10)	125.7(3)
C(8)-C(9)-C(10)	124.8(3)	C(7)-C(8)-C(9)	107.4(3)
C(4)-C(3)-C(2)	107.9(4)	Mg-N(5)-C(55)	116.3(3)
Mg-N(5)-C(51)	116.9(2)	C(55)-N(5)-C(51)	110.2(4)
N(2)-C(6)-C(7)	109.3(3)	N(2)-C(6)-C(5)	125.3(3)
C(7)-C(6)-C(5)	125.3(4)	N(1)-C(4)-C(3)	109.0(3)
N(1)-C(4)-C(5)	125.4(3)	C(3)-C(4)-C(5)	125.6(4)
C(23)-C(24)-C(25)	119.2(4)	C(3)-C(2)-C(1a)	107.3(4)
C(54)-C(53)-C(52)	109.1(4)	C(24)-C(23)-C(22)	120.9(5)
C(9)-C(10)-C(1)	125.8(3)	C(9)-C(10)-C(21)	117.6(3)
C(1)-C(10)-C(21)	116.6(3)	N(5)-C(55)-C(54)	115.0(5)
C(53)-C(54)-C(55)	110.8(4)	C(24)-C(25)-C(26)	120.5(4)
C(10)-C(1)-N(1a)	125.5(4)	C(10)-C(1)-C(2a)	125.6(4)
N(1a)-C(1)-C(2a)	108.9(3)	C(23)-C(22)-C(21)	120.2(4)
C(10)-C(21)-C(22)	121.8(3)	C(10)-C(21)-C(26)	120.2(4)
C(22)-C(21)-C(26)	118.0(3)	C(25)-C(26)-C(21)	121.2(5)
N(5)-C(51)-C(52)	114.3(3)	C(53)-C(52)-C(51)	111.4(5)
C(6)-C(5)-C(4)	126.5(4)	C(6)-C(5)-C(31)	117.1(3)
C(4)-C(5)-C(31)	116.4(3)	C(5)-C(31)-C(32)	122.0(4)
C(5)-C(31)-C(36)	120.7(4)	C(32)-C(31)-C(36)	117.3(4)
C(33)-C(34)-C(35)	119.0(5)	C(31)-C(32)-C(33)	121.2(4)
C(31)-C(36)-C(35)	121.0(4)	C(34)-C(33)-C(32)	120.5(4)
C(34)-C(35)-C(36)	120.9(4)	Mg-N(1a)-C(1)	126.1(3)
N(1)-C(1a)-C(2)	108.9(3)		

3 UV-visible spectrophotometer.

Several attempts to record the electronic spectra of single crystals were unsuccessful because of intense fluorescence of the sample.

Infra-red measurements were recorded on a Shimadzu IR-27G spectrophotometer.

The densities of the crystals were determined in triplicate by flotation using KI-water solutions.

Observed and calculated structure factor amplitudes are available in Appendices A to C.

6.3 RESULTS

6.3.1 Description of the Structures

A perspective view of $MgTPP(1\text{-}MeIm)_2$ is shown in Figure 6.1 which also defines the numbering system used throughout this paper. The Mg atom lies at the centroid of the porphyrin core which is slightly deviated from planarity. The perpendicular displacements of the atoms from this core are illustrated in the lower half of Figure 6.2. The pyrrole rings are planar to ±0.012Å. They are inclined at 8.9° and 2.4° to the plane of the four chelating nitrogen atoms and mutually at 7.7°. The averaged bond lengths for the chemically analogous types of bonds are Mg-N = 2.078(6), N-Ca = 1.365(5), Ca-Cb = 1.444(15), Cb-Cb = 1.352(0), Ca-Cm = 1.409(4) and $Cm\text{-}C_{phenyl}$ = 1.502(8) Å, where the numbers in parentheses are the estimated standard deviations for the averaged values (Figure 6.1). Important bond lengths of the core are given in the upper half of the centrosymmetric molecule in Figure 6.2. The distances between N(1) and N(3), and N(3) and N(2) are 3.097Å and 3.136Å respectively, which are slightly longer than the 3Å van der Waals radii for nitrogen [115]. The averaged values

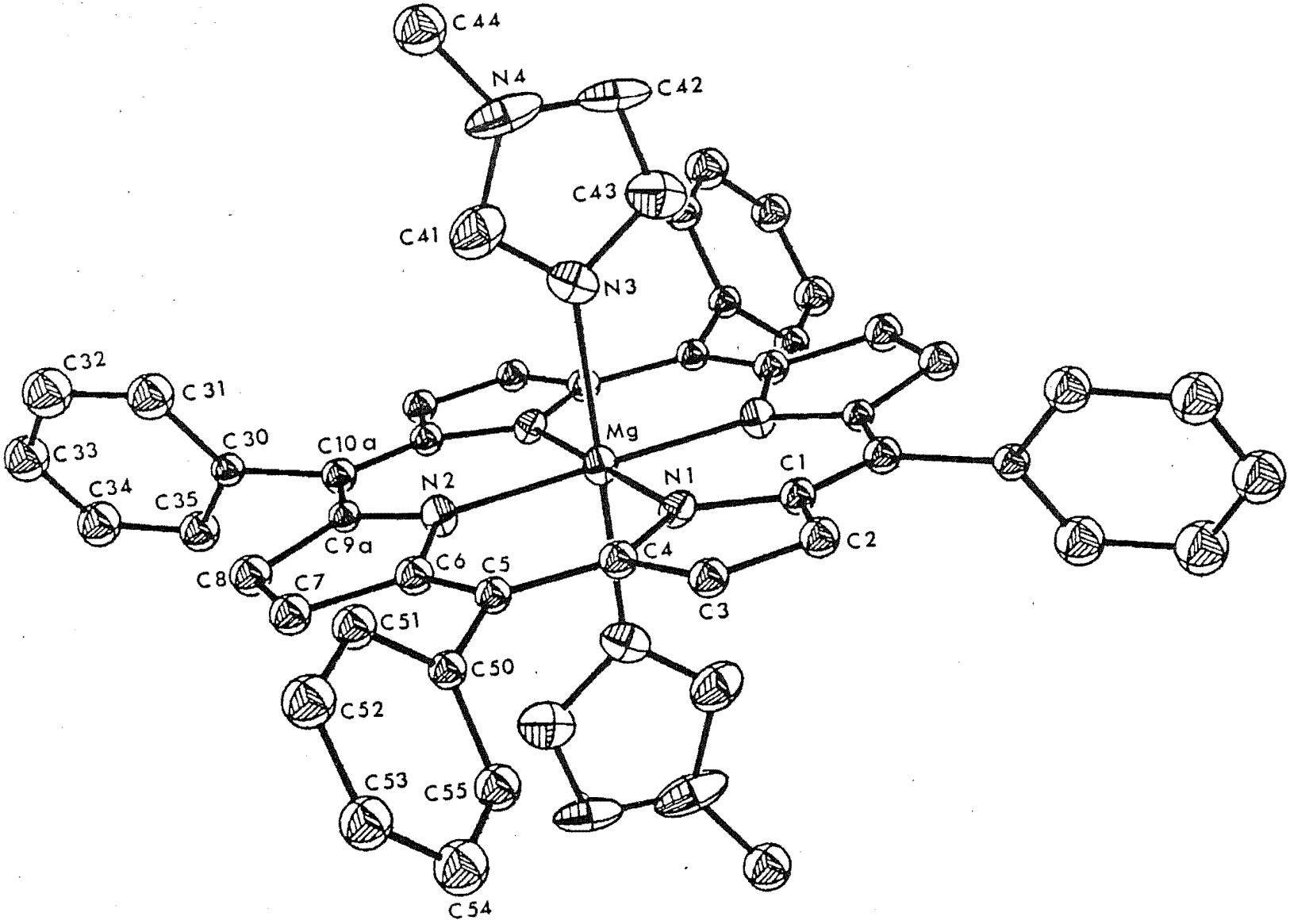

Figure 6.1 : Computer drawn structure of MgTPP(1-MeIm)$_2$ showing the numbering scheme (30% probability ellipsoids)

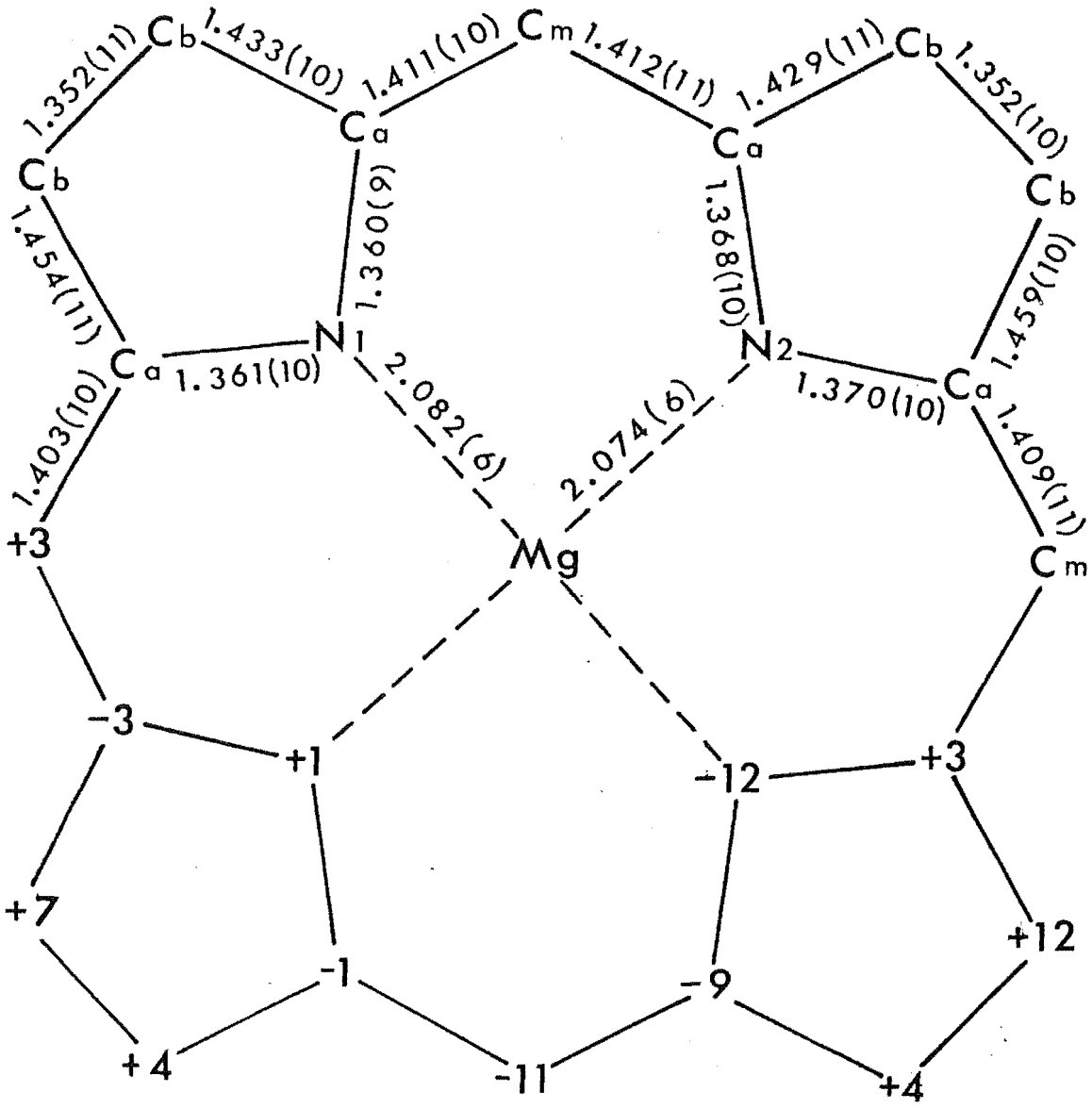

Figure 6.2 : Diagram of the porphyrin core of MgTPP(1-MeIm)$_2$ displaying on the upper half, the structurally independent bond lengths. On the lower half of the centrosymmetric diagram, atomic displacements in units of 0.01Å, from the mean porphyrin plane are given

for the bond angles are NMgN = 90.0(2), MgNCa = 125.8(8), CaNCa = 107.9(4), CaCmCa = 126.2(5), NCaCb = 108.8(5), NCaCm = 125.9(7), CaCbCb = 107.2(18). The averaged values for the internal angles and bond lengths of the phenyl rings are 120°(1) and 1.382(20) Å respectively. The dihedral angles between the mean plane of the porphyrin core and the mean planes of the phenyl groups are 62.3° and 69.3°. The dihedral angle between the mean planes of the imidazole ring and the four chelating nitrogen atoms is 87° while the dihedral angle between the mean planes of the core and the four chelating nitrogen atoms is only 3.2°. The angle between the lines joining C(41) to C(43) and N(1) and N(1a) is 13.2°. A stereoscopic drawing to highlight the dihedral angles of the imidazole to the porphyrin is given in Figure 6.3. The bond angles and distances of the imidazole ring agree well with the previously reported values [382].

Figure 6.4 is a perspective diagram of $MgTPP(4\text{-pic})_2$ with Mg at the centre of the four chelating nitrogen atoms and an octahedral configuration. The porphyrin core as a whole is slightly non-planar and the deviations of atoms from the mean plane of this core are given in the lower half of Figure 6.5. Individually, the pyrrole rings are planar to 0.008Å with angles of 8.3° and 8.7° to the plane of the four chelating nitrogen atoms and mutually at 6.1°. The averaged bond length for Mg-N = 2.071(2), N-Ca = 1.378(3), Ca-Cb = 1.449(3), Cb-Cb = 1.341(1), Cm-Ca = 1.407(2) and $Cm\text{-}C_{phenyl}$ = 1.503(7)Å. The upper half of Figure 6.5 shows important bond lengths of the porphyrin core. The distances between the nitrogen atoms of the pyrrole and pyridine rings are 3.066Å and 3.056Å.

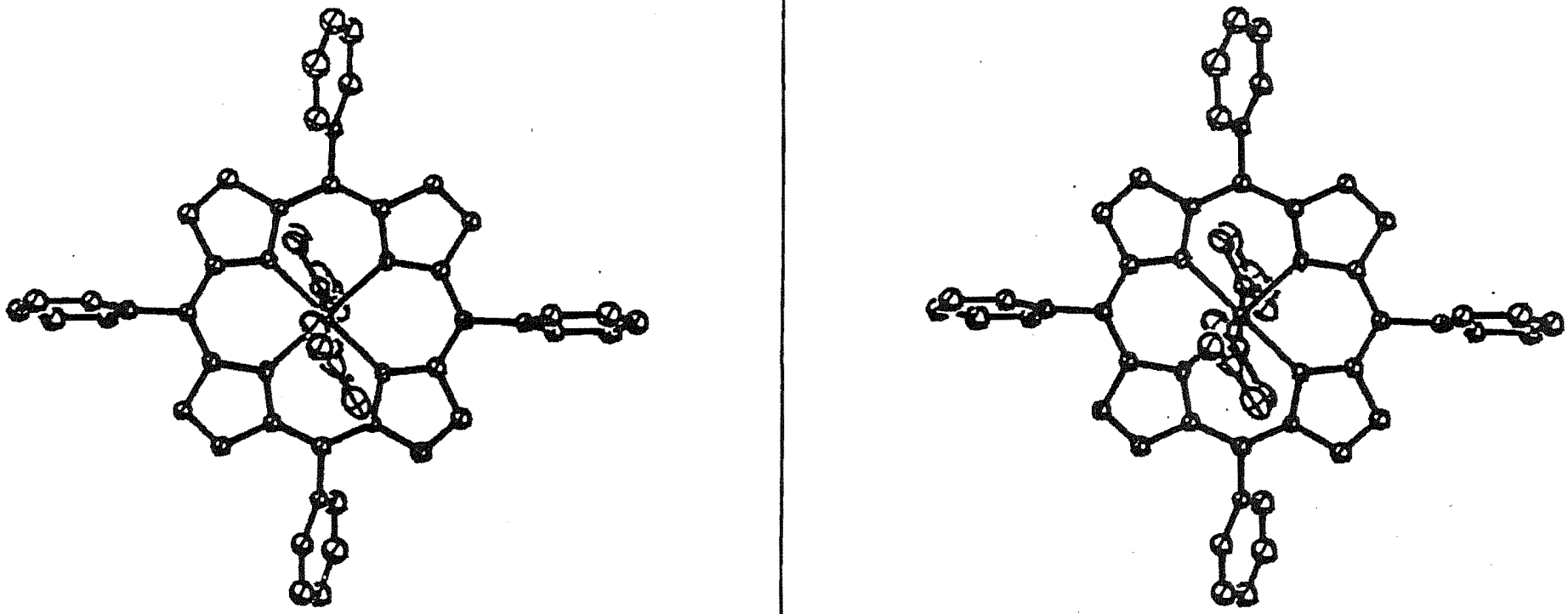

Figure 6.3 : Stereoscopic diagram of $MgTPP(1\text{-}MeIm)_2$, illustrating the relative orientation of the imidazole rings.

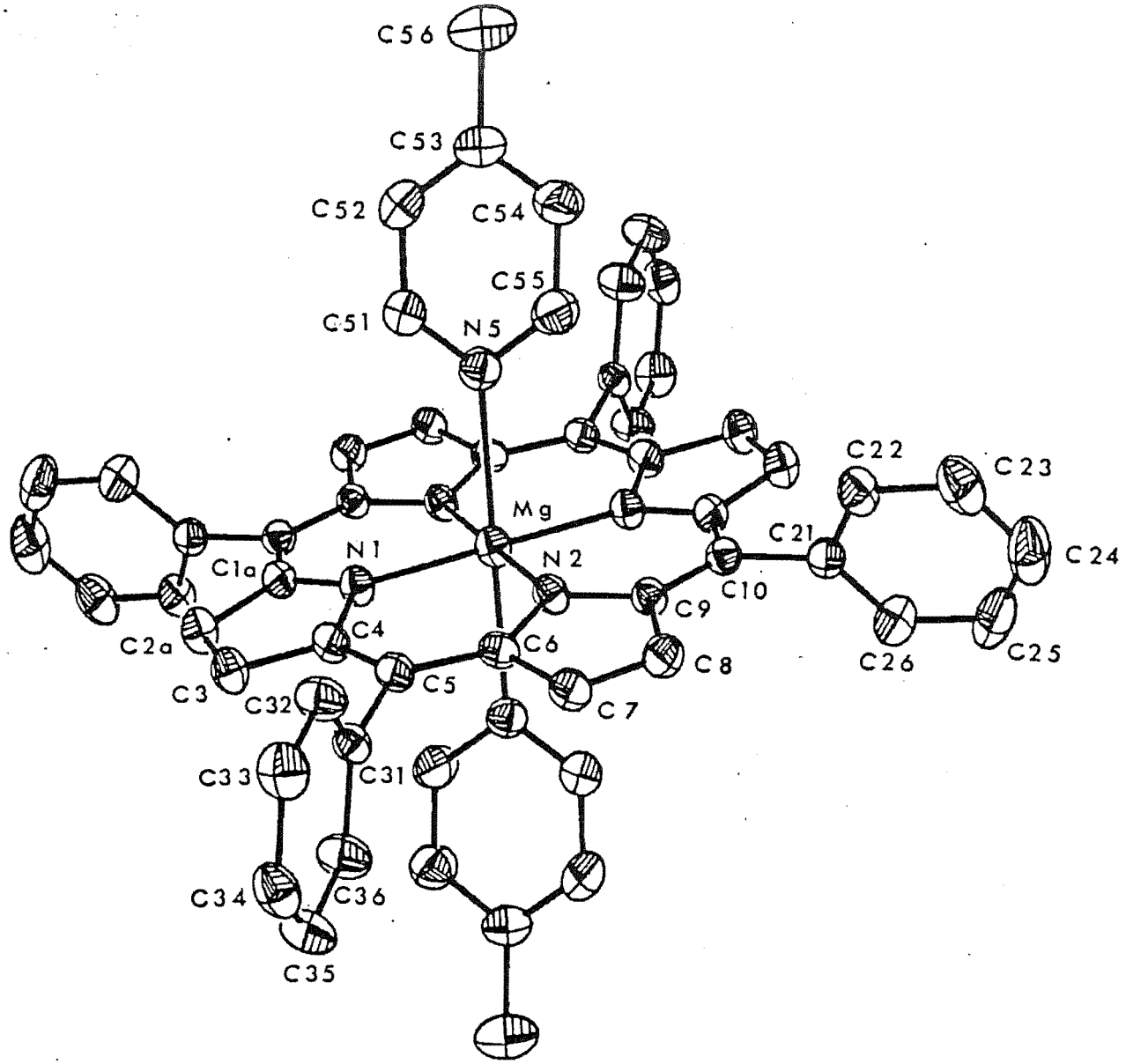

Figure 6.4 : Computer drawn structure of MgTPP(4-pic)$_2$ showing the numbering system (30% probability ellipsoids)

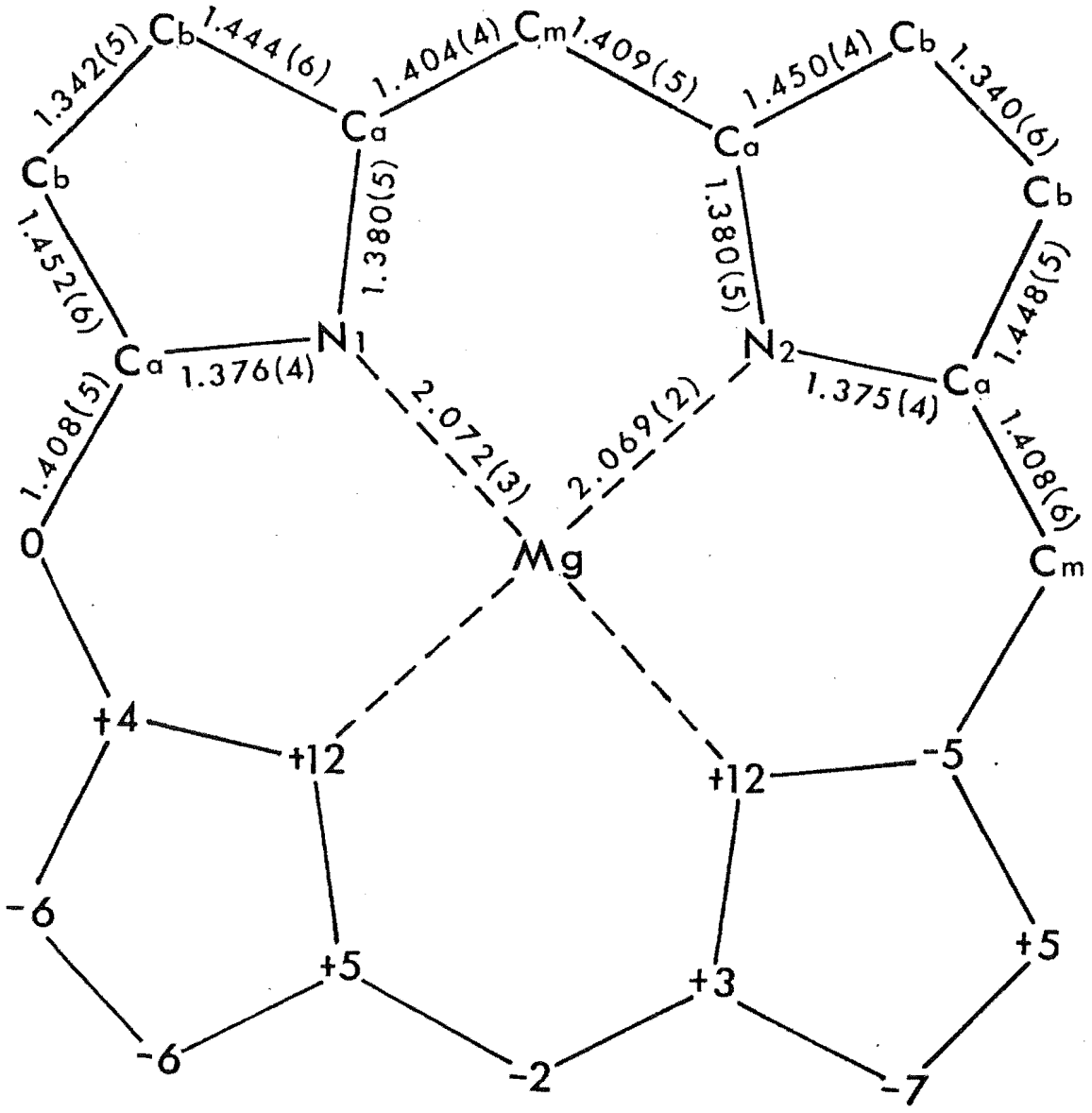

Figure 6.5 : A formal diagram of the porphyrin core of $MgTPP(4\text{-pic})_2$ displaying, on the upper half, the structurally independent bond lengths. On the lower half of the centrosymmetric diagram, the numbered symbol for each atom is replaced by its perpendicular displacement, in units of 0.01Å, from the mean plane of the porphyrin core.

The averaged bond angles are NMgN = 90(1), MgNCa = 126.1(12), CaNCa = 106.8(3), CaCmCa = 126.7(7), NCaCb = 109.1(2), NCaCm = 125.2(3), CaCbCb = 107.5(1)°. The averaged values of the internal angles and bond lengths of the phenyl rings are 120(1)° and 1.378(12)Å respectively. The two unique phenyl groups form dihedral angles of 84.9° and 70.3° with the mean plane of the core, while the dihedral angle between the mean planes of the pyridine ring and the four coordinating nitrogen atoms is 74.5°. The angle between the lines C(51)-C(55) and N(1)-N(1a) is 41.2°. A stereo diagram to illustrate the differences in dihedral angles between this complex and $MgTPP(1\text{-}MeIm)_2$ is given in Figure 6.6. The averaged bond lengths of the pyridine ring are N-C = 1.330(1)Å and C-C = 1.371(10)Å, while the averaged bond angles are MgNC = 122.2(7)°, CCC = 119(3)°, CCN = 124.2(7)°.

An illustration of a single molecule of $MgTPP(pip)_2$ with labelling of the atoms is given in Figure 6.7. This complex shows a basically similar octahedral structure to that of $MgTPP(4\text{-}pic)_2$. On the whole, the porphyrin core shows small but significant departures from planarity which are listed in the lower half of Figure 6.8. The pyrrole rings are planar to ±0.006Å with angles of 9.7° and 7.7° to the plane of the four chelating nitrogen atoms, and mutually at 7.5°. The averaged bond lengths for Mg-N = 2.073(2), N-Ca = 1.375(5), Ca-Cb = 1.445(3), Cb-Cb = 1.344(8), Ca-Cm = 1.412(3), $Cm\text{-}C_{phenyl}$ = 1.500(5) Å. The upper half of Figure 6.8 gives some important bond lengths of the porphyrin core. The distances between the nitrogen atoms of the pyrrole rings and piperidine are 3.180 and 3.163 Å.

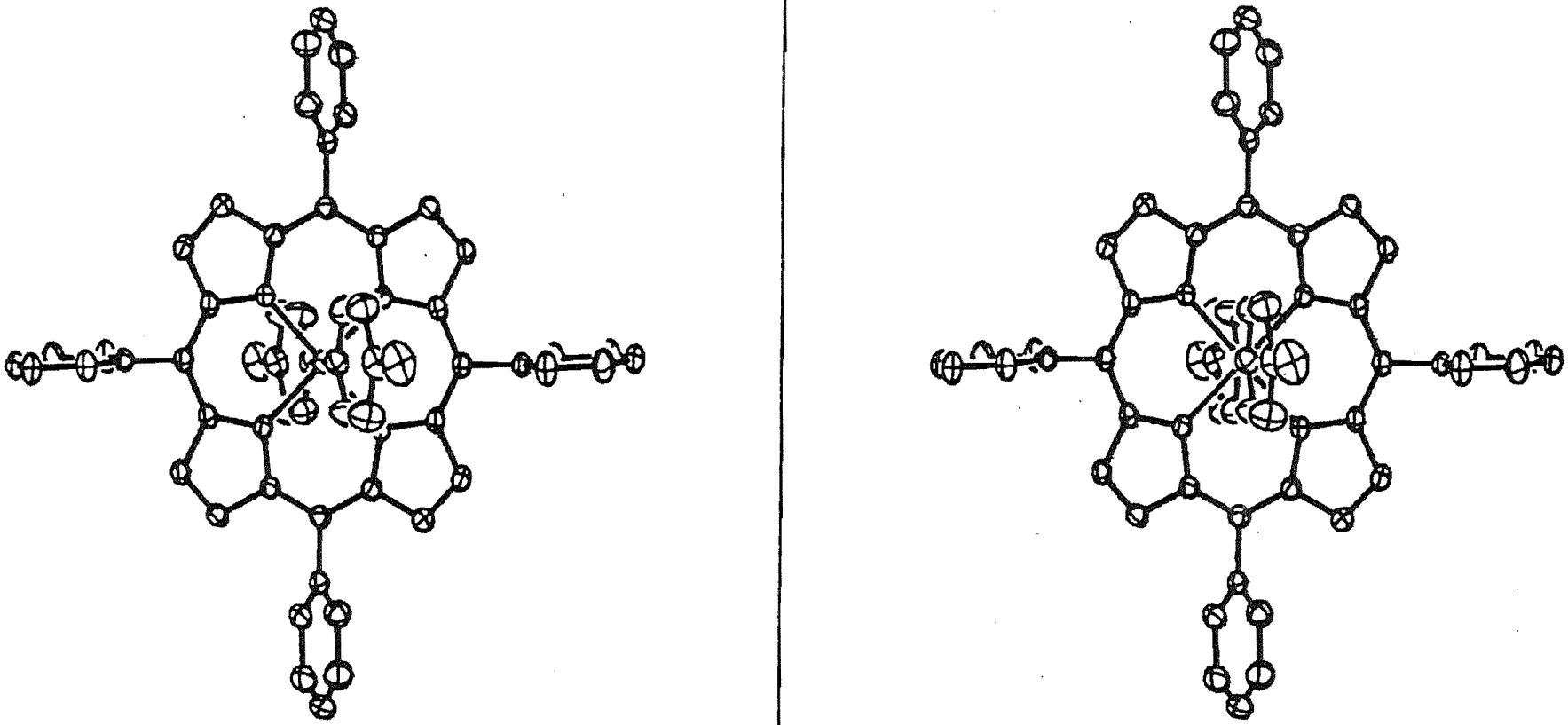

Figure 6.6 : Stereoscopic diagram of $MgTPP(4\text{-pic})_2$ illustrating the relative orientation of the pyridine rings

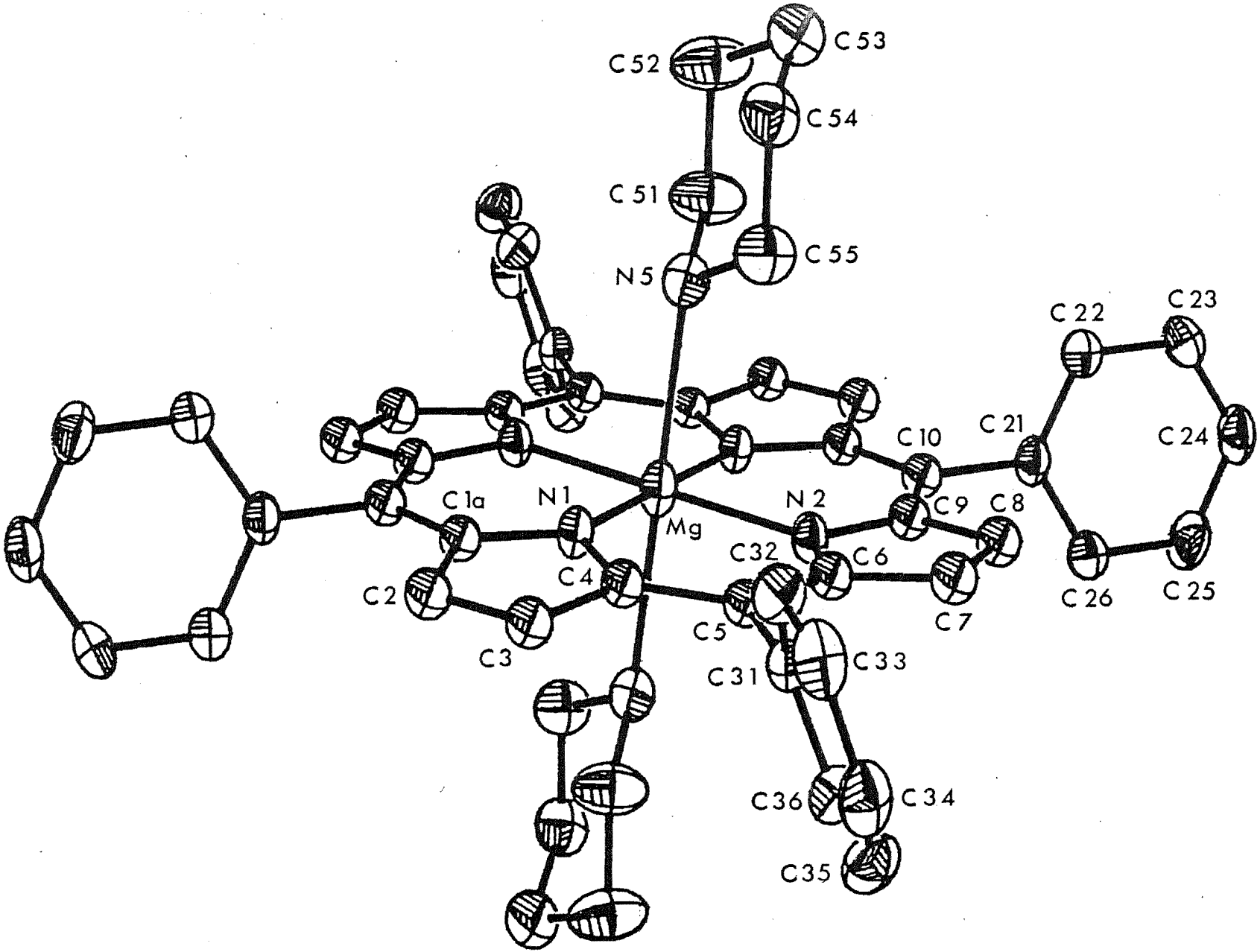

Figure 6.7 : Computer drawn structure of $MgTPP(pip)_2$ showing the numbering scheme (30% probability ellipsoids)

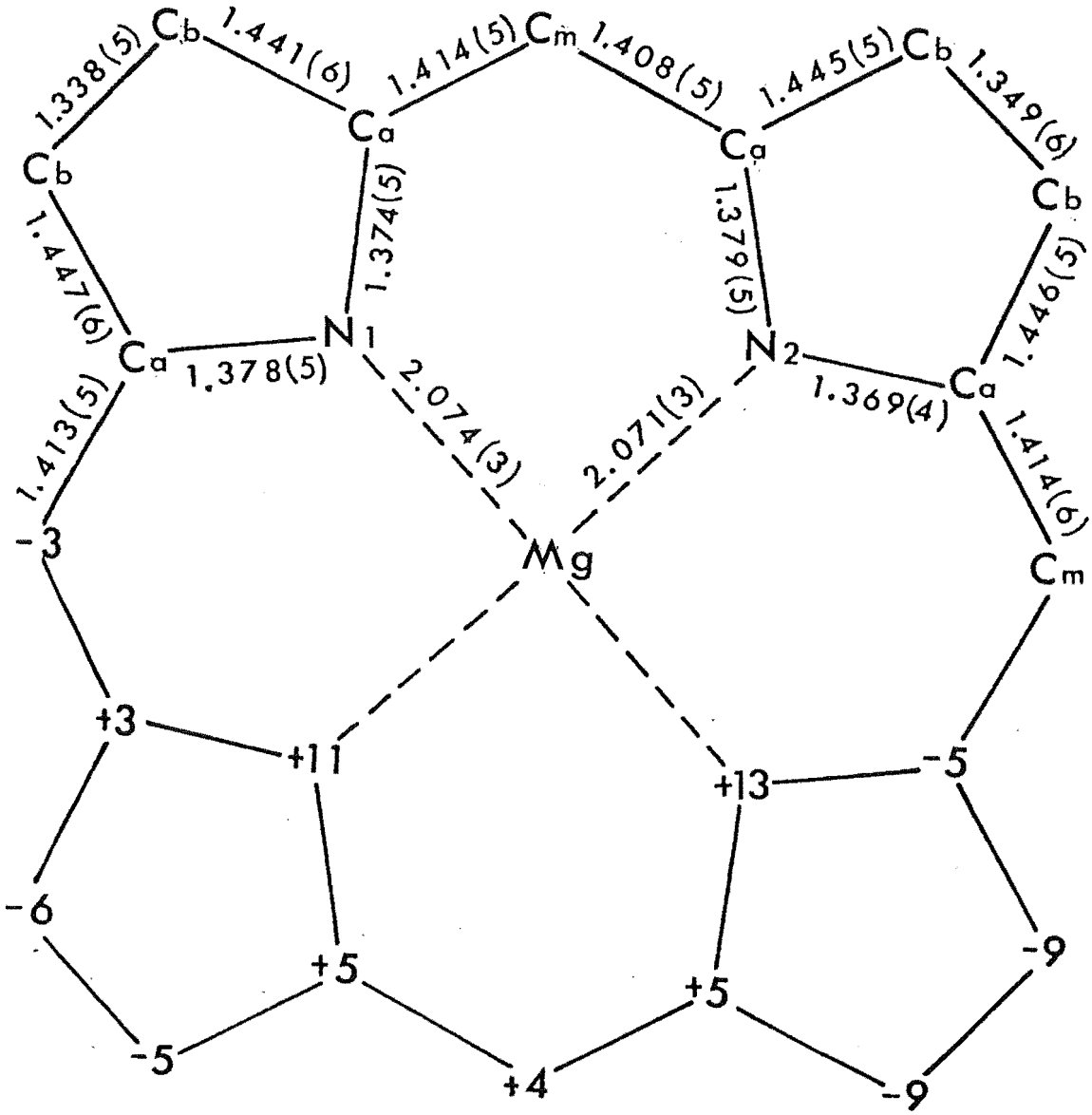

Figure 6.8 : Diagram of the porphyrin core of MgTPP(pip)$_2$ displaying on the upper half, the structurally independent bond lengths. On the lower half of the centrosymmetric diagram, atomic displacements in units of 0.01Å, from the mean plane of the porphyrin core.

The averaged values for the bond angles are NMgN = 90.0(1), MgNCa = 126.1(3), CaNCa = 106.9(1), CaCmCa = 126.2(5), NCaCb = 109.2(2), NCaCm = 125.5(2), CaCbCb = 107.4(3)°. The averaged internal angles and bond lengths of the phenyl rings are 120(1)° and 1.377(10)Å respectively. The phenyl groups form dihedral angles of 81.7° and 70.2° with the mean plane of the core, while the dihedral angle between the mean plane of the piperidine and the four coordinating nitrogen atoms is 79°. The angle between the lines C(51)-C(55) and N(1)-N(1a) is 43.9°. The similarity between this complex and MgTPP(4-pic)$_2$ is shown in a stereodiagram, Figure 6.9. The piperidine ring is in the chair form with averaged angles of CNMg = 116.6(4), CCC = 110.4(12)° and NCC = 114.7(5)°.

6.3.2 Electronic Spectra of MgTPP(1-MeIm)$_2$, MgTPP(4-pic)$_2$ and MgTPP(pip)$_2$

The electronic spectra of these complexes as KBr disc and Nujol mull films show dichroic properties and variable band intensities. Generally, three or four bands are observed in the visible region (Table 6.17). From reported equilibrium studies [82], the positions of these bands correlate to five- and six-coordinate MgTPP complexes. This suggests that grinding of the crystals and addition of Nujol has decomposed six-coordinate MgTPP complexes to five-coordinate ones. This suggestion is supported by the observation that increasing the Nujol concentration increases the intensities of the five-coordinate species.

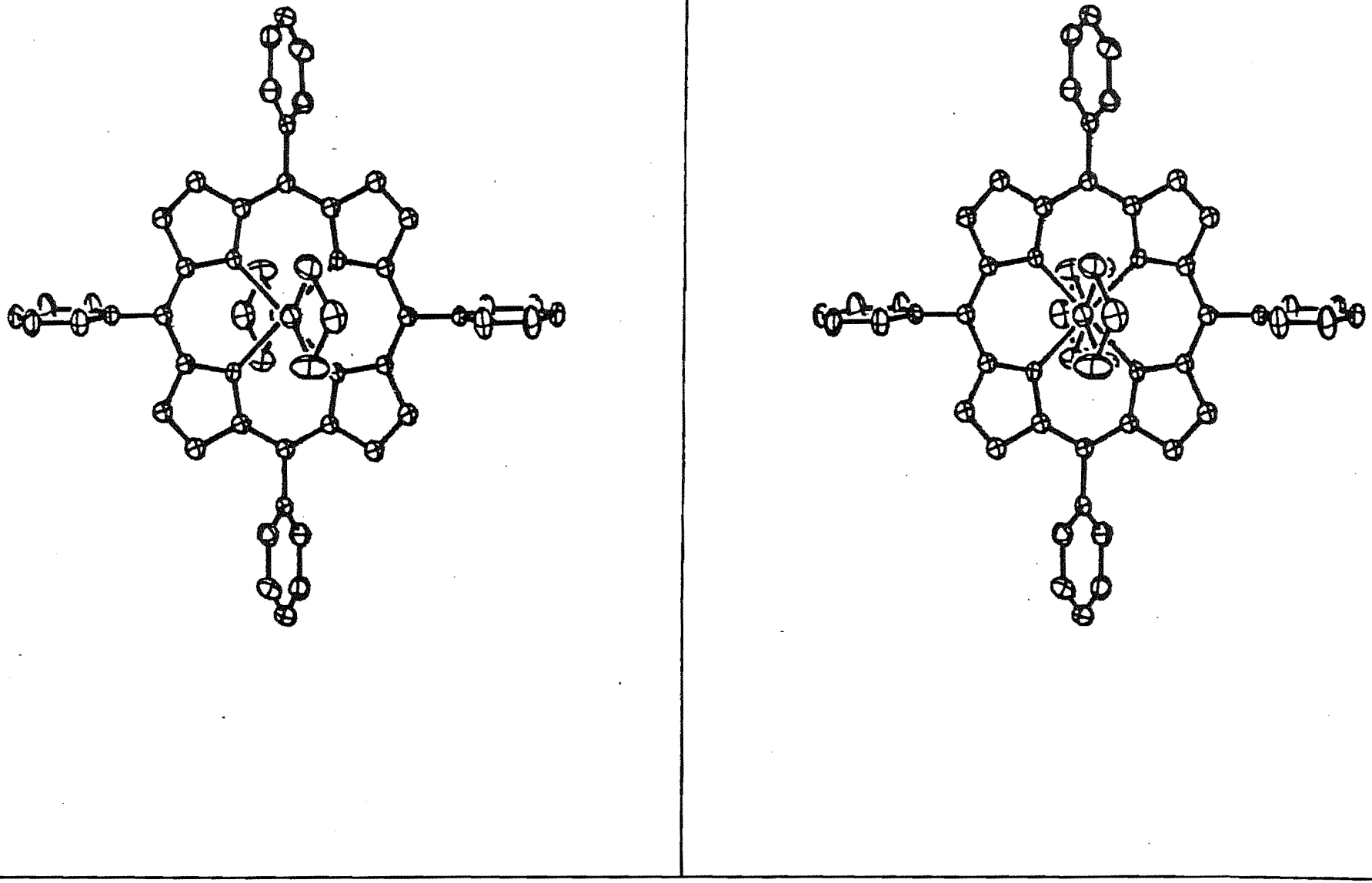

Figure 6.9 : Stereoscopic diagram of $MgTPP(pic)_2$ illustrating the relative orientation of the piperidine rings

Table 6.17 Electronic data for $MgTPP(L)_2$ in KBr disc, Nujol mull and CH_2Cl_2 solution

Compound	Electronic Bands (nm)					
	KBr disc		Nujol Mull		CH_2Cl_2 solution*	
	Q_o	Q_1	Q_o	Q_1	Q_o	Q_1
$MgTPP(1\text{-}MeIm)_2$	634	591[a]	640	595[a]	629	566
MgTPP(1-MeIm)	604	566			603	563
$MgTPP(4\text{-}pic)_2$	621		629	585[a]	623	577
MgTPP(4-pic)	603.5	565(broad)			603	563
$MgTPP(pip)_2$	619	576[a]	624	584[a]	620	576
MgTPP(pip)	603.5	565	604	565	603	563
$MgTPP(py)_2$			630	588	622	579
MgTPP(py)					603	563

* Data obtained from Kadish and Shiue [82]

a Peak probably due to overlapping of Q_1 band of six-coordinate $MgTPP(L)_2$ and Q_o band of five-coordinate MgTPP(L).

6.3.3 Infra-red Spectra

The formation of complexes between nitrogenous bases and MgTPP was established by infra-red spectroscopy because additional ligand bands are observed. The infra-red spectra of these complexes in KBr disc and Nujol solution are similar (Figure 6.10).

The infra-red spectrum of MgTPP(4-pic)$_2$ is similar to that for MgTPP(pip)$_2$ except for two extra bands at 1215 cm^{-1} and 1612 cm^{-1}. These bands are likely to result from C=N- groups in the pyridine ring because MgTPP(py)$_2$ has these bands too. The infra-red spectrum of MgTPP(1-MeIm)$_2$ has more complex bands than those observed for MgTPP(pip)$_2$ and MgTPP(4-pic)$_2$. However, the positions of the characteristic porphyrin bands remain the same for these three (Mg porphyrin)(nitrogenous base)$_2$ complexes.

6.4 DISCUSSION

6.4.1 Comparison of Axial Ligand Binding for Mg Porphyrin Complexes

X-ray results indicate that MgTPP(pip)$_2$ and MgTPP(4-pic)$_2$ are isostructural while MgTPP(1-MeIm)$_2$ adopts a different structure. Generally, the Mg-N(axial) ligand distances are long and very weak, so that it is understandable that grinding can decompose six-coordinate MgTPP complexes to five-coordinate ones. The Mg-N(axial) bond lengths of MgTPP(pip)$_2$ are by far the longest reported Mg-N bond distances, and they are even longer than those of 7-coordinate Mg complexes [393] (Table 6.18).

The Mg-N(axial) bond lengths are pip >4-pic >1-MeIm. This order obviously bears no correlation to the basicity of the ligands where the pKa value order is pip >1-MeIm >4-pic

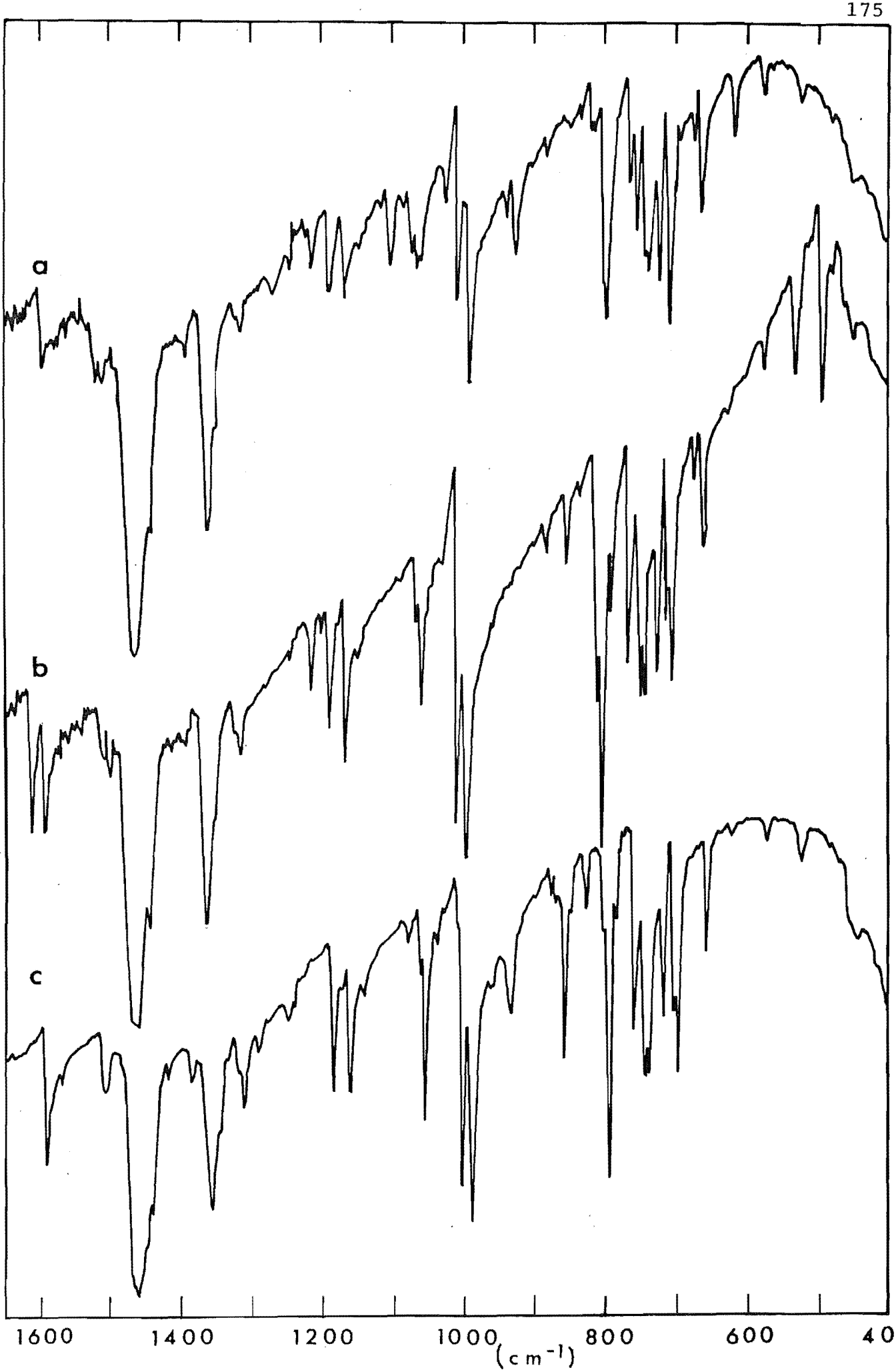

Figure 6.10 : Infra-red spectra of (a) $MgTPP(1\text{-}MeIm)_2$, (b) $MgTPP(4\text{-}pic)_2$ and (c) $MgTPP(pip)_2$

Table 6.18 Comparison of Mg-Nitrogen Bond Distances (Å)

Compound	Coordination Number	Mg-N (Å) (average)	Reference
$[Mg(Br)(Et)(Et_3N)]_2$	4	2.15	383
$Mg(C_6H_5)_2TMEDA$	4	2.202	384
$((THF)Mg)(HAlN\text{-}t\text{-}Bu)_3$	4	2.090	385
$[(CH_3)_2N(CH_2)_2N(CH_3)MgCH_3]_2$	4	2.132	386
$MgPc(H_2O)(py)_2$	5	2.040[a]	367
ethyl chlorophyllide a	5	2.086[a]	24
ethyl chlorophyllide b	5	2.081[a]	368
methylchlorophyllide a	5	2.093[a]	369
methylpyrochlorophyllide a	5	2.090[a]	370
$MgTPP^+ClO_4^-$	5	2.096[a]	366
$MgTPP(H_2O)(2\text{-pic})_{2.5}$	5	2.087[a]	Chapter 7 of this work
$MgTPP(1\text{-MeIm})_2$	6	2.078[a] 2.297[b]	this work
$MgTPP(4\text{-pic})_2$	6	2.071[a] 2.386[b]	this work
$MgTPP(pip)_2$	6	2.073[a] 2.419[b]	this work
$Mg(C{\equiv}CPh)_2(TMEDA)_2$	6	2.375	387
$Mg[(EtO)_2POS]_2(NC_5H_5)_4$	6	2.229 2.280	388
$Mg(C_5H_4NCOO)_2(H_2O)_2$	6	2.22	389
$Mg(C_6H_4NO_2)_2(H_2O)_4$	6	2.271	390
$Mg(Br)_2(C_5H_5N)_4$	6	2.17 2.28	391
$Mg(H_2O)(EDTA)^{2-}$	7	2.378	392
$Mg_2(EDTA)(H_2O)_9$	7	2.396	393
Mg(benzo-15-crown-5)$(NCS)_2$	7	2.061	394
$Mg(N_5H_{23}C_{15})(Cl)_2(H_2O)_6$	7	2.24-2.31	395

a Mg-N (equatorial) bond length

b Mg-N (axial) bond length

[396]. Instead, steric effects between the porphyrin and the hydrogen atoms of the ligands can be considered to be important in determining these bond lengths. Although both piperidine and pyridine are six-membered rings, the presence of the aromatic ring in pyridine suggests that steric effects would be reduced for pyridine compared with piperidine. It is observed that the Mg-N(axial) bond lengths for MgTPP(4-pic)$_2$ are slightly shorter than those for MgTPP(pip)$_2$. The five-membered imidazole ring exhibits even smaller steric effects than pyridine and shorter Mg-N(axial) bond lengths are indeed observed. This kind of steric effect has also been observed for low-spin Fe(II)TPP complexes [397]. However, the metal-N(axial) bond distances for six-coordinate MgTPP complexes are significantly longer than those for corresponding Fe(II) complexes, so that steric interaction would be expected to be decreased at longer distances. Consequently, it is possible that there are some electronic effects contributing to the shorter Mg-N(axial) ligand bonds for MgTPP(1-MeIm)$_2$ compared with MgTPP(pip)$_2$ and MgTPP(4-pic)$_2$. A possible electronic factor is the overlapping of the empty d orbitals of the metal ion and filled p orbitals of the nitrogen atoms of the ligand.

The small differences in the Mg-N(equatorial) bond lengths for MgTPP(1-MeIm)$_2$ may be related to this interaction (Mg-N(1) = 2.074Å, Mg-N(2) = 2.082Å). By contrast, the corresponding values for MgTPP(pip)$_2$ and MgTPP(4-pic)$_2$ differ by only ~0.003Å.

The relative orientation of the imidazole ring to the plane of the four chelating nitrogen atoms is different from those of 4-picoline and piperidine. This difference is

likely to be a result of the intermolecular packing effect of the unit cell of MgTPP(1-MeIm)$_2$ complex. Figure 6.11 indicates that there is relatively close contact between one of the phenyl groups of tetraphenylporphyrin and the coordinated imidazole group. The closest non-bonding interatomic distances for these two groups are 3.37Å (Table 6.19). For the unit cells of MgTPP(pip)$_2$ and MgTPP(4-pic)$_2$, the interatomic distances are longer (Figure 6.12).

Thus, X-ray results indicate that the Mg-N(axial) bond lengths for six-coordinate MgTPP complexes are strongly influenced by steric effects of the ligands.

6.4.2 Comparison of Fe(II)TPP and MgTPP Complexes

The detailed X-ray results for isostructural pairs of Fe(II) and MgTPP(L)$_2$ complexes, where L=pip and L=1-MeIm, enable a direct comparison of the binding properties of these two metal ions to be made. Fe(II) and Mg(II) ions have closely similar ionic radii (0.64Å and 0.65Å respectively [398]). The insignificant differences for the bond angles/bond lengths of six-coordinate MgTPP and Fe(II)TPP complexes indicate that the metal ions do not affect the porphyrin core. However, there are significant differences in the metal-nitrogen bond lengths. The equatorial and axial bond lengths are shorter by about 0.07Å and 0.3Å respectively for the corresponding Fe(II) complexes (Table 6.20, Figure 6.13). These shorter bond lengths are due to π-bonding between the electrons of 3d orbitals of Fe(II) and the empty p orbitals of nitrogen atoms (Figure 6.14) [399]. For Fe(II), there are five 3d orbitals. The $3d_{z^2}$ and $3d_{x^2-y^2}$ orbitals are incorporated into metal hybrids which are involved in metal-ligand

Table 6.19 Interatomic distances (within 4.0Å) for non-bonding atoms of $MgTPP(1\text{-}MeIm)_2$

Atoms	Distance (Å)	Atoms	Distance (Å)
N4-C33'	3.366	N4-C44'	3.726
C42-C33'	3.367	C41-C44'	3.728
N4-N4'	3.386	C43-C33'	3.745
C43-C44'	3.452	N3-C32	3.791
C41-C32'	3.478	C44-C34	3.799
C32-N4	3.516	C41'-C33	3.812
C43-C44'	3.529	C42'-C32	3.845
N3-C44	3.556	C44-C32'	3.897
N4-C42	3.571	C42-C54'	3.921
C43-C54'	3.573	C35-C33'	3.947
C55-C54'	3.605	C43-C32'	3.956
C42-C44'	3.615	C43-N4'	3.956
N3-C44'	3.622	C35-C32'	3.960
C44-C33'	3.670	N4-C34	3.966
N4-C41'	3.706	C53'-C55	3.969
C41-C42'	3.718	C43-C53'	3.977

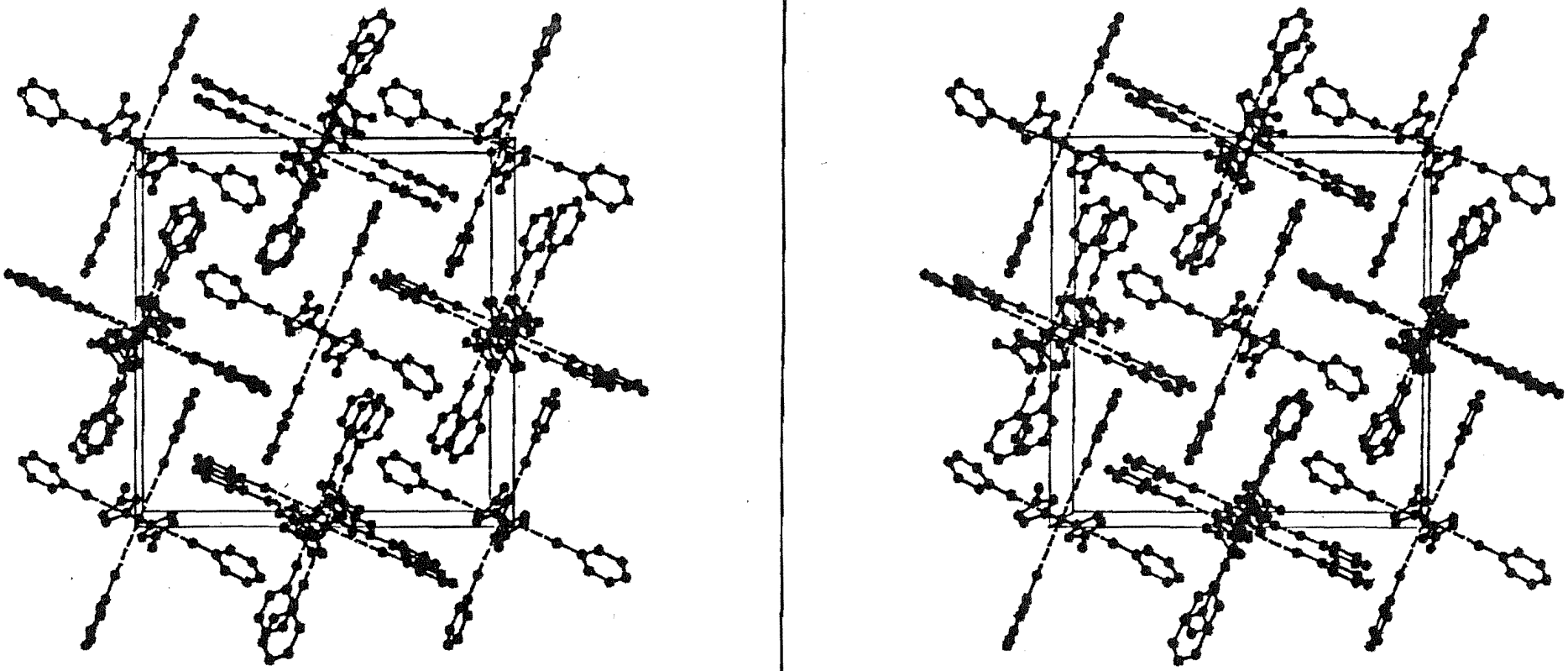

Figure 6.11 : Stereoscopic diagram of the cell contents of $MgTPP(1\text{-}MeIm)_2$ excluding the porphyrin core

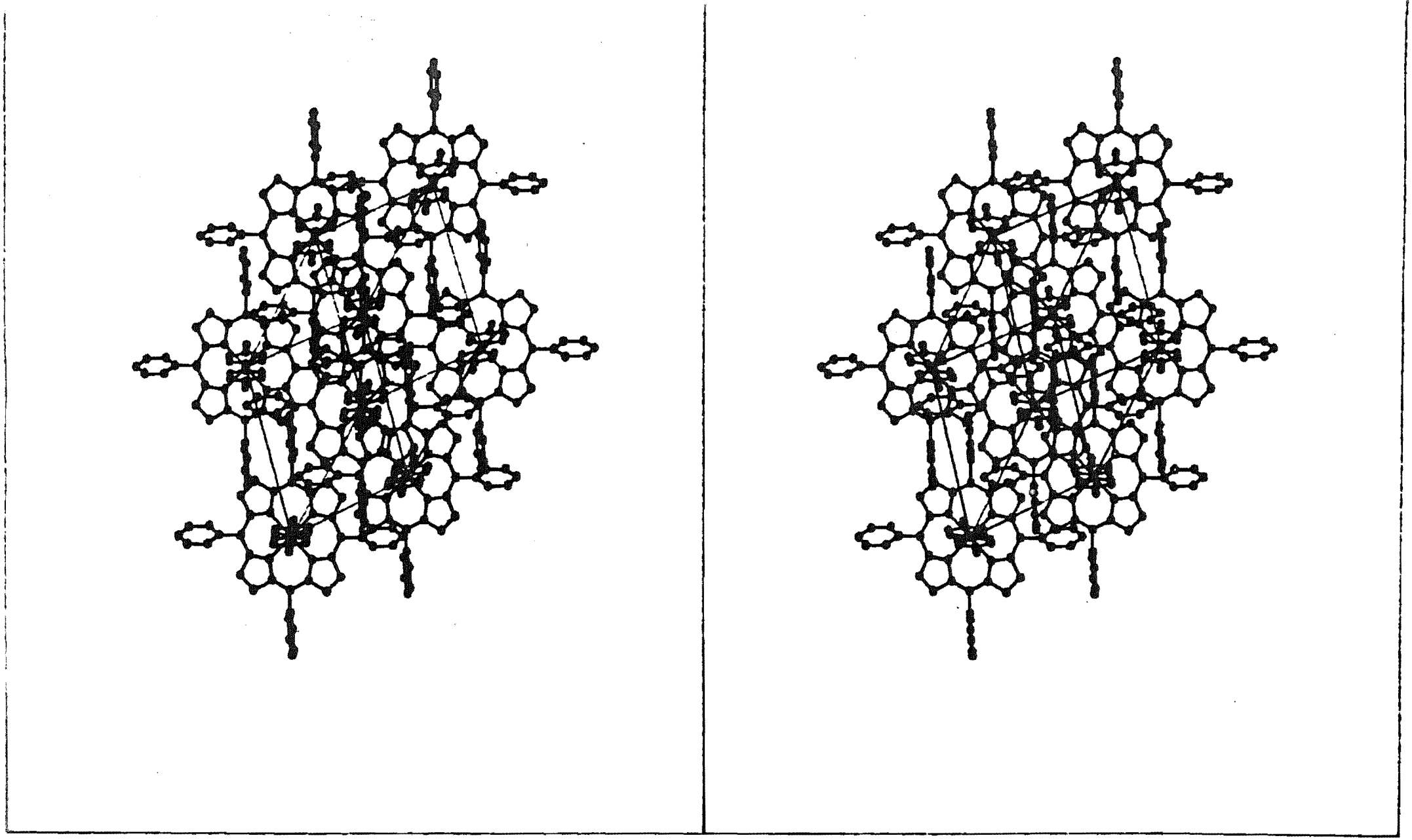

Figure 6.12 (i): Stereoscopic diagram of the cell contents of $MgTPP(4\text{-pic})_2$

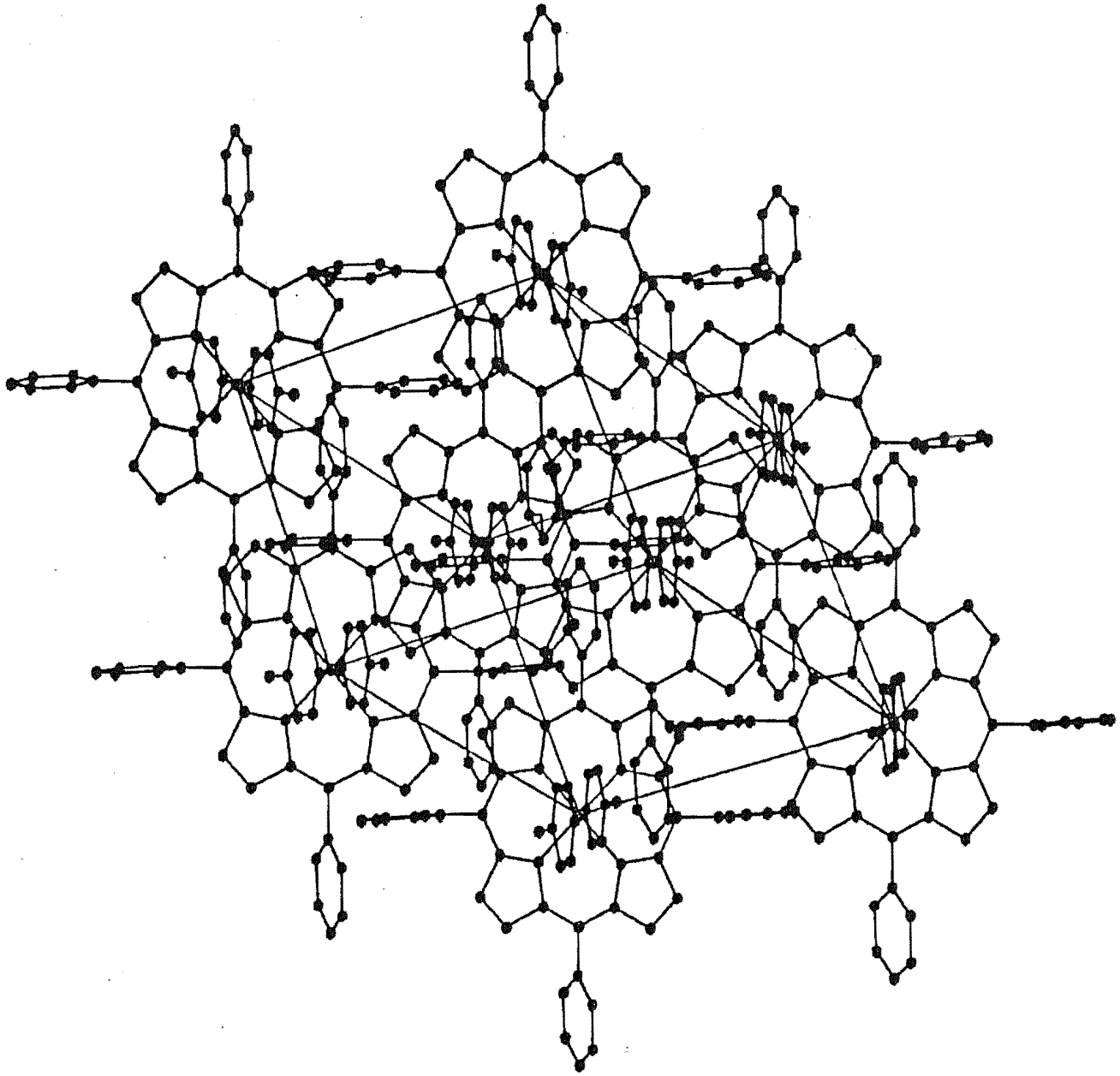

Figure 6.12(ii) : Unit cell packing arrangement in $MgTPP(4\text{-pic})_2$

Table 6.20 Comparison of the nitrogenous base complexes of Mg-, Fe(II)- and Co(III)-TPP

Compound	Oxidation Number	Crystal System	Space Group	Cell Dimensions	Number of Molecules per unit cell	Averaged bond length		Reference
						M-N equatorial	M-N axial	
$MgTPP(1\text{-}MeIm)_2$	2	Tetragonal	$P4_2/n$	a=20.764(5) c=9.659(3)	4	2.071	2.297	this work
$FeTPP(1\text{-}MeIm)_2$	2	Tetragonal	$P4_2/n$	a=20.651(4) c=9.526(1)	4	1.997	2.014	375
$MgTPP(pip)_2$	2	Triclinic	$P\bar{1}$	a=9.944(3) b=11.436(3) c=11.914(3) α=101.78° β=104.59° γ=115.60°	1	2.071	2.419	this work
$FeTPP(pip)_2$	2	Triclinic	$P\bar{1}$	a=11.113(3) b=12.071(3) c=9.797(3) α=105.67° β=113.70° γ=101.02°	1	2.004	2.127	374
$CoTPP(pip)_2^+$	3	Triclinic	$P\bar{1}$	a=12.049(3) b=12.911(3) c=10.405(5) α=102.73° β=92.04° γ=65.24°	1	1.978	2.060	401
$MgTPP(4\text{-}pic)_2$	2	Triclinic	$P\bar{1}$	a=10.146(2) b=11.210(2) c=11.643(3) α=65.63° β=76.32° γ=67.42°	1	2.071	2.386	this work

Table 6.20 continued over ...

Table 6.20 continued

Compound	Oxidation Number	Crystal System	Space Group	Cell Dimensions	Number of Molecules per unit cell	Averaged bond length		Reference
						M-N equatorial	M-N axial	
$MgOEP(py)_2$	2	Triclinic	$P\bar{1}$	a=10.607(3) b=10.423(4) c=9.957(4) $\alpha=114.69^{\circ}$ $\beta=90.56^{\circ}$ $\gamma=99.27^{\circ}$	1	2.068	2.389	373

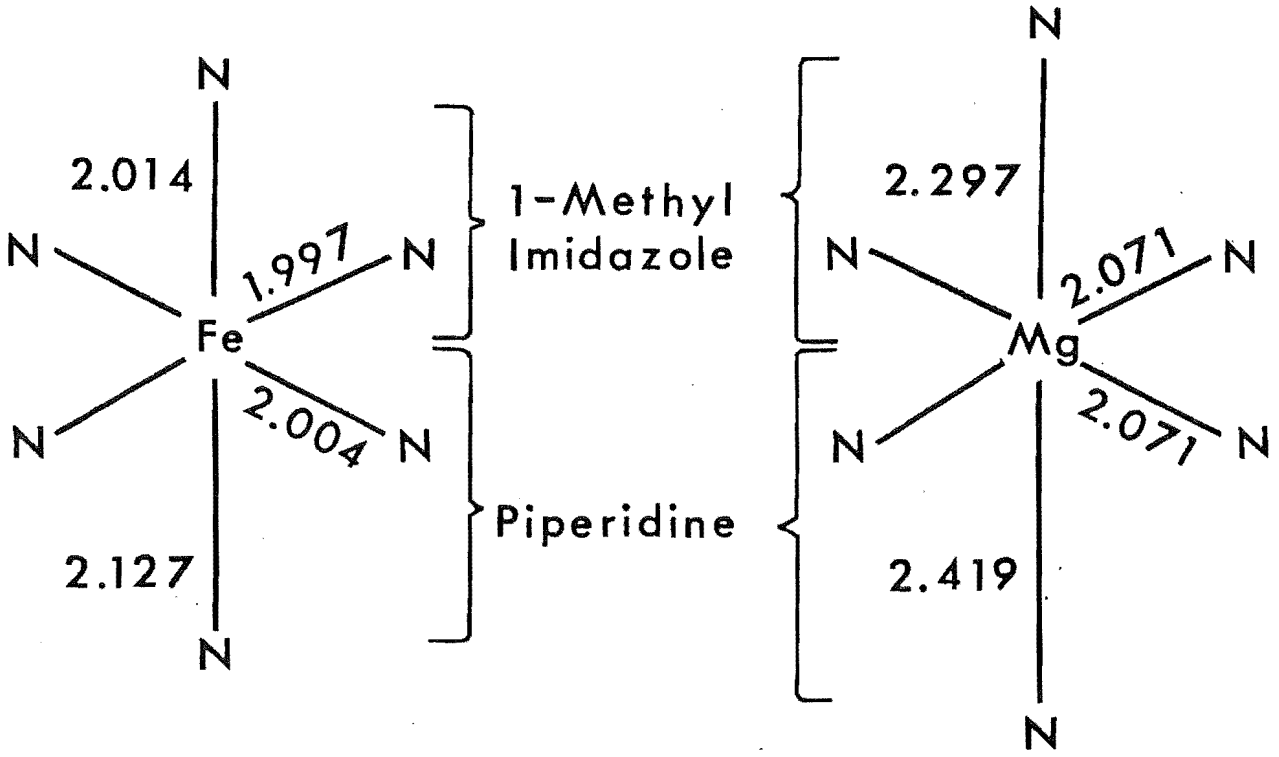

Figure 6.13 : Comparison of bond lengths for Fe(II)- and Mg(II)-TPP(L)$_2$

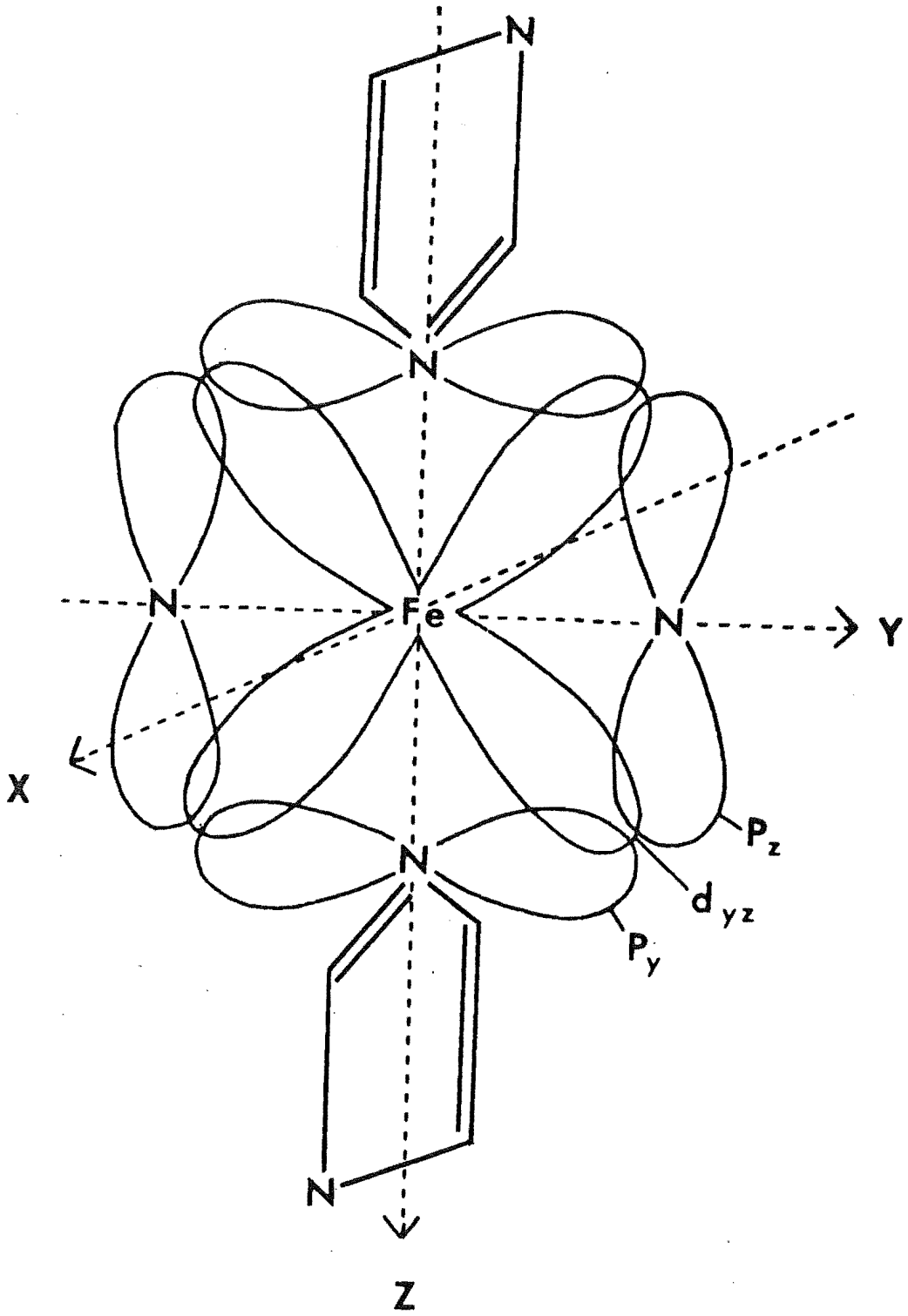

Figure 6.14 : Intreactions of the $3d_{yz}$ atomic orbital of iron of $Fe(II)TPP(L)_2$ with the π^*-orbitals of the ligand nitrogen atoms

σ-bonds. The $3d_{xy}$ orbital is occupied but it does not take part in bonding because of its symmetry [158,400]. Finally, the $3d_{xz}$ and $3d_{yz}$ orbitals which are also filled are of the correct symmetry to combine with p π^*-orbitals of nitrogen atoms in the axial and equatorial positions. This π-bonding leads to a flow of charge away from the metal to the ligand which, in turn, can donate more electron density back to the metal via the σ-bonds. On the whole, shorter metal-nitrogen bond lengths are observed.

Shorter metal-nitrogen bond lengths have also been observed for the TPP complex of Co(III), which is isoelectronic with Fe(II) and has an ionic radius of 0.63Å [401]. This is because of the increase in formal charge for Co(III) which can increase the strength of axial binding.

This comparison shows that the presence of d electrons for Fe(II) and Co(III) considerably enhances the binding of nitrogen donors, especially in the axial positions. For Mg, having no d electrons, there is lower affinity for axial ligands in porphyrin systems.

6.4.3 Comparison of Mg Porphyrin Complexes

A comparison of the structures of $MgOEP(py)_2$ [373] and $MgTPP(4\text{-pic})_2$ indicates that the porphyrin core and metal-nitrogen bond lengths are very similar. Thus substitutions of the porphyrin ring at the Cb atoms and at Cm atoms do not appear to affect Mg-N distances in Mg porphyrin complexes. Furthermore, substitution of a methyl group for hydrogen at the 4-position of pyridine has no significant steric effect on the metal-nitrogen bond lengths. This result contrasts with that for 2-picoline where a five-coordinate hydrated MgTPP complex, $MgTPP(H_2O)(2\text{-pic})_{2.5}$,

is formed (Chapter 7). The bond distance between the centre of the core and one of the chelating nitrogen atoms for $MgTPP(H_2O)(2\text{-pic})_{2.5}$ is ~2.05Å. The slightly longer Mg-N(equatorial) bond lengths of ~2.07Å for six-coordinate MgTPP shows that there is a radial expansion of the Mg-N bonds to accommodate the Mg^{2+} ion into the centre of the core for these complexes. This radial expansion is also observed for high-spin six-coordinate FeTPP complexes [402].

For all three Mg structures reported here, the phenyl groups of the porphyrin ring make angles greater than 60° with the core. This is considered to be an indication that there are insignificant steric interactions between the hydrogen atoms of pyrrole and phenyl hydrogen atoms within the porphyrin ring [403].

Generally, the bond distances around the porphyrin core remain the same. This holds even for radial cations like $MgTPP^+$ [366].

6.4.4 Effects of Structures on the Spectral Properties of $MgTPP(L)_2$ Complexes

The solid state properties of metalloporphyrin compounds have been of considerable interest because their modes of energy transfer have been considered to be models for the energy transfer phenomena in heme proteins, antenna chlorophyll and accessory pigments in photosynthesis [404]. In addition, these properties also provide an understanding of their molecular characteristics [405] which are important for the development of solar cells (Chapter 9). The common method for determining the solid state properties of the metalloporphyrin compounds is by electronic spectroscopy.

The electronic spectra of crystalline MgTPP complexes indicate that the Q_o and Q_1 bands for MgTPP(1-MeIm), MgTPP(pip) and MgTPP(4-pic) species, are at 603.5 and 565 nm respectively. These positions correlate well with those observed in solution [82] and suggest that the spectral properties of five-coordinate MgTPP(L) complexes are not affected by the different types of ligands. However, the positions of the bands for the six-coordinate $MgTPP(L)_2$ complexes show significant differences for different axial ligands for KBr disc, CH_2Cl_2 solution and Nujol mull states. The most reliable band for the determination of the red-shift in six-coordinate MgTPP is the Q_o band, because the red-shifted Q_1 band can overlap with the Q_o band of five-coordinate MgTPP to produce another peak. For example, the peak at 595 nm of $MgTPP(1\text{-MeIm})_2$ in Nujol is probably a result of this type of overlap.

Although the peak positions of the Q_o bands for these six-coordinate MgTPP complexes in Nujol mull, KBr and CH_2Cl_2 solution [82] are different, the order for their red-shifts remains the same. It is observed that the Q_o band of $MgTPP(1\text{-MeIm})_2$ is red-shifted the most, followed by $MgTPP(4\text{-pic})_2$ and then $MgTPP(pip)_2$. The X-ray results in this work show that that the Mg-N(axial) bond lengths are in the reverse order, pip>4-pic>1-MeIm. Thus the closer the ligand to the Mg centre, the greater is the red-shift.

This result agrees well with the suggestion by Katz and coworkers that the red-shift in six-coordinate chlorophyll-bifunctional ligand adducts, (which are models for the reaction centre), is related to the distance between

the nucleophilic centres of axial ligands [18]. The greater the distance at which the ligands are held, the smaller the red-shift.

Overall, the X-ray and spectral studies of MgTPP complexes indicate that the Mg-N bond distances of the nitrogenous bases which are coordinated to Mg in the axial positions determine the magnitudes of the red-shift. This type of study could be extended to bifunctional ligands and other nucleophilic atoms like oxygen and sulphur which are likely to be coordinated to Mg in chlorophyll [18].

6.4.5 Effects of Coordination State on the Stabilities of $MgTPP(L)_2$ Complexes

Under the influence of light, Mg porphyrin in hydrophobic environments readily photo-decomposes to a variety of products (Chapter 4). However, it was observed that addition of nitrogenous bases suppress these photo-reactions [314]. The extra stability to photo-oxidation by Mg porphyrin in nitrogenous bases has been suggested to be a result of the formation of six-coordinate Mg porphyrin complexes which stabilises the magnesium-porphyrin bonds. Furthermore, these complexes prevent the dissociation of Mg from the porphyrin ring.

The crystal structures show that the Mg ion is exactly in the centre of the porphyrin core and the two axial ligands are coordinated symmetrically. Dissociation of Mg through the axial positions is therefore unfavourable compared to five-coordinate MgTPP complexes where the Mg ion is displaced out of the porphyrin ring (Chapter 7). Thus, six-coordination stabilises the Mg centres of metalloporphyrin. It is possible that in the reaction centres of photosynthetic organisms, this type of six-coordination may also be

important for the stabilisation of Mg ions. The stability of six-coordinate MgTPP complexes to light in the crystalline state shows that these compounds can be used as photosensitizing compounds in energy generating processes (Chapter 9).

Thus, the detailed crystal and molecular structural determination of six-coordinate Mg porphyrin has provided an insight into one of the important photochemical properties of metalloporphyrin. Furthermore, these structures and properties may be related to the chlorophyll-ligand interactions in photosynthetic systems.

CHAPTER 7

CRYSTAL STRUCTURE OF MONOHYDRATE 2-PICOLINE MAGNESIUM PORPHYRIN COMPLEX

7.1 INTRODUCTION

The coordination states of Mg tetrapyrrole complexes have always been of considerable importance because of their relationship to chlorophyll and its related compounds [60]. It has been generally accepted that the Mg centre is preferentially five-coordinated but under "forcing" conditions, six-coordination can be observed (Chapter 2).

Katz and coworkers have suggested that the six-coordinate Mg centre is situated close to the mean plane of the chelating nitrogen atoms of the macrocyclic ring, while the five-coordinate Mg centre is displaced out of the plane [62]. The relative position of the Mg centre to this plane is of considerable interest in the understanding of the effect of light on the potential energy curves of Mg tetrapyrrole complexes [406]. An effective way of determining the relative position of the Mg centre accurately is by X-ray diffraction studies. Most of these studies indicate that the five-coordinate Mg centre is displaced out of the plane, by values ranging from 0.273Å to 0.496Å [24,60,366-370].

In this chapter, the X-ray structure of another five-coordinate Mg tetrapyrrole complex, $MgTPP(H_2O)(2\text{-pic})_{2.5}$ is reported. The structure has not been fully refined because of the disordered half molecule of 2-picoline in the crystal, which gives, overall, 2.5 molecules of 2-picoline. However,

the main features of Mg porphyrin entity have been established. Distinct structural differences are observed between this complex and MgTPP(H_2O) [60]. In addition, under the same experimental conditions, six-coordinate MgTPP complexes are obtained in solutions of 4-picoline, 1-methylimidazole and piperidine (Chapter 6). These differences in coordination state enable the steric effects of substitution at the carbon atom adjacent to the nitrogen atoms of the pyridine ring to be assessed in detail.

Another interesting feature is the close similarity of the structure to that of MgPc(H_2O)$(py)_2$ [367], especially when it is considered that the tetradentate ligand in the latter complex is quite different from TPP and also that the unit cell packing arrangement differs significantly from that of TPP. The structural similarity between the two molecular entities therefore indicates that this is a favourable electronic and bonding arrangement for magnesium porphyrin complexes. In both cases displacement of Mg from planar rings is increased by hydrogen bonding of nitrogen donors to a coordinated water molecule. Such an arrangement could also arise in a protein environment through favourable orientation of amino acid side chain groups. Thus, this type of structural feature may be important in facilitating the displacement and charge separation required in the primary events of photosynthesis.

7.2 EXPERIMENTAL

MgTPP(H_2O) was prepared according to the methods described in Chapter 6. It was then heated in 2-pic until

boiling and shiny, red-purple, needle-like crystals were obtained from an air-exposed solution of 2-pic-chloroform solution.

A crystal of approximate dimensions 0.35x0.125x0.163 mm was used for the structure determination. Intensity data were collected at room temperature on a computer-controlled Nicolet R3 m four-circle diffractometer using graphite monochromated Mo K_α radiation (Table 7.1). The cell parameters were determined by least squares refinement using 25 accurately centred reflections ($28° < 2\theta < 32°$). A total of 6566 reflections were collected using the θ-2θ scan technique ($3° < 2\theta < 45°$). Crystal stability was monitored by recording three standard reflections for every 100 reflections and no significant variation was observed. Data reduction gave 6319 unique reflections of which 2507 having $I_o \geq 3\sigma(I_o)$, were used in the subsequent structural analysis. Intensities were corrected for Lorentz-polarisation effects and an empirical absorption correction based on ψ-scan data was applied. Scattering factors for Mg were taken from Cromer and Mann [380] and anomalous dispersion corrections were from Cromer and Liberman [381].

The Mg atom and 48 non-hydrogen atoms of the porphyrin ring were located by direct methods using the programme RANT. All the programmes used for data reduction and structure solution are included in the SHELXTL (version 3.0) package [379]. The remaining non-hydrogen atoms were located by difference Fourier techniques and the structure was refined using blocked cascade least squares method. Hydrogen atoms were then fixed in theoretically idealised positions (C-H=0.96Å) except Ha and Hb which were refined, with

Table 7.1 : Crystal data

Compound	$MgTPP(H_2O)(2\text{-pic})_{2.5}$
Molecular weight	887.9
Crystal system	Triclinic
Space group	$P\bar{1}$
Cell dimensions, a (Å)	10.247(2)
b (Å)	13.325(3)
C (Å)	17.700(3)
α	87.23(2)°
β	88.69(2)°
γ	86.88(2)°
Volume	2409.9
Dm	1.23
Dc	1.22
Z	2
F(000)	939.81
$\mu(cm^{-1})$	0.85
Crystal dimension (mm)	0.35x0.125x0.163
Mosaicity	0.22
Radiation	Mo K_α
2θ range	3-45
Total independent reflections	6319
Reflections used in refinements for which $I_o \geq 3\sigma(I_o)$	2507
g	-0.00201

thermal parameters equal to 1.2xU of their carrier atoms.

The difference map showed disordered 2-picoline molecules with occupancy factor of half. The measured density also indicates the presence of half a molecule of 2-picoline in the structure. In all refinements, the function minimised was $R = \Sigma||F_o|-|F_c|| / \Sigma|F_o|$, $R_w = (\Sigma w(|F_o|-|F_c|)^2/\Sigma w|F_o|^2)^{\frac{1}{2}}$. Using 433 variables, the present values of R and R_w are 0.084 and 0.081 respectively. Table 7.2 gives the atomic positions. Important interatomic distances and bond angles are listed in Tables 7.3 and 7.4 respectively.

7.3 RESULTS

A perspective view of $MgTPP(H_2O)(2\text{-pic})_{2.5}$ is shown in Figure 7.1 which also defines the numbering system used throughout this chapter. The average bond distances for Ca-N = 1.384, Cb-Cb = 1.339, Ca-Cb = 1.448, Ca-Cm = 1.394 and $Cm-C_{phenyl}$ = 1.498Å. The average bond angles are CaNCa = 107.1°, NCaCb = 108.5°, NCaCm = 125.6°, CaCbCb = 107.9° and CaCmCa = 125.8°. These values agree well with those reported for other metallotetraphenylporphyrin complexes (Chapter 6).

An important structural feature is the hydrogen bonding of the coordinated water molecule to two 2-picoline groups. The Ha-N(80)and Hb-N(70)distances for these interactions are 1.717Å and 1.951Å respectively.

A third group, presumably 2-picoline, is located in the lattice but it is disordered. Refinement on this structure is still in progress.

Overall, the porphyrin is non-planar with large displacements at the Cb atoms (Figure 7.2). Individually,

Table 7.2 Atom coordinates of $MgTPP(H_2O)(2\text{-pic})_{2.5}$ excluding disordered 2-picoline ($x10^4$)

Atom	x	y	z
Mg	8361	2023	7675
N(1)	7739	832	7056
C(9)	10168	3310	6656
N(4)	8013	1130	8650
N(3)	9620	2822	8311
C(16)	8217	1398	9385
C(19)	7150	358	8711
C(6)	9177	2237	5975
C(11)	10414	3560	8021
N(2)	9370	2509	6711
C(1)	7034	36	7344
C(4)	7809	784	6284
C(14)	9703	2783	9092
C(10)	10656	3807	7253
C(18)	6776	188	9498
C(8)	10439	3573	5865
C(5)	8415	1440	5783
C(7)	9835	2922	5450
C(15)	9060	2125	9590
C(13)	10630	3512	9293
C(41)	11119	5511	6688
C(42)	11933	6290	6518
C(43)	13240	6175	6722
C(44)	13685	5318	7115
C(45)	12867	4534	7277
C(40)	11557	4628	7073
C(12)	11010	3991	8655
C(17)	7434	806	9901
C(51)	9076	3045	10808
C(52)	9313	3078	11566
C(53)	9802	2228	11961
C(54)	10069	1354	11592
C(55)	9832	1323	10830
C(50)	9316	2194	10422
C(31)	7072	1317	4621
C(32)	6947	1119	3877

cont...

Table 7.2 (continued)

Atom	x	y	z
C(33)	8039	864	3443
C(34)	9253	824	3749
C(35)	9377	1028	4500
C(30)	8285	1273	4957
O(1)	6749	2961	7597
N(80)	7061	4765	6749
C(81)	6888	4972	6062
C(82)	6902	5879	5609
C(85)	7404	5533	7187
C(83)	7330	6499	6033
C(86)	6539	4206	5624
C(84)	7499	6432	6887
C(20)	6741	-166	8099
C(2)	6715	-559	6731
C(3)	7174	-122	6085
C(61)	6463	-1883	8692
C(62)	5712	-2705	8884
C(63)	4461	-2708	8650
C(64)	3915	-1888	8255
C(65)	4666	-1074	8076
C(60)	5929	-1044	8287
N(70)	4426	2010	7752
C(75)	4105	1864	8484
C(71)	3575	1764	7234
C(73)	2090	1225	8202
C(72)	2397	1399	7459
C(74)	2931	1451	8728
C(76)	3950	1930	6443
Ha	6778	3623	7196
Hb	5896	2823	7455

Table 7.3 Bond lengths (Å) of $MgTPP(H_2O)(2\text{-pic})_{2.5}$

Atoms	Distance	Atoms	Distance
Mg-N(1)	2.106	Mg-N(4)	2.084
Mg-N(3)	2.097	Mg-N(2)	2.070
Mg-O(1)	2.020	N(1)-C(1)	1.386
N(1)-C(4)	1.372	C(9)-N(2)	1.378
C(9)-C(10)	1.390	C(9)-C(8)	1.450
N(4)-C(16)	1.389	N(4)-C(19)	1.391
N(3)-C(11)	1.382	N(3)-C(14)	1.386
C(16)-C(15)	1.398	C(16)-C(17)	1.438
C(19)-C(18)	1.448	C(19)-C(20)	1.401
C(6)-N(2)	1.391	C(6)-C(5)	1.410
C(6)-C(7)	1.452	C(11)-C(10)	1.402
C(11)-C(12)	1.448	C(1)-C(20)	1.379
C(1)-C(2)	1.429	C(4)-C(5)	1.376
C(4)-C(3)	1.463	C(14)-C(15)	1.393
C(14)-C(13)	1.456	C(10)-C(40)	1.488
C(18)-C(17)	1.334	C(8)-C(7)	1.348
C(13)-C(12)	1.330	C(41)-C(42)	1.384
C(41)-C(40)	1.390	C(42)-C(43)	1.393
C(43)-C(44)	1.370	C(44)-C(45)	1.390
C(45)-C(40)	1.395	C(51)-C(52)	1.373
C(51)-C(50)	1.360	C(52)-C(53)	1.378
C(53)-C(54)	1.375	C(54)-C(55)	1.379
C(55)-C(50)	1.421	C(31)-C(32)	1.365
C(31)-C(30)	1.388	C(32)-C(33)	1.379
C(33)-C(34)	1.365	C(34)-C(35)	1.380
C(35)-C(30)	1.399	N(80)-C(81)	1.248
N(80)-C(85)	1.379	C(81)-C(82)	1.419
C(81)-C(86)	1.378	C(82)-C(83)	1.245
C(85)-C(84)	1.295	C(83)-C(84)	1.523
C(20)-C(60)	1.493	C(2)-C(3)	1.345
C(61)-C(62)	1.396	C(61)-C(60)	1.391
C(62)-C(63)	1.357	C(63)-C(64)	1.368
C(64)-C(65)	1.384	C(65)-C(60)	1.359
N(70)-C(75)	1.336	N(70)-C(71)	1.343
C(71)-C(76)	1.454	C(71)-C(72)	1.370
C(73)-C(74)	1.339	C(73)-C(72)	1.356
C(15)-C(50)	1.509	C(5)-C(30)	1.500

Table 7.4 Bond angles (deg) of $MgTPP(H_2O)(2\text{-pic})_{2.5}$

Atoms	Angle	Atoms	Angle
N(1)-Mg-N(4)	87.2	N(1)-Mg-N(3)	157.6
N(4)-Mg-N(3)	87.7	N(1)-Mg-N(2)	87.8
N(4)-Mg-N(2)	156.5	N(3)-Mg-N(2)	88.2
N(1)-Mg-O(1)	99.4	N(4)-Mg-O(1)	103.9
N(3)-Mg-O(1)	103.0	N(2)-Mg-O(1)	99.6
Mg-N(1)-C(1)	125.9	Mg-N(1)-C(4)	125.5
C(1)-N(1)-C(4)	108.1	N(2)-C(9)-C(10)	126.6
N(2)-C(9)-C(8)	109.5	C(10)-C(9)-C(8)	123.9
Mg-N(4)-C(16)	125.4	Mg-N(4)-C(19)	125.3
C(16)-N(4)-C(19)	105.9	Mg-N(3)-C(11)	125.1
Mg-N(3)-C(14)	126.3	C(11)-N(3)-C(14)	108.2
N(4)-C(16)-C(17)	109.4	N(4)-C(16)-C(17)	109.4
C(15)-C(16)-C(17)	125.4	N(4)-C(19)-C(18)	109.0
N(4)-C(19)-C(20)	124.4	C(18)-C(19)-C(20)	126.6
N(2)-C(6)-C(5)	124.3	N(2)-C(6)-C(7)	109.3
C(5)-C(6)-C(7)	126.4	N(3)-C(11)-C(10)	126.4
N(3)-C(11)-C(12)	107.3	C(10)-C(11)-C(12)	126.2
Mg-N(2)-C(9)	125.8	Mg-N(2)-C(6)	126.7
C(9)-N(2)-C(6)	106.3	N(1)-C(1)-C(20)	125.5
N(1)-C(1)-C(2)	108.3	C(20)-C(1)-C(2)	126.1
N(1)-C(4)-C(5)	126.6	N(1)-C(4)-C(3)	107.7
C(5)-C(4)-C(3)	125.7	N(3)-C(14)-C(15)	125.7
N(3)-C(14)-C(13)	107.8	C(15)-C(14)-C(13)	126.5
C(9)-C(10)-C(11)	124.8	C(9)-C(10)-C(40)	118.2
C(11)-C(10)-C(40)	117.0	C(19)-C(18)-C(17)	107.7
C(9)-C(8)-C(7)	107.6	C(6)-C(5)-C(4)	126.1
C(6)-C(7)-C(8)	107.2	C(16)-C(15)-C(14)	125.7
C(14)-C(13)-C(12)	107.5	C(42)-C(41)-C(40)	122.0
C(41)-C(42)-C(43)	119.1	C(42)-C(43)-C(44)	119.8
C(43)-C(44)-C(45)	120.8	C(44)-C(45)-C(40)	120.3
C(10)-C(40)-C(41)	120.8	C(10)-C(40)-C(45)	121.3
C(41)-C(40)-C(45)	117.9	C(11)-C(12)-C(13)	109.1
C(16)-C(17)-C(18)	108.0	C(52)-C(51)-C(50)	122.2
C(51)-C(52)-C(53)	119.9	C(52)-C(53)-C(54)	119.9
C(53)-C(54)-C(55)	120.2	C(54)-C(55)-C(50)	120.2
C(51)-C(50)-C(55)	117.7	C(32)-C(31)-C(30)	121.4
C(31)-C(32)-C(33)	117.7	C(32)-C(33)-C(34)	120.4

cont...

Table 7.4 (continued)

Atoms	Angle	Atoms	Angle
C(33)-C(34)-C(35)	119.4	C(34)-C(35)-C(30)	121.5
C(31)-C(30)-C(35)	117.2	C(81)-N(80)-C(85)	117.3
N(80)-C(81)-C(82)	133.3	N(80)-C(81)-C(86)	117.4
C(82)-C(81)-C(86)	109.1	C(81)-C(82)-C(83)	104.3
N(80)-C(85)-C(84)	120.0	C(82)-C(83)-C(84)	129.9
C(85)-C(84)-C(83)	113.7	C(19)-C(20)-C(1)	126.6
C(19)-C(20)-C(60)	116.5	C(1)-C(20)-C(60)	117.0
C(1)-C(2)-C(3)	108.4	C(4)-C(3)-C(2)	107.4
C(62)-C(61)-C(60)	120.9	C(61)-C(62)-C(63)	119.9
C(62)-C(63)-C(64)	120.1	C(63)-C(64)-C(65)	119.3
C(64)-C(65)-C(60)	122.6	C(20)-C(60)-C(61)	120.1
C(20)-C(60)-C(65)	122.8	C(61)-C(60)-C(65)	117.1
C(75)-N(70)-C(71)	118.3	N(70)-C(75)-C(74)	122.6
N(70)-C(71)-C(72)	120.1	N(70)-C(71)-C(76)	117.2
C(72)-C(71)-C(76)	122.7	C(72)-C(73)-C(74)	119.5
C(71)-C(72)-C(73)	121.3	C(75)-C(74)-C(73)	118.0
		N(4)-C(16)-C(15)	125.3

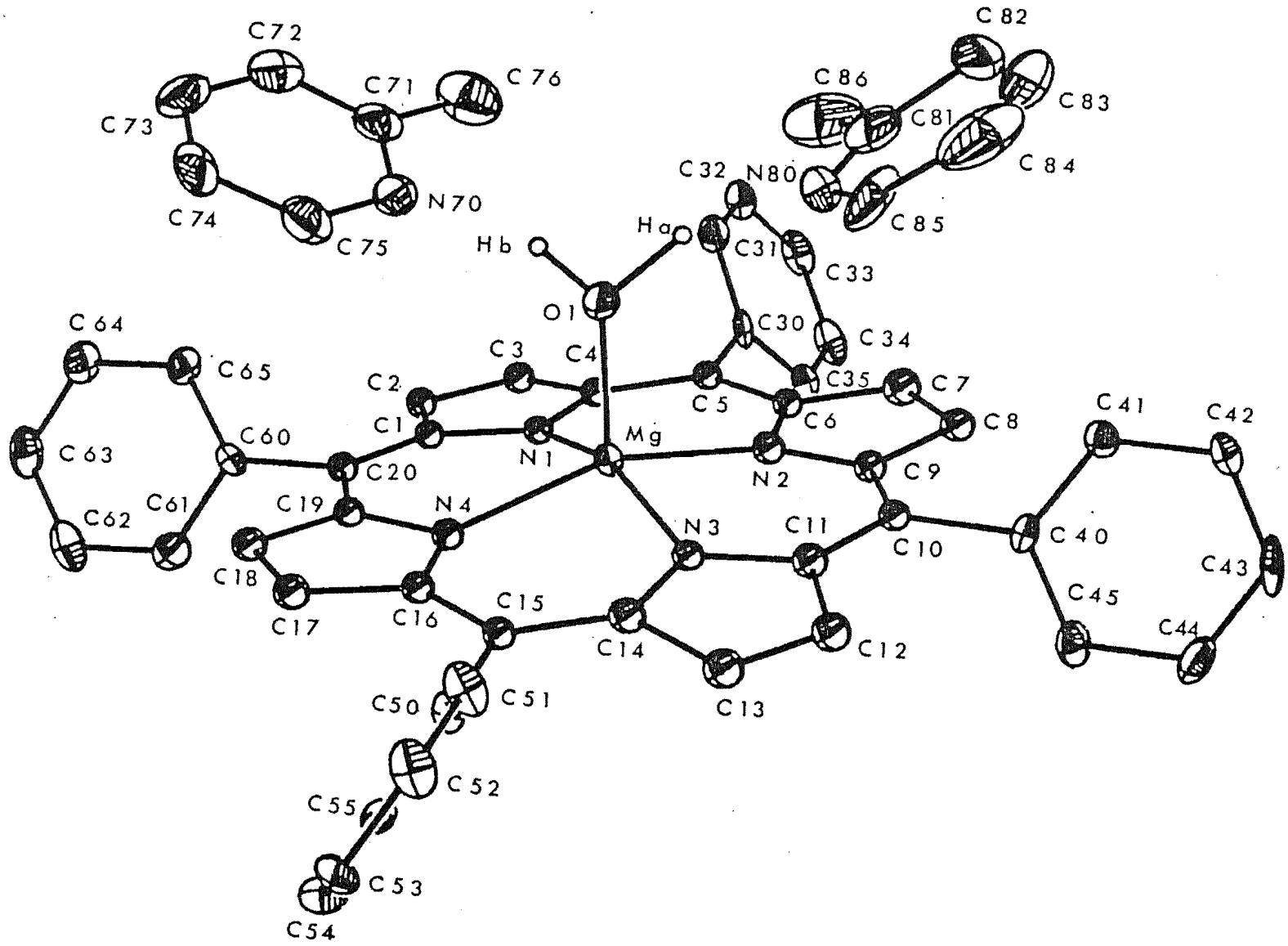

Figure 7.1 : Computer drawn structure of $MgTPP(H_2O)(2\text{-pic})_{2.5}$ showing the numbering system

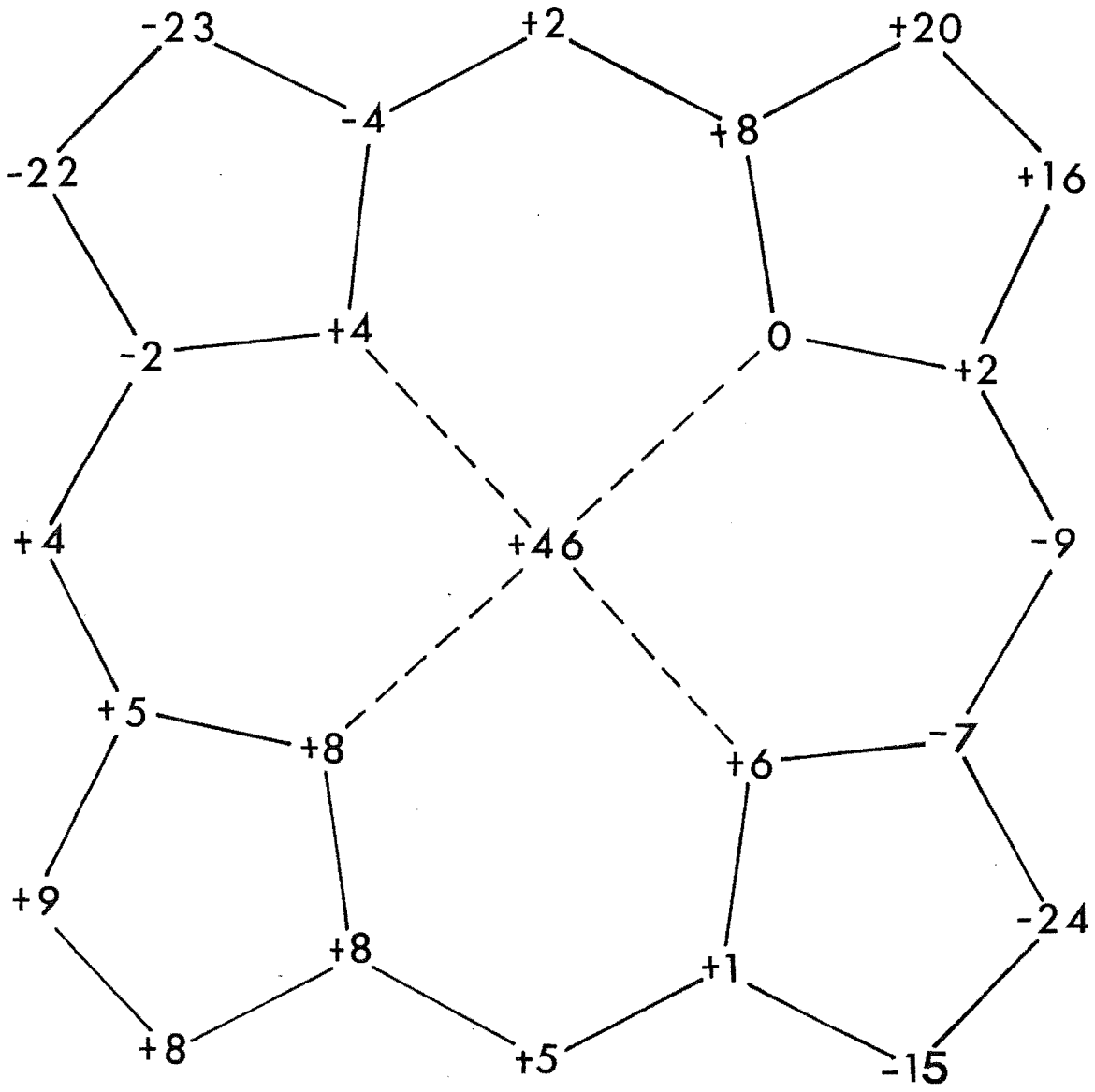

Figure 7.2 : Atomic displacements of $MgTPP(H_2O)(2\text{-pic})_{2.5}$ in units of 0.01Å, from the mean plane of the four chelating nitrogen atoms of the porphyrin ring

the pyrrole rings are planar to 0.02Å and they are inclined at 7.5°, 0.6°, 7.2° and 5.1° to the mean plane of the core. The smaller angle of inclination of the pyrrole ring, $N_2C_6C_7C_8C_9$, is likely to be a result of a weak interaction with the aromatic ring of 2-picoline. Distances between atoms contained in the two groups are 4.124Å (for C(7) to C(81) of 2-picoline) and 4.058Å and 4.030Å (for C(8) to N(80) and C(81) of 2-picoline).

The greatest deviation from non-planarity is at the Mg centre which is displaced by 0.416Å out of the plane of the four chelating nitrogen atoms.

7.4 DISCUSSION

7.4.1 General Discussion

The large deviation of 0.416Å for the Mg centre out of the plane of the four chelating atoms, compared with a corresponding value of 0.273Å for MgTPP(H_2O) [60], suggests that the increased displacement is probably due to hydrogen bonding of two 2-picoline groups to the coordinated water molecule. This bonding effectively increases the electronegativity of the oxygen atom which attracts the Mg ion even more. Therefore the displacement of Mg ion from the plane of the four chelating nitrogen atoms is enhanced. In addition, the Mg-OH_2 bond length of 2.020Å is significantly shorter than that observed for the corresponding value for MgTPP(H_2O), (2.099Å), although there is some doubt about the accuracy of the latter value [367].

The hydrogen bonds to the 2-picoline groups also localise the coordinated water molecule. A similar type

of hydrogen bonding with the nitrogen atom of an imidazole group may be important in the stabilisation of the bonding of a water molecule to Mg ion in Mg porphyrin-Mb complexes (Chapter 3). In the case of six-coordinate Fe(III)TPP $(H_2O)_2(ClO_4)_2(THF)_2$ [407], hydrogen bonding between water and other molecules has also been observed.

The basic structure of $MgTPP(H_2O)(2\text{-pic})_{2.5}$ shows many similarities to that of $MgPc(H_2O)(pyridine)_2$ [367]. In both cases, the coordinated water molecule is hydrogen bonded to the nitrogen donor groups to produce relatively large displacements of the Mg atom from the porphyrin (0.496Å for Pc and 0.416Å for TPP). For the TPP complex, the 2-picoline rings form dihedral angles of 27.2° and 29.5° with the plane through the four central nitrogen atoms of MgTPP, compared with corresponding values for the Pc complex of 8.6° and 30.8° [367]. The existence of a significantly lower value for one pyridine in the latter case is probably due to two factors:- (1) In the TPP complex the phenyl substituents are oriented at angles of 65.9°, 62.7°, 59.9° and 56.1° to the core (angles which preclude steric interactions between pyrrole hydrogen and phenyl hydrogen atoms [367]). As can be seen clearly in Figure 7.3 phenyl rings oriented this way prevent the 2-picoline groups from lying approximately parallel to the MgTPP entity (as observed especially for one pyridine ring in the Pc complex). (2) In the Pc complex there is parallel stacking of the groups, in particular for pairs of MgPc units, at the favoured ~3.4Å distance for aromatic rings, which tends to make the pyridine groups lie parallel with the MgPc units. Such a stacking effect is absent in the TPP complex because of the presence and

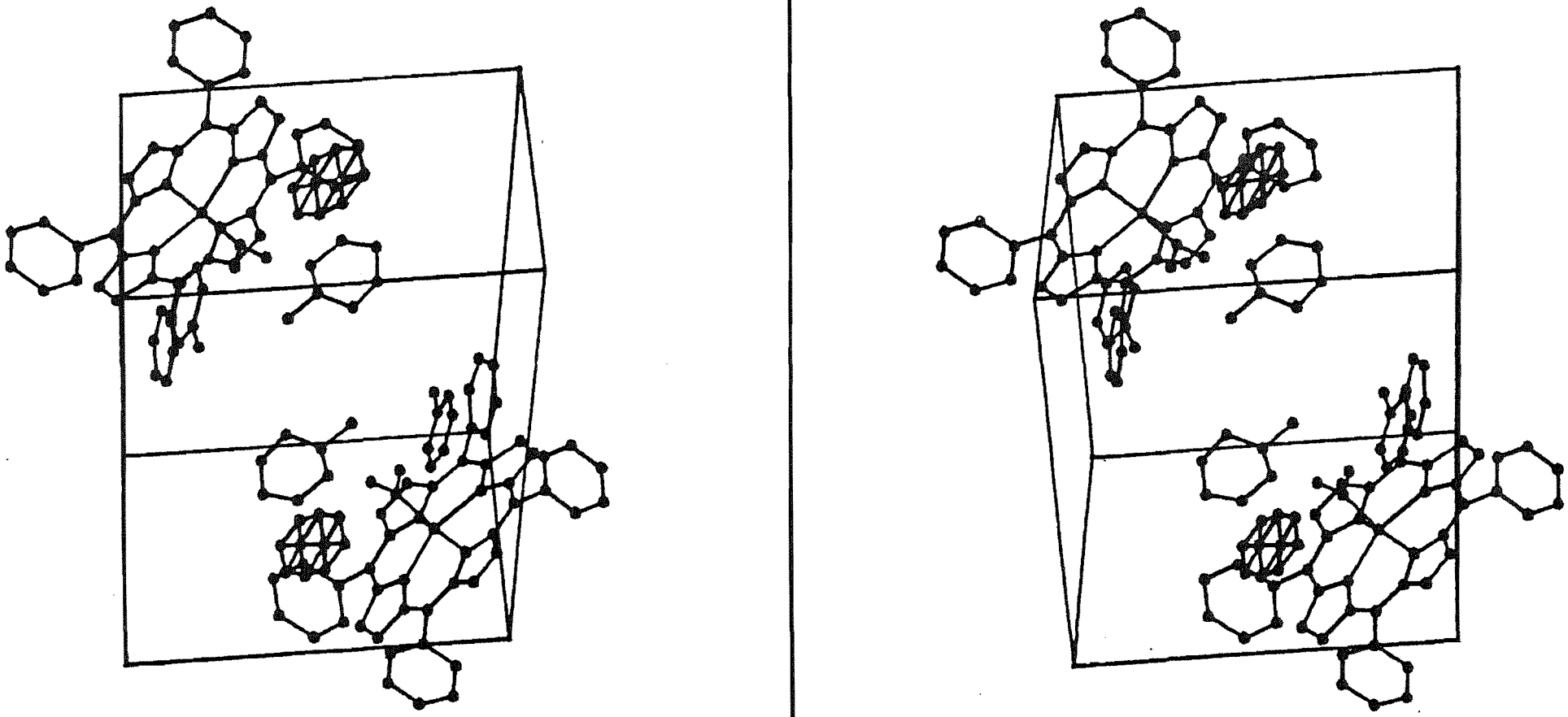

Figure 7.3 : Stereoscopic diagram of the cell contents of $MgTPP(H_2O)(2\text{-pic})_{2.5}$

orientation of the phenyl substituents which prevents close association of MgTPP units.

The average Mg-N(equatorial) bond distance of 2.089Å confirms the suggestion that when Mg porphyrin is under the same environment as $MgPc(H_2O)(py)_2$, this distance is at least 2.070Å [367]. It is significant that this type of molecular geometry is adopted by two different compounds. The tetradentate ligands, TPP and Pc, are dissimilar and the overall unit cell packing shows that the hydrogen bonding effect is not simply a result of favourable intermolecular interactions. Thus this special kind of geometry appears to be a particular arrangement that can be readily adopted by magnesium porphyrin systems and possibly, chlorophyll molecules.

Several attempts to obtain $MgTPP(H_2O)(py)_2$ complex using the MgPc/pyridine conditions, produced only six-coordinate $MgTPP(pyridine)_2$ which is similar to that of $MgOEP(pyridine)_2$ (Chapter 6). Five-coordination is favoured over six-coordination presumably because of steric interaction between the methyl group of 2-picoline and the porphyrin ring for the octahedral geometry. In addition, equilibrium studies also provide evidence that the formation of a six-coordinate 2-picoline complex is hindered by steric factors [82]. This sort of steric interaction may be important in determining the coordination behaviours of Mg complexes in chlorophyll systems (Section 7.4.2) [408].

Thus, the results indicate that steric effects between the ligand and the porphyrin ring generally tend to favour five-coordination. Furthermore the five-coordinate

Mg centre is displaced out of the plane of the porphyrin ring and the relative position of the Mg centre is influenced by hydrogen bonding to the axial ligand.

7.4.2 Hydrogen Bonding in Biological Systems

Hydrogen bonding to axial ligand plays a very important role in biological systems. X-ray studies of hemoproteins show that the proximal histidine is invariably hydrogen bonded to an electronegative group on the apoprotein [409-411]. This bonding modulates the imidazole basicity [412,413], serves as a control for dioxygen affinity [414] and red-shifts the electronic spectra [415].

Hydrogen bonding of groups to a water molecule in five-coordinate Mg complexes may also be a key feature adopted by chlorphyll molecules *in vivo*. Physical studies of chlorophyll molecules *in vitro* show that the Mg centre has a high affinity for a water molecule [18]. The coordinated water molecule is hydrogen bonded to the carbonyl group of the cyclopentanone ring of another chlorophyll molecule [24,416,417]. Similarly, X-ray results of the chlorophyll protein complex of *Prosthecochloris aestuarii* indicate that one of the chlorophyll groups is coordinated to a water molecule [4]. The coordinated water molecule is likely to be hydrogen bonded to electronegative groups on the protein chain. This bonding can enhance the displacement of the excited magnesium ion from the chlorin ring by a significant amount as shown by the comparison of MgTPP(H_2O) (0.273Å) and MgTPP(H_2O)(2-pic)$_{2.5}$ (0.416Å). This increased displacement can thereby facilitate the charge separation in the reaction centres of photosynthetic systems.

It has been recently suggested that an increase in the displacement of the Mg centre from the chlorin ring is an important factor associated with the primary events of photosynthesis [406]. It was concluded that upon excitation of light, the excited state entity undergoes an internal conversion to a $^1A_2$ charge-transfer state that involves an increase in the displacement of the Mg ion from 0.79Å to nearly 1.01Å out of the ring [406]. Any feature such as hydrogen bonding to a coordinated water molecule, which enhances the displacement of the Mg atom could facilitate such electronic changes in chlorophyll systems.

Overall, hydrogen bonding to the axial ligand of metalloporphyrin appears to be common in natural systems. Such bonding enables biological systems to exhibit complex reactions which are necessary for the maintenance of their biochemical functions.

CHAPTER 8

CHEMICAL STUDIES OF COUPLING IN TWO OSCILLATING REACTOR CELL SYSTEM

8.1 INTRODUCTION

Oscillating chemical reactions are particularly interesting because of the discovery of such oscillators in biological systems [418]. Such oscillating behaviour in chemical systems is known to be associated with non-equilibrium conditions [29]. It is therefore not surprising that oscillations have been observed for living systems as they are essentially non-equilibrium in character.

Organised non-equilibrium systems exhibit a variety of gross spatiotemporal characteristics which are probably independent of the degree of complexity of the systems. While overall living systems are very complex, they may nonetheless be adequately modelled from the point of view of spatiotemporal effects, by relatively simple non-biological, non-equilibrium chemical systems, including oscillators. Thus the interaction of two or more organised living cells with each other may be modelled by studying the interaction of chemical oscillators of the B-Z reaction type reported in this work. Certainly, many reports have highlighted the similarities between biological and non-biological oscillators [419,420].

It has been suggested that in living organisms, the interaction between cells is dependent upon three periodic events [421,422]. The first event is the "off and sensitive" state. When a cell is isolated from its neighbours,

it oscillates autonomously. It can be signalled by a nearest neighbouring cell which is itself passing through the signalling aspect. This signal then phase shifts the entire cycle of the cell. The second event is the "on and signalling" state. During this time, the signalling substance is produced and functional coupling with the cell's nearest neighbours can still occur. The third event is the "off and insensitive" state. At this state, reception of a signal from another cell produces no response. Furthermore, the phase of the cycle of the cell is not shifted by the signal.

Recently, model studies of such living cell interaction have been carried out using chemical oscillations [30,44,46,53,54]. These studies generally involve a two reactor cell system which is also a model for circadian [48], neural [50] and other coupled oscillators [51]. The results indicate that the extent of synchronisation in the system is dependent upon the difference between the frequencies of interacting oscillators and degree of chemical interaction [30].

In this chapter, the interaction of an organised reactor cell on the starting of another is reported. Such a study may be relevant to the replication of cells where it can be envisaged that the organised system of the parent cell is maintained for one of the daughter cells and at the same time influencing the organisation of newly replicated molecules for the construction of the second daughter cell. The influence of apparatus design and geometry is also analysed. These studies provide a broader understanding of chemical coupling and also enable some mathematical

theories of biological processes to be assessed to some extent.

This work incorporates results obtained in a research assistant study carried out just prior to Ph.D. registration.

8.2 EXPERIMENTAL

Two different types of reactor cell systems were used to determine the coupling constant. The first type, System 1, shown in Figure 8.1 was made of perspex and the reactor cells were coupled through the holes in two side plates. The degree of coupling was controlled by changing the amount of insertion of the middle non-flexible perspex plate. This system is similar to that used by Fujii and Sawada [44]. It was difficult to ensure absolute tight seals between the reactor cells for this system. The second type, System 2, was made of glass and a flexible plastic sheet separated the two reactor cells (Figure 8.2). The reactor cells were coupled through holes by sliding the plastic sheet horizontally. These two reactor cells were held together by high vacuum silicone grease. In both reactor cell systems, the reactor cells were filled with oscillating reagents and stirred independently by two stirrers. The stirring speed was the same for each reactor cell so that there was no dependence on the oxygen in the air [39]. Chemical oscillators in the reactor cells were monitored by platinum and reference calomel electrodes purchased from Corning. The change in redox potential was recorded on a CR503 recorder and the reactor cell systems were surrounded by water thermostated at 25.0 ± 0.5 °C.

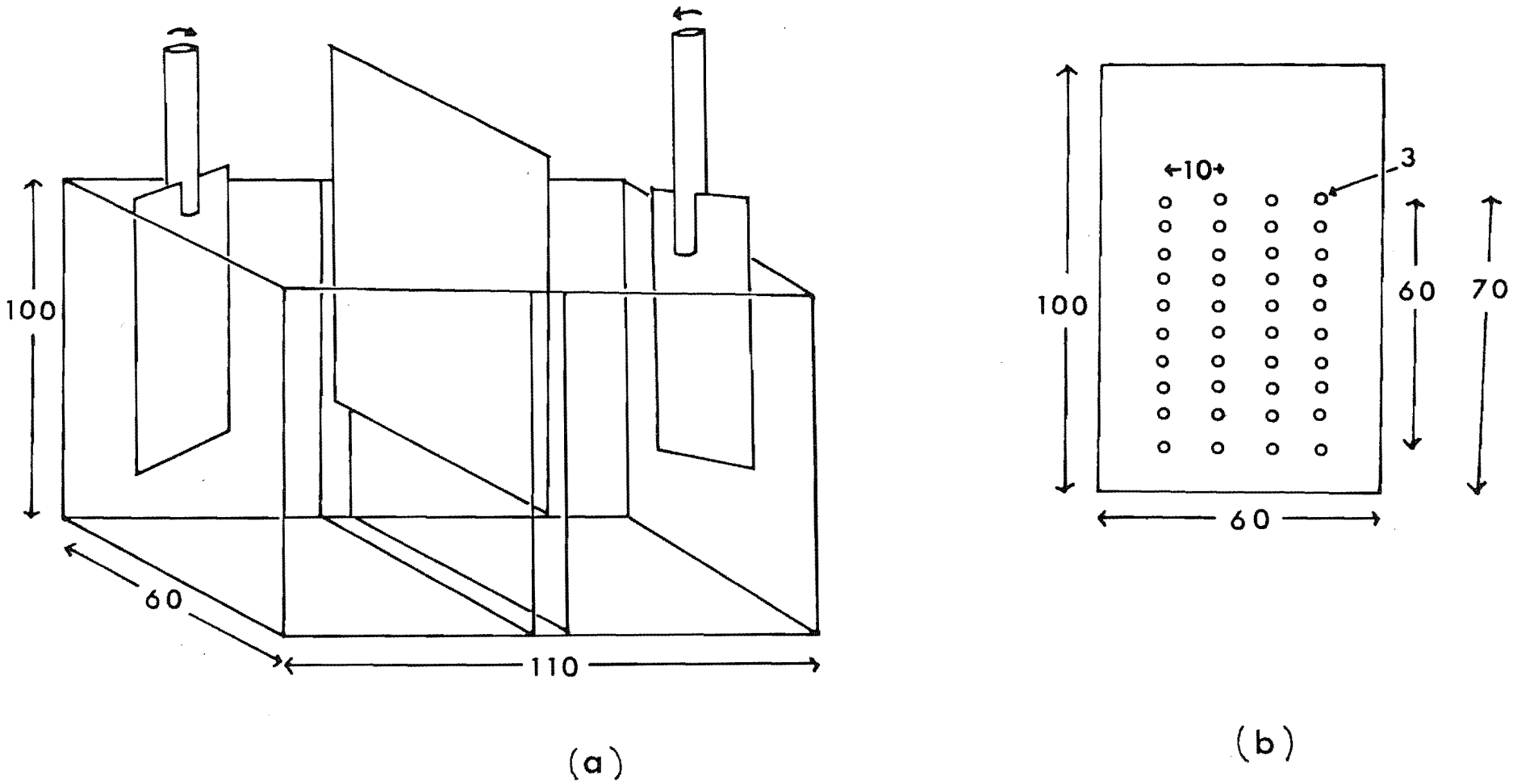

Figure 8.1 : Experimental set-up (a) System 1, (b) two perforated plates at the sides of the movable middle plate which divides the system into two parts

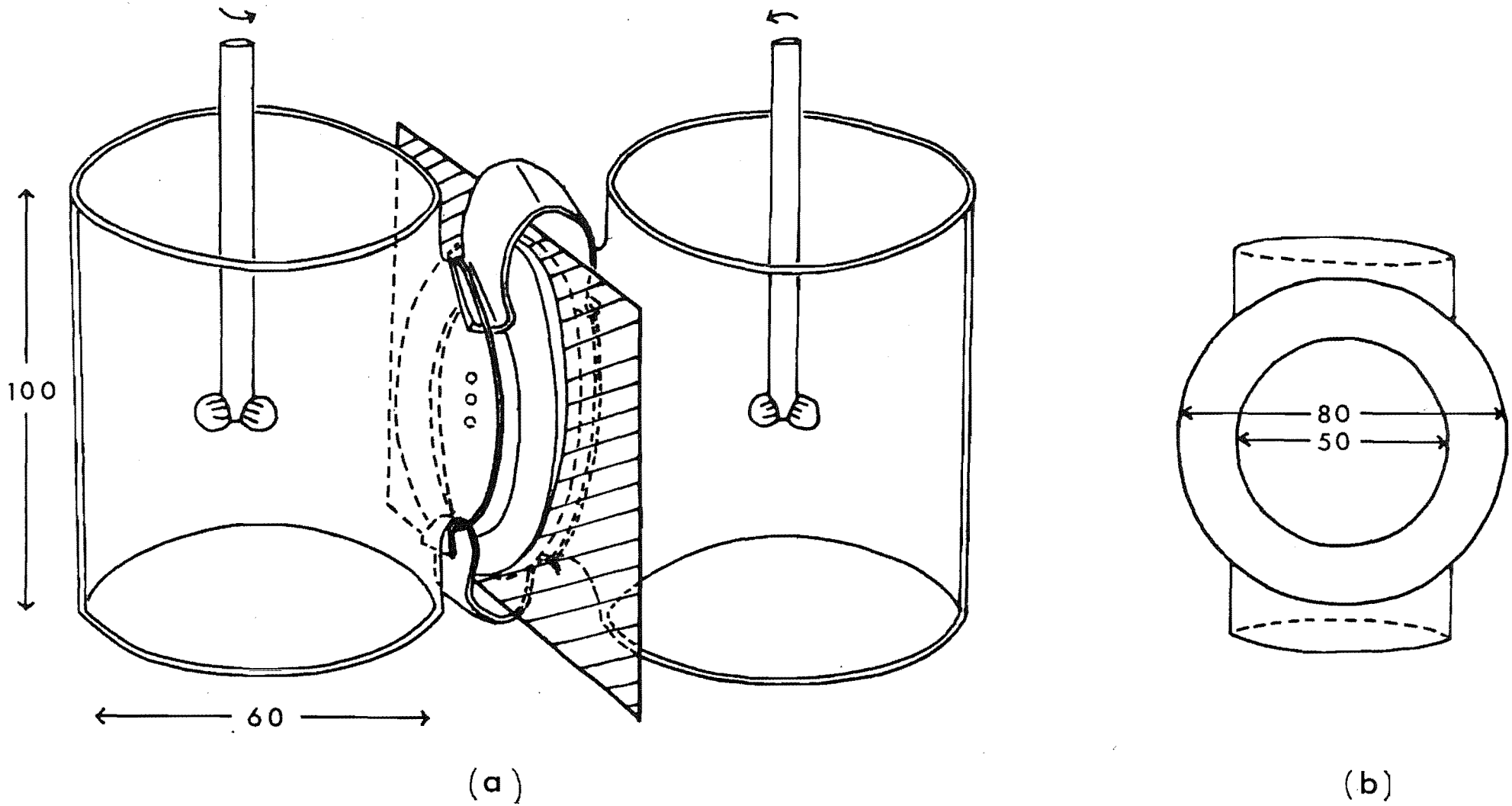

Figure 8.2 : Experimental set-up (a) System 2, (b) side view of one reactor cell

Most of the oscillating reagents were prepared according to the concentrations described in Table 8.1 (Mixture 1). However, oscillating reagents (Mixture 2) prepared by the procedure of Fujii and Sawada [44] were also used to compare the effect of different oscillating reagents (Table 8.2).

The determination of the coupling constant between two organised reactor cells was carried out by starting one reactor cell and after a while, starting the second reactor cell. Initially, the reactor cells were oscillating independently of one another. At time = 0, the two reactor cells were brought into contact by moving the middle plate (or plastic sheet) to a certain level and the two reactor cells were coupled through the holes. The phases of the two reactor cells start to change mutually and the phase differences for different numbers of coupling holes were plotted.

The influence of an organised reactor cell on the starting of another was determined by allowing one reactor cell to oscillate independently. Then at time = 0, the second reactor cell was allowed to organise itself by adding sulphuric acid, $MnSO_4.2H_2O$ and ferroin. Simultaneously, the middle plate (or plastic sheet) was moved to a certain level and there was interaction between the two reactor cells. The phase difference for various coupling holes was again determined.

8.3 RESULTS

In the Belousov-Zhabotinskii (B-Z) reaction, there is an induction period and temporal oscillations are observed after one minute. The wavelength of the first periodic

Table 8.1 : Reagents used for Mixture 1

$MnSO_4$ $2H_2O$	0.1 g
Malonic acid	5 g
$KBrO_3$	3.8 g
Ferroin	0.5 ml
Water	250 ml
Conc. H_2SO_4	10 ml

Table 8.2 : Reagents used for Mixture 2 and their ratio in volume

1.5M	H_2SO_4	12
4 mM	$Ce_2(SO_4)_3$	12
0.35 M	$KBrO_3$	12
1.2 M	Malonic acid	12
25 mM	Ferroin solution	1

oscillation varies between the values 9 and 13 mm, when Mixture 1 is used. The wavelength for subsequent oscillations changed rapidly for a short while and then increased linearly with time (Figure 8.3). The two straight lines indicate that there is no coupling between the reactor cells.

The degree of coupling between the reactor cells was calculated from the equation, $C = \frac{2\pi N}{\Delta W}$, where C is the coupling constant, N is the number of holes and ΔW is the difference between the natural limit cycle frequencies [44]. Using the same oscillating reagents (Mixture 2) and the apparatus described by Fujii and Sawada [44], the coupling between two organised reactor cells was found to occur when the value of the coupling constant was greater than 7.5 hours (Table 8.3, Figures 8.4 and 8.5). Below this value, no coupling was observed (Figure 8.6). In all cases, the higher frequency reactor cell entrained the lower frequency one. The phase difference which was calculated from the formula, $\phi = \cos^{-1}\left(\frac{\text{difference between wavelength}}{\text{wavelength}} \times 360°\right)$ (Figure 8.7) gives a better pictorial indication of coupling (Figure 8.8).

Using the same apparatus, System 1, the coupling constant was found to be 4.0 hours when Mixture 2 was changed to Mixture 1 (Table 8.4). Under the same experimental conditions, the coupling constant between an established reactor cell and a starting reactor cell was found to be 1.0 hour (Table 8.5).

When System 1 was changed to System 2, and Mixture 1 was used, the coupling constant between an established reactor cell and a starting one was found to be 0.5 hour (Table 8.6). However, the coupling is weak and on some occasions, two different phase angles which change sign are observed. The

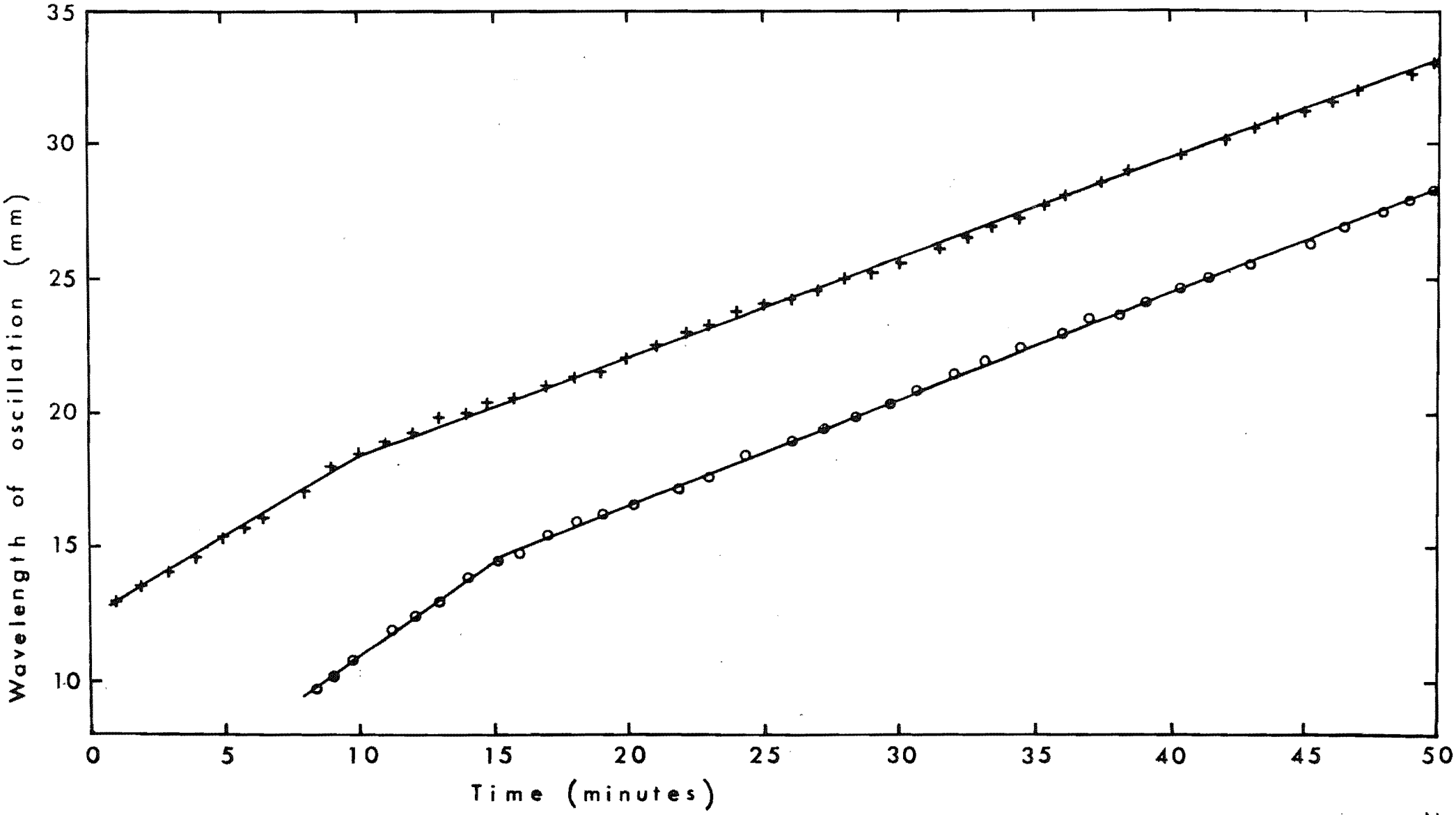

Figure 8.3 : Wavelength of oscillation as a function of time

Table 8.3 : Comparison of coupling constants for organised-organised reactor cells using Mixture 2 and System 1

Wavelength (mm) Reactor Cell 1	Wavelength (mm) Reactor Cell 2	Time (sec) Reactor Cell 1	Time (sec) Reactor Cell 2	Number of holes N	ΔW	$\frac{2\pi N}{\Delta W}$ (hr)	Overall Effect
15.5	13.0	31	26	36	6.20×10^{-3}	10.13	Coupling
29.0	19.5	58	39	36	8.40×10^{-3}	7.48	Coupling
28.0	19.0	56	38	36	8.46×10^{-3}	7.43	Coupling
30.0	19.5	60	39	36	8.97×10^{-3}	7.00	No coupling
30.0	19.0	60	38	20	9.65×10^{-3}	3.62	No coupling
41.0	14.0	82	28	36	2.35×10^{-2}	2.67	No coupling

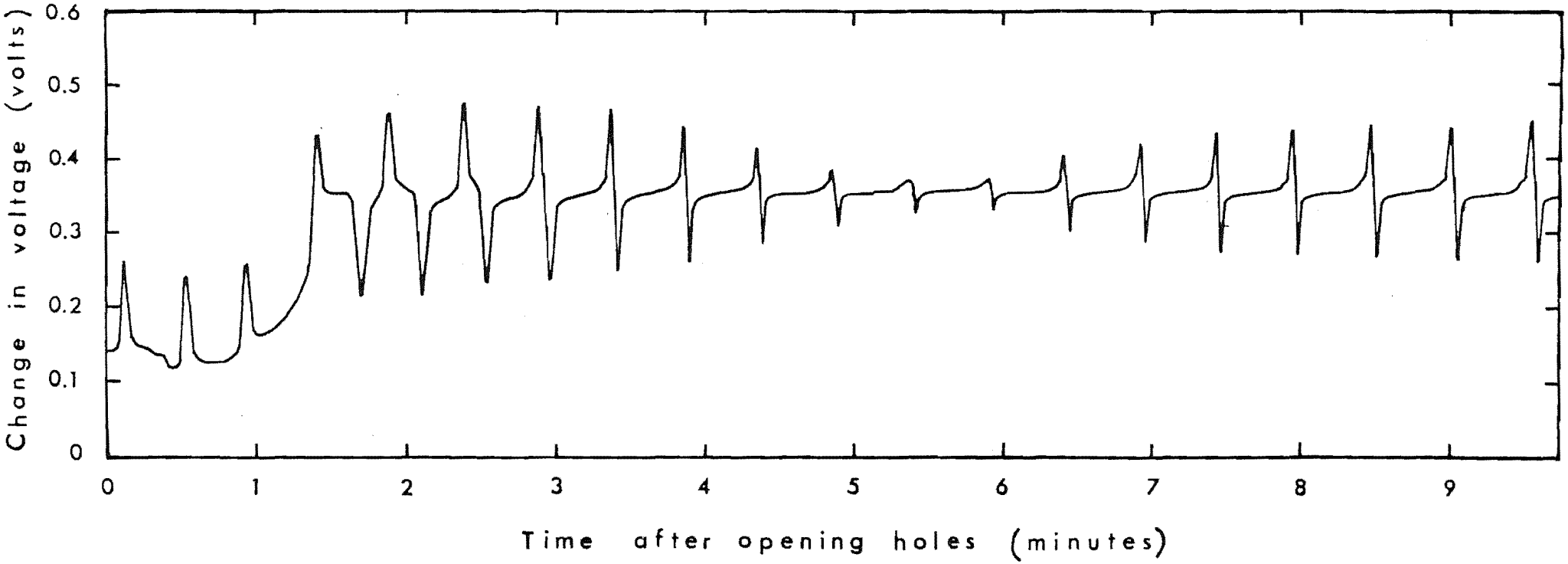

Figure 8.4 : Change in voltage as a function of time after opening holes to illustrate coupling in the reactor cell system.

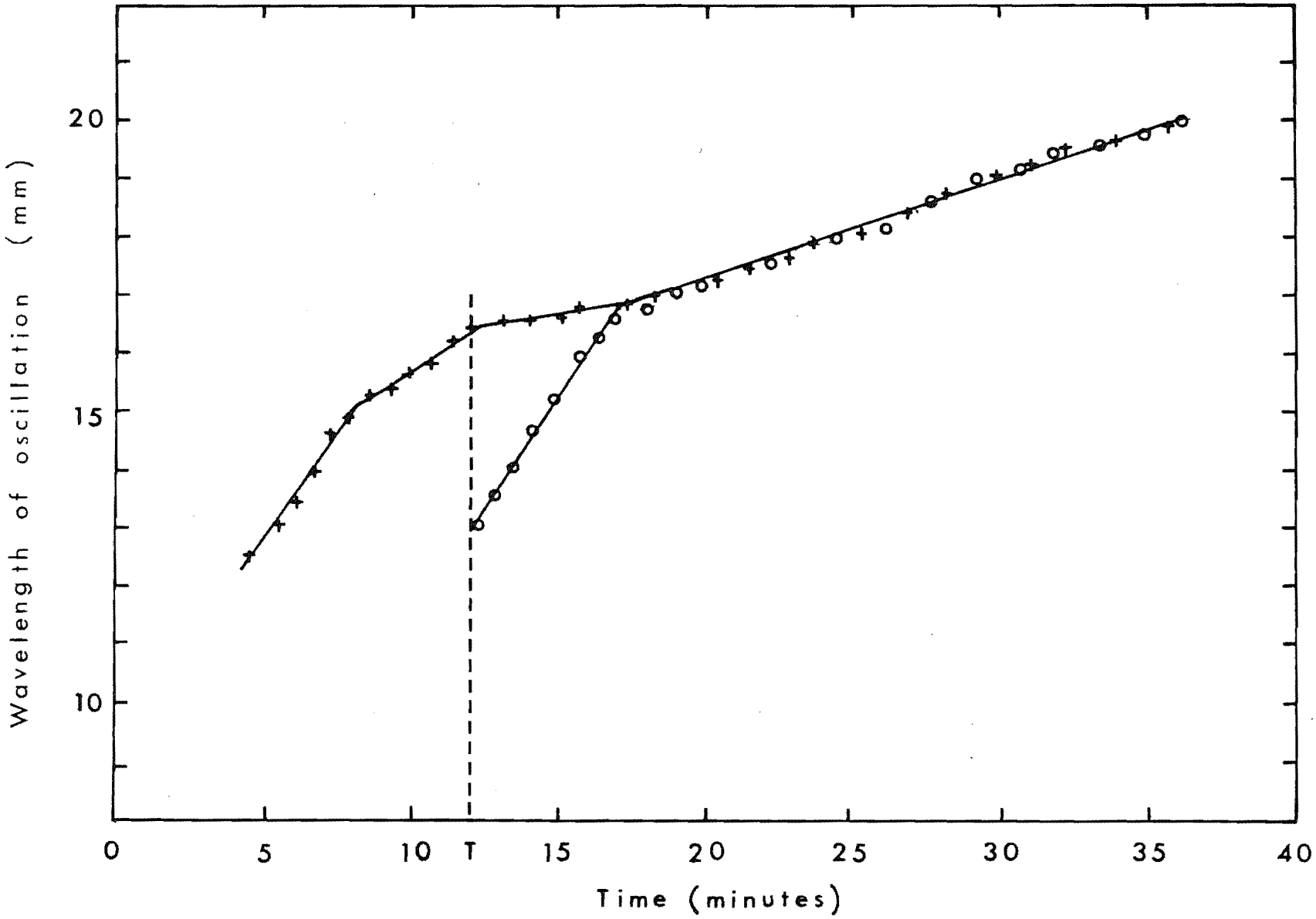

Figure 8.5 : Wavelength of oscillation as a function of time to illustrate coupling in the reactor cell system. T is the time when the holes are opened.

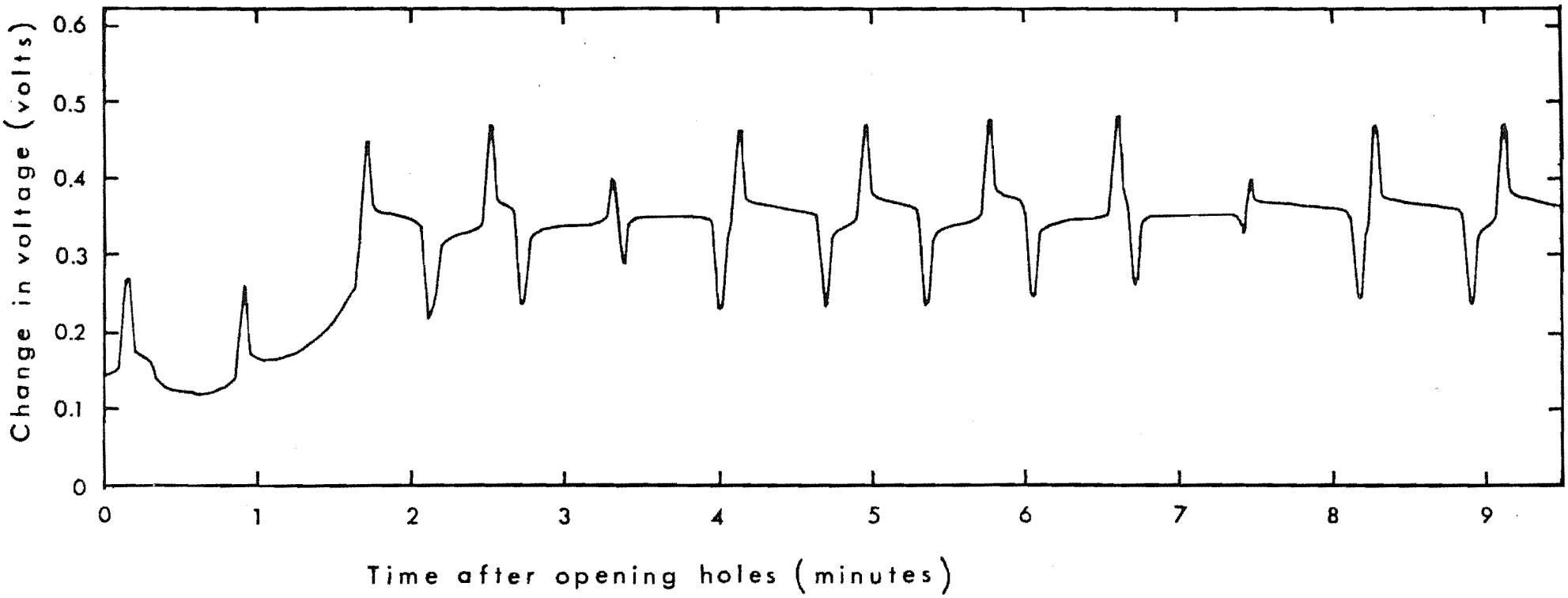

Figure 8.6 : Change in voltage as a function of time after opening holes to illustrate no coupling in the reactor cell system

Table 8.4 : Comparison of coupling constants for organised-organised reactor cells using Mixture 1 and System 1

Wavelength (mm) Reactor 1	Wavelength (mm) Cell 2	Time (sec) Reactor 1	Time (sec) Cell 2	Number of holes N	ΔW	$\frac{2\pi N}{\Delta W}$ (hr)	Overall Effect
19.0	18.5	38	37	24	7.11×10^{-4}	58.9	Coupling
19.0	17.5	38	35	36	2.25×10^{-3}	27.9	Coupling
18.0	13.0	36	26	36	1.07×10^{-2}	5.88	Coupling
15.0	11.0	30	22	36	1.12×10^{-2}	5.18	Coupling
14.5	10.5	29	21	36	1.31×10^{-2}	4.78	Coupling
20.0	13.0	40	26	36	1.35×10^{-2}	4.67	Coupling
16.5	12.0	33	24	28	1.14×10^{-2}	4.30	Coupling
12.5	9.0	25	18	36	1.56×10^{-2}	4.04	Coupling
13.5	9.5	27	19	36	1.59×10^{-2}	4.03	No coupling
18.0	12.5	36	25	28	1.22×10^{-2}	3.99	No coupling
13.5	12.0	27	24	10	4.63×10^{-3}	3.77	No coupling
14.0	11.5	28	23	16	7.76×10^{-3}	3.60	No coupling
17.5	13.0	35	26	20	9.89×10^{-3}	3.53	No coupling
16.5	12.0	33	24	28	1.14×10^{-2}	3.07	No coupling
16.5	9.0	33	18	36	2.53×10^{-2}	2.49	No coupling
13.0	10.0	26	20	14	1.15×10^{-2}	2.12	No coupling
15.5	9.5	31	19	20	2.04×10^{-2}	1.71	No coupling
15.0	9.0	30	18	12	2.22×10^{-2}	0.94	No coupling
15.5	12.0	31	24	4	9.41×10^{-3}	0.74	No coupling
14.0	11.0	28	22	4	9.74×10^{-3}	0.72	No coupling

Table 8.5 : Comparison of coupling constants for starting-organised reactor cells using Mixture 1 and System 1

Wavelength (mm) Reactor Cell 1	Wavelength (mm) Reactor Cell 2	Time (sec) Reactor Cell 1	Time (sec) Reactor Cell 2	Number of holes N	ΔW	$\frac{2\pi N}{\Delta W}$ (hr)	Overall Effect
14.0	13.5	28	27	36	1.32×10^{-3}	47.5	Coupling
15.0	13.5	30	27	16	3.70×10^{-3}	7.54	Coupling
18.0	14.5	36	29	5	6.71×10^{-3}	1.30	Coupling
17.5	11.5	35	23	10	1.49×10^{-2}	1.17	Coupling
18.0	11.5	36	23	8	1.57×10^{-2}	0.89	No coupling
17.5	11.5	35	23	6	1.49×10^{-2}	0.70	No coupling

Table 8.6 : Comparison of coupling constants for starting-organised reactor cells using Mixture 1 and System 2

Wavelength (mm) Reactor 1	Wavelength (mm) Cell 2	Time (sec) Reactor 1	Time (sec) Cell 2	Number of holes N	ΔW	$\frac{2\pi N}{\Delta W}$ (hr)	Overall Effect
13.6	12.3	32.1	29.0	3	3.3×10^{-3}	1.59	Coupling
18.3	15.6	43.2	36.9	3	4.0×10^{-3}	1.31	Coupling
14.5	12.5	34.3	29.5	3	4.74×10^{-3}	1.10	Coupling
18.5	15.0	43.7	35.4	3	5.3×10^{-3}	1.00	Coupling
13.5	11.4	31.9	26.9	3	5.78×10^{-3}	0.91	Coupling
11.6	9.8	27.4	23.2	3	6.7×10^{-3}	0.78	Coupling
17.2	13.4	40.6	31.7	3	6.98×10^{-3}	0.75	Coupling
19.8	14.9	46.8	35.2	3	7.04×10^{-3}	0.74	Coupling
17.9	13.7	42.3	32.4	3	7.22×10^{-3}	0.73	Coupling
18.0	13.7	42.5	32.4	3	7.38×10^{-3}	0.71	Coupling
11.0	9.1	26.0	21.5	3	8.06×10^{-3}	0.65	Coupling
17.0	12.8	40.2	30.2	3	8.17×10^{-3}	0.64	Coupling
16.1	12.2	38.0	28.8	3	8.38×10^{-3}	0.63	Coupling
13.0	10.3	30.7	24.3	3	8.53×10^{-3}	0.61	Coupling
13.4	10.5	31.7	24.8	3	8.72×10^{-3}	0.60	Coupling
14.9	11.4	35.2	26.9	3	8.76×10^{-3}	0.60	Coupling
17.5	12.8	41.3	30.2	3	8.86×10^{-3}	0.59	Coupling
16.6	12.3	39.2	29.1	3	8.92×10^{-3}	0.59	Coupling

cont...

Table 8.6 continued

Wavelength (mm) Reactor Cell 1	Wavelength (mm) Reactor Cell 2	Time (sec) Reactor Cell 1	Time (sec) Reactor Cell 2	Number of holes N	ΔW	$\frac{2\pi N}{\Delta W}$ (hr)	Overall Effect
16.5	12.0	39.0	28.3	3	9.64×10^{-3}	0.54	Coupling
14.0	10.6	33.1	25.0	3	9.7×10^{-3}	0.54	Coupling
16.8	12.1	39.7	28.6	3	9.8×10^{-3}	0.54	Coupling
15.7	11.5	37.1	27.2	3	9.86×10^{-3}	0.53	Coupling
12.5	9.6	29.5	22.7	3	1.02×10^{-2}	0.51	Coupling
14.0	10.4	33.1	24.6	3	1.04×10^{-2}	0.50	Coupling
21.0	13.8	49.6	32.6	3	1.05×10^{-2}	0.50	No coupling
21.0	13.6	49.6	32.1	3	1.10×10^{-2}	0.48	No coupling
15.9	11.2	37.6	26.5	3	1.11×10^{-2}	0.47	No coupling
21.8	13.8	51.5	32.6	3	1.13×10^{-2}	0.47	No coupling
23.0	13.9	54.3	32.8	3	1.21×10^{-2}	0.43	No coupling
13.0	9.3	30.7	22.0	3	1.29×10^{-2}	0.41	No coupling

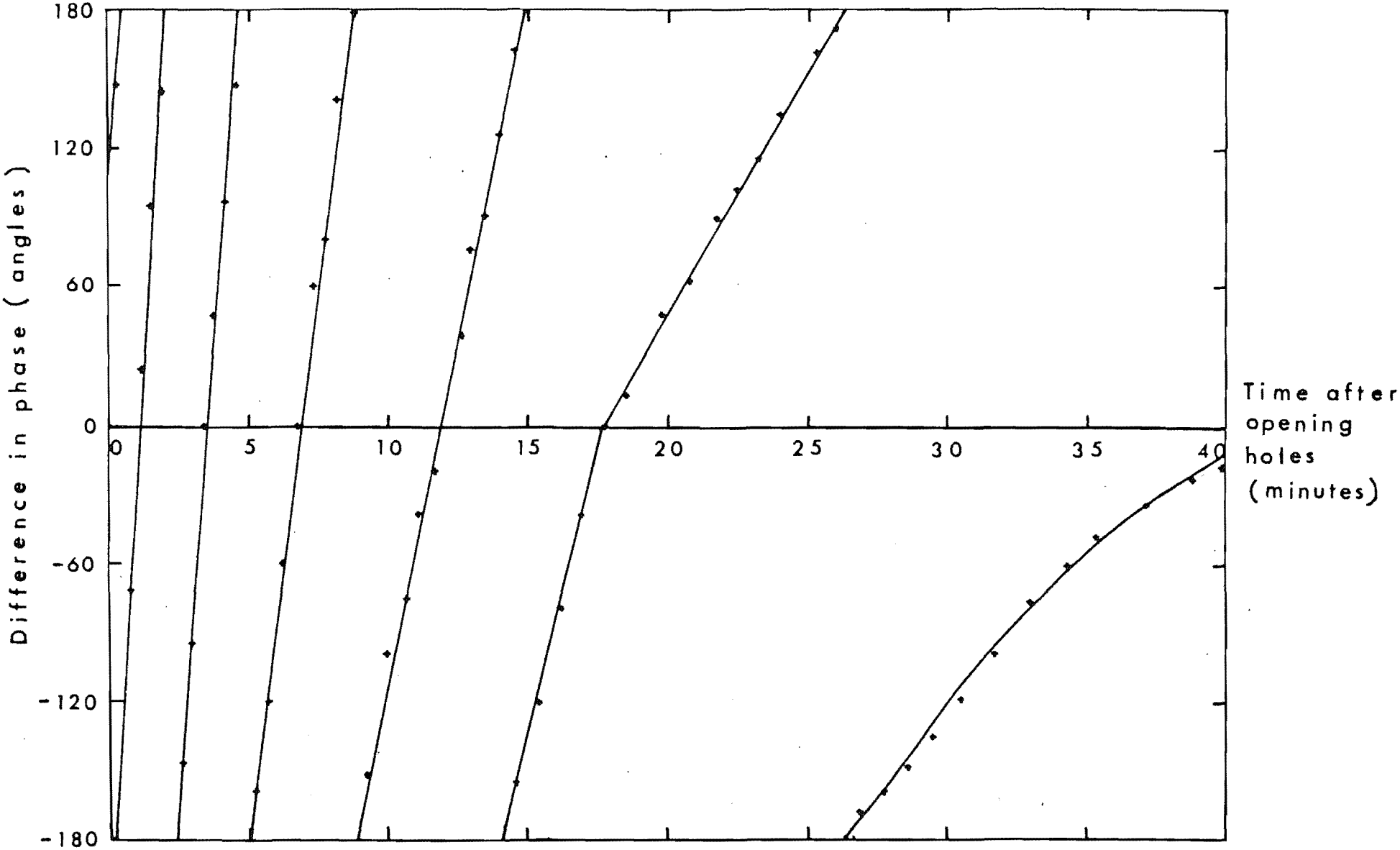

Figure 8.7 : Difference in phase as a function of time after opening holes to illustrate no coupling in the reactor cell system

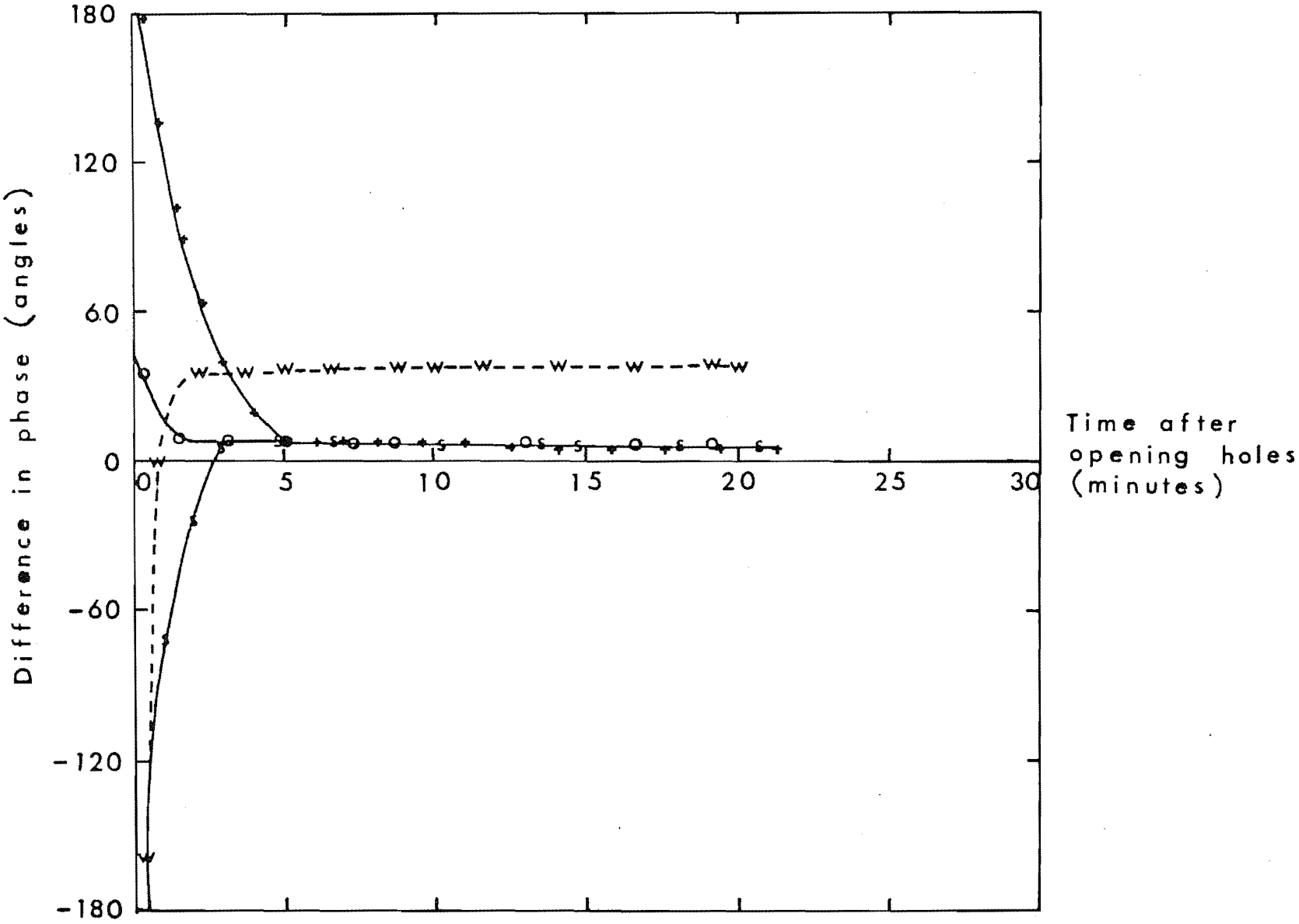

Figure 8.8 : Difference in phase as a function of time after opening holes to illustrate coupling in the reactor cell system

corresponding coupling constant between two organised reactor cells was found to be 3.0 hours (Table 8.7).

It was observed that at values close to the coupling constant, the phase of the two oscillating reagents determine whether the two reactor cell systems couple.

The flow speed of the chemical reagents from one reactor cell to another, v, is determined from the coupling constant, C, by the expression, $C = \frac{\pi N V_o}{Sv}$ where S is the total area of the coupling holes and V_o is the total volume of the chemical system. Rearranging this expression and taking $S = \pi r^2 N$ gives $v = \frac{V_o}{Cr^2}$ where r is the radius of the coupling holes. Using the apparatus and oscillating reagent described by Fujii and Sawada, the value of v for two organised reactor cells is 0.9cm/sec. which is close to that found by Fujii and Sawada [44].

8.4 DISCUSSION

8.4.1 General Discussion

The observation of synchronisation in the two reactor cells enables the coupling constant to be determined accurately. Using the same oscillating reagent (Mixture 2) and the apparatus (System 1) described by Fujii and Sawada [44], the coupling constant of 7.5 hours was slightly higher than the reported value of 6 hours. This difference is probably due to the methods of obtaining frequency differences between the reactor cells. Fujii and Sawada achieved these frequency differences by varying the stirring speed, while the frequency differences reported here, were attained by starting the reactor cells at different times.

Table 8.7 : Comparison of coupling constants for organised-organised reactor cells using Mixture 1 and System 2

Wavelength (mm) Reactor Cell 1	Wavelength (mm) Reactor Cell 2	Time (sec) Reactor Cell 1	Time (sec) Reactor Cell 2	Number of holes N	ΔW	$\frac{2\pi N}{\Delta W}$ (hr)	Overall Effect
19.5	19.0	46.1	44.9	3	5.80×10^{-4}	9.03	Coupling
21.1	19.8	50.1	46.8	4	1.41×10^{-3}	4.94	Coupling
19.0	17.6	44.9	41.6	3	1.77×10^{-3}	2.96	Coupling
21.1	19.8	50.1	46.8	2	1.41×10^{-3}	2.27	No coupling
16.5	15.0	39.0	35.4	3	2.61×10^{-3}	2.03	No coupling
19.0	17.0	44.9	40.2	3	2.63×10^{-3}	1.99	No coupling

It has been suggested that the flow speed of the chemical reagents from one cell to the other, influences the coupling constant [44]. The smaller coupling constant of 4.0 hours obtained for different concentrations of oscillating chemical reagents (Mixture 1) but the same apparatus (System 1), suggests that the concentrations of the oscillating chemical reagents do affect the coupling constant. This is probably due to Mixture 1 having more of the essential reagent for entrainment, in a fixed volume, than Mixture 2. Consequently, the critical volume of exchanged material between the two reactor cells for coupling is less for Mixture 1 and the two reactor cells couple faster.

A comparison of the coupling constants using different apparatus but the same oscillating reagents (Mixture 1) indicates that the apparatus design affects this constant by only a small amount. The value of 3.0 hours for the coupling constant using Mixture 1 and System 2 shows that the coupling strength of System 2 is stronger than that of System 1 by a small amount. The increased coupling strength is probably due to either the shape of the reactor cells or the flexibility of the walls separating them. This result agrees well with that of the well-known sympathetic pendulum system [423]. In the sympathetic pendulum system, the two pendula are fixed to the same beam which can transfer energy from one pendulum to the other. Coupling across the beam between the two pendula is observed and the coupling strength depends on various factors particularly the rigidity of the mount holding the pendulum and the coupling effect of the beam. Thus the two reactor cell system and the sympathetic pendulum system share properties of a more general class of coupled oscillators. Phenomena like synchronisation and

beats can also be observed for coupled systems [424,425].

The observation of small changes in the wavelengths for the later oscillations compared to the starting oscillations is likely to be due to either the changing concentrations of bromomalonic acid or changing compositions of the reagents. For an open system where the reagents are continuously supplied to the reactor cells and the by-products are removed, the wavelengths for all the oscillations under these experimental conditions, are the same. However, in this work, the systems are closed and the wavelengths therefore tend to increase with time. Closed systems would generally be regarded to be inappropriate models for living cells which are open systems. However, the B-Z reaction can continue to oscillate for a relatively long period of time so that overall it can be considered to be a pseudo-open one, and therefore a reasonably satisfactory model system.

In the B-Z reaction, the possibility of two limit cycles, an unstable one and a stable one, has been highlighted by Stanshine [426] and Pacault [427]. The starting and organised reactor cells could be in such unstable and stable cycles respectively. In this work, one of the reactor cells was allowed to organise itself until it was in the stable limit cycle. Then, depending upon the time of reaction of the second reactor before coupling, the two reactor cell system can experience two different limit cycle couplings: (1) unstable-stable limit cycles (for short times) and (2) stable-stable limit cycles (for longer times - as studied by Sawada and coworkers [44]). Therefore two different coupling constants may be determined for coupled oscillators.

Using System 2, the results show that the relative coupling constant between a starting reactor cell and an organised one is six times smaller than between two organised reactor cells, while using System 1, the coupling constant is four times smaller. This suggests that in both cases, an oscillating system that is organising itself is influenced more by external environmental effects than an organised one. Thus any slight environmental asymmetry is more likely to be captured by a starting oscillating reaction than by an organised one. The capture of external asymmetry in oscillating reactions has been suggested as the origin of preferred chirality in living systems [350].

8.4.2 Relevance of Coupled Oscillating Chemical Reactions as Models for Biological Systems

It has been generally accepted that coupled oscillators are involved in the circadian [427,428], neural [429,430] and stomata [431,432] systems. Consequently, their overall biochemical properties can be modelled by the B-Z reactions in coupled reactor cell systems. In the biological systems, it has been suggested that synchronisation and interaction are dependent upon the flow of stimuli from one oscillator to another [421,422]. These stimuli can be AMP [433], electrical impulse [434], water [431], hydrogen ion [435], fatty acids [436] and chemical compounds called morphogens [10,437]. They are transmitted through gap junctions (which are discussed in more detail below). The observation of critical coupling constants in the coupled reactor cell systems suggests that there is synchronisation in the oscillators of biological systems only after a certain amount of stimuli is passed from one oscillator to another. This amount of stimuli is

commonly known as the threshold perturbation [29]. Thus in marine animals, only the solar-day rhythm can influence the circadian oscillators because it is more intense than the lunar-day rhythm [438]. This work suggests that the intensity of the solar-day rhythm is above the threshold perturbation level.

The observation of coupling between organised reactor cells shows that there could be the same mutual interaction between two mature cells in biological systems. Such interaction could enable a cell to determine the state of its neighbours and a model based on this idea has already been proposed [439]. This model is interesting because it shows that living organisms can regenerate missing structures through such an interaction.

Spatial and temporal organisation in cells are considered to be important in living systems for the control of the positions and sequence of events in embryonic development [422]. The spatial organisation is envisaged to be controlled by a morphogen which is generated by source cells. This morphogen is transported to other cells by diffusion and active transport [421]. In the B-Z reactions, most of these characteristics are also observed. The "morphogen" is likely to be bromomalonic acid [33,37], and the higher frequency reactor cell which entrains the lower one, is comparable to the organising centre [440]. Furthermore, the calculated flow speed of bromomalonic acid from this study gives reasonable values, which are of a similar magnitude to that found by Fujii and Sawada [44].

The temporal organisation in a cell is likely to be dependent upon the signalling time of its neighbours [421, 440]. In each cell, three different events were suggested;

namely the "off and sensitive" state, "on and signalling" state and "off and insensitive" state (see Introduction). In the B-Z reaction, the existence of unstable and stable limit cycles enables the signalling time to be modelled and the chemical properties of multiple limit cycles to be determined. This is important because multiple limit cycle states are commonly found during the synthesis of protein [29,441]. Generally, the presence of multiple limit cycles enables small perturbations to vary the period of oscillatory motion over a wide range of values. The change from one limit cycle to another can lead to synchronisation instead of beat frequencies [442].

This behaviour is found during cell division where the cells pass from the clock state to the cell division state. Sorensen and Castillo have suggested that this change in limit cycle states affects the rate constant of the reactions. This can in turn disturb the stability threshold of cells. Such disturbance can lead to cancer growth [442]. The change from one state to another may also be important for the understanding of regulatory processes in living systems, such as the mechanism that turns on and off the copying of a strand of DNA or the contraction of a muscle [420].

The differing coupling constants between a starting-organised reactor cell system and an organised-organised reactor cell system indicate that there is indeed a difference in the sensitivity of the reactor cell which is influenced by the signalling time. The results therefore indicate that a living cell in an unstable limit cycle state is more likely to be entrained by environmental factors than another cell in a stable limit cycle. Thus, the threshold

perturbation level required for a newly formed cell is less and this provides a very sensitive regulatory mechanism for selectively controlling the behaviour of new cells by the organising centre.

It is possible that this mechanism gives rise to the development of different types of cells in higher organisms during embryonic growth. The signals from the organising centre have been suggested to be in contact with every cell [421,422]. If these signals are below the threshold perturbation level for organised cells but above the threshold perturbation level for new cells, only the latter will be affected by the organising centre. The frequency of this signal from the organising centre can change with time, and the coupled frequency of these new cells is therefore different from that of the organised cell at an earlier stage. This difference in frequency could in turn determine the amount of morphogen in each cell and thus enable different types of cells to be formed.

Communication between cells is another important process in higher organisms because it controls growth, development, division and metabolism in these living systems [42]. It has been suggested that gap junctions on the surface of the cells provide direct communication between them [443,444]. Several methods are being used to probe the biochemical properties of the surfaces of different cells [445-447] and various models of gap junctions have been postulated [43]. However, the influences of different gap junctions and geometry of the cells (on the communication between cells) are still not well understood. The different coupling constant obtained when another reaction cell system was used, suggests that the type of gap

junction and geometry of the cells could play a small but significant role during the communication between cells. This result is consistent with early theoretical predictions by Cohen which showed that a small geometric correction was essential for the calculations of coupling in cells [448]. The magnitude of this correction term in living systems is dependent on several factors including the degree of irregularity in the packing of the cells and the amount of interstitial space. Recent theoretical calculations suggest that the cell facets, edges and vertices also play an important role in the biochemical activities of cells [449]. The results indicate that the system which has a cylindrical geometry and a more flexible membrane separating the cells is more likely to have a smaller correction term.

The overall results obtained here agree well with theoretical predictions of coupled cells. Thus the coupled reactor cell system using the B-Z reaction may be considered to be a good model for studying the oscillatory behaviour of interacting cells of higher organisms. The observation of new chemical properties like different sensitivity to environmental factors which are not found under equilibrium situations, suggests that living systems are able to show complex biochemical behaviour by utilising non-equilibrium conditions. By determining coupling constants under different conditions, model systems can be used to help elucidate gross behaviour of complicated biochemical entities.

CHAPTER 9

SIGNIFICANCE OF CHEMICAL STUDIES ON MAGNESIUM PORPHYRIN COMPLEXES AND COUPLED OSCILLATORS FOR A GREATER UNDERSTANDING OF IMPORTANT BIOLOGICAL AND TECHNOLOGICAL PROCESSES

9.1 INTRODUCTION

Porphyrins, metal ions, proteins and coupled oscillators play important roles in most of the biological processes in living systems. The elucidation of their chemical behaviour is therefore crucial to a greater understanding of biological processes and their applications for technological purposes.

The importance and diversity of porphyrins in biological systems can hardly be rivalled by any compound in nature [450]. Basically, all life forms depend on the redox potential of chlorophyll and the electron-transferring properties of heme-containing cytochromes,for converting light to chemical energy. Furthermore, during respiration, heme enzymes and hemoproteins are usually responsible for the transportation, storage, reduction and activation of dioxygen. Other biochemical processes like the reduction of soil nitrite to ammonia in plants, is also mediated by reduced porphyrins (isobacteriochlorin and chlorin) [451].

The ability of porphyrins to accommodate extreme redox changes is due to the unusual chemical properties of the π-system. When a metal ion is coordinated to the centre of the porphyrin, the chemical properties are further enhanced because axial ligations and valence change can occur at the metal centre.

Metal ions are responsible for several biochemical processes because of their stereochemical and electronic environments. Some of these processes require specific metal centres, while for others, replacement of the metal ion by another, can still give the same effect but with the reactivity significantly altered [452].

Mg ions are generally required for the synthesis of chlorophyll and the transfer of phosphate groups to form ATP [453]. Generally, Mg ions are six-coordinate but three- [454], four- [455-457], five- [60,458], seven- [394] and eight-coordinate Mg ions [459] have also been observed. In the photosynthetic system, the Mg ion is coordinated to a tetrapyrrole ring and the axial positions can be coordinated by water or protein amino acid residues. The association of the Mg centre with a protein environment is important because it allows for the possibility of interaction of substituted groups around the chlorophyll ring with other amino acid residues in the protein chain [7]. Furthermore, the protein environment can also influence the coordination state of the metal ion, as found for myoglobin and hemoglobin [166].

Proteins are essentially made up of 20 different kinds of amino acid residues which are either hydrophilic, neutral or hydrophobic in nature [88]. These amino acid residues are joined together by peptide bonds or amide links, -CO-NH-, to give the linear sequence or primary structure (Figure 9.1). There is no branching of chains in proteins but this deficiency is overcome by the possibility of cross-linking of peptide chains. The peptide bond limits the way amino acids can move relative to one another, because

the N-C=O unit is planar. The secondary structure is derived from the primary structure and it causes proteins to have random coil structures or regular α-helical structures. The presence of α-helical structure is due to hydrogen bonding along the axis between the carbonyl and NH groups. Other secondary structure features are determined by the effects of the substituents on the α-carbon atoms and the formation of disulphide bridges between two cysteines (Figure 9.1). Hydrogen bonding and disulphide bridges tend to hold the chains together, while steric hindrance and electrostatic repulsion in the substituents on the α-carbon atoms tend to give either a polypeptide "bend" or random coil. The tertiary structure of proteins is the folding in three-dimensions into a specific configuration characteristic of that protein [460]. This tertiary structure is strongly dependent on the hydrophobicity of the primary structure and the secondary structure which serves as a nucleation position for folding [461]. The non-polar or hydrophobic residues are attracted to each other by van der Waals forces and are usually found in the interior of the protein. Similarly, the polar or hydrophilic residues tend to be on the surface of the protein. Often, these hydrophilic groups can form weak bonds with the hydrophilic groups of another protein to give what is called quarternary structure [462]. This structure is used for allosteric control [460] and it can influence the overall conformation of the protein [463,464]. Thus, changes in the amino acid sequences are likely to produce different protein conformations which can then affect the biochemical properties of metal ions and porphyrins reconstituted into the protein. Thus a full

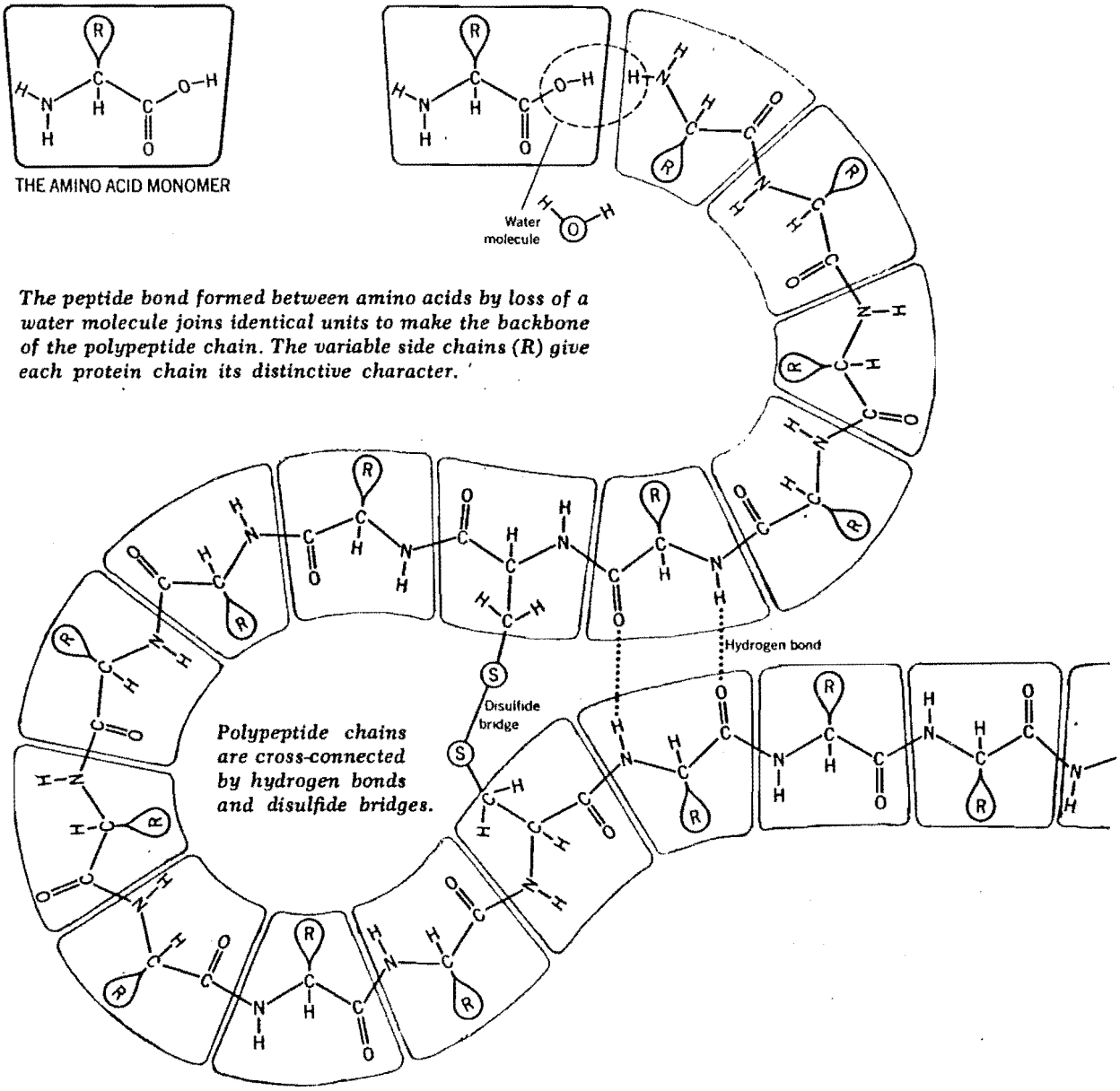

Figure 9.1 : The primary structure of a protein is the sequence of amino acids specified by their sidechains R along the polypeptide chain. Hydrogen bonds, disulphide bonds and interaction between the R groups give rise to elements of secondary structure helices etc. and the overall tertiary structure from ref. 88

understanding of all these effects will ultimately be required in order to understand the action of chlorophyll in detail.

Coupling between oscillators is an important aspect of living systems because living cells show oscillating behaviour and they are coupled chemically to one another by gap junctions or microtubules [443]. In higher organisms, there is evidence which suggests that their biological clocks [427] and neural senses [429] are coupled. The most successful chemical reaction for modelling this coupling is the B-Z reaction. Other oscillating reactions like the Briggs-Rauscher [465,466] and chlorite-iodate-arsenite system [467,468] can also be used but the conditions for prolonged oscillations are more stringent. Furthermore, the B-Z reactions show both smooth and chaotic oscillations [419].

Although porphyrin, metal ions, proteins and naturally occurring coupled oscillators have been extensively studied, most of their chemical properties are still not well understood. In some cases, the importance of these studies to biological systems and their applications is not obvious. Consequently, an attempt will be made in this concluding chapter to indicate the relevance of this work to photosynthetic systems, coupled biological oscillators and DNA-metalloporphyrin interaction. The first two have been the focus of attention in this thesis, while the last one indicates how results obtained here could be extended to another different biological system.

9.2 PHOTOSYNTHETIC SYSTEM

The fossil fuel in the world is running out fast and the petroleum era may be close to its end [469]. There has been an increasing need for new sources of energy especially since the energy crisis of the early 1970's [470]. The potential, large-scale energy resources considered suitable for the future are nuclear, solar, wind, waves, geothermal and tides [471]. Recent studies have suggested that the most feasible source of energy for the future is solar energy [472], and several experiments have been performed to trap this energy [473-476]. Solar heating devices [477,478], photogalvanic cells [479-481] including semiconductor electrodes [482] and solar biomass [476,483] are some of the direct methods for collecting this energy. However, storage of this energy can be a major problem if steady energy is required [471].

In nature, the most common and inexpensive process for collecting and storing solar energy efficiently, is the photosynthetic one. The overall photosynthetic process can be represented as

$$CO_2 + H_2O \xrightarrow{h\nu} {}^1/6(C_6H_{12}O_6) + O_2 \quad \Delta H = 468 \text{ kJ mol}^{-1}$$

where $C_6H_{12}O_6$ is a monomeric unit of carbohydrate. Most of the important primary events in photosynthesis are performed by chlorophyll molecules and it is therefore important to elucidate their chemical properties.

9.2.1 Chlorophyll Molecules *in vivo*

The chemical properties and environments of chlorophyll *in vivo* are still not completely understood. The red-shift in the spectrum of antenna chlorophyll *in vivo* has been

suggested to be a result of either the association of protein [3] or the aggregation of chlorophyll molecules [23]. The studies reported here on Mg porphyrin-globin complexes indicate that most of the red-shift is due to chlorophyll-protein interactions and partially to the formation of a six-coordinate Mg centre. Theoretical calculations [484] and other model studies of chlorophyll-protein complexes by Boxer [12-15] and Pearlstein [17] appear to support this suggestion.

Molecular orbital calculations by Eccles and Honig [484] have shown that the red-shifts induced in the transition energies of chlorophyll by external amino acid charges are comparable in magnitude to those observed *in vivo*. Furthermore, the size of the shift increases in the order bacteriochlorophyll b > bacteriochlorophyll a > chlorophyll a which is the observed trend. They concluded that the red-shift in photosynthetic systems was mainly a result of interaction between the chlorophyll molecules and the amino acid residues in the protein chain.

Boxer and coworkers observed no change in the positions of the spectral bands of pyrochlorophyllide in apomyoglobin and in organic solvent [12-15]. However, crystallisation of pyrochlorophyllide-Mb complex red-shifted one of the bands by 9 nm. They suggested that interaction between the protein environment and the substituents around the chlorophyll ring led to this red-shift. Pearlstein and coworkers observed red-shifted and intense CD bands for some of the chlorophyllide-Mb complexes [17]. They suggested that this red-shift was due to the aggregation of chlorophyll molecules, involving the formation of six-coordinate Mg centres.

Equilibrium studies and observations of induced Cotton effects for Mg porphyrin confirm that six-coordinate Mg centres can red-shift the electronic and CD spectra significantly.

X-ray studies show that six-coordinate Mg centres are obtained under high ligand concentration. The Mg ion is situated at the centre of the porphyrin ring and the magnitude of the red-shift is dependent upon the bond distance between the coordinating atom and the Mg centre. Steric interaction increases this bond distance and the amount of red-shift is diminished. This type of six-coordinate Mg centre is of particular interest as suitable models for the reaction centres of photosynthetic organisms, as discussed in Section 2.4.2.

X-ray studies also show that for Mg porphyrins, the nitrogen atoms of aromatic rings and the oxygen atom of water molecule are preferentially coordinated to Mg. This result supports the suggestion that most of the Mg atoms in chlorophyll molecules *in vivo* are coordinated to either water molecules [18] or nitrogen atoms of histidine groups [3]. When there is steric interaction between Mg porphyrin and the ligand, a five-coordinate square pyramidal structure is favoured. An important feature, highlighted in this work, is that for the structure with water coordinated, the Mg ion is displaced further out of the plane of the porphyrin ring when there is hydrogen bonding between the water molecule and other molecules. This result suggests that in reaction centres of photosynthetic systems, the same effect could enhance the excited Mg ion out of the chlorophyll plane which then initiates the charge separation that is so

important in photosynthesis [406].

Chlorophyll molecules and Mg porphyrin are insoluble in water. The stability of Mg porphyrin-globin complexes indicates that in photosynthetic systems, reconstitution of chlorophyll molecules into proteins enables the complex to become soluble in water. The photolysis results for Mg porphyrin-globin complexes reported here suggest that the protein environment can significantly slow down the photo-oxidation of chlorophyll molecules *in vivo*. This is possibly another reason why antenna chlorophyll molecules, which collect sunlight, are closely associated with proteins.

This work has provided an insight into the biochemical behaviour of chlorophyll molecules *in vivo*. Furthermore, the importance of Mg porphyrin as a model compound for chlorophyll molecule has also been highlighted. These results can also be relevant to the development of a more efficient artificial photosynthetic system.

9.2.2 Artificial Photosynthetic System

The disintegration of water to produce dihydrogen and dioxygen gases is an efficient way of storing energy indefinitely in a recoverable form [485]. Furthermore, the gases produced do not pollute the atmosphere and hydrosphere [486]. The dihydrogen gas can be used in (1) catalytic processes for the production of gasoline, (2) the Haber process for production of ammonia, (3) the edible oil industry where hydrogenation of unsaturated bonds is important, (4) the production of polyurethane, (5) the metallurgical industry for reduction of metal oxides, (6) rockets as a fuel and (7) ionization detectors as a fuel gas. At present, these uses account for more than 90% of the hydrogen consumed [487].

The three general methods of generating dihydrogen gas from water are (1) steam reformation of hydrocarbon [487] and coal [488], (2) electrolysis [489] and (3) solar processes [490]. Solar energy conversion is by far the most interesting because solar energy is available everywhere and the total supply far outstrips man's requirement [491]. Furthermore, this solar energy conversion is accomplished readily in nature by photosynthetic systems.

In natural systems, photosynthesis requires the interaction of two kinds of photosystems called photosystem I and II, to overcome an electrochemical gradient of 1.23 V for the oxidation of water (Figure 9.2) [492,493]. In photosystem II, light energy absorbed by antenna chlorophyll is transferred very rapidly to the reaction centre, P_{680}, which absorbs at 680 nm. This energy creates a very strong oxidant, P_{680}^{+}, and a weak reductant called Q^{-}. The electronically excited Q^{-} then reduces a molecule of plastoquinone and the electron is transferred through a series of pigments (including cytochromes b, cytochromes f and plastocyanin) until it reaches P_{700}^{+} in photosystem I to regenerate P_{700}. P_{680}^{+} can extract an electron from an unknown donor, Z, to regenerate P_{680} and produce Z^{+}. Z^{+} then extracts an electron from a manganese compound, M. The accumulation of four positive charges on M can then oxidise water to oxygen molecules. The overall reaction is

$$2H_2O \longrightarrow 4H^{+} + O_2 + 4e^{-}$$

Similarly in photosystem I, the energy trapped by the antenna chlorophyll is used to excite the reaction centre, P_{700}, which absorbs at 700 nm. This excitation results in a weak oxidant, P_{700}^{+} and a strong reductant. The excited

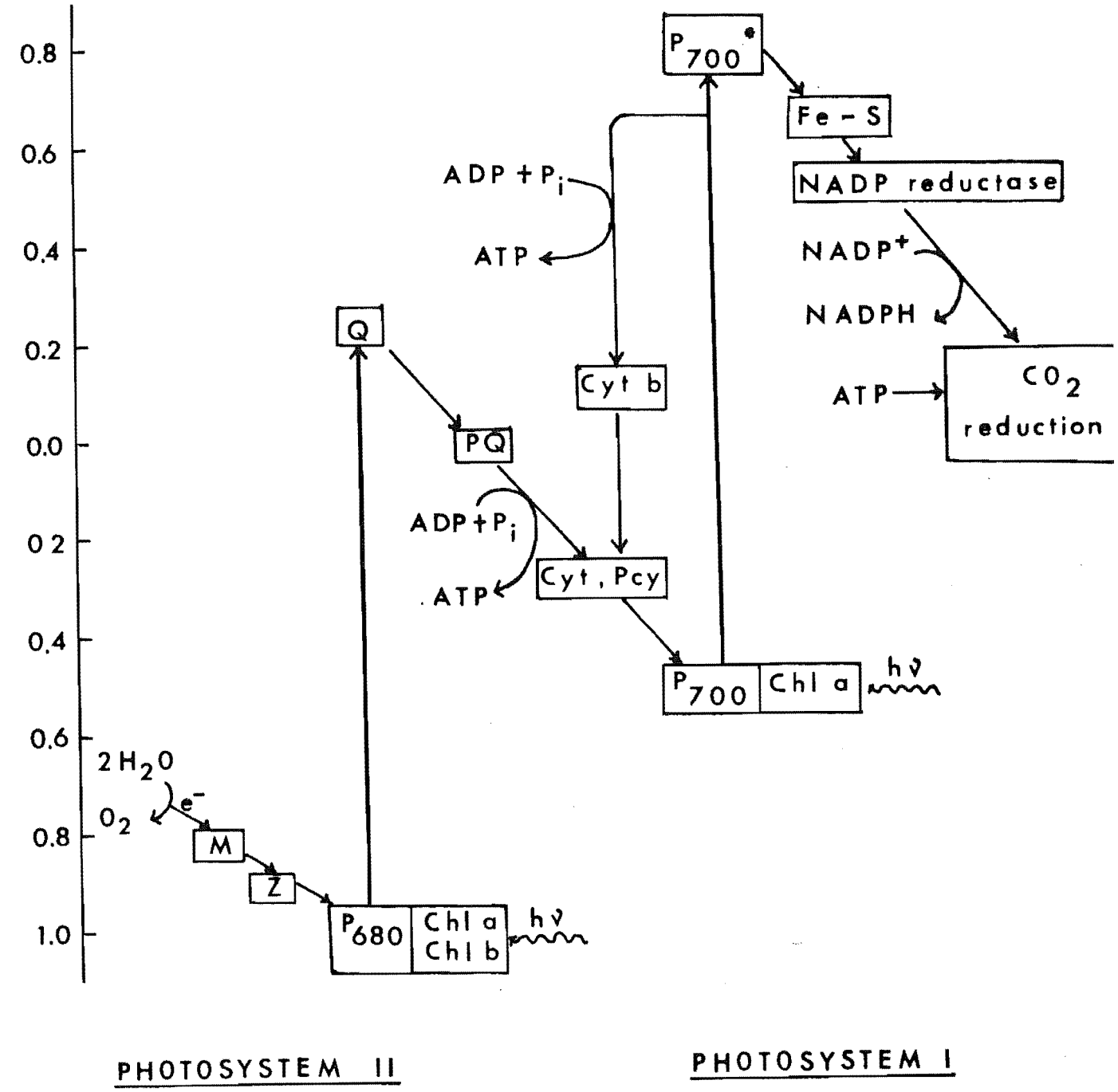

Figure 9.2 : Photosynthetic electron transfer scheme. The two light reactions of photosystem I and photosystem II operate in series, connected by quinones (Q,PQ), cytochrome b(Cyt b) and the copper protein, plastocyanin (Pcy). Strong oxidants produced by photosystem II remove electrons from the Mn-containing complex (M) via Z (unknown) that results in water oxidation. Photosystem I produces powerful reductants that donate electrons to ferredoxin (Fe-S) and NADP and are ultimately responsible for CO_2 reduction

electron at P_{700} is captured by iron-sulphur centres (Fe-S), which then reduces ferredoxin (an iron containing protein). The reduced ferredoxin can react with either (1) $NADP^+$ and H^+ to give NADPH in the presence of ferredoxin NADP reductase, or (2) cytochrome b_6, and the electron then flows back to P_{700}^+ through cytochrome f and plastocyanin to generate ATP.

During the flow of electrons through the two photosystems, ATP is also produced. By utilising ATP (an energy carrier) and NADPH (a reducing agent), CO_2 can be reduced to yield carbohydrates in the Calvin cycle.

The understanding of these chemical properties has led to the development of several artificial photosynthetic systems [494,495]. One such newly discovered system consists of Pt, RuO_2, TiO_2, methylviologen and a photosensitizer [496-498]. The photosensitizers that have been generally used are Ru complexes and metalloporphyrins (including their derivatives). In this system, photoredox reactions occur on Pt and RuO_2 adsorbed on TiO_2.

Light energy of the appropriate wavelength is essential to excite the photosensitizer and an electron from the excited photosensitizer is then passed into the conduction band of TiO_2 (Figure 9.3). The existence of a small Schottky potential barrier at the Pt/TiO_2 junction assists the movement of the electrons to reduce H^+ to H_2 [499]. The oxidised photosensitizer is then converted back to its original form by oxidising water to oxygen through RuO_2, which is an excellent electrocatalyst for water oxidation. Thus, this system is capable of cleaving water in a cyclical manner (Figure 9.4). The main drawbacks

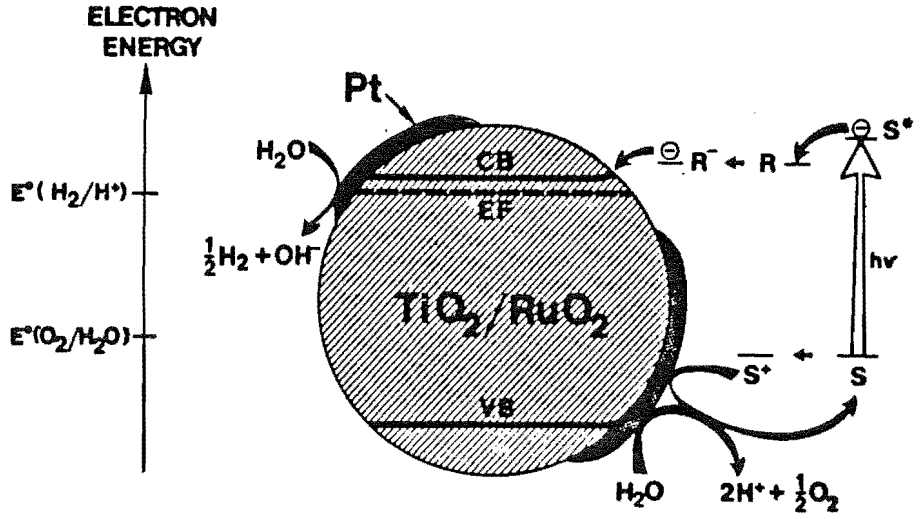

Figure 9.3 : Schematic illustration of the intervention of a TiO_2-based catalyst in simultaneous H_2 and O_2 formation (from ref. 496)

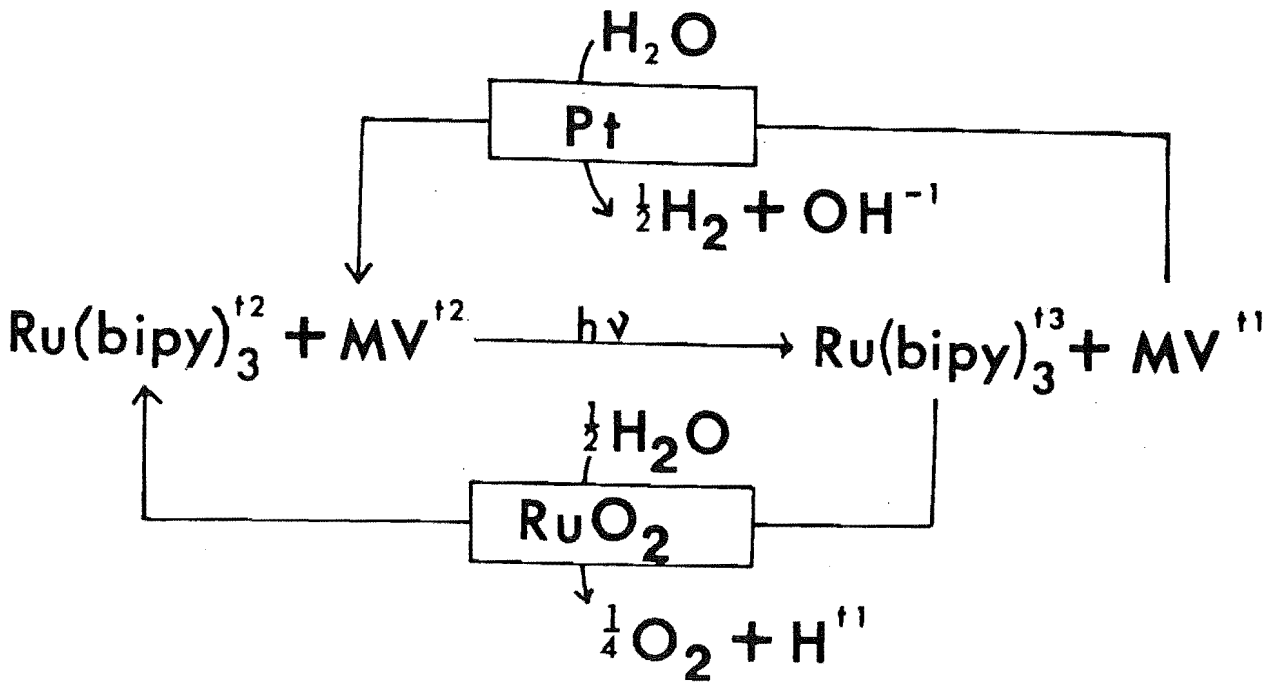

Figure 9.4 : Schematic diagram of cyclic cleavage of water

are that it works for a relatively short period of time [500] and the production of a mixture of dihydrogen and dioxygen gases is not useful [501]. However, in the future, these disadvantages are likely to be overcome.

In the past, $Ru(bipy)_3^{2+}$ has been the most popular photosensitizer but recently, water-soluble metalloporphyrins have been commonly used [501]. These porphyrins have many advantages including low cost and high quantum yield of at least 60 percent in green light for zinc tetramethyl-pyridylporphyrin. It is possible to develop an artificial photosynthetic system which can perform better than the natural ones because efficient storage of energy is not the prime purpose of photosynthetic organisms [491]. Recent studies support this possibility and the results show that the quantum yield for ZnTPP as photosensitizer in DMSO-water solution is higher than that of chlorophyll [311].

Mg porphyrin and its derivatives have also been used as photosensitizers in artificial photosynthetic systems because the magnesium ion has been found to promote spin-orbit coupling [502]. This coupling is necessary for multiplicity forbidden crossing processes to occur, especially $S_1 \rightarrow T_1$, where S_1 and T_1 are the singlet and triplet excited electronic states respectively. Replacement of Mg by heavier atoms, e.g. Zn, increases the process $S_1 \rightarrow T_1$ further but it also enhances the process $T_1 \rightarrow S_o$, where S_o is the singlet ground state (Figure 9.5). The overall result for the heavier atom is a lower triplet state. Thus the Mg(II) ion is ideal for the production of the triplet state which is essential for photochemical reactions, particularly the cleavage of water.

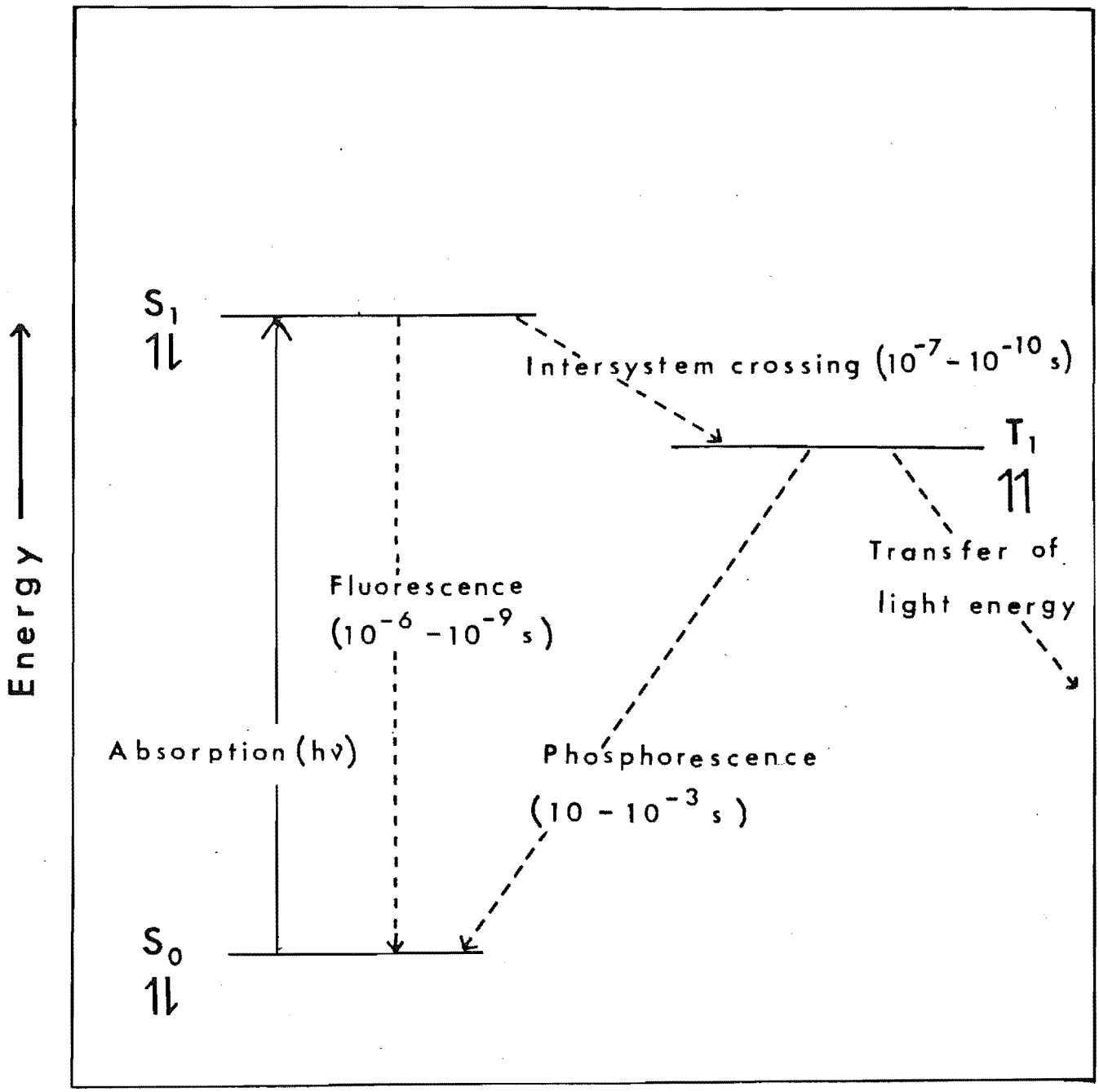

Figure 9.5 : Possible electronic transitions

Recent results show that the quantum yields of Mg tetraphenylporphyrin [311] and Mg phthalocyanine [503] in DMSO-water are 10 and 47 percent respectively. The lower quantum yield of MgTPP compared to ZnTPP (which has a quantum yield of 40 percent) is surprising because MgTPP has a longer lifetime for the triplet state (46 ms). A possible reason for the low quantum yield is the lower oxidation potential of MgTPP (0.78 V) relative to ZnTPP (0.95 V) [311].

Stellwagen has proposed that the exposure of metalloporphyrin-globin complex to an aqueous solvent can primarily determine the redox potential [504]. Therefore, reconstitution of Mg porphyrin into globin may affect the potential of Mg porphyrin which could lead to a higher quantum yield.

This work indicates that incorporation of metalloporphyrin into globin enables metalloporphyrins which are insoluble in water to be "dissolved", and used as potential photosensitizers. Furthermore, these metalloporphyrin-globin complexes are more stable to light than metalloporphyrin, alone.

Another advantage of these complexes is that they could be used in the formation of mixed hybrid species. In these species, Mg porphyrin can be reconstituted into the α_2 strand and Fe porphyrin incorporated into the β_2 strand of apohemoglobin. Light energy collected by Mg porphyrin-(α_2)Hb could be used to disintegrate water and the dioxygen gas produced may be effectively removed by Fe(II)porphyrin-(β_2)Hb. The removal of dioxygen gas may be important because dioxygen gas can sometimes poison the reaction [485]. The presence of such a mixed hybrid species could enable dihydrogen and dioxygen gases produced in artificial

photosynthetic systems to be separated efficiently.

It is possible that light energy can be used for direct cleavage of the water coordinated to Mg porphyrin-Mb complex. The photolysis experiments reported here indicate that water coordinated to Mg can indeed be affected by light. The energy required for such cleavage is large but the presence of a protein environment enables the energy to be transferred efficiently from one chromophore to another. Results for a mixed hybrid hemoglobin consisting of Zn chlorophyllide and heme [505] or Zn porphyrin and heme [211,506] have shown that intramolecular energy transfer is possible. Thus energy collected by Mg porphyrin-Hb (which can be considered to be the analogue of antenna chlorophyll) could be transferred to a "reaction centre", like Mg porphyrin-Mb.

The overall results indicate that metalloporphyrin-globin complexes can be considered as suitable photosensitizers. Furthermore, these complexes can possibly mimic the photochemical mechanisms in antenna chlorophyll and reaction centres of natural photosynthetic systems to cleave water.

9.3 DNA-METALLOPORPHYRIN COMPLEXES

Metal complexes [507] which intercalate with deoxyribonucleic acid (DNA) are of considerable importance because of their potential anticancer properties. This anticancer activity was first discovered for the complex, cis-$Pt(NH_3)_2Cl_2$, by Rosenberg and coworkers [508,509]. Since then many other metal complexes [510,511] including metalloporphyrin [512-514] have been found to show such

activity.

When tetrakis(4-N-methylpyridyl)porphyrin(H_2TMpyP-4) (Figure 9.6) intercalates to DNA, it is observed that (1) the intensities of the electronic bands of DNA and H_2TMpyP-4 in the ultra-violet region are altered, and the positions of these bands are red-shifted, (2) there is an induced Cotton effect for H_2TMpyP-4 in the visible region, (3) the ellipticity of the DNA in the ultra-violet region is changed, (4) the relative viscosity of solutions of these complexes is increased, (5) there is stabilisation of DNA helix against thermal denaturation, and (6) the covalently closed superhelical DNA is unwinded [515].

Results obtained from Mg protoporphyrin-globin complexes (Chapter 3) suggest that the red-shift in DNA-(H_2TMpyP-4) complex is probably due to interaction between DNA and the peripheral substituents of H_2TMpyP-4. Construction of a molecular model of a stable structure of DNA-(H_2TMpyP-4) correlates with this suggestion and shows that the positively charged meso-substituents of H_2TMpyP-4 interact with the negatively charged phosphate groups of the DNA backbone [515]. This red-shift is large because charge transfer is possible for this type of interaction. It is likely that this charge interaction stabilise the complex against random dissociation of H_2TMpyP-4.

The observation of an induced Cotton effect in the visible region of DNA-(H_2TMpyP-4) suggests that H_2TMpyP-4 is closely associated with the chiral groups of DNA. The magnitude of the induced optical activity is dependent upon the metal ions substituted into H_2TMpyP-4, but it is generally weak. This activity is probably due to the

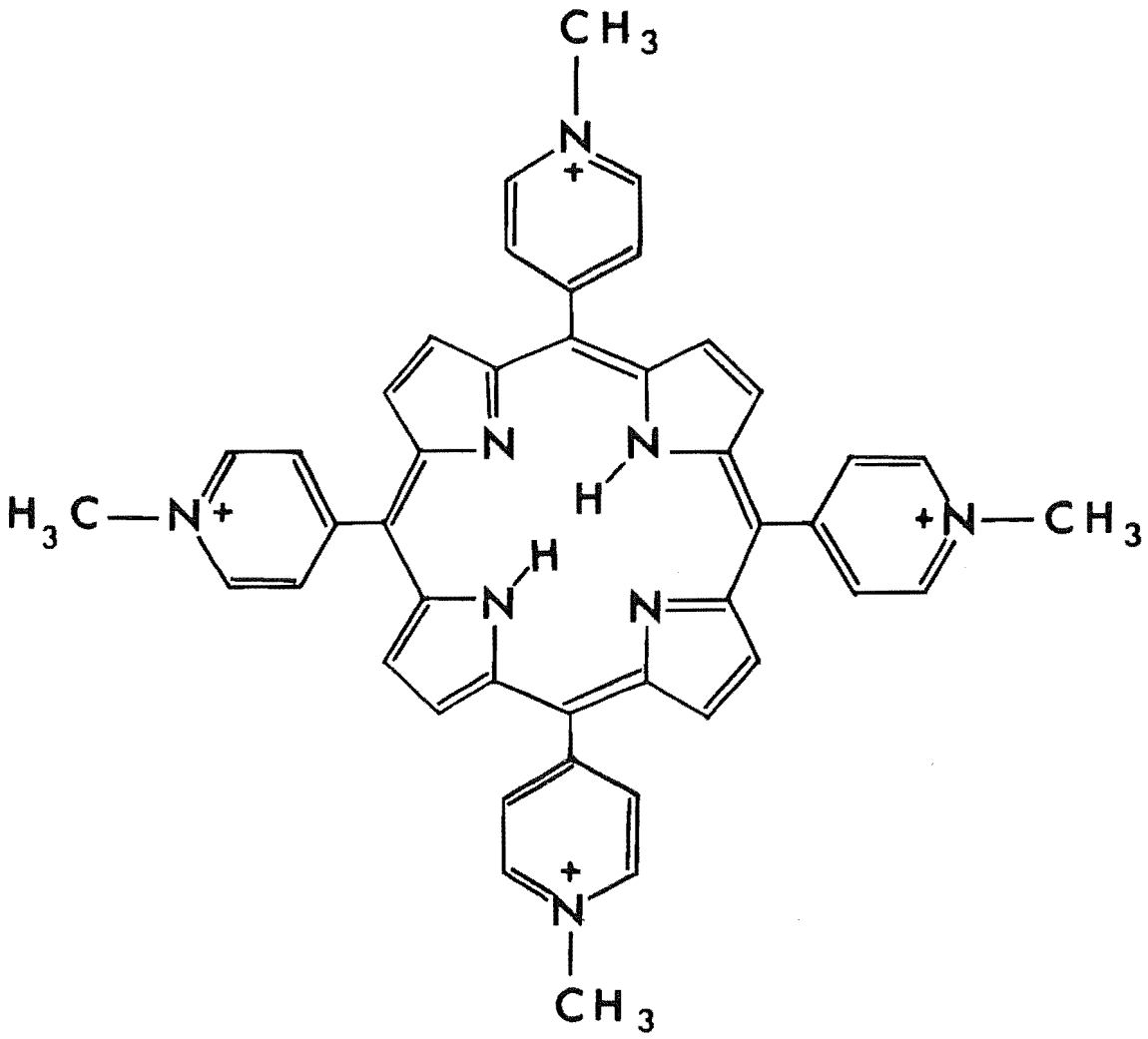

Figure 9.6 : Structure of H_2TMpyP-4

coupled oscillator mechanism, which also gives rise to induced Cotton effects in Mg porphyrin-globin complexes (Chapter 4). In this mechanism, the most important coupling is likely to be between the porphyrin π-π^* transitions and the π-π^* transitions of the base pair in DNA. Other couplings may also contribute to this optical activity.

The stability of the DNA-(H_2TMpyP-4) complex against thermal denaturation suggests that the porphyrin is tightly accommodated into DNA. Similar results were observed for Mg porphyrin-globin complexes. The apohemoglobin and apomyoglobin are unstable at room temperature and denature rapidly (Chapter 3). However, reconstitution of Mg porphyrin prevents the denaturation and Mg porphyrin-globin complexes are stable for a long period of time. This suggestion for the DNA-(H_2TMpyP-4) complex is supported by molecular models. These models are constructed by building the DNA portion around the porphyrin [515]. When they are completed, the packing is so tight that the porphyrin cannot slide out of the DNA chain.

X-ray studies of Mg tetraphenylporphyrin complexes indicate that the phenyl groups are nearly perpendicular to the plane of the porphyrin ring (Chapters 6 and 7). It is likely that for H_2TMpyP-4, the N-methylpyridyl groups are also oriented at right angles to the porphyrin core and for intercalation of H_2TMpyP-4, the N-methylpyridyl groups have to rotate to a position nearly coplanar to the porphyrin core [515]. X-ray results also show that six-coordinate metalloporphyrin complexes of Group IIA are unlikely to be intercalated because the bond distance of ligand-metal-ligand are too long to be accommodated into DNA.

Another interesting aspect is the photochemistry of the DNA-(H_2TMpyP-4) complex. Results of Mg porphyrin-globin complex show that the protein chain is affected after prolonged irradiation. It is possible that under the influence of light, H_2TMpyP-4 can also act as a photosensitizer and affect the function of DNA. Fiel and coworkers have obtained evidence which indicates that such photochemical processes do occur [514].

Overall, the intercalation of porphyrin and its metal complexes to DNA exhibits several physical properties which are similar to those observed for Mg porphyrin complexes. The detailed studies of Mg porphyrin complexes may therefore assist in the understanding of the biochemical behaviour of complexes of the DNA-(H_2TMpyP-4) type.

9.4 COUPLED OSCILLATOR SYSTEM

It has been suggested that coupling of at least two components can lead to new chemical behaviour [95]. In the reaction centres of the photosynthetic systems, the coupling of the two chlorophyll molecules is generally believed to give rise to the exciton effect [95]. The exciton effect is comparable to the sympathetic pendulum system (Section 8.4.1) [424], where the beat phenomenon observed is not present in either of the two isolated pendula.

Similarly for metalloporphyrin, DNA and protein, there are no CD spectral features in the visible region. However, when the metalloporphyrin is coupled to DNA or protein, the coupled oscillator mechanism gives rise to the induced Cotton effect in the visible region (Section 3.4.4).

The work on coupled reactor cell systems also supports

this suggestion and the results show that coupling can indeed lead to new chemical features like beats and synchronisation. The results also indicate that the geometry of the components is important for determining the critical coupling behaviour. This result suggests that in the photosynthetic system, the relative orientation and arrangement of the chlorophyll molecules are also likely to be crucial for the exciton effect.

In circadian oscillations, it is generally accepted that there are at least two types of oscillators [516]. These oscillators are influenced by light [517], food [518] and other stimuli [519]. These oscillators exhibit rhythm splitting, synchronisation and beats [520] which are also observed in coupled reactor cell systems. Thus the results from reactor cell systems may be important for an understanding of circadian oscillation.

It has been observed that circadian oscillations can show "spontaneous internal desynchronisation", where the temperature and activity rhythms which were originally synchronised become non-synchronised [521]. This "flip-flop" type of coupling is important because it enables higher organisms to regulate their temperature and activity [522]. The results from the coupled reactor cell system (Chapter 8) suggest that there are at least 2 limit cycles in one of the oscillators, while the other oscillator remains in the same limit cycle. This would enable coupled systems to switch from one state to another. Depending on the conditions of coupling, there are therefore two modes of interaction which can be measured by the periods of the driving oscillators.

Although this study of coupled B-Z systems involved intrinsic coupling between chemical oscillators, the results indicate that their characteristics are also generally found in other more complex physical and biological systems. Consequently, some of the biochemical properties of living systems can be successfully modelled by relatively simple coupled reactor cell systems. The results obtained so far agree well with theoretical predictions of biological behaviour.

9.5 CONCLUDING REMARKS

The work shows that detailed biochemical properties may be obtained from model studies which can give an insight into the chemical behaviour of living systems. However, the functions of biological systems are generally very subtle. Thus, direct studies of natural biological components are still essential for a complete understanding of such complex systems. For example, the cooperative mechanism of the four heme groups in hemoglobin has been determined from a range of physical studies of hemoglobin itself, because it is unlikely that model studies alone can provide such information. Nonetheless, as highlighted in this Chapter, results from model studies may also be of value to other major areas of interest, particularly in the medical and technological fields.

APPENDIX A

OBSERVED AND CALCULATED STRUCTURE FACTORS FOR MG TPPINIOAZOLE PAGE 1

H	K	L	FO	FC	H	K	L	FO	FC	H	K	L	FO	FC	H	K	L	FO	FC	H	K	L	FO	FC
0	2	0	184	182	9	9	0	19	18	-4	14	0	64	65	4	18	0	19	13	3	5	1	137	135
2	2	0	87	87	-9	10	0	49	46	-2	14	0	63	62	12	18	0	39	38	4	5	1	56	57
3	3	0	103	104	-4	10	0	24	29	0	14	0	26	22	-10	20	0	20	25	5	5	1	19	23
-2	4	0	264	262	-2	10	0	149	145	4	14	0	52	50	-5	20	0	34	33	-5	6	1	20	21
0	4	0	96	99	0	10	0	57	57	6	14	0	105	107	0	20	0	72	69	-4	6	1	24	23
2	4	0	78	82	2	10	0	109	102	10	14	0	29	26	2	20	0	33	32	-3	6	1	40	41
4	4	0	134	133	5	10	0	35	32	12	14	0	41	43	-7	21	0	21	21	-2	6	1	28	29
-3	5	0	43	47	8	10	0	39	42	14	14	0	57	59	1	21	0	19	13	-1	6	1	80	79
-1	5	0	70	69	-7	11	0	17	16	-13	15	0	28	27	4	22	0	36	32	0	6	1	39	39
1	5	0	66	68	-5	11	0	18	14	-5	15	0	25	23	1	1	1	156	160	1	6	1	32	32
3	5	0	72	72	-3	11	0	20	17	1	15	0	41	43	-1	2	1	39	36	2	6	1	73	73
5	5	0	31	31	1	11	0	24	24	3	15	0	20	15	0	2	1	29	29	3	6	1	57	56
0	6	0	19	21	3	11	0	31	31	5	15	0	38	44	1	2	1	34	36	4	6	1	33	34
2	6	0	80	79	5	11	0	40	45	7	15	0	25	26	-2	3	1	17	19	6	6	1	22	27
4	6	0	134	139	9	11	0	30	33	11	15	0	24	22	-1	3	1	148	148	-5	7	1	137	134
6	6	0	57	58	11	11	0	31	31	15	15	0	25	17	0	3	1	97	92	-4	7	1	33	35
-5	7	0	61	60	-8	12	0	57	57	-14	16	0	39	42	1	3	1	56	59	-3	7	1	95	91
-3	7	0	60	60	-6	12	0	26	27	-10	16	0	26	33	2	3	1	34	34	-2	7	1	37	31
-1	7	0	65	63	-4	12	0	38	32	-8	16	0	27	26	3	3	1	146	147	-1	7	1	44	47
1	7	0	71	74	-2	12	0	17	15	0	16	0	30	30	-3	4	1	168	169	0	7	1	52	52
3	7	0	21	22	0	12	0	71	71	4	16	0	21	21	-2	4	1	72	72	1	7	1	37	37
5	7	0	64	66	2	12	0	88	88	6	16	0	57	58	-1	4	1	126	126	2	7	1	55	56
7	7	0	25	30	4	12	0	45	41	8	16	0	50	50	0	4	1	30	29	3	7	1	152	152
-6	8	0	119	114	6	12	0	57	56	-11	17	0	24	22	1	4	1	21	19	4	7	1	19	20
-4	8	0	44	44	8	12	0	42	43	-9	17	0	22	11	2	4	1	76	77	5	7	1	16	12
-2	8	0	54	52	-9	13	0	42	44	-7	17	0	19	19	3	4	1	188	189	6	7	1	19	16
0	8	0	49	53	-7	13	0	45	45	-5	17	0	36	36	4	4	1	40	40	7	7	1	54	56
2	8	0	21	24	3	13	0	23	24	5	17	0	31	35	-4	5	1	17	18	-6	8	1	25	26
6	8	0	126	120	7	13	0	28	25	7	17	0	23	23	-3	5	1	137	135	-5	9	1	25	25
8	8	0	20	14	9	13	0	19	20	-10	18	0	34	35	-2	5	1	69	70	-4	9	1	20	24
-5	9	0	45	49	-12	14	0	26	22	-9	19	0	32	32	-1	5	1	133	130	-2	9	1	28	26
-3	9	0	40	41	-10	14	0	48	49	-6	18	0	35	33	0	5	1	56	55	-1	9	1	70	67
1	9	0	33	36	-8	14	0	31	30	-2	18	0	56	60	1	5	1	94	95	1	9	1	19	20
5	9	0	30	32	-6	14	0	47	44	2	18	0	25	27	2	5	1	41	35	2	9	1	34	36

OBSERVED AND CALCULATED STRUCTURE FACTORS FOR MG TPPINIOAZOLE PAGE 2

H	K	L	FO	FC	H	K	L	FO	FC	H	K	L	FO	FC	H	K	L	FO	FC	H	K	L	FO	FC
3	8	1	17	19	-2	11	1	21	16	-7	14	1	21	14	7	17	1	63	64	3	3	2	73	74
4	8	1	33	33	-1	11	1	53	52	-6	14	1	21	21	13	17	1	39	37	-3	4	2	35	39
5	8	1	33	31	0	11	1	25	22	-5	14	1	23	19	-10	18	1	18	8	-2	4	2	77	75
6	8	1	19	13	2	11	1	26	27	0	14	1	14	12	-9	18	1	22	25	0	4	2	72	74
8	8	1	28	29	3	11	1	16	12	4	14	1	25	20	1	18	1	29	24	2	4	2	33	35
-8	9	1	24	21	4	11	1	31	29	6	14	1	21	20	8	18	1	25	25	3	4	2	28	28
-7	9	1	35	38	5	11	1	73	77	8	14	1	20	20	9	18	1	20	16	4	4	2	44	44
-5	9	1	90	78	7	11	1	16	15	11	14	1	25	25	11	18	1	19	2	-3	5	2	44	42
-4	9	1	37	36	8	11	1	28	28	-13	15	1	50	49	-11	19	1	26	27	-2	5	2	22	27
-3	9	1	42	44	9	11	1	21	21	-11	15	1	35	37	-9	19	1	39	41	-1	5	2	65	65
-1	9	1	114	111	10	11	1	19	15	-9	15	1	19	18	-7	19	1	31	33	0	5	2	20	19
0	9	1	44	45	-11	12	1	23	19	-8	15	1	28	29	-5	19	1	19	20	1	5	2	28	33
1	9	1	48	48	-10	12	1	20	14	-7	15	1	21	21	-1	19	1	19	18	3	5	2	85	88
3	9	1	92	86	-8	12	1	19	23	-6	15	1	18	10	1	19	1	48	45	5	5	2	74	71
4	9	1	34	30	-2	12	1	16	22	-5	15	1	44	40	7	19	1	19	20	-4	6	2	69	67
5	9	1	52	46	0	12	1	20	19	-3	15	1	55	55	-5	20	1	20	23	-3	6	2	15	13
6	9	1	34	37	1	12	1	35	32	-2	15	1	24	22	8	20	1	19	3	-2	6	2	28	28
7	9	1	46	45	2	12	1	19	23	0	15	1	16	11	-5	21	1	30	32	0	6	2	25	33
9	9	1	25	25	4	12	1	21	20	5	15	1	27	28	-1	21	1	37	33	1	6	2	16	22
-8	10	1	19	18	-11	13	1	38	38	7	15	1	73	81	1	21	1	37	39	2	6	2	49	48
-7	10	1	39	38	-10	13	1	40	37	8	15	1	36	24	2	21	1	27	15	4	6	2	42	44
-5	10	1	35	33	-9	13	1	34	30	12	15	1	22	20	5	21	1	33	35	5	6	2	37	36
-4	10	1	20	19	-7	13	1	50	50	13	15	1	27	33	0	0	2	351	350	6	6	2	25	25
-2	10	1	40	39	-5	13	1	29	28	15	15	1	35	34	0	1	2	263	266	-6	7	2	61	57
0	10	1	32	33	-3	13	1	29	29	-12	16	1	19	16	1	1	2	98	92	-4	7	2	28	22
3	10	1	37	38	-1	13	1	34	35	-11	16	1	20	18	-1	2	2	51	50	-2	7	2	19	23
4	10	1	27	31	1	13	1	21	24	-8	16	1	33	25	0	2	2	51	51	-1	7	2	19	18
5	10	1	30	30	3	13	1	26	25	6	16	1	18	10	1	2	2	97	98	0	7	2	24	24
6	10	1	72	72	4	13	1	23	27	-11	17	1	20	18	2	2	2	25	25	3	7	2	29	30
7	10	1	23	23	5	13	1	81	79	-8	17	1	24	25	-2	3	2	23	23	6	7	2	55	55
-9	11	1	22	19	6	13	1	17	4	-7	17	1	39	35	-1	3	2	91	94	-6	8	2	103	103
-8	11	1	17	18	7	13	1	55	52	-3	17	1	39	42	0	3	2	99	99	-5	8	2	50	51
-7	11	1	29	29	13	13	1	39	39	-1	17	1	32	28	1	3	2	68	71	-4	8	2	66	67
-5	11	1	32	30	-9	14	1	30	27	3	17	1	19	19	2	3	2	58	59	-3	8	2	29	28

continued..

APPENDIX A (continued)

OBSERVED AND CALCULATED STRUCTURE FACTORS FOR MG TPPIMIDAZOLE PAGE 3

H	K	L	FO	FC	H	K	L	FO	FC	H	K	L	FO	FC	H	K	L	FO	FC	H	K	L	FO	FC
-9	8	2	58	57	-3	11	2	28	22	-6	14	2	45	42	-13	17	2	19	17	2	3	3	32	33
-8	8	2	27	28	-1	11	2	26	25	-4	14	2	37	35	-11	17	2	24	22	3	3	3	47	45
-2	8	2	35	34	0	11	2	27	27	-2	14	2	41	37	-5	17	2	20	15	-2	4	3	67	65
-5	8	2	17	13	1	11	2	16	16	-1	14	2	23	22	-4	17	2	29	28	-1	4	3	54	55
-6	8	2	27	27	2	11	2	34	34	0	14	2	21	23	-2	17	2	32	29	0	4	3	52	51
-7	8	2	60	56	4	11	2	41	39	2	14	2	22	18	-1	17	2	30	28	1	4	3	16	19
-8	9	2	95	94	6	11	2	44	43	4	14	2	31	35	4	17	2	19	19	3	4	3	35	39
-8	9	2	18	16	7	11	2	17	16	6	14	2	73	76	8	17	2	23	21	4	4	3	61	60
-7	9	2	77	75	9	11	2	17	20	7	14	2	36	36	-10	18	2	33	29	-4	5	3	61	63
-6	9	2	18	20	11	11	2	31	36	9	14	2	20	18	-8	18	2	35	36	0	5	3	59	60
-5	9	2	16	19	-9	12	2	26	28	10	14	2	27	27	-6	18	2	29	29	1	5	3	22	17
-2	9	2	41	41	-8	12	2	42	42	14	14	2	38	36	-5	18	2	20	19	2	5	3	32	31
-1	9	2	15	14	-6	12	2	44	46	-11	15	2	28	29	0	18	2	25	23	4	5	3	51	51
0	9	2	36	36	-4	12	2	19	20	-9	15	2	26	23	-4	19	2	25	19	-5	6	3	42	44
1	9	2	36	37	-2	12	2	19	20	-6	15	2	19	16	-2	19	2	16	17	-4	6	3	31	30
3	9	2	21	19	1	12	2	22	19	0	15	2	28	27	0	19	2	19	23	-3	6	3	50	49
5	9	2	53	49	2	12	2	30	30	4	15	2	28	25	3	19	2	19	13	-2	6	3	29	24
7	9	2	45	50	4	12	2	37	39	9	15	2	22	24	9	19	2	19	13	1	6	3	33	33
-9	10	2	39	42	6	12	2	87	85	9	15	2	19	16	11	19	2	21	16	2	6	3	46	43
-6	10	2	31	35	8	12	2	30	34	13	15	2	19	13	-5	20	2	35	42	3	6	3	37	39
-4	10	2	42	43	9	12	2	28	32	15	15	2	19	8	-4	20	2	30	35	-6	7	3	45	46
-3	10	2	26	26	12	12	2	23	22	-13	16	2	19	24	-1	20	2	31	31	-5	7	3	55	52
-2	10	2	74	73	-10	13	2	25	26	-9	16	2	34	35	0	20	2	44	40	-3	7	3	46	47
-1	10	2	18	17	-6	13	2	19	19	-7	16	2	18	14	2	20	2	29	30	0	7	3	16	21
0	10	2	25	25	-4	13	2	41	37	-6	16	2	46	50	4	20	2	25	22	1	7	3	32	37
1	10	2	45	43	-3	13	2	29	24	-4	16	2	39	38	0	1	3	27	26	2	7	3	33	39
3	10	2	19	9	-2	13	2	31	29	0	16	2	25	23	1	1	3	110	110	3	7	3	32	34
6	10	2	37	36	-1	13	2	30	28	1	16	2	18	17	-1	2	3	125	123	4	7	3	35	35
9	10	2	19	1	1	13	2	19	15	3	16	2	20	15	0	2	3	69	69	-5	8	3	39	39
-9	11	2	19	13	5	13	2	21	21	5	16	2	27	27	1	2	3	172	173	-4	8	3	27	26
-8	11	2	29	27	7	13	2	25	23	6	16	2	60	62	2	2	3	133	135	-2	9	3	70	73
-7	11	2	34	41	9	13	2	18	6	8	16	2	37	36	-2	3	3	69	69	-1	9	3	16	12
-6	11	2	24	25	-10	14	2	26	26	9	16	2	22	24	-1	3	3	41	38	0	9	3	42	42
-5	11	2	28	30	-9	14	2	43	45	14	16	2	22	15	0	3	3	37	36	2	9	3	24	21

OBSERVED AND CALCULATED STRUCTURE FACTORS FOR MG TPPIMIDAZOLE PAGE 4

H	K	L	FO	FC	H	K	L	FO	FC	H	K	L	FO	FC	H	K	L	FO	FC	H	K	L	FO	FC
3	8	3	48	48	-1	11	3	58	47	-11	14	3	19	17	-12	17	3	23	16	2	2	4	67	70
4	9	3	35	38	0	11	3	44	44	-10	14	3	29	34	-11	17	3	22	15	-2	3	4	60	59
7	9	3	52	52	1	11	3	27	27	-6	14	3	23	23	-7	17	3	47	50	-1	3	4	69	72
-7	9	3	34	33	3	11	3	35	35	-2	14	3	19	13	-6	17	3	22	23	0	3	4	46	44
-4	9	3	28	23	4	11	3	19	18	1	14	3	35	39	-4	17	3	18	21	1	3	4	59	60
-3	9	3	39	41	5	11	3	20	14	2	14	3	38	35	1	17	3	30	32	2	3	4	36	40
-2	9	3	26	24	7	11	3	42	42	3	14	3	40	37	6	17	3	25	22	3	3	4	80	77
-1	9	3	54	51	-4	12	3	17	15	4	14	3	24	25	8	17	3	37	36	-3	4	4	19	14
0	9	3	35	34	-3	12	3	25	24	5	14	3	21	23	10	17	3	22	15	-2	4	4	29	30
1	9	3	22	25	-2	12	3	54	54	6	14	3	49	46	12	17	3	21	23	-1	4	4	37	35
2	9	3	39	39	-1	12	3	30	29	8	14	3	37	36	-8	18	3	25	22	0	4	4	35	33
5	9	3	20	23	0	12	3	45	44	12	14	3	20	17	-3	18	3	21	16	1	4	4	58	58
7	9	3	17	18	1	12	3	23	22	-12	15	3	35	45	-1	18	3	22	21	2	4	4	47	47
9	9	3	23	23	2	12	3	39	40	-5	15	3	25	28	0	18	3	24	20	3	4	4	19	15
-9	10	3	34	36	3	12	3	25	24	-3	15	3	25	26	1	18	3	29	29	4	4	4	43	42
-8	10	3	27	23	5	12	3	18	13	-2	15	3	31	29	5	18	3	24	22	-4	5	4	41	41
-6	10	3	17	18	6	12	3	22	21	-1	15	3	20	23	-9	19	3	22	22	-3	5	4	72	72
-5	10	3	57	57	7	12	3	21	27	4	15	3	22	15	-4	19	3	35	30	-1	5	4	28	24
-4	10	3	34	34	9	12	3	21	21	5	15	3	50	50	-3	19	3	19	14	0	5	4	21	16
-3	10	3	54	53	10	12	3	48	48	6	15	3	19	23	3	19	3	25	21	1	5	4	33	22
0	10	3	24	21	11	12	3	27	24	7	15	3	31	29	4	19	3	18	9	2	5	4	31	31
2	10	3	26	23	-12	13	3	56	56	15	15	3	23	23	-6	20	3	20	16	3	5	4	29	31
3	10	3	24	19	-6	13	3	27	29	-12	16	3	19	24	1	20	3	21	20	-4	6	4	25	27
4	10	3	39	40	-5	13	3	50	50	-9	16	3	25	23	2	20	3	19	4	-3	6	4	52	51
7	10	3	28	26	-3	13	3	29	26	-7	16	3	25	29	5	20	3	21	26	-2	6	4	45	44
9	10	3	17	18	-1	13	3	31	33	-4	16	3	30	30	-2	21	3	26	25	-1	6	4	38	36
9	10	3	28	26	1	13	3	50	51	-3	16	3	49	49	-1	21	3	27	27	0	6	4	28	23
10	10	3	18	13	3	13	3	50	49	-1	16	3	41	41	1	21	3	21	21	3	6	4	30	30
-8	11	3	19	19	4	13	3	39	39	0	16	3	32	25	0	0	4	62	62	5	6	4	23	19
-7	11	3	33	29	5	13	3	31	34	4	16	3	31	29	0	1	4	74	76	-6	7	4	43	44
-6	11	3	18	18	7	13	3	34	39	5	16	3	22	19	1	1	4	21	22	-5	7	4	34	35
-4	11	3	32	35	8	13	3	39	43	8	16	3	31	30	-1	2	4	21	23	-2	7	4	25	22
-3	11	3	32	34	12	13	3	31	32	9	16	3	25	24	0	2	4	67	64	-1	7	4	22	23
-2	11	3	29	28	13	13	3	25	19	14	16	3	19	14	1	2	4	64	67	2	7	4	38	38

continued..

APPENDIX A (continued)

OBSERVED AND CALCULATED STRUCTURE FACTORS FOR MG TPPIMIDAZOLE PAGE 5

H	K	L	FO	FC	H	K	L	FO	FC	H	K	L	FO	FC	H	K	L	FO	FC	H	K	L	FO	FC
3	7	4	19	15	5	10	4	36	37	4	14	4	25	28	7	17	4	20	22	-3	6	5	64	62
4	7	4	29	28	7	10	4	21	22	5	14	4	32	27	-10	18	4	21	27	-1	6	5	51	55
5	7	4	18	18	10	10	4	49	50	7	14	4	21	21	0	18	4	21	14	0	6	5	33	32
6	7	4	28	25	-9	11	4	43	44	8	14	4	52	54	3	16	4	24	15	1	6	5	28	24
-7	8	4	28	18	-8	11	4	18	15	9	14	4	28	24	7	18	4	25	20	2	6	5	17	17
-6	8	4	24	28	-4	11	4	27	28	11	14	4	30	31	-4	19	4	27	27	4	6	5	26	22
-5	8	4	23	23	-3	11	4	18	9	-10	15	4	21	22	0	19	4	22	28	6	6	5	16	17
-4	8	4	44	46	0	11	4	23	24	-9	15	4	22	14	2	19	4	25	25	-5	7	5	41	39
-3	8	4	20	19	3	11	4	25	25	-5	15	4	21	9	3	19	4	28	14	-3	7	5	41	44
-2	8	4	48	47	4	11	4	43	43	-3	15	4	24	19	8	19	4	22	9	-2	7	5	18	16
-1	8	4	33	36	6	11	4	25	25	-2	15	4	30	33	-5	20	4	29	31	-1	7	5	29	15
0	8	4	38	37	7	11	4	65	67	-1	15	4	21	19	-1	20	4	21	21	0	7	5	21	19
2	8	4	42	42	-11	12	4	18	11	0	15	4	36	38	0	1	5	35	36	1	7	5	21	23
4	8	4	19	20	-9	12	4	34	33	2	15	4	25	25	-1	2	5	34	34	2	7	5	52	52
5	8	4	32	30	-7	12	4	17	8	9	15	4	21	24	2	2	5	78	79	3	7	5	28	28
6	8	4	44	47	-6	12	4	28	28	13	15	4	21	16	-2	3	5	65	68	5	7	5	32	33
7	8	4	37	37	-4	12	4	20	22	-10	16	4	22	24	-1	3	5	54	55	-6	8	5	20	24
-8	9	4	30	30	-1	12	4	19	18	-9	16	4	29	31	0	3	5	42	43	-3	8	5	37	39
-7	9	4	19	12	0	12	4	25	27	-5	16	4	22	21	1	3	5	32	33	-2	8	5	37	38
-6	9	4	25	23	4	12	4	39	40	-2	16	4	21	24	2	3	5	57	59	0	8	5	29	29
-5	9	4	42	41	11	12	4	30	27	-1	16	4	27	25	3	3	5	64	65	2	8	5	33	33
-4	9	4	40	35	-11	13	4	24	21	1	16	4	21	16	-2	4	5	16	19	4	8	5	21	23
-3	9	4	38	35	-9	13	4	22	23	3	16	4	20	19	-1	4	5	70	71	5	8	5	18	33
1	9	4	37	38	-7	13	4	20	25	5	16	4	37	39	2	4	5	22	7	-7	9	5	27	28
4	9	4	19	15	3	13	4	38	35	10	16	4	20	15	3	4	5	20	19	-5	9	5	30	28
7	9	4	35	33	4	13	4	20	16	12	16	4	25	27	4	4	5	40	39	-1	9	5	23	23
-6	10	4	21	18	7	13	4	20	12	-9	17	4	22	24	-3	5	5	51	51	0	9	5	20	19
-5	10	4	40	41	8	13	4	19	20	-8	17	4	25	28	-2	5	5	29	35	1	9	5	25	24
-4	10	4	27	29	-12	14	4	31	29	-5	17	4	26	27	0	5	5	30	30	5	9	5	46	50
-3	10	4	20	21	-9	14	4	45	47	-4	17	4	18	19	1	5	5	28	30	7	9	5	46	50
-2	10	4	28	26	-4	14	4	18	17	-1	17	4	56	56	2	5	5	19	22	9	9	5	22	19
0	10	4	14	17	-1	14	4	18	14	1	17	4	19	20	4	5	5	42	39	-9	10	5	41	40
2	10	4	24	25	0	14	4	19	16	3	17	4	40	41	5	5	5	21	20	3	10	5	30	33
5	10	4	52	52	3	14	4	40	40	4	17	4	18	3	-5	6	5	33	33	4	10	5	20	21

OBSERVED AND CALCULATED STRUCTURE FACTORS FOR MG TPPIMIDAZOLE PAGE 6

H	K	L	FO	FC	H	K	L	FO	FC	H	K	L	FO	FC	H	K	L	FO	FC	H	K	L	FO	FC
7	10	5	26	27	8	13	5	45	51	1	1	6	33	33	-4	7	6	22	24	-7	12	6	23	25
8	10	5	43	46	-13	14	5	23	14	0	2	6	28	26	-3	7	6	17	10	-6	12	6	25	19
10	10	5	23	17	-9	14	5	28	18	1	2	6	34	34	2	7	6	28	24	-1	12	6	23	19
-10	11	5	23	24	-8	14	5	25	26	2	2	6	19	20	-4	8	6	22	19	0	12	6	20	22
-9	11	5	19	25	0	14	5	24	23	-2	3	6	43	44	-3	8	6	30	38	1	12	6	35	34
-7	11	5	30	28	1	14	5	36	36	-1	3	6	34	34	0	8	6	23	22	2	12	6	19	19
-5	11	5	43	42	6	14	5	24	23	0	3	6	30	33	2	8	6	26	29	3	12	6	24	23
-1	11	5	19	12	9	14	5	24	18	1	3	6	44	45	4	8	6	38	31	9	12	6	24	16
0	11	5	25	24	-11	15	5	29	27	2	3	6	46	50	5	8	6	28	22	13	12	6	20	13
2	11	5	23	25	-6	15	5	23	20	3	3	6	37	36	7	8	6	22	19	-11	13	6	33	29
5	11	5	17	14	-4	15	5	35	32	-3	4	6	32	33	-5	9	6	20	15	-3	13	6	18	15
7	11	5	30	32	0	15	5	39	40	-2	4	6	26	28	-1	9	6	19	20	0	13	6	19	20
8	11	5	27	28	6	15	5	24	27	-1	4	6	16	17	2	9	6	32	32	4	13	6	18	26
9	11	5	20	14	-7	16	5	29	33	1	4	6	21	10	3	9	6	26	26	5	13	6	31	29
10	11	5	21	20	-4	16	5	26	28	2	4	6	37	38	4	9	6	25	23	-1	14	6	21	11
-3	12	5	19	13	0	16	5	25	27	3	4	6	34	41	9	9	6	25	20	2	14	6	21	27
-2	12	5	27	25	4	16	5	30	31	4	4	6	59	61	-9	10	6	18	19	9	14	6	25	26
-1	12	5	30	31	5	16	5	23	23	-4	5	6	25	23	-4	10	6	25	23	10	14	6	20	22
0	12	5	27	27	-8	17	5	25	28	-3	5	6	24	23	-2	10	6	26	29	-9	15	6	22	9
5	12	5	19	22	-5	17	5	20	14	-2	5	6	16	13	1	10	6	20	22	-8	15	6	24	17
6	12	5	32	27	0	17	5	23	16	-1	5	6	23	22	2	10	6	23	17	-4	16	6	27	21
8	12	5	22	26	2	17	5	20	22	0	5	6	27	28	3	10	6	19	10	-2	16	6	38	37
9	12	5	23	28	3	17	5	23	17	1	5	6	17	15	4	10	6	35	35	-1	16	6	26	29
10	12	5	27	26	6	17	5	21	17	2	5	6	29	32	6	10	6	18	4	2	16	6	21	18
11	12	5	24	26	8	17	5	20	17	4	5	6	21	14	7	10	6	21	16	3	16	6	23	24
-12	13	5	29	34	-3	18	5	25	26	5	5	6	20	16	10	10	6	26	24	4	16	6	27	29
-6	13	5	29	30	-2	18	5	18	17	-4	6	6	29	28	-6	11	6	20	29	7	16	6	20	9
-5	13	5	22	26	2	18	5	19	19	-3	6	6	20	22	0	11	6	40	40	-1	17	6	19	18
-4	13	5	19	11	3	18	5	20	17	-2	6	6	24	19	3	11	6	29	26	0	17	6	16	16
1	13	5	20	16	-4	19	5	20	14	0	6	6	24	28	4	11	6	28	33	-2	18	6	25	23
2	13	5	21	22	0	19	5	18	16	2	6	6	20	18	5	11	6	24	16	0	18	6	31	31
3	13	5	29	26	3	19	5	20	16	4	6	6	17	9	7	11	6	24	24	2	18	6	30	34
4	13	5	33	33	5	19	5	20	21	5	6	6	21	19	8	11	6	28	26	0	1	7	16	16
6	13	5	45	49	0	0	6	53	48	-6	7	6	17	19	11	11	6	29	25	1	1	7	24	22

continued..

APPENDIX A (continued)

OBSERVED AND CALCULATED STRUCTURE FACTORS FOR MG TPPIMIDAZOLE PAGE 7

H	K	L	FO	FC	H	K	L	FO	FC	H	K	L	FO	FC	H	K	L	FO	FC	H	K	L	FO	FC
0	2	7	15	20	5	9	7	20	16	5	13	7	20	18	2	6	8	43	40	-6	13	8	25	29
0	3	7	22	21	8	9	7	35	36	-6	14	7	19	18	3	6	8	20	22	0	14	8	18	18
1	3	7	27	21	-3	10	7	18	15	-5	15	7	23	20	4	6	8	24	28	1	1	9	21	24
2	3	7	49	52	2	10	7	20	19	-3	15	7	27	32	5	6	8	20	15	-1	2	9	19	22
3	3	7	38	38	3	10	7	32	39	3	15	7	22	21	0	7	8	25	23	2	3	9	24	25
0	4	7	15	19	5	10	7	21	25	-2	16	7	20	2	4	7	8	31	28	3	3	9	37	37
1	4	7	21	20	-9	11	7	27	24	0	2	8	24	22	-3	8	8	22	20	3	4	9	34	35
3	4	7	33	34	-8	11	7	31	33	0	3	8	54	60	0	8	8	15	13	-3	5	9	31	32
-3	5	7	26	26	-5	11	7	29	29	2	3	8	27	33	2	8	8	28	34	1	5	9	20	15
0	5	7	22	23	-3	11	7	28	27	3	3	8	37	40	3	8	8	28	26	3	5	9	26	22
4	5	7	19	13	-1	11	7	25	22	-2	4	8	31	34	4	8	8	29	26	5	5	9	25	25
-5	6	7	27	24	1	11	7	27	31	-1	4	8	31	34	7	8	8	20	19	-1	6	9	22	21
1	6	7	31	28	4	11	7	28	23	2	4	8	38	38	-8	9	8	37	35	2	7	9	28	27
2	6	7	32	30	5	11	7	27	24	3	4	8	27	24	0	10	8	28	31	3	7	9	22	23
4	6	7	18	13	9	11	7	30	31	4	4	8	41	43	4	10	8	21	23	-5	8	9	21	17
5	6	7	29	25	11	11	7	31	31	-3	5	8	33	40	8	10	8	23	22	3	8	9	19	15
3	7	7	19	25	-10	12	7	24	24	1	5	8	29	32	10	10	8	26	25	-1	9	9	20	13
5	7	7	19	13	-3	12	7	20	21	4	5	8	25	29	-7	11	8	29	34	-5	10	9	23	23
6	7	7	25	23	1	12	7	22	19	-5	6	8	19	16	-4	11	8	23	20	3	10	9	26	25
0	8	7	25	27	4	12	7	30	27	-4	6	8	24	26	6	11	8	28	26	2	2	10	19	13
1	8	7	28	23	-9	13	7	24	23	-2	6	8	24	26	-7	12	8	20	15	0	3	10	22	21
3	8	7	26	25	3	13	7	19	23	0	6	8	17	17	5	12	8	22	24	4	4	10	26	28
4	8	7	26	24	4	13	7	19	20															

APPENDIX B

OBSERVED AND CALCULATED STRUCTURE FACTORS FOR MGTPP(4-METHYLPYRIDINE) OCC PAGE 1

H	K	L	FO	FC	H	K	L	FO	FC	H	K	L	FO	FC	H	K	L	FO	FC	H	K	L	FO	FC
1	0	0	54	50	1	2	0	25	23	4	4	0	17	17	4	7	0	5	5	2	11	0	4	4
2	0	0	7	6	2	2	0	64	61	5	4	0	27	27	5	7	0	6	7	3	11	0	5	6
3	0	0	7	8	3	2	0	45	43	6	4	0	19	19	6	7	0	6	5	4	11	0	7	7
4	0	0	8	9	4	2	0	24	24	9	4	0	6	6	8	7	0	10	10	5	11	0	4	1
7	0	0	9	8	5	2	0	16	17	10	4	0	5	4	9	7	0	5	3	-6	-11	1	5	6
8	0	0	13	14	6	2	0	5	6	11	4	0	7	7	10	7	0	4	4	-4	-11	1	9	11
9	0	0	8	8	7	2	0	17	17	-6	5	0	4	4	-3	8	0	6	6	-7	-10	1	6	6
10	0	0	7	7	9	2	0	14	14	-5	5	0	4	3	-2	8	0	5	5	-6	-10	1	7	7
-9	1	0	5	3	11	2	0	5	5	-3	5	0	5	6	-1	8	0	5	6	-4	-10	1	10	10
-8	1	0	9	10	-8	3	0	6	5	-2	5	0	6	5	0	8	0	19	19	-3	-10	1	11	12
-7	1	0	4	4	-7	3	0	7	8	-1	5	0	9	9	1	8	0	4	2	-2	-10	1	5	4
-5	1	0	13	14	-6	3	0	5	6	0	5	0	5	5	2	8	0	11	12	-1	-10	1	5	6
-4	1	0	11	10	-5	3	0	11	12	1	5	0	35	32	3	8	0	11	12	0	-10	1	6	4
-2	1	0	26	25	-4	3	0	7	8	2	5	0	22	22	4	8	0	13	13	-7	-9	1	9	9
-1	1	0	22	21	-3	3	0	21	21	3	5	0	26	26	5	8	0	4	2	-6	-9	1	7	7
0	1	0	57	54	-2	3	0	7	8	5	5	0	12	12	6	8	0	5	6	-5	-9	1	4	4
1	1	0	34	33	-1	3	0	27	25	6	5	0	5	5	7	8	0	9	10	-4	-9	1	4	4
2	1	0	5	6	0	3	0	10	12	7	5	0	6	6	8	8	0	8	7	-3	-9	1	7	6
3	1	0	31	31	1	3	0	5	6	9	5	0	5	3	-2	9	0	5	5	-2	-9	1	8	9
4	1	0	32	32	2	3	0	32	32	-5	6	0	4	4	-1	9	0	6	5	-1	-9	1	4	3
5	1	0	28	28	3	3	0	7	7	-2	6	0	8	8	0	9	0	5	4	1	-9	1	8	9
6	1	0	4	3	5	3	0	4	3	-1	6	0	4	3	3	9	0	5	5	2	-9	1	6	5
7	1	0	18	16	6	3	0	4	3	1	6	0	6	5	4	9	0	13	13	4	-9	1	5	4
8	1	0	6	4	8	3	0	4	3	2	6	0	18	18	5	9	0	10	11	-7	-8	1	8	9
9	1	0	12	12	-7	4	0	5	6	3	6	0	18	18	6	9	0	4	1	-6	-8	1	8	9
10	1	0	5	4	-6	4	0	16	16	4	6	0	8	7	7	9	0	16	16	-5	-8	1	9	10
-8	2	0	7	7	-5	4	0	4	3	5	6	0	7	6	8	9	0	6	7	-2	-8	1	6	7
-7	2	0	12	12	-3	4	0	13	13	8	6	0	10	11	9	9	0	4	3	-1	-8	1	5	5
-6	2	0	5	6	-2	4	0	15	16	9	6	0	7	6	-1	10	0	4	4	0	-8	1	9	9
-5	2	0	8	8	-1	4	0	12	13	-5	7	0	8	9	3	10	0	6	4	1	-8	1	8	9
-4	2	0	8	8	0	4	0	12	12	-3	7	0	12	12	5	10	0	13	13	2	-8	1	5	5
-2	2	0	11	13	1	4	0	7	7	0	7	0	7	8	7	10	0	6	4	4	-8	1	6	7
-1	2	0	44	41	2	4	0	16	13	1	7	0	5	5	0	11	0	5	4	-9	-7	1	4	4
0	2	0	32	32	3	4	0	32	29	2	7	0	8	7	1	11	0	6	6	-7	-7	1	8	10

OBSERVED AND CALCULATED STRUCTURE FACTORS FOR MGTPP(4-METHYLPYRIDINE) OCC PAGE 2

H	K	L	FO	FC	H	K	L	FO	FC	H	K	L	FO	FC	H	K	L	FO	FC	H	K	L	FO	FC
-6	-7	1	5	3	-5	-3	1	8	7	-1	-1	1	22	23	3	1	1	11	9	7	3	1	10	10
-5	-7	1	4	3	-4	-3	1	50	50	0	-1	1	26	24	4	1	1	18	17	8	3	1	11	12
-4	-7	1	9	9	-2	-3	1	15	13	1	-1	1	166	152	5	1	1	8	7	10	3	1	5	5
-3	-7	1	8	7	-1	-3	1	4	6	2	-1	1	50	49	7	1	1	4	5	-7	4	1	4	4
-2	-7	1	18	18	1	-3	1	55	54	3	-1	1	41	41	8	1	1	14	15	-6	4	1	13	12
3	-7	1	10	8	2	-3	1	32	29	4	-1	1	13	14	10	1	1	5	5	-5	4	1	7	6
-10	-6	1	5	6	5	-3	1	9	9	6	-1	1	4	3	11	1	1	5	5	-4	4	1	8	9
-9	-6	1	12	11	7	-3	1	6	5	7	-1	1	5	5	-5	2	1	8	8	-3	4	1	7	8
-7	-6	1	7	6	-9	-2	1	6	6	9	-1	1	5	6	-5	2	1	11	11	-2	4	1	7	9
-4	-6	1	6	6	-8	-2	1	22	23	10	-1	1	5	5	-4	2	1	7	6	-1	4	1	34	32
-3	-6	1	23	21	-7	-2	1	13	12	-9	0	1	5	7	-3	2	1	7	8	1	4	1	22	23
-2	-6	1	29	26	-6	-2	1	28	27	-7	0	1	24	25	-2	2	1	10	10	3	4	1	22	22
-1	-6	1	19	21	-5	-2	1	27	29	-6	0	1	7	7	-1	2	1	49	48	4	4	1	34	34
0	-6	1	16	14	-4	-2	1	4	5	-5	0	1	17	16	0	2	1	27	28	8	4	1	9	9
-8	-5	1	7	7	-3	-2	1	35	32	-4	0	1	24	22	1	2	1	44	43	9	4	1	6	4
-6	-5	1	9	9	-2	-2	1	23	24	-3	0	1	10	9	2	2	1	99	99	11	4	1	5	4
-5	-5	1	5	4	-1	-2	1	23	22	-2	0	1	78	74	3	2	1	34	34	-6	5	1	4	4
-3	-5	1	8	6	0	-2	1	7	8	0	0	1	47	43	4	2	1	14	13	-5	5	1	11	10
-2	-5	1	7	6	1	-2	1	99	93	1	0	1	45	42	5	2	1	7	7	-4	5	1	8	8
-1	-5	1	4	3	2	-2	1	74	70	2	0	1	9	8	6	2	1	7	6	-3	5	1	9	9
0	-5	1	5	7	3	-2	1	15	15	3	0	1	36	35	7	2	1	7	6	-1	5	1	14	12
2	-5	1	5	3	4	-2	1	4	5	4	0	1	11	10	8	2	1	7	8	0	5	1	8	7
-9	-4	1	5	5	5	-2	1	8	8	5	0	1	8	7	10	2	1	5	6	1	5	1	3	3
-8	-4	1	14	15	6	-2	1	7	6	7	0	1	4	2	-5	3	1	22	22	2	5	1	9	10
-7	-4	1	5	6	7	-2	1	13	12	8	0	1	9	9	-4	3	1	15	13	3	5	1	8	7
-6	-4	1	7	7	8	-2	1	7	7	10	0	1	8	8	-3	3	1	23	23	4	5	1	24	25
-5	-4	1	6	6	10	-2	1	8	6	-7	1	1	6	5	-2	3	1	26	26	5	5	1	17	16
-4	-4	1	8	7	-9	-1	1	12	11	-5	1	1	5	6	-1	3	1	5	6	10	5	1	8	8
-3	-4	1	17	14	-8	-1	1	11	12	-4	1	1	8	7	0	3	1	28	26	-5	6	1	10	10
-2	-4	1	13	14	-7	-1	1	21	21	-3	1	1	4	3	2	3	1	11	10	-4	6	1	9	9
2	-4	1	23	23	-5	-1	1	15	13	-1	1	1	59	56	3	3	1	11	11	-3	6	1	4	5
5	-4	1	7	6	-4	-1	1	19	20	0	1	1	46	44	4	3	1	34	34	-2	6	1	6	6
-8	-3	1	13	14	-3	-1	1	20	19	1	1	1	8	7	5	3	1	21	20	-1	6	1	15	15
-6	-3	1	6	6	-2	-1	1	51	49	2	1	1	49	47	6	3	1	13	13	0	6	1	8	9

continued..

APPENDIX B (continued)

OBSERVED AND CALCULATED STRUCTURE FACTORS FOR MGTPP(4-METHYLPYRIDINE) OCC PAGE 3

H	K	L	FO	FC	H	K	L	FO	FC	H	K	L	FO	FC	H	K	L	FO	FC	H	K	L	FO	FC
1	5	1	20	19	-1	10	1	5	5	-5	-6	2	4	2	3	-3	2	32	32	-9	0	2	11	12
2	6	1	13	15	0	10	1	7	7	-4	-6	2	10	11	5	-3	2	9	9	-6	0	2	9	9
3	6	1	6	6	1	10	1	9	9	-1	-6	2	7	7	6	-3	2	5	5	-5	0	2	6	5
4	5	1	20	19	2	10	1	14	12	0	-6	2	11	12	9	-3	2	9	9	-4	0	2	3	1
5	6	1	12	13	5	10	1	5	6	1	-6	2	4	5	-8	-2	2	10	9	-3	0	2	26	26
6	5	1	6	5	7	10	1	6	5	4	-5	2	7	8	-7	-2	2	7	7	-2	0	2	13	13
8	5	1	19	17	1	11	1	6	6	-7	-5	2	5	4	-6	-2	2	10	9	-1	0	2	54	53
9	5	1	10	9	2	11	1	11	10	-6	-5	2	5	7	-5	-2	2	9	9	0	0	2	43	44
-7	7	1	6	5	4	11	1	6	6	-5	-5	2	8	9	-4	-2	2	20	19	1	0	2	30	29
-4	7	1	9	9	5	11	1	5	5	-4	-5	2	7	8	-2	-2	2	30	30	3	0	2	8	9
-1	7	1	5	5	6	12	1	5	5	-1	-5	2	4	3	-1	-2	2	7	3	4	0	2	38	38
1	7	1	31	28	-5	-11	2	6	5	3	-5	2	7	7	0	-2	2	47	44	5	0	2	10	10
2	7	1	8	9	-5	-10	2	9	8	5	-5	2	5	6	1	-2	2	35	33	6	0	2	9	9
4	7	1	8	6	-5	-10	2	6	6	-8	-4	2	7	5	2	-2	2	81	76	-9	1	2	5	3
5	7	1	13	14	-2	-10	2	9	8	-7	-4	2	20	21	3	-2	2	32	33	-7	1	2	13	14
7	7	1	9	9	-5	-9	2	9	7	-6	-4	2	16	17	4	-2	2	25	26	-6	1	2	5	5
8	7	1	7	7	-4	-9	2	7	9	-5	-4	2	10	8	5	-2	2	5	5	-5	1	2	9	9
9	7	1	15	15	-2	-9	2	5	6	-4	-4	2	10	12	-9	-1	2	5	5	-4	1	2	9	10
-1	8	1	5	3	-8	-9	2	5	5	-3	-4	2	24	22	-8	-1	2	9	11	-3	1	2	14	14
0	8	1	13	13	-7	-8	2	6	5	-1	-4	2	9	11	-6	-1	2	10	10	-2	1	2	17	17
4	8	1	12	12	-6	-8	2	7	7	0	-4	2	23	22	-5	-1	2	12	12	-1	1	2	54	53
5	8	1	11	10	-5	-8	2	8	8	1	-4	2	17	17	-4	-1	2	35	35	0	1	2	17	17
6	8	1	7	5	-4	-8	2	4	5	2	-4	2	24	24	-3	-1	2	25	24	1	1	2	60	59
8	8	1	6	7	-1	-8	2	15	15	3	-4	2	21	21	-2	-1	2	30	29	2	1	2	48	44
9	8	1	12	13	0	-8	2	9	9	5	-4	2	6	5	-1	-1	2	49	48	3	1	2	4	3
9	8	1	5	6	-4	-7	2	9	8	-8	-3	2	12	12	0	-1	2	25	25	4	1	2	8	8
10	8	1	5	5	-3	-7	2	6	5	-7	-3	2	13	13	1	-1	2	44	45	5	1	2	12	11
-4	9	1	5	5	-2	-7	2	6	6	-6	-3	2	37	37	2	-1	2	52	57	7	1	2	6	6
0	9	1	9	10	0	-7	2	9	9	-5	-3	2	30	28	3	-1	2	12	12	8	1	2	5	4
1	9	1	7	6	3	-7	2	5	4	-4	-3	2	25	25	4	-1	2	8	8	-8	2	2	5	6
2	9	1	7	8	5	-7	2	5	5	-2	-3	2	4	5	5	-1	2	8	7	-7	2	2	8	8
4	9	1	10	10	-9	-6	2	7	8	0	-3	2	12	10	6	-1	2	9	9	-6	2	2	6	7
5	9	1	8	9	-8	-6	2	5	4	1	-3	2	18	15	7	-1	2	8	8	-5	2	2	21	19
8	9	1	6	6	-6	-6	2	5	6	2	-3	2	45	45	9	-1	2	11	11	-4	2	2	35	33

OBSERVED AND CALCULATED STRUCTURE FACTORS FOR MGTPP(4-METHYLPYRIDINE) OCC PAGE 4

H	K	L	FO	FC	H	K	L	FO	FC	H	K	L	FO	FC	H	K	L	FO	FC	H	K	L	FO	FC
-3	2	2	14	14	3	4	2	28	27	1	7	2	14	15	4	12	2	8	7	-7	-4	3	25	27
-1	2	2	4	4	4	4	2	14	15	2	7	2	15	15	6	12	2	5	4	-6	-4	3	15	15
0	2	2	54	52	5	4	2	17	17	4	7	2	15	14	-1	-10	3	4	2	-5	-4	3	20	19
1	2	2	19	19	6	4	2	9	10	5	7	2	12	11	-4	-9	3	6	6	-4	-4	3	13	13
2	2	2	53	53	9	4	2	9	8	6	7	2	10	10	-7	-8	3	5	5	-3	-4	3	11	11
4	2	2	17	18	10	4	2	7	7	7	7	2	5	7	-5	-8	3	5	5	-2	-4	3	6	5
5	2	2	6	6	11	4	2	5	6	9	7	2	14	13	-2	-8	3	5	6	-1	-4	3	10	10
8	2	2	6	7	-7	5	2	5	5	10	7	2	7	7	-1	-8	3	7	6	1	-4	3	5	6
10	2	2	7	7	-4	5	2	5	5	-4	8	2	7	7	0	-8	3	5	5	3	-4	3	27	27
-2	3	2	5	5	-3	5	2	12	12	-2	8	2	10	10	-5	-7	3	5	5	4	-4	3	18	19
-1	3	2	5	5	-1	5	2	19	19	-1	8	2	5	4	-4	-7	3	7	7	5	-4	3	9	9
0	3	2	16	16	0	5	2	20	21	0	8	2	4	5	-3	-7	3	12	13	-9	-3	3	4	5
-4	3	2	7	8	1	5	2	7	7	1	8	2	10	10	-2	-7	3	9	9	-8	-3	3	8	8
-3	3	2	20	21	2	5	2	12	12	2	8	2	13	12	0	-7	3	13	12	-6	-3	3	14	15
-2	3	2	6	7	3	5	2	5	5	3	8	2	9	10	1	-7	3	4	2	-5	-3	3	12	12
-1	3	2	15	14	4	5	2	20	21	5	8	2	13	13	2	-7	3	4	4	-4	-3	3	13	14
0	3	2	42	42	5	5	2	8	8	6	8	2	7	7	-7	-6	3	4	5	-3	-3	3	7	6
1	3	2	54	53	6	5	2	8	8	7	8	2	11	12	-5	-6	3	9	9	-2	-3	3	20	19
2	3	2	18	18	7	5	2	7	6	8	8	2	5	5	-4	-6	3	11	11	-1	-3	3	6	6
3	3	2	15	15	8	5	2	20	20	9	8	2	4	4	-3	-6	3	16	15	0	-3	3	11	11
4	3	2	7	6	9	5	2	12	12	10	8	2	4	4	-1	-6	3	7	8	1	-3	3	22	22
5	3	2	35	36	10	5	2	7	7	0	9	2	7	7	0	-6	3	11	11	2	-3	3	5	4
6	3	2	17	17	-6	6	2	6	6	3	9	2	8	9	1	-6	3	6	6	3	-3	3	52	52
7	3	2	8	8	-4	6	2	16	17	4	9	2	10	10	3	-6	3	6	6	4	-3	3	18	18
8	3	2	6	7	-1	6	2	6	6	8	10	2	6	6	4	-6	3	9	9	5	-3	3	5	4
-7	4	2	9	9	0	6	2	10	9	9	10	2	5	6	-10	-5	3	6	6	6	-3	3	8	7
-5	4	2	4	6	1	6	2	17	18	3	10	2	15	14	-9	-5	3	6	6	7	-3	3	5	6
-4	4	2	8	8	2	6	2	33	33	3	10	2	6	5	-6	-5	3	11	11	-7	-2	3	4	3
-3	4	2	13	13	4	6	2	8	9	8	10	2	5	5	-5	-5	3	9	10	-5	-2	3	5	6
-2	4	2	5	5	5	6	2	9	9	2	11	2	7	6	-4	-5	3	22	21	-4	-2	3	11	11
-1	4	2	4	4	6	6	2	18	18	3	11	2	10	10	-3	-5	3	9	9	-3	-2	3	20	18
0	4	2	19	20	8	6	2	5	6	5	11	2	10	9	1	-5	3	9	9	-2	-2	3	12	13
1	4	2	23	23	10	6	2	6	6	6	11	2	7	8	2	-5	3	4	4	-1	-2	3	9	9
2	4	2	7	7	-4	7	2	7	7	7	11	2	5	6	4	-5	3	15	15	0	-2	3	22	23

continued..

APPENDIX B (continued)

OBSERVED AND CALCULATED STRUCTURE FACTORS FOR MGTPP(4-METHYLPYRIDINE) OCC PAGE 5

H	K	L	FO	FC	H	K	L	FO	FC	H	K	L	FO	FC	H	K	L	FO	FC	H	K	L	FO	FC
1	-2	3	10	10	-8	1	3	6	7	0	3	3	49	48	7	5	3	9	10	6	8	3	5	4
2	-2	3	41	41	-6	1	3	7	7	1	3	3	22	22	9	5	3	9	10	-2	9	3	6	6
3	-2	3	15	15	-5	1	3	7	8	3	3	3	21	20	10	5	3	6	7	-1	9	3	6	5
4	-2	3	4	4	-3	1	3	36	36	4	3	3	19	19	11	5	3	7	7	0	9	3	9	9
7	-2	3	18	18	-2	1	3	22	22	5	3	3	19	20	-5	6	3	4	5	1	9	3	8	9
8	-2	3	5	4	0	1	3	65	63	6	3	3	8	7	-4	6	3	5	4	3	9	3	22	22
10	-2	3	4	3	1	1	3	55	55	7	3	3	5	6	-3	6	3	9	10	4	9	3	10	10
11	-1	3	4	3	2	1	3	45	44	8	3	3	7	7	-2	6	3	5	5	5	9	3	10	9
-8	-1	3	7	7	3	1	3	3	3	11	3	3	5	4	-1	6	3	12	11	7	9	3	5	6
-6	-1	3	7	7	4	1	3	5	5	-8	4	3	6	6	0	6	3	6	5	8	9	3	7	7
-5	-1	3	15	15	5	1	3	9	8	-7	4	3	9	9	2	6	3	9	9	-2	10	3	6	6
-4	-1	3	16	17	6	1	3	13	13	-5	4	3	6	6	3	6	3	6	6	-1	10	3	7	7
-3	-1	3	7	6	7	1	3	9	9	-3	4	3	19	19	4	6	3	5	5	1	10	3	7	7
-1	-1	3	17	18	-9	2	3	6	6	-2	4	3	31	31	6	6	3	12	12	4	10	3	14	14
1	-1	3	4	4	-5	2	3	6	6	0	4	3	23	23	7	6	3	28	28	5	10	3	13	12
3	-1	3	16	16	-4	2	3	14	14	1	4	3	15	15	8	6	3	11	11	6	10	3	10	10
4	-1	3	4	3	-3	2	3	7	7	2	4	3	9	10	10	6	3	6	5	7	10	3	10	11
5	-1	3	4	4	-1	2	3	23	23	3	4	3	19	18	11	6	3	7	7	8	10	3	5	4
7	-1	3	19	19	0	2	3	38	37	4	4	3	11	12	-6	7	3	7	6	-2	11	3	5	5
-8	0	3	6	7	1	2	3	97	91	9	4	3	12	13	-5	7	3	4	4	2	11	3	5	5
-6	0	3	4	4	2	2	3	4	5	10	4	3	7	6	-1	7	3	12	12	3	11	3	9	10
-4	0	3	8	9	3	2	3	11	10	11	4	3	7	7	0	7	3	10	10	4	11	3	11	11
-3	0	3	34	34	4	2	3	35	35	-7	5	3	8	6	2	7	3	18	18	5	11	3	8	7
-2	0	3	6	7	5	2	3	32	32	-6	5	3	8	8	3	7	3	4	3	8	11	3	6	6
-1	0	3	26	25	7	2	3	19	19	-5	5	3	5	6	5	7	3	11	11	2	12	3	5	5
0	0	3	19	19	8	2	3	5	4	-4	5	3	11	11	6	7	3	10	10	5	12	3	6	5
1	0	3	25	24	-9	3	3	5	5	-3	5	3	28	27	8	7	3	12	12	4	13	3	5	4
2	0	3	55	53	-8	3	3	6	6	0	5	3	22	23	-4	8	3	5	5	5	13	3	6	7
3	0	3	6	5	-6	3	3	6	7	1	5	3	27	26	-1	8	3	4	4	-5	-8	4	5	6
4	0	3	4	3	-5	3	3	6	5	2	5	3	22	22	0	8	3	4	5	-3	-8	4	5	4
5	0	3	17	17	-4	3	3	9	10	3	5	3	47	47	1	8	3	5	4	-2	-8	4	10	10
7	0	3	4	4	-3	3	3	9	11	4	5	3	17	17	3	8	3	5	6	-1	-8	4	6	5
9	0	3	7	7	-2	3	3	9	9	5	5	3	7	7	4	8	3	15	16	0	-8	4	4	3
11	0	3	5	5	-1	3	3	11	12	6	5	3	8	8	5	8	3	8	8	-4	-7	4	6	6

OBSERVED AND CALCULATED STRUCTURE FACTORS FOR MGTPP(4-METHYLPYRIDINE) OCC PAGE 6

H	K	L	FO	FC	H	K	L	FO	FC	H	K	L	FO	FC	H	K	L	FO	FC	H	K	L	FO	FC
-2	-7	4	4	3	2	-3	4	14	14	-3	0	4	5	7	-3	2	4	4	3	2	4	4	21	21
-9	-6	4	5	5	3	-3	4	4	5	-2	0	4	37	35	-2	2	4	9	10	3	4	4	35	35
-7	-6	4	4	4	4	-3	4	16	16	-1	0	4	13	12	-1	2	4	9	9	4	4	4	49	46
-6	-6	4	5	3	-9	-2	4	5	4	0	0	4	22	23	0	2	4	20	20	5	4	4	5	4
-5	-6	4	16	17	-7	-2	4	7	7	1	0	4	12	12	1	2	4	29	31	9	4	4	10	10
-4	-6	4	10	10	-6	-2	4	4	5	2	0	4	6	5	2	2	4	23	24	10	4	4	5	5
-3	-6	4	14	15	-5	-2	4	14	15	3	0	4	6	7	3	2	4	5	5	-8	5	4	6	6
-1	-6	4	19	19	-4	-2	4	6	6	4	0	4	9	10	4	2	4	11	12	-5	5	4	7	6
0	-6	4	8	8	-3	-2	4	12	12	5	0	4	9	9	5	2	4	12	13	-3	5	4	10	10
2	-6	4	6	6	-2	-2	4	7	6	6	0	4	8	7	6	2	4	11	11	-2	5	4	12	12
5	-6	4	8	8	-1	-2	4	11	11	7	0	4	9	9	7	2	4	12	12	-1	5	4	12	12
-7	-5	4	8	8	0	-2	4	10	10	9	0	4	11	11	8	2	4	5	4	0	5	4	31	31
-6	-5	4	9	9	1	-2	4	15	14	-9	1	4	5	3	-9	3	4	5	4	1	5	4	21	19
-5	-5	4	19	19	2	-2	4	3	3	-8	1	4	6	6	-7	3	4	12	12	2	5	4	33	33
-3	-5	4	24	24	3	-2	4	20	20	-6	1	4	5	5	-6	3	4	10	10	3	5	4	8	8
-2	-5	4	4	2	4	-2	4	6	7	-5	1	4	7	7	-5	3	4	12	12	4	5	4	12	12
4	-5	4	17	17	5	-2	4	11	12	-4	1	4	4	4	-4	3	4	4	3	5	5	4	6	6
5	-5	4	14	14	9	-2	4	5	5	-3	1	4	26	25	-2	3	4	25	25	6	5	4	5	5
-8	-4	4	4	2	-9	-1	4	7	6	-2	1	4	18	18	-1	3	4	29	28	7	5	4	18	19
-5	-4	4	7	7	-5	-1	4	4	3	-1	1	4	27	26	1	3	4	10	11	8	5	4	15	14
-4	-4	4	11	11	-4	-1	4	9	8	0	1	4	15	15	2	3	4	42	42	9	5	4	6	6
-3	-4	4	11	11	-3	-1	4	4	4	1	1	4	19	19	3	3	4	5	5	11	5	4	7	7
0	-4	4	9	9	-2	-1	4	25	26	2	1	4	5	5	4	3	4	18	19	-6	6	4	4	4
1	-4	4	10	11	-1	-1	4	6	7	3	1	4	27	26	5	3	4	5	4	-5	6	4	12	11
3	-4	4	13	13	0	-1	4	5	4	4	1	4	17	16	6	3	4	15	13	-4	6	4	7	7
4	-4	4	32	33	1	-1	4	11	11	5	1	4	30	29	7	3	4	4	4	-3	6	4	5	5
5	-4	4	10	11	2	-1	4	7	7	6	1	4	13	14	10	3	4	7	6	-1	6	4	14	14
-7	-3	4	6	7	3	-1	4	19	19	7	1	4	15	15	-8	4	4	5	6	0	6	4	14	15
-6	-3	4	4	4	4	-1	4	18	18	-9	2	4	5	6	-6	4	4	4	3	1	6	4	17	16
-5	-3	4	4	1	5	-1	4	10	10	-8	2	4	10	11	-5	4	4	12	12	2	6	4	8	9
-4	-3	4	16	16	8	-1	4	10	10	-7	2	4	11	11	-2	4	4	22	21	4	6	4	4	4
-1	-3	4	14	14	-7	0	4	6	6	-6	2	4	7	6	-1	4	4	24	24	5	6	4	4	4
0	-3	4	8	9	-5	0	4	6	6	-5	2	4	14	14	0	4	4	41	40	8	6	4	4	5
1	-3	4	4	4	-4	0	4	23	23	-4	2	4	5	6	1	4	4	26	27	9	6	4	16	16

continued..

APPENDIX B (continued)

OBSERVED AND CALCULATED STRUCTURE FACTORS FOR MGTPP(4-METHYLPYRIDINE) ODC PAGE 7

H	K	L	FO	FC	H	K	L	FO	FC	H	K	L	FO	FC	H	K	L	FO	FC	H	K	L	FO	FC
-5	7	4	13	13	6	10	4	6	7	-8	-4	5	7	7	-1	-1	5	34	33	5	1	5	5	5
-4	7	4	8	8	7	10	4	8	8	-6	-4	5	6	7	0	-1	5	12	12	6	1	5	7	6
-3	7	4	10	10	8	10	4	4	4	-4	-4	5	7	7	1	-1	5	35	35	7	1	5	5	5
0	7	4	5	5	-1	11	4	7	8	-3	-4	5	19	19	2	-1	5	15	15	-9	2	5	6	5
2	7	4	13	12	3	11	4	7	8	-2	-4	5	5	5	3	-1	5	5	5	-8	2	5	7	7
3	7	4	5	7	4	11	4	15	15	-1	-4	5	7	7	4	-1	5	11	11	-5	2	5	6	6
4	7	4	7	8	5	12	4	5	6	0	-4	5	10	10	5	-1	5	8	9	-4	2	5	17	18
5	7	4	27	27	6	12	4	12	12	3	-4	5	6	7	7	-1	5	11	11	-3	2	5	9	9
6	7	4	20	19	7	12	4	6	6	4	-4	5	8	8	8	-1	5	13	13	-2	2	5	15	17
7	7	4	5	5	8	12	4	6	5	5	-4	5	10	11	-8	0	5	8	7	-1	2	5	32	32
-8	8	4	6	6	-9	-9	5	5	5	-8	-4	5	8	8	-7	0	5	19	19	0	2	5	46	47
-6	8	4	4	3	-1	-8	5	5	4	-7	-3	5	5	5	-5	0	5	6	6	1	2	5	4	6
-3	8	4	6	5	-8	-7	5	5	4	-5	-3	5	10	10	-4	0	5	4	4	2	2	5	22	22
-2	8	4	11	11	-4	-7	5	9	9	-4	-3	5	10	10	-2	0	5	10	10	3	2	5	5	6
-1	8	4	18	19	-3	-7	5	8	7	-1	-3	5	7	7	-1	0	5	16	16	4	2	5	5	4
0	8	4	19	19	-1	-7	5	6	7	0	-3	5	9	8	0	0	5	21	21	5	2	5	15	15
1	8	4	19	18	0	-7	5	7	8	2	-3	5	8	8	2	0	5	19	20	6	2	5	8	9
2	8	4	18	19	-5	-6	5	7	6	3	-3	5	9	8	3	0	5	17	18	9	2	5	5	4
4	8	4	15	15	-4	-6	5	18	18	4	-3	5	11	11	4	0	5	12	11	-8	3	5	5	5
5	8	4	7	7	-3	-6	5	6	6	5	-3	5	12	13	5	0	5	4	3	-7	3	5	6	6
7	8	4	9	9	-2	-6	5	14	13	6	-3	5	6	6	6	0	5	5	5	-6	3	5	12	11
9	8	4	17	17	0	-6	5	7	9	-6	-3	5	7	7	8	0	5	4	5	-3	3	5	13	13
0	9	4	9	8	1	-6	5	11	12	-1	-2	5	10	10	9	0	5	6	6	-1	3	5	17	15
3	9	4	11	10	-6	-5	5	9	9	0	-2	5	5	5	-8	1	5	10	10	-2	3	5	21	19
4	9	4	12	12	-5	-5	5	6	6	1	-2	5	16	15	-7	1	5	12	13	0	3	5	15	17
7	9	4	5	4	-4	-5	5	11	12	4	-2	5	7	8	-6	1	5	4	4	1	3	5	4	4
8	9	4	5	5	-3	-5	5	6	6	5	-2	5	5	5	-5	1	5	5	5	2	3	5	18	20
-8	10	4	7	7	-2	-5	5	9	10	6	-2	5	14	14	-4	1	5	23	22	3	3	5	17	17
-1	10	4	10	9	0	-5	5	8	7	7	-2	5	5	5	-3	1	5	4	3	5	3	5	31	30
1	10	4	5	6	1	-5	5	12	13	-7	-1	5	6	7	-1	1	5	8	8	9	3	5	19	18
2	10	4	15	15	2	-5	5	12	12	-5	-1	5	4	3	0	1	5	17	17	-7	4	5	14	14
3	10	4	15	15	4	-5	5	7	8	-3	-1	5	7	7	1	1	5	25	26	-5	4	5	9	9
4	10	4	12	12	5	-5	5	12	13	-2	-1	5	32	31	2	1	5	5	5	-3	4	5	9	10
															3	1	5	4	3	-1	4	5	6	5

OBSERVED AND CALCULATED STRUCTURE FACTORS FOR MGTPP(4-METHYLPYRIDINE) ODC PAGE 9

H	K	L	FO	FC	H	K	L	FO	FC	H	K	L	FO	FC	H	K	L	FO	FC	H	K	L	FO	FC
0	4	5	5	3	-4	7	5	9	9	11	9	5	4	0	-1	-5	6	4	4	-4	-1	5	5	5
1	4	5	48	46	-3	7	5	4	2	-1	10	5	12	12	0	-5	6	14	14	-1	-1	5	4	5
2	4	5	20	18	-2	7	5	11	11	0	10	5	16	16	-7	-4	6	5	4	0	-1	5	9	9
3	4	5	6	7	-1	7	5	17	17	1	10	5	5	5	-5	-4	6	9	9	1	-1	5	15	15
5	4	5	17	17	0	7	5	17	18	3	10	5	5	5	-3	-4	6	9	9	2	-1	5	10	12
6	4	5	5	5	1	7	5	24	25	5	10	5	15	15	-2	-4	6	10	10	3	-1	5	5	5
7	4	5	9	9	2	7	5	11	11	6	10	5	4	3	-1	-4	6	4	4	4	-1	5	5	5
8	4	5	11	10	3	7	5	5	4	7	10	5	9	9	0	-4	6	7	6	7	-1	5	5	5
9	4	5	12	12	4	7	5	10	9	-1	11	5	13	12	2	-4	6	6	6	-7	0	5	15	16
-8	5	5	5	5	5	7	5	15	17	0	11	5	7	7	5	-4	6	5	5	-6	0	5	9	9
-4	5	5	13	12	6	7	5	13	13	1	11	5	6	6	-9	-3	6	7	4	-5	0	5	4	5
-3	5	5	6	6	8	7	5	11	11	2	11	5	6	4	-8	-3	6	6	5	-3	0	5	14	14
-2	5	5	7	7	10	7	5	9	8	6	11	5	10	9	-7	-3	6	10	10	-2	0	5	3	4
-1	5	5	16	16	-5	8	5	5	4	7	11	5	9	8	-2	-3	6	6	5	-1	0	5	3	3
0	5	5	5	5	-4	8	5	6	6	3	12	5	9	7	-1	-3	6	10	10	0	0	5	10	9
1	5	5	9	11	-2	8	5	8	7	8	12	5	5	5	0	-3	6	14	14	1	0	5	15	15
2	5	5	14	13	0	8	5	13	12	9	12	5	5	4	1	-3	6	11	11	2	0	5	4	4
4	5	5	15	15	2	8	5	14	14	3	13	5	8	8	2	-3	6	10	10	4	0	5	6	5
5	5	5	8	7	4	8	5	10	10	4	13	5	5	4	3	-3	6	15	15	5	0	5	7	8
7	5	5	7	7	8	8	5	13	12	-3	-8	5	5	6	-6	-2	6	15	15	6	0	5	10	9
-9	5	5	5	5	9	8	5	7	7	-1	-8	6	6	4	-5	-2	6	7	7	8	0	5	7	5
-7	5	5	5	5	10	8	5	5	5	-4	-7	6	8	8	-4	-2	6	9	9	-8	1	5	6	6
-6	5	5	7	7	-3	9	5	5	4	-3	-7	6	12	12	-3	-2	6	8	8	-7	1	5	9	10
-5	5	5	11	10	-2	9	5	5	5	-2	-7	6	13	13	-2	-2	6	4	3	-6	1	5	5	5
-4	5	5	11	12	8	9	5	7	5	-1	-7	6	9	9	-1	-2	6	25	25	-5	1	5	8	8
-3	5	5	11	11	1	9	5	7	6	3	-7	6	5	1	0	-2	6	29	28	-4	1	5	10	10
-2	5	5	5	5	2	9	5	6	7	-6	-6	6	4	2	1	-2	6	10	10	-3	1	5	22	23
-1	5	5	15	15	3	9	5	6	7	-4	-6	6	5	4	2	-2	6	5	4	-2	1	5	8	7
1	5	5	25	25	4	9	5	9	9	-1	-6	6	5	5	3	-2	6	9	9	0	1	5	14	13
3	5	5	18	17	5	9	5	11	12	0	-6	6	7	7	4	-2	6	6	6	1	1	5	29	29
4	6	5	22	22	6	9	5	4	6	1	-6	6	5	1	5	-2	6	4	2	2	1	6	3	2
5	6	5	10	10	7	9	5	10	10	2	-6	6	6	6	7	-2	6	5	6	3	1	6	9	9
6	6	5	17	18	8	9	5	7	8	4	-6	6	5	4	-6	-1	6	11	10	4	1	6	7	8
7	6	5	12	12	9	9	5	7	7	-3	-5	6	6	6	-5	-1	6	6	5	6	1	6	6	7

continued..

APPENDIX B (continued)

OBSERVED AND CALCULATED STRUCTURE FACTORS FOR MGTPP(4-METHYLPYRIDINE) OCC

H	K	L	FO	FC	H	K	L	FO	FC	H	K	L	FO	FC	H	K	L	FO	FC	H	K	L	FO	FC
7	1	5	4	4	0	4	5	16	16	-6	7	6	5	4	5	11	6	5	4	-1	-2	7	4	4
8	1	6	4	5	1	4	6	7	7	-4	7	6	12	13	7	11	6	4	4	0	-2	7	6	6
10	1	6	6	6	2	4	6	17	18	-3	7	6	21	20	9	11	6	5	5	1	-2	7	7	6
-7	2	6	7	5	3	4	6	13	13	-2	7	6	6	5	4	12	6	8	8	2	-2	7	6	5
-6	2	6	7	9	4	4	6	11	11	1	7	6	37	36	9	12	6	5	3	3	-2	7	6	6
-5	2	6	13	12	5	4	6	13	13	9	7	6	11	11	3	13	6	5	4	-6	-1	7	15	16
-2	2	6	4	4	6	4	6	4	3	10	7	6	9	8	4	13	6	5	5	-5	-1	7	19	19
-1	2	6	10	11	7	4	6	5	4	11	7	6	5	5	-3	-5	7	5	4	-4	-1	7	12	12
0	2	6	34	34	8	4	6	5	5	1	8	6	19	19	-2	-5	7	5	4	-3	-1	7	5	4
1	2	6	11	10	9	4	6	6	7	2	8	6	5	5	1	-5	7	5	5	2	-1	7	8	7
2	2	6	9	8	-7	5	6	5	4	5	8	6	6	6	-6	-5	7	6	6	5	-1	7	12	12
4	2	6	3	3	-6	5	6	8	7	8	8	6	10	9	-5	-5	7	5	5	7	-1	7	5	5
5	2	6	11	11	-5	5	6	7	8	9	8	6	9	8	9	-5	7	11	11	-6	0	7	8	8
6	2	6	19	19	-4	5	6	14	13	-3	9	6	5	4	1	-5	7	10	9	-5	0	7	4	3
7	2	6	4	3	-3	5	6	19	20	-1	9	6	5	5	2	-5	7	4	4	-4	0	7	8	9
8	2	6	4	4	-2	5	6	9	9	0	9	6	23	23	-8	-4	7	6	4	-3	0	7	13	13
10	2	6	8	7	-1	5	6	6	6	1	9	6	19	19	-6	-4	7	9	8	-2	0	7	12	12
-6	3	6	7	7	0	5	6	15	15	2	9	6	5	5	-5	-4	7	7	7	0	0	7	9	9
-4	3	6	14	13	2	5	6	20	19	5	9	6	7	7	-2	-4	7	4	3	1	0	7	14	14
-3	3	6	6	5	3	5	6	22	22	6	9	6	12	13	1	-4	7	6	7	2	0	7	23	22
-2	3	6	5	5	4	5	6	6	7	8	9	6	14	14	3	-4	7	15	15	3	0	7	5	5
-1	3	6	6	6	7	5	6	9	9	10	9	6	5	5	3	-4	7	7	8	4	0	7	7	7
0	3	6	8	8	9	5	6	5	5	-2	10	6	5	5	4	-4	7	10	9	5	0	7	5	5
1	3	6	15	15	-6	6	6	6	6	0	10	6	14	14	5	-4	7	7	6	7	0	7	6	7
2	3	6	9	9	-5	6	6	5	4	1	10	6	5	5	-5	-3	7	5	4	8	0	7	6	7
3	3	6	30	30	-3	6	6	14	14	3	10	6	7	7	-4	-3	7	13	13	-5	1	7	11	12
6	3	6	13	12	-2	6	6	5	4	4	10	6	7	7	-3	-3	7	6	5	-4	1	7	8	8
9	3	6	5	4	-1	6	6	6	6	5	10	6	5	5	-2	-3	7	7	8	-3	1	7	7	7
10	3	6	5	5	0	6	6	11	12	8	10	6	5	6	-1	-3	7	4	4	-2	1	7	8	9
-7	4	6	5	3	2	6	6	7	7	10	10	6	5	5	0	-3	7	7	7	-1	1	7	5	4
-4	4	6	10	9	3	6	6	6	5	-1	11	6	5	6	1	-3	7	8	8	0	1	7	3	3
-3	4	6	16	16	6	6	6	8	7	0	11	6	7	7	-7	-2	7	5	5	1	1	7	18	18
-2	4	6	15	16	7	6	6	9	8	2	11	6	8	8	-6	-2	7	9	8	2	1	7	8	9
-1	4	6	11	12	9	6	6	6	4	4	11	6	12	12	-3	-2	7	16	17	4	1	7	7	7

OBSERVED AND CALCULATED STRUCTURE FACTORS FOR MGTPP(4-METHYLPYRIDINE) OCC

H	K	L	FO	FC	H	K	L	FO	FC	H	K	L	FO	FC	H	K	L	FO	FC	H	K	L	FO	FC
5	1	7	9	9	-4	5	7	7	6	3	8	7	7	7	1	-4	8	7	4	-3	1	8	7	7
7	1	7	5	6	-1	5	7	7	7	4	8	7	5	6	2	-4	8	9	9	-2	1	8	4	4
-7	2	7	5	5	0	5	7	11	10	7	8	7	9	10	4	-4	8	5	5	-1	1	8	12	11
-3	2	7	17	17	1	5	7	5	5	9	8	7	6	6	-5	-3	8	8	8	0	1	8	10	10
-2	2	7	6	7	2	5	7	15	15	10	8	7	4	4	-4	-3	8	7	5	1	1	8	11	12
-1	2	7	9	9	3	5	7	31	31	-4	9	7	5	4	-3	-3	8	5	5	2	1	8	6	5
1	2	7	14	14	4	5	7	19	19	-1	9	7	8	7	-2	-3	8	8	7	4	1	8	8	9
5	2	7	6	6	8	5	7	6	5	0	9	7	7	7	1	-3	8	5	4	5	1	8	7	7
9	2	7	5	4	11	5	7	5	5	1	9	7	23	23	3	-3	8	6	6	-4	2	8	5	5
10	2	7	5	4	-4	6	7	4	5	2	9	7	4	3	-5	-2	8	5	5	-3	2	8	5	5
-5	3	7	5	6	-3	6	7	9	9	9	9	7	12	11	-4	-2	8	11	10	-1	2	8	10	10
-5	3	7	6	5	-2	6	7	8	9	-2	10	7	4	2	-3	-2	8	7	7	0	2	8	6	5
-3	3	7	11	10	0	6	7	6	6	-1	10	7	4	5	-1	-2	8	12	12	1	2	8	4	5
-2	3	7	24	24	2	6	7	22	22	1	10	7	7	8	1	-2	8	4	4	4	2	8	9	9
-1	3	7	21	21	3	6	7	19	18	4	10	7	7	7	-7	-1	8	5	1	5	2	8	5	6
0	3	7	7	7	5	6	7	10	10	5	10	7	15	15	-6	-1	8	8	7	10	2	8	5	3
1	3	7	10	10	7	6	7	6	5	6	10	7	7	8	-5	-1	8	8	7	-5	3	8	6	5
2	3	7	11	12	10	6	7	8	7	7	10	7	4	1	-3	-1	8	10	10	-5	3	8	5	6
3	3	7	4	3	11	6	7	7	8	8	10	7	5	5	-2	-1	8	11	11	-3	3	8	4	3
4	3	7	6	5	-6	7	7	9	8	10	10	7	9	7	-1	-1	8	12	11	-2	3	8	8	8
5	3	7	8	7	-5	7	7	9	8	4	11	7	9	8	2	-1	8	5	5	-1	3	8	13	13
8	3	7	4	2	-4	7	7	7	8	5	11	7	14	14	3	-1	8	9	9	2	3	8	10	11
-7	4	7	6	5	-3	7	7	6	6	6	11	7	5	5	-5	0	8	6	5	3	3	8	11	12
-6	4	7	7	7	0	7	7	10	11	8	11	7	4	3	-3	0	8	7	7	4	3	8	14	13
-5	4	7	8	7	2	7	7	35	35	5	12	7	8	9	-2	0	8	13	12	5	3	8	7	7
-4	4	7	7	7	3	7	7	7	7	3	13	7	4	3	-1	0	8	4	4	6	3	8	9	9
-2	4	7	9	9	5	7	7	4	4	-3	-6	8	4	3	0	0	8	7	6	9	3	8	7	7
1	4	7	4	4	6	7	7	12	12	-5	-5	8	7	6	2	0	8	11	11	-5	4	8	10	9
2	4	7	32	32	7	7	7	13	13	0	-5	8	6	6	3	0	8	5	6	-4	4	8	6	6
3	4	7	4	3	8	7	7	9	8	1	-5	8	6	6	4	0	8	9	9	-2	4	8	9	9
5	4	7	4	4	10	7	7	6	6	-5	-4	8	4	4	5	0	8	6	6	-1	4	8	5	5
7	4	7	5	5	-1	8	7	6	5	-4	-4	8	9	9	7	0	8	5	4	0	4	8	4	3
8	4	7	12	11	1	8	7	22	22	-3	-4	8	6	6	8	0	8	7	6	1	4	8	13	13
-5	5	7	8	8	2	8	7	16	16	-1	-4	8	5	5	-6	1	8	5	3	2	4	8	19	18

continued..

APPENDIX B (continued)

OBSERVED AND CALCULATED STRUCTURE FACTORS FOR MGTPP(4-METHYLPYRIDINE) DCC — PAGE 11

H	K	L	FO	FC	H	K	L	FO	FC	H	K	L	FO	FC	H	K	L	FO	FC	H	K	L	FO	FC
3	4	8	16	16	-2	8	8	7	7	-4	-3	9	11	10	-3	3	9	13	13	-3	7	9	7	5
4	4	8	25	25	-1	8	8	4	4	-3	-3	9	7	7	0	3	9	7	6	-2	7	9	11	10
5	4	8	15	16	2	8	8	22	23	0	-3	9	6	6	2	3	9	10	11	-1	7	9	14	15
6	4	8	5	5	3	8	8	5	5	2	-3	9	4	9	3	3	9	15	15	0	7	9	9	10
-5	5	8	5	6	4	8	8	11	11	-4	-2	9	5	4	4	3	9	15	16	1	7	9	5	5
-4	5	8	9	8	5	8	8	9	9	-3	-2	9	5	3	5	3	9	20	20	3	7	9	14	14
-2	5	8	19	11	6	8	8	10	10	-2	-2	9	7	7	-5	4	9	5	3	4	7	9	12	12
-1	5	8	19	19	7	8	8	10	10	-1	-2	9	7	7	-4	4	9	7	7	5	7	9	10	9
0	5	8	10	11	8	8	8	8	7	0	-2	9	12	11	-3	4	9	7	7	6	7	9	15	15
3	5	8	24	23	9	8	8	5	6	2	-2	9	5	5	-1	4	9	9	10	7	7	9	13	13
4	5	8	19	19	10	8	8	6	7	4	-2	9	9	8	0	4	9	16	16	8	7	9	5	5
6	5	8	6	5	-3	9	8	9	9	-2	-1	9	7	7	2	4	9	13	13	9	7	9	7	7
-5	6	8	7	6	-2	9	8	5	5	-1	-1	9	11	11	3	4	9	8	9	10	7	9	14	13
-4	6	8	13	13	2	9	8	18	18	0	-1	9	6	6	4	4	9	15	15	-2	8	9	10	10
-3	6	8	7	9	4	9	8	4	2	1	-1	9	4	4	5	4	9	8	8	-1	8	9	10	10
-2	6	8	7	7	5	9	8	8	8	-4	0	9	5	5	6	4	9	5	6	3	8	9	4	3
-1	6	8	5	4	6	9	8	16	17	-3	0	9	10	10	8	4	9	5	5	4	8	9	9	9
2	6	8	8	8	7	9	8	10	10	-2	0	9	5	5	9	4	9	5	4	7	8	9	9	9
3	6	8	15	15	-2	10	8	5	3	-1	0	9	8	7	10	4	9	5	6	8	8	9	5	5
4	6	8	9	9	-1	10	8	5	3	1	0	9	9	9	11	5	9	5	4	1	9	9	5	5
5	6	8	15	15	0	10	8	4	4	-4	1	9	12	12	-4	5	9	5	5	3	9	9	5	5
6	6	8	8	9	1	10	8	4	3	1	1	9	6	6	-3	5	9	7	7	4	9	9	5	5
7	6	8	13	12	5	10	8	3	4	3	1	9	5	5	-2	5	9	11	12	5	9	9	5	5
8	6	8	14	14	6	10	8	11	11	6	1	9	5	6	-1	5	9	9	9	6	9	9	5	5
9	6	8	5	7	7	10	8	9	8	-4	2	9	7	8	1	5	9	7	7	7	9	9	10	10
-11	5	8	5	3	2	11	8	5	5	-3	2	9	13	13	2	5	9	6	5	10	9	9	5	4
-10	7	8	5	5	3	11	8	7	6	-3	2	9	9	9	5	5	9	5	5	0	10	9	8	8
-1	7	8	7	5	4	11	8	5	5	-1	2	9	9	9	6	5	9	8	9	7	10	9	4	5
1	7	8	10	10	3	12	8	6	4	0	2	9	15	15	7	5	9	4	4	3	11	9	5	4
2	7	8	8	9	4	12	8	5	4	3	2	9	7	8	9	5	9	5	5	4	11	9	9	10
3	7	8	14	15	5	12	8	5	5	4	2	9	6	6	-4	6	9	5	5	5	11	9	5	6
6	7	8	4	4	-3	-5	9	8	7	5	2	9	15	16	-3	6	9	6	6	2	12	9	5	4
8	7	8	8	9	-3	-4	9	6	6	7	2	9	6	7	3	6	9	22	23	4	12	9	5	5
10	7	8	4	3	1	-4	9	7	8	-4	3	9	7	5	4	5	9	25	27	-2	-4	10	6	5

OBSERVED AND CALCULATED STRUCTURE FACTORS FOR MGTPP(4-METHYLPYRIDINE) DCC — PAGE 12

H	K	L	FO	FC	H	K	L	FO	FC	H	K	L	FO	FC	H	K	L	FO	FC	H	K	L	FO	FC
1	-4	10	6	6	2	3	10	10	9	7	8	10	6	5	-4	3	11	7	6	2	8	11	5	5
-2	-3	10	5	4	5	3	10	12	11	8	8	10	8	8	-2	3	11	12	12	6	8	11	6	5
-1	-3	10	8	8	9	3	10	5	4	-1	9	10	5	5	-1	3	11	11	11	7	8	11	6	5
-1	-2	10	4	5	-5	4	10	5	3	0	9	10	6	5	3	3	11	4	2	1	9	11	5	5
2	-2	10	5	6	-3	4	10	6	6	1	9	10	12	11	6	3	11	10	10	2	9	11	5	4
0	-1	10	5	5	-2	4	10	8	9	3	9	10	8	8	-4	4	11	6	5	5	9	11	4	5
-5	0	10	7	4	3	4	10	7	6	5	9	10	5	3	-2	4	11	8	8	6	9	11	7	6
-3	0	10	9	10	5	4	10	13	13	6	9	10	8	8	0	4	11	5	4	6	10	11	5	5
-1	0	10	5	3	-4	5	10	6	5	8	9	10	6	6	1	4	11	13	13	3	11	11	6	7
0	0	10	6	6	0	5	10	12	11	1	10	10	5	6	2	4	11	12	12	-1	0	12	6	6
1	0	10	9	8	1	5	10	11	12	5	10	10	8	8	3	4	11	8	8	0	0	12	6	5
2	0	10	9	9	2	5	10	14	14	6	10	10	5	6	5	4	11	7	6	2	0	12	6	5
4	0	10	4	5	4	5	10	15	15	1	11	10	6	4	6	4	11	9	9	0	1	12	6	6
5	0	10	4	5	5	5	10	21	21	0	-3	11	5	3	7	4	11	5	5	2	1	12	6	6
-4	1	10	10	10	8	5	10	6	5	-2	-2	11	5	2	-3	5	11	4	1	-3	2	12	8	7
-3	1	10	12	13	-3	6	10	5	5	-2	-1	11	7	7	-1	5	11	5	4	-1	2	12	7	7
-2	1	10	13	12	-1	6	10	10	10	-1	-1	11	9	8	0	5	11	8	7	0	2	12	8	7
-1	1	10	9	9	0	6	10	12	13	1	-1	11	5	5	1	5	11	8	8	3	2	12	4	7
1	1	10	9	9	1	6	10	12	12	2	-1	11	5	4	2	5	11	6	4	-3	3	12	7	7
2	1	10	5	5	2	6	10	9	9	3	-1	11	5	5	3	5	11	11	12	2	3	12	9	9
3	1	10	4	3	4	6	10	10	10	-3	0	11	5	4	4	5	11	6	5	3	3	12	9	9
5	1	10	6	6	8	6	10	11	11	-2	0	11	10	11	5	5	11	11	11	5	3	12	6	5
6	1	10	10	11	9	6	10	9	9	-1	0	11	8	8	9	5	11	4	4	7	3	12	6	4
7	1	10	6	6	-1	7	10	11	11	0	0	11	5	5	8	6	11	13	13	2	4	12	9	9
-4	2	10	4	5	0	7	10	7	7	-4	1	11	5	4	1	6	11	9	9	3	4	12	5	5
-3	2	10	14	14	1	7	10	5	5	-1	1	11	6	6	2	6	11	9	8	6	4	12	5	5
-4	3	10	4	5	4	7	10	5	4	3	1	11	6	6	4	6	11	9	9	1	5	12	12	12
5	2	10	8	8	6	7	10	11	12	4	1	11	5	5	6	6	11	7	6	2	5	12	7	6
-4	3	10	4	3	8	7	10	7	7	7	1	11	6	5	8	6	11	5	5	5	5	12	6	6
-3	3	10	4	4	9	7	10	6	5	-3	2	11	8	7	9	6	11	8	8	8	6	12	4	3
-2	3	10	7	7	-1	8	10	4	3	0	2	11	5	7	1	7	11	5	3	1	6	12	5	5
-1	3	10	9	9	2	8	10	6	6	1	2	11	15	15	7	7	11	5	5	2	6	12	5	5
0	3	10	19	20	3	8	10	5	6	6	2	11	7	7	9	7	11	7	7	3	6	12	7	7
1	3	10	18	19	6	8	10	6	6	7	2	11	5	4	1	8	11	5	6	2	7	12	7	6

continued..

APPENDIX B (continued)

OBSERVED AND CALCULATED STRUCTURE FACTORS FOR NGTPP(4-METHYLPYRIDINE) OCC PAGE 13

H	K	L	FO	FC	H	K	L	FO	FC	H	K	L	FO	FC	H	K	L	FO	FC	H	K	L	FO	FC
3	7	13	7	7	3	8	13	5	5	4	3	13	5	4	4	3	13	7	6	4	6	13	7	6
5	7	13	7	6	7	8	13	4	5	-1	3	13	5	4	2	4	13	7	7	3	7	13	5	5
6	7	13	4	4	1	9	13	6	5	0	3	13	7	7	3	4	13	7	6	5	9	13	7	6
7	7	13	6	5	3	9	13	5	5	3	3	13	13	13	4	4	13	5	4					

APPENDIX C

OBSERVED AND CALCULATED STRUCTURE FACTORS FOR MG TPP PIPERIDINE

H	K	L	FO	FC	H	K	L	FO	FC	H	K	L	FO	FC	H	K	L	FO	FC	H	K	L	FO	F
1	0	0	38	39	6	2	0	6	6	-7	5	0	20	20	0	0	0	18	18	4	-10	1	11	1
2	0	0	52	52	7	2	0	14	13	-4	5	0	6	7	-11	0	0	4	4	5	-10	1	6	6
3	0	0	3	4	-10	3	0	4	3	-1	5	0	4	5	-10	0	0	7	8	6	-10	1	11	1
4	0	0	13	14	-9	3	0	4	5	0	5	0	7	6	-9	0	0	9	9	7	-10	1	6	6
5	0	0	14	14	-7	3	0	7	9	1	5	0	13	13	-8	0	0	8	8	-2	-9	1	9	10
8	0	0	9	9	-5	3	0	21	21	2	5	0	9	10	-6	0	0	9	9	-1	-9	1	5	4
9	0	0	3	4	-4	3	0	16	17	3	5	0	8	8	-5	0	0	10	10	0	-9	1	7	6
-9	1	0	9	10	-3	3	0	11	10	4	5	0	13	13	-3	0	0	3	3	1	-9	1	7	8
-7	1	0	5	5	-2	3	0	21	21	5	5	0	12	12	0	0	0	6	6	4	-9	1	10	10
-5	1	0	24	24	-1	3	0	30	30	-10	6	0	6	6	-9	10	0	4	3	5	-9	1	5	4
-4	1	0	5	5	0	3	0	25	25	-7	6	0	10	10	-8	10	0	6	6	9	-9	1	7	5
-3	1	0	46	47	1	3	0	3	3	-5	6	0	9	8	-6	10	0	10	10	-2	-8	1	11	11
-2	1	0	12	13	2	3	0	21	22	-4	6	0	7	8	-4	10	0	3	2	-1	-8	1	6	4
-1	1	0	49	50	3	3	0	23	23	-3	6	0	16	15	-3	10	0	10	11	0	-8	1	5	6
0	1	0	56	58	4	3	0	8	8	-2	6	0	5	6	-2	10	0	4	4	1	-8	1	5	4
1	1	0	33	32	7	3	0	8	7	-1	6	0	14	14	-1	10	0	4	4	2	-8	1	5	6
2	1	0	28	29	-10	4	0	4	3	0	6	0	5	5	1	10	0	6	6	3	-8	1	9	9
3	1	0	37	38	-9	4	0	4	4	2	6	0	11	11	-8	11	0	4	3	4	-8	1	3	3
4	1	0	7	7	-8	4	0	4	4	3	6	0	4	4	-5	11	0	4	4	5	-8	1	10	10
6	1	0	5	4	-7	4	0	4	4	5	6	0	4	4	-3	11	0	4	4	8	-8	1	3	4
7	1	0	8	9	-6	4	0	9	8	-11	7	0	4	4	-2	11	0	7	7	9	-8	1	4	5
8	1	0	7	8	-5	4	0	14	14	-9	7	0	11	12	-5	12	0	6	7	-3	-7	1	4	4
-9	2	0	6	6	-4	4	0	4	3	-7	7	0	8	7	-3	12	0	4	5	-2	-7	1	5	4
-8	2	0	18	18	-3	4	0	4	4	-5	7	0	3	3	-5	13	0	5	5	-1	-7	1	5	5
-6	2	0	17	17	-2	4	0	20	20	-3	7	0	7	7	5	-13	1	4	4	1	-7	1	11	11
-5	2	0	3	3	-1	4	0	16	17	-2	7	0	8	8	1	-12	1	4	1	4	-7	1	20	19
-4	2	0	15	16	0	4	0	11	12	-1	7	0	4	4	2	-12	1	5	3	5	-7	1	17	17
-3	2	0	35	36	1	4	0	31	31	0	7	0	8	8	5	-12	1	4	1	6	-7	1	4	1
-1	2	0	13	14	2	4	0	16	15	2	7	0	5	5	2	-11	1	5	5	7	-7	1	21	20
0	2	0	23	23	4	4	0	13	13	-9	8	0	10	11	4	-11	1	9	9	9	-7	1	6	9
1	2	0	15	15	5	4	0	6	6	-8	8	0	11	11	5	-11	1	5	5	9	-7	1	5	6
2	2	0	28	28	-10	5	0	6	5	-6	8	0	14	14	10	-11	1	5	4	-6	-6	1	5	5
3	2	0	20	19	-9	5	0	8	9	-5	8	0	16	16	-1	-10	1	7	5	-5	-6	1	5	6
5	2	0	10	10	-8	5	0	4	3	-2	8	0	4	4	0	-10	1	7	8	-1	-6	1	29	29

OBSERVED AND CALCULATED STRUCTURE FACTORS FOR MG TPP PIPERIDINE

H	K	L	FO	FC	H	K	L	FO	FC	H	K	L	FO	FC	H	K	L	FO	FC	H	K	L	FO	FC
0	-6	1	4	4	-3	-3	1	5	5	-2	-1	1	12	12	0	1	1	18	17	4	3	1	8	8
1	-6	1	6	4	-2	-3	1	5	4	-1	-1	1	48	48	1	1	1	38	38	5	3	1	8	9
2	-6	1	11	11	-1	-3	1	20	20	0	-1	1	48	51	2	1	1	9	7	6	3	1	7	7
3	-6	1	18	17	0	-3	1	22	22	1	-1	1	3	2	3	1	1	9	8	7	3	1	7	8
4	-6	1	11	10	1	-3	1	31	31	2	-1	1	38	39	5	1	1	4	2	-10	4	1	6	5
5	-6	1	4	5	3	-3	1	19	18	3	-1	1	26	26	6	1	1	5	5	-9	4	1	12	12
6	-6	1	6	7	4	-3	1	15	15	4	-1	1	48	47	7	1	1	11	11	-7	4	1	11	11
7	-6	1	24	24	5	-3	1	23	23	5	-1	1	10	10	-10	2	1	4	3	-4	4	1	15	15
9	-6	1	26	27	6	-3	1	6	6	6	-1	1	9	9	-9	2	1	13	13	-3	4	1	32	32
10	-6	1	4	2	7	-3	1	11	11	7	-1	1	9	8	-8	2	1	13	14	-2	4	1	77	78
-4	-5	1	11	10	9	-3	1	7	7	9	-1	1	4	4	-7	2	1	5	4	-1	4	1	57	58
-2	-5	1	13	13	-7	-2	1	5	5	-9	0	1	9	10	-6	2	1	5	5	0	4	1	7	6
-1	-5	1	16	16	-6	-2	1	4	5	-7	0	1	11	10	-5	2	1	19	18	1	4	1	8	9
1	-5	1	22	22	-5	-2	1	12	11	-6	0	1	5	5	-4	2	1	9	9	2	4	1	28	29
2	-5	1	22	23	-4	-2	1	25	24	-5	0	1	12	12	-3	2	1	16	16	3	4	1	11	12
3	-5	1	13	13	-3	-2	1	6	6	-4	0	1	32	31	-2	2	1	10	11	4	4	1	4	4
5	-5	1	9	7	-2	-2	1	6	7	-3	0	1	13	13	-1	2	1	162	170	5	4	1	6	6
6	-5	1	5	5	0	-2	1	18	18	-2	0	1	94	98	0	2	1	7	7	6	4	1	7	7
7	-5	1	13	12	1	-2	1	62	61	-1	0	1	2	2	1	2	1	7	7	-10	5	1	6	6
8	-5	1	17	18	2	-2	1	60	61	0	0	1	45	44	2	2	1	22	22	-9	5	1	4	3
-5	-4	1	4	4	3	-2	1	34	34	1	0	1	37	39	3	2	1	16	15	-8	5	1	9	9
-5	-4	1	5	4	4	-2	1	6	8	2	0	1	26	28	4	2	1	7	7	-7	5	1	8	9
-4	-4	1	11	11	5	-2	1	4	4	3	0	1	4	6	7	2	1	9	10	-5	5	1	3	3
-2	-4	1	12	12	6	-2	1	10	10	4	0	1	4	5	8	2	1	5	4	-4	5	1	13	13
-1	-4	1	4	3	7	-2	1	9	9	7	0	1	7	7	-7	3	1	5	5	-2	5	1	9	9
0	-4	1	10	10	8	-2	1	7	6	9	0	1	5	3	-6	3	1	6	6	-1	5	1	14	13
1	-4	1	5	5	9	-2	1	7	7	-9	1	1	11	10	-4	3	1	16	16	0	5	1	11	11
3	-4	1	9	10	-9	-1	1	4	0	-8	1	1	12	13	-3	3	1	33	34	1	5	1	19	18
4	-4	1	28	27	-8	-1	1	9	9	-7	1	1	4	2	-2	3	1	30	30	2	5	1	16	16
5	-4	1	16	15	-7	-1	1	5	5	-5	1	1	4	4	-1	3	1	76	76	3	5	1	4	4
6	-4	1	28	26	-6	-1	1	4	4	-4	1	1	28	28	0	3	1	5	5	6	5	1	6	4
8	-4	1	9	9	-5	-1	1	17	17	-3	1	1	30	30	1	3	1	6	6	-11	6	1	6	6
-6	-3	1	9	8	-4	-1	1	40	39	-2	1	1	51	51	2	3	1	8	9	-8	6	1	8	7
-5	-3	1	13	12	-3	-1	1	26	27	-1	1	1	48	48	3	3	1	24	23	-6	6	1	5	4

continued..

APPENDIX C (continued)

OBSERVED AND CALCULATED STRUCTURE FACTORS FOR MG TPP PIPERIDINE PAGE 3

H	K	L	FO	FC	H	K	L	FO	FC	H	K	L	FO	FC	H	K	L	FO	FC	H	K	L	FO	FC
-5	6	1	4	5	-2	11	1	4	3	9	-8	2	9	8	4	-5	2	11	11	-2	-2	2	15	15
-4	6	1	9	8	-4	12	1	6	5	-3	-7	2	6	6	6	-5	2	12	12	-1	-2	2	65	66
-3	6	1	5	5	4	-12	2	4	4	-2	-7	2	5	5	7	-5	2	7	8	0	-2	2	77	79
-2	6	1	19	20	7	-12	2	7	7	-1	-7	2	10	10	8	-5	2	12	12	1	-2	2	59	61
0	6	1	11	10	2	-11	2	5	4	0	-7	2	4	3	-7	-4	2	5	6	2	-2	2	15	15
1	6	1	4	2	3	-11	2	4	3	1	-7	2	5	5	-5	-4	2	6	7	3	-2	2	27	27
2	6	1	6	6	4	-11	2	5	5	2	-7	2	4	4	-3	-4	2	5	5	4	-2	2	18	17
3	6	1	5	5	5	-11	2	5	5	3	-7	2	21	22	-2	-4	2	34	33	5	-2	2	34	34
4	6	1	7	8	7	-11	2	6	6	4	-7	2	15	15	-1	-4	2	6	5	6	-2	2	25	25
-11	7	1	4	3	8	-11	2	5	4	5	-7	2	19	19	0	-4	2	28	27	7	-2	2	4	3
-10	7	1	7	7	0	-10	2	5	5	8	-7	2	10	11	1	-4	2	13	13	-7	-1	2	13	14
-9	7	1	6	7	2	-10	2	4	5	-6	-6	2	5	6	2	-4	2	8	8	-6	-1	2	18	17
-8	7	1	8	8	4	-10	2	13	13	-5	-6	2	8	8	3	-4	2	17	17	-5	-1	2	10	11
-4	7	1	5	5	6	-10	2	5	5	-3	-6	2	9	9	4	-4	2	18	18	-4	-1	2	21	21
-1	7	1	6	6	-4	-9	2	9	9	-2	-6	2	10	11	6	-4	2	18	18	-3	-1	2	25	25
3	7	1	13	13	-2	-9	2	4	4	-1	-6	2	14	14	7	-4	2	21	23	-2	-1	2	30	31
4	7	1	11	12	1	-9	2	8	8	1	-6	2	7	7	9	-4	2	4	5	-1	-1	2	9	10
-9	8	1	4	4	2	-9	2	5	5	2	-6	2	7	7	-5	-3	2	15	14	0	-1	2	19	20
-8	8	1	6	7	3	-9	2	5	4	3	-6	2	19	18	-4	-3	2	20	18	1	-1	2	31	31
-7	8	1	12	13	4	-9	2	4	5	4	-6	2	34	33	-3	-3	2	4	3	2	-1	2	37	36
-6	8	1	11	11	5	-9	2	6	6	5	-6	2	11	11	-1	-3	2	25	25	3	-1	2	6	6
-5	8	1	4	4	6	-9	2	6	6	6	-6	2	13	13	0	-3	2	45	47	4	-1	2	23	23
0	8	1	8	7	7	-9	2	5	5	7	-6	2	4	4	1	-3	2	17	16	5	-1	2	7	6
-9	9	1	7	8	9	-9	2	8	8	8	-6	2	8	8	2	-3	2	23	23	6	-1	2	7	7
-8	9	1	7	7	-3	-8	2	8	9	-7	-5	2	5	6	3	-3	2	28	30	7	-1	2	6	6
-6	9	1	7	6	-2	-8	2	9	9	-6	-5	2	10	9	4	-3	2	29	27	-7	0	2	5	5
-3	9	1	6	6	-1	-8	2	4	4	-4	-5	2	10	8	5	-3	2	12	10	-6	0	2	17	16
-1	9	1	6	7	1	-8	2	7	6	-3	-5	2	9	10	6	-3	2	30	30	-5	0	2	6	6
0	9	1	4	6	2	-8	2	4	3	-2	-5	2	18	17	7	-3	2	16	17	-4	0	2	14	13
1	9	1	5	6	3	-8	2	10	11	-1	-5	2	8	8	9	-3	2	7	7	-3	0	2	11	11
-9	10	1	5	4	4	-8	2	5	6	0	-5	2	10	10	-7	-2	2	5	5	-2	0	2	33	33
-3	10	1	9	9	5	-8	2	8	8	1	-5	2	5	5	-6	-2	2	4	5	-1	0	2	46	46
-1	10	1	9	9	6	-8	2	6	5	2	-5	2	12	12	-5	-2	2	8	7	0	0	2	38	37
-10	11	1	6	6	7	-8	2	9	8	3	-5	2	17	18	-3	-2	2	17	17	1	0	2	45	43

OBSERVED AND CALCULATED STRUCTURE FACTORS FOR MG TPP PIPERIDINE PAGE 4

H	K	L	FO	FC	H	K	L	FO	FC	H	K	L	FO	FC	H	K	L	FO	FC	H	K	L	FO	FC
2	0	2	29	28	-5	3	2	9	9	0	5	2	6	5	-2	9	2	4	4	8	-9	3	9	9
4	0	2	15	15	-4	3	2	20	20	1	5	2	4	3	-9	10	2	7	7	-5	-8	3	7	7
5	0	2	10	10	-3	3	2	13	13	2	5	2	7	6	-8	10	2	4	5	-4	-8	3	6	5
6	0	2	6	8	-2	3	2	55	56	4	5	2	9	9	-7	10	2	6	6	-3	-8	3	8	8
8	0	2	6	7	-1	3	2	51	51	5	5	2	6	7	-5	10	2	7	7	-1	-8	3	5	7
-9	1	2	8	7	0	3	2	3	3	6	5	2	8	7	-4	10	2	4	4	1	-8	3	9	8
-8	1	2	5	5	1	3	2	8	9	-11	6	2	4	4	-10	11	2	6	6	3	-8	3	20	20
-7	1	2	8	7	2	3	2	4	4	-10	6	2	7	7	-9	11	2	4	4	5	-8	3	7	8
-5	1	2	22	22	3	3	2	6	5	-9	6	2	5	6	-8	11	2	4	6	7	-8	3	8	7
-4	1	2	10	9	4	3	2	8	9	-7	6	2	5	4	-4	11	2	6	5	-4	-7	3	8	7
-2	1	2	39	38	5	3	2	6	8	-6	6	2	12	12	2	-13	3	8	6	-3	-7	3	10	9
-1	1	2	24	24	-10	4	2	6	7	-5	6	2	14	15	5	-13	3	5	4	-1	-7	3	6	6
0	1	2	28	29	-9	4	2	13	13	-4	6	2	17	18	6	-13	3	6	5	0	-7	3	7	6
1	1	2	5	5	-6	4	2	5	5	-3	6	2	26	27	1	-12	3	6	3	1	-7	3	5	3
2	1	2	3	2	-5	4	2	4	3	-2	6	2	20	19	2	-12	3	4	4	2	-7	3	12	12
3	1	2	26	24	-4	4	2	27	26	0	6	2	12	12	5	-12	3	6	5	3	-7	3	17	17
4	1	2	6	6	-3	4	2	21	21	3	6	2	6	5	8	-12	3	4	5	4	-7	3	5	5
7	1	2	5	3	-2	4	2	81	84	-10	7	2	6	6	9	-12	3	5	6	5	-7	3	5	5
-9	2	2	8	9	-1	4	2	16	16	-9	7	2	8	8	1	-11	3	8	8	6	-7	3	11	10
-8	2	2	16	15	0	4	2	20	19	-7	7	2	7	7	2	-11	3	7	7	8	-7	3	6	7
-6	2	2	8	8	2	4	2	8	8	-4	7	2	5	5	3	-11	3	4	3	-5	-6	3	6	5
-5	2	2	30	29	3	4	2	4	4	-3	7	2	16	16	4	-11	3	4	5	-4	-6	3	14	14
-4	2	2	8	8	4	4	2	4	5	-1	7	2	6	6	5	-11	3	4	3	-3	-6	3	14	14
-3	2	2	3	2	5	4	2	7	6	0	7	2	7	7	6	-11	3	5	5	-2	-6	3	4	3
-2	2	2	12	12	6	4	2	8	8	1	7	2	14	14	8	-11	3	6	6	-1	-6	3	5	6
-1	2	2	52	53	-10	5	2	5	7	2	7	2	4	3	6	-10	3	7	8	0	-6	3	4	3
0	2	2	51	52	-9	5	2	8	8	-7	8	2	5	5	-3	-9	3	6	6	1	-6	3	9	8
1	2	2	6	6	-8	5	2	10	10	-6	8	2	4	5	-1	-9	3	6	7	2	-6	3	24	24
4	2	2	8	8	-6	5	2	6	5	-5	8	2	4	2	0	-9	3	5	6	3	-6	3	8	7
6	2	2	7	8	-5	5	2	6	6	0	8	2	5	6	1	-9	3	7	8	4	-6	3	18	18
-10	3	2	7	8	-4	5	2	16	17	2	8	2	8	7	3	-9	3	11	11	5	-6	3	8	8
-9	3	2	8	9	-3	5	2	9	9	-8	9	2	8	6	4	-9	3	15	15	6	-6	3	7	7
-8	3	2	16	16	-2	5	2	32	33	-7	9	2	5	5	5	-9	3	9	10	9	-6	3	6	5
-6	3	2	13	13	-1	5	2	12	11	-5	9	2	6	5	7	-9	3	6	6	-6	-5	3	10	9

continued..

APPENDIX C (continued)

OBSERVED AND CALCULATED STRUCTURE FACTORS FOR MG TPP PIPERIDINE

H	K	L	FO	FC	H	K	L	FO	FC	H	K	L	FO	FC	H	K	L	FO	FC	H	K	L	FO	FC
-5	-5	3	14	14	1	-3	3	22	23	6	-1	3	7	9	-5	2	3	12	12	-7	5	3	12	12
-4	-5	3	11	10	2	-3	3	35	37	7	-1	3	5	6	-4	2	3	32	32	-6	5	3	9	8
-3	-5	3	13	13	3	-3	3	45	46	8	-1	3	4	4	-3	2	3	4	5	-5	5	3	13	13
-1	-5	3	14	13	4	-3	3	24	24	-8	0	3	5	6	-2	2	3	59	58	-4	5	3	12	12
0	-5	3	18	19	5	-3	3	4	3	-7	0	3	7	6	-1	2	3	6	5	-3	5	3	13	15
1	-5	3	6	6	6	-3	3	14	14	-6	0	3	14	14	0	2	3	16	16	-2	5	3	18	18
2	-5	3	11	11	7	-3	3	27	28	-5	0	3	4	4	1	2	3	6	7	-1	5	3	4	6
3	-5	3	6	6	-8	-2	3	7	7	-4	0	3	10	11	2	2	3	8	7	0	5	3	8	9
4	-5	3	4	3	-7	-2	3	4	3	-3	0	3	6	6	3	2	3	8	8	1	5	3	12	13
5	-5	3	4	3	-6	-2	3	7	7	-2	0	3	14	14	4	2	3	13	13	2	5	3	9	9
6	-5	3	5	5	-5	-2	3	8	7	-1	0	3	61	60	-8	3	3	5	5	4	5	3	6	6
8	-5	3	5	5	-4	-2	3	6	7	1	0	3	12	11	-6	3	3	21	20	-11	6	3	7	7
10	-5	3	9	7	-3	-2	3	51	50	2	0	3	8	8	-5	3	3	14	14	-10	6	3	5	3
-7	-4	3	6	7	-2	-2	3	3	3	3	0	3	9	8	-4	3	3	4	5	-7	6	3	8	8
-6	-4	3	8	8	-1	-2	3	32	32	4	0	3	13	13	-2	3	3	28	27	-6	6	3	4	4
-5	-4	3	9	10	0	-2	3	24	23	5	0	3	13	14	0	3	3	7	7	-3	6	3	55	57
-4	-4	3	18	18	2	-2	3	3	3	6	0	3	4	4	1	3	3	7	7	-2	6	3	8	8
-3	-4	3	7	7	3	-2	3	5	4	-10	1	3	4	4	3	3	3	14	14	-1	6	3	7	7
-2	-4	3	12	13	4	-2	3	14	13	-9	1	3	6	4	4	3	3	7	8	0	6	3	7	6
-1	-4	3	26	25	5	-2	3	17	18	-8	1	3	17	19	-10	4	3	6	7	1	6	3	5	5
0	-4	3	9	9	6	-2	3	21	23	-7	1	3	18	17	-9	4	3	11	11	2	6	3	4	3
1	-4	3	10	11	7	-2	3	7	7	-6	1	3	7	7	-7	4	3	10	10	3	6	3	4	4
2	-4	3	5	4	-8	-1	3	5	6	-5	1	3	3	3	-6	4	3	30	29	-11	7	3	5	5
3	-4	3	30	30	-6	-1	3	12	11	-4	1	3	23	22	-5	4	3	6	6	-7	7	3	5	6
4	-4	3	7	7	-4	-1	3	15	15	-3	1	3	6	6	-3	4	3	19	20	-6	7	3	5	5
5	-4	3	14	15	-3	-1	3	17	17	-2	1	3	48	48	-2	4	3	38	37	-5	7	3	4	4
9	-4	3	4	3	-2	-1	3	9	10	-1	1	3	23	22	-1	4	3	30	31	-4	7	3	11	11
-9	-3	3	4	4	-1	-1	3	73	75	2	1	3	15	14	0	4	3	3	4	-3	7	3	21	23
-8	-3	3	5	5	0	-1	3	58	58	3	1	3	11	11	1	4	3	7	7	-2	7	3	4	4
-7	-3	3	10	10	1	-1	3	27	27	4	1	3	19	19	3	4	3	13	13	-1	7	3	7	7
-4	-3	3	6	6	2	-1	3	11	11	5	1	3	9	8	-11	5	3	7	8	0	7	3	12	11
-3	-3	3	10	9	3	-1	3	29	25	6	1	3	4	5	-10	5	3	10	11	1	7	3	8	7
-2	-3	3	25	27	4	-1	3	10	9	-8	2	3	11	12	-9	5	3	4	4	2	7	3	5	3
0	-3	3	50	50	5	-1	3	19	19	-6	2	3	3	1	-8	5	3	4	5	-6	8	3	13	13

OBSERVED AND CALCULATED STRUCTURE FACTORS FOR MG TPP PIPERIDINE

H	K	L	FO	FC	H	K	L	FO	FC	H	K	L	FO	FC	H	K	L	FO	FC	H	K	L	FO	FC
-5	8	3	6	5	-2	-8	4	9	9	0	-5	4	34	34	-5	-2	4	31	31	-2	0	4	20	20
-4	8	3	12	11	-1	-8	4	8	7	1	-5	4	23	24	-4	-2	4	8	7	-1	0	4	5	6
-2	8	3	5	7	0	-8	4	16	16	2	-5	4	13	12	-3	-2	4	10	9	0	0	4	22	21
0	8	3	5	5	3	-8	4	7	8	3	-5	4	12	12	-2	-2	4	12	12	2	0	4	7	6
-7	9	3	9	10	5	-8	4	14	15	4	-5	4	6	5	-1	-2	4	12	11	3	0	4	4	5
-5	9	3	7	7	6	-8	4	5	5	5	-5	4	7	7	0	-2	4	22	23	4	0	4	13	12
-4	9	3	13	14	9	-8	4	4	4	7	-5	4	5	6	1	-2	4	19	19	5	0	4	17	18
-7	10	3	5	5	-5	-7	4	6	6	-6	-4	4	6	6	2	-2	4	33	32	6	0	4	5	5
0	10	3	4	3	-4	-7	4	17	18	-5	-4	4	5	3	3	-2	4	4	3	-9	1	4	12	12
0	-12	4	5	5	-3	-7	4	12	13	-4	-4	4	11	10	4	-2	4	7	9	-8	1	4	4	4
1	-12	4	8	7	-2	-7	4	14	15	-2	-4	4	3	4	5	-2	4	4	3	-6	1	4	9	9
5	-12	4	7	9	-1	-7	4	15	15	-1	-4	4	4	3	7	-2	4	8	9	-4	1	4	10	10
-2	-11	4	5	5	2	-7	4	20	19	0	-4	4	28	27	-7	-1	4	9	10	-3	1	4	5	5
0	-11	4	5	2	3	-7	4	5	4	1	-4	4	27	26	-6	-1	4	16	15	-2	1	4	6	6
1	-11	4	9	9	5	-7	4	10	10	2	-4	4	9	9	-5	-1	4	6	5	-1	1	4	6	7
3	-11	4	5	6	6	-7	4	6	5	3	-4	4	27	27	-4	-1	4	22	22	0	1	4	10	10
4	-11	4	7	7	7	-7	4	10	11	4	-4	4	21	21	-3	-1	4	27	28	3	1	4	9	9
5	-11	4	9	8	-7	-6	4	6	5	5	-4	4	4	4	-2	-1	4	31	32	4	1	4	7	7
7	-11	4	6	5	-6	-6	4	9	10	6	-4	4	8	8	-1	-1	4	9	10	5	1	4	17	18
9	-11	4	6	6	-5	-6	4	4	4	-7	-3	4	10	8	0	-1	4	13	14	-9	2	4	8	9
-3	-10	4	4	2	-4	-6	4	8	8	-5	-3	4	7	6	1	-1	4	14	14	-8	2	4	6	7
2	-10	4	5	5	-3	-6	4	9	9	-2	-3	4	36	34	2	-1	4	22	21	-7	2	4	11	11
3	-10	4	6	6	-2	-6	4	10	11	-1	-3	4	31	31	3	-1	4	7	7	-5	2	4	6	6
5	-10	4	5	3	-1	-6	4	13	14	0	-3	4	10	9	4	-1	4	9	9	-4	2	4	10	10
7	-10	4	11	12	1	-6	4	13	13	1	-3	4	15	15	5	-1	4	5	6	-3	2	4	10	10
8	-10	4	12	12	2	-6	4	25	24	2	-3	4	29	29	6	-1	4	11	12	-2	2	4	8	8
-1	-9	4	8	8	3	-6	4	4	5	3	-3	4	6	6	7	-1	4	5	5	-1	2	4	10	10
0	-9	4	11	11	5	-6	4	4	3	4	-3	4	11	10	-9	0	4	11	12	0	2	4	10	10
1	-9	4	15	15	9	-6	4	5	3	5	-3	4	18	17	-8	0	4	6	6	1	2	4	11	11
2	-9	4	5	5	-7	-5	4	8	7	6	-3	4	6	6	-7	0	4	6	6	3	2	4	24	24
5	-9	4	5	5	-5	-5	4	5	5	9	-3	4	7	6	-6	0	4	4	4	4	2	4	9	10
6	-9	4	7	7	-4	-5	4	19	18	-8	-2	4	6	6	-5	0	4	7	6	-10	3	4	4	2
7	-9	4	10	10	-2	-5	4	10	10	-7	-2	4	8	8	-4	0	4	46	44	-9	3	4	14	16
-3	-8	4	8	8	-1	-5	4	17	16	-6	-2	4	14	15	-3	0	4	12	11	-8	3	4	14	13

continued..

APPENDIX C (continued)

OBSERVED AND CALCULATED STRUCTURE FACTORS FOR MG TPP PIPERIDINE PAGE 7

H	K	L	FO	FC	H	K	L	FO	FC	H	K	L	FO	FC	H	K	L	FO	FC	H	K	L	FO	FC
-7	3	4	6	6	0	6	4	4	4	0-10	5	13	14	3	-7	5	9	9	2	-4	5	22	23
-5	3	4	21	20	2	6	4	10	10	1-10	5	4	3	4	-7	5	9	10	3	-4	5	5	7
-4	3	4	23	23	-5	7	4	10	9	2-10	5	4	5	5	-7	5	9	8	5	-4	5	4	4
-2	3	4	3	4	-4	7	4	19	20	4-10	5	10	10	6	-7	5	7	6	9	-4	5	5	5
-1	3	4	13	15	-3	7	4	17	17	5-10	5	6	5	7	-7	5	8	9	-9	-3	5	6	5
0	3	4	4	5	-8	8	4	10	10	7-10	5	4	5	-6	-6	5	6	6	-7	-3	5	8	7
3	3	4	16	16	-7	8	4	9	9	8-10	5	5	4	-4	-6	5	6	6	-6	-3	5	7	9
4	3	4	6	5	-5	8	4	7	9	-3	-9	5	4	4	-3	-6	5	6	7	-3	-3	5	23	23
5	3	4	7	8	-4	8	4	34	37	-2	-9	5	4	4	-2	-6	5	16	16	-2	-3	5	22	19
-9	4	4	4	4	-3	8	4	4	4	-1	-9	5	4	4	-1	-6	5	22	22	-1	-3	5	53	51
-8	4	4	10	10	-2	9	4	5	6	0	-9	5	4	4	0	-6	5	11	10	0	-3	5	25	24
-6	4	4	8	8	-9	9	4	6	6	2	-9	5	11	11	1	-6	5	9	9	1	-3	5	29	29
-5	4	4	25	24	-5	9	4	5	5	3	-9	5	4	4	3	-6	5	12	11	3	-3	5	7	7
-4	4	4	4	5	-4	9	4	12	13	4	-9	5	4	4	4	-6	5	19	19	5	-3	5	7	6
-3	4	4	32	32	-7	10	4	5	5	6	-9	5	5	6	5	-6	5	5	6	-9	-2	5	5	5
-2	4	4	18	18	-5	10	4	8	8	7	-9	5	7	6	7	-6	5	8	8	-7	-2	5	7	7
0	4	4	15	16	-9	11	4	5	4	8	-9	5	8	8	-6	-5	5	11	10	-6	-2	5	4	5
2	4	4	4	4	-5	11	4	6	6	-3	-8	5	5	6	-5	-5	5	17	17	-5	-2	5	20	19
4	4	4	6	6	4	-13	5	6	5	-1	-8	5	9	9	-4	-5	5	10	10	-4	-2	5	24	24
-11	5	4	7	7	0	-12	5	7	6	0	-8	5	16	15	-3	-5	5	4	5	-2	-2	5	9	7
-7	5	4	13	15	1	-12	5	10	9	1	-8	5	19	19	-2	-5	5	7	8	-1	-2	5	9	10
-6	5	4	16	16	3	-12	5	4	3	2	-8	5	6	6	-1	-5	5	29	29	0	-2	5	39	39
-5	5	4	6	6	4	-12	5	4	6	3	-8	5	11	12	1	-5	5	9	8	2	-2	5	14	13
-4	5	4	18	18	7	-12	5	6	5	4	-8	5	7	7	2	-5	5	20	19	3	-2	5	11	11
-3	5	4	6	7	-2	-11	5	4	3	5	-8	5	8	8	3	-5	5	13	13	5	-2	5	14	14
-2	5	4	11	12	0	-11	5	10	10	6	-8	5	12	12	4	-5	5	14	14	6	-2	5	6	5
1	5	4	18	19	1	-11	5	8	8	7	-8	5	13	13	5	-5	5	7	7	-9	-1	5	6	7
-10	6	4	5	6	2	-11	5	6	5	8	-8	5	5	6	8	-5	5	7	8	-8	-1	5	11	11
-9	6	4	5	5	4	-11	5	10	11	-4	-7	5	10	9	-8	-4	5	4	4	-7	-1	5	4	4
-8	6	4	4	3	5	-11	5	6	7	-2	-7	5	5	5	-7	-4	5	8	9	-6	-1	5	14	14
-7	6	4	14	15	7	-11	5	8	9	-1	-7	5	15	14	-5	-4	5	11	11	-5	-1	5	6	7
-6	6	4	5	4	8	-11	5	5	3	0	-7	5	15	16	-4	-4	5	11	11	-4	-1	5	11	11
-5	6	4	8	9	-3	-10	5	8	8	1	-7	5	7	8	0	-4	5	4	6	-3	-1	5	3	1
-3	6	4	12	12	-1	-10	5	5	5	2	-7	5	6	6	1	-4	5	34	33	-2	-1	5	5	6

OBSERVED AND CALCULATED STRUCTURE FACTORS FOR MG TPP PIPERIDINE PAGE 8

H	K	L	FO	FC	H	K	L	FO	FC	H	K	L	FO	FC	H	K	L	FO	FC	H	K	L	FO	FC
-1	-1	5	4	3	-3	2	5	5	4	-4	6	5	4	4	3	-11	6	7	8	4	-7	6	12	12
0	-1	5	18	18	-2	2	5	25	24	-3	6	5	8	10	4	-11	6	10	10	5	-7	6	10	10
1	-1	5	19	18	-1	2	5	39	38	-2	6	5	8	9	6	-11	6	10	8	7	-7	6	13	14
2	-1	5	24	23	3	2	5	5	6	-1	6	5	17	18	7	-11	6	6	5	-5	-6	6	6	5
4	-1	5	8	9	4	2	5	20	20	0	6	5	7	7	8	-10	6	13	13	-4	-5	6	8	7
8	-1	5	5	3	-10	3	5	6	5	-10	7	5	5	3	3	-10	6	15	16	-3	-6	6	5	3
-9	0	5	8	8	-8	3	5	8	9	-9	7	5	5	2	5	-10	6	4	2	-2	-6	6	5	5
-8	0	5	14	14	-7	3	5	4	4	-7	7	5	6	5	6	-10	6	6	6	-1	-6	6	25	25
-7	0	5	7	7	-5	3	5	10	10	-6	7	5	14	14	-4	-9	6	5	6	0	-6	6	16	16
-6	0	5	17	17	-4	3	5	9	10	-5	7	5	6	6	-2	-9	6	8	8	2	-6	6	15	15
-4	0	5	6	5	-3	3	5	22	22	-4	7	5	7	9	-1	-9	6	12	12	3	-6	6	12	12
-3	0	5	10	9	-2	3	5	10	11	-2	7	5	8	8	0	-9	6	14	15	5	-6	6	7	7
-2	0	5	5	5	-1	3	5	14	13	-1	7	5	8	9	1	-9	6	7	7	6	-6	6	10	11
-1	0	5	23	23	0	3	5	10	10	0	7	5	9	10	2	-9	6	6	6	9	-6	6	7	7
0	0	5	16	16	2	3	5	9	9	-8	8	5	10	11	3	-9	6	14	14	-5	-5	6	5	5
1	0	5	37	37	4	3	5	7	9	-7	8	5	9	9	4	-9	6	9	9	-2	-5	6	9	8
2	0	5	7	7	-9	4	5	6	5	-6	8	5	11	10	6	-9	6	7	7	0	-5	6	16	16
3	0	5	7	7	-8	4	5	10	10	-5	8	5	8	7	8	-9	6	6	5	1	-5	6	10	11
4	0	5	5	6	-4	4	5	3	4	-1	8	5	4	2	-4	-8	6	8	8	3	-5	6	7	7
5	0	5	6	6	-3	4	5	24	25	-8	9	5	5	5	-2	-8	6	5	4	4	-5	6	5	5
-7	1	5	10	9	-1	4	5	6	7	-6	9	5	7	8	-1	-8	6	23	24	5	-5	6	7	7
-5	1	5	21	21	1	4	5	5	7	-5	9	5	9	11	0	-8	6	8	8	6	-5	6	9	10
-3	1	5	3	3	2	4	5	16	16	-4	9	5	7	9	2	-8	6	9	8	8	-5	6	4	3
-2	1	5	5	5	3	4	5	7	7	-1	9	5	6	5	3	-8	6	18	17	-8	-4	6	10	10
-1	1	5	12	11	-10	5	5	5	6	-9	10	5	4	4	4	-8	6	6	7	-5	-4	6	12	11
0	1	5	15	16	-9	5	5	9	10	-6	10	5	4	6	6	-8	6	8	8	-3	-4	6	5	5
1	1	5	9	9	-6	5	5	6	5	-5	10	5	12	15	7	-8	6	9	9	-2	-4	6	15	15
2	1	5	5	4	-5	5	5	8	7	-5	11	5	9	9	-6	-7	6	4	3	-1	-4	6	9	8
3	1	5	21	21	-3	5	5	5	6	3	-13	6	5	4	-4	-7	6	9	8	0	-4	6	16	16
4	1	5	14	15	-1	5	5	10	10	1	-12	6	5	5	-3	-7	6	7	8	3	-4	6	31	30
5	1	5	10	11	2	5	5	5	6	4	-12	6	4	5	-2	-7	6	4	6	5	-4	6	4	5
-10	2	5	6	8	-11	6	5	6	6	6	-12	6	7	7	-1	-7	6	21	21	6	-4	6	16	16
-6	2	5	6	5	-10	6	5	6	7	0	-11	6	7	7	2	-7	6	11	10	7	-4	6	10	10
-5	2	5	35	34	-9	6	5	8	9	2	-11	6	4	4	3	-7	6	14	14	-9	-3	6	6	5

continued..

APPENDIX C (continued)

OBSERVED AND CALCULATED STRUCTURE FACTORS FOR MG TPP PIPERIDINE PAGE 9

H	K	L	FO	FC	H	K	L	FO	FC	H	K	L	FO	FC	H	K	L	FO	FC	H	K	L	FO	FC
-6	-3	6	10	10	1	0	6	11	12	0	3	6	15	15	-6	7	6	4	4	4	-8	7	4	5
-5	-3	6	4	3	-9	1	6	9	10	4	3	6	11	11	0	7	6	4	3	-5	-7	7	11	11
-3	-3	6	9	10	-7	1	6	8	7	-11	4	6	5	6	1	7	6	5	4	-4	-7	7	8	6
-2	-3	6	23	22	-5	1	6	13	12	-10	4	6	5	5	-10	8	6	6	7	-3	-7	7	5	4
-1	-3	6	6	7	-3	1	6	3	1	-9	4	6	6	7	-8	8	6	4	4	-2	-7	7	8	8
0	-3	6	9	9	-2	1	6	4	4	-6	4	6	14	13	-4	8	6	8	7	-1	-7	7	8	8
1	-3	6	9	8	-1	1	6	15	15	-5	4	6	10	10	-2	8	6	6	7	0	-7	7	4	4
2	-3	6	8	7	0	1	6	15	15	-3	4	6	4	3	-7	9	6	7	6	2	-7	7	8	8
3	-3	6	13	12	1	1	6	26	25	-2	4	6	9	9	-1	9	6	4	3	-5	-6	7	14	13
4	-3	6	5	5	2	1	6	5	4	-1	4	6	8	7	2-12		7	5	4	-4	-6	7	4	4
5	-3	6	9	9	3	1	6	8	9	1	4	6	8	8	3-12		7	4	3	-2	-6	7	19	20
7	-3	6	7	6	4	1	6	4	4	3	4	6	16	15	5-12		7	7	6	-1	-6	7	4	5
-8	-2	6	12	12	-10	2	6	7	7	-9	5	6	7	9	1-11		7	7	7	1	-6	7	12	12
-5	-2	6	10	9	-9	2	6	10	11	-7	5	6	4	2	5-11		7	4	2	2	-6	7	8	7
-3	-2	6	26	27	-8	2	6	5	3	-6	5	6	6	7	7-11		7	6	4	3	-6	7	11	10
-2	-2	6	11	13	-7	2	6	13	12	-5	5	6	4	5	-3-10		7	4	3	4	-6	7	6	7
-1	-2	6	3	2	-6	2	6	7	7	-4	5	6	5	6	0-10		7	4	4	5	-6	7	13	14
0	-2	6	30	30	-5	2	6	7	7	-3	5	6	8	9	1-10		7	6	5	6	-6	7	11	11
3	-2	6	5	6	-4	2	6	7	6	-2	5	6	9	10	2-10		7	4	5	-6	-5	7	7	6
4	-2	6	8	7	-3	2	6	15	15	-1	5	6	4	3	3-10		7	10	10	-5	-5	7	10	10
-8	-1	6	13	13	-1	2	6	13	12	0	5	6	10	11	4-10		7	5	5	-2	-5	7	31	32
-3	-1	6	7	6	0	2	6	25	24	1	5	6	6	6	5-10		7	10	9	-1	-5	7	6	6
-2	-1	6	16	14	1	2	6	8	8	2	5	6	11	11	6-10		7	7	6	0	-5	7	11	10
0	-1	6	11	11	2	2	6	13	13	3	5	6	5	5	-1	-9	7	10	10	1	-5	7	11	10
1	-1	6	6	5	3	2	6	9	10	-9	6	6	4	4	0	-9	7	4	4	2	-5	7	23	22
3	-1	6	10	11	4	2	6	4	4	-8	6	6	6	7	1	-9	7	7	7	3	-5	7	17	16
5	-1	6	10	10	-11	3	6	5	4	-6	6	6	9	8	2	-9	7	6	6	4	-5	7	9	10
-10	0	6	6	6	-10	3	6	8	8	-4	6	6	11	13	3	-9	7	10	10	5	-5	7	4	3
-6	0	6	4	4	-8	3	6	5	5	-3	6	6	13	13	4	-9	7	9	9	6	-5	7	13	13
-5	0	6	9	9	-6	3	6	14	13	-2	6	6	7	8	5	-9	7	9	9	-6	-4	7	5	4
-4	0	6	6	5	-5	3	6	14	14	1	6	6	7	8	6	-9	7	5	5	-4	-4	7	6	6
-3	0	6	22	21	-4	3	6	9	10	2	6	6	5	5	-1	-8	7	26	26	-3	-4	7	12	13
-1	0	6	32	30	-2	3	6	8	8	-10	7	6	6	7	0	-8	7	7	7	-2	-4	7	19	20
0	0	6	6	4	-1	3	6	9	8	-7	7	6	4	4	2	-8	7	9	8	-1	-4	7	5	5

OBSERVED AND CALCULATED STRUCTURE FACTORS FOR MG TPP PIPERIDINE PAGE 10

H	K	L	FO	FC	H	K	L	FO	FC	H	K	L	FO	FC	H	K	L	FO	FC	H	K	L	FO	FC
0	-4	7	9	9	-5	-1	7	5	6	-3	2	7	7	7	-3	6	7	7	7	2	-7	8	11	11
1	-4	7	25	24	-4	-1	7	15	14	-2	2	7	22	22	-2	6	7	12	12	3	-7	8	5	6
2	-4	7	5	4	-3	-1	7	8	8	0	2	7	9	10	-7	7	7	8	7	4	-7	8	6	5
3	-4	7	10	9	-2	-1	7	10	9	2	2	7	5	5	-3	7	7	6	7	5	-7	8	4	4
4	-4	7	4	6	-1	-1	7	21	21	4	2	7	5	5	-10	8	7	4	5	-2	-6	8	20	20
5	-4	7	17	17	0	-1	7	5	4	-10	3	7	7	8	-5	8	7	7	6	-1	-6	8	6	6
6	-4	7	5	7	2	-1	7	5	4	-9	3	7	5	5	-1	8	7	4	2	1	-6	8	10	11
-8	-3	7	7	7	3	-1	7	16	17	-8	3	7	5	5	3-12		8	7	7	2	-6	8	11	11
-7	-3	7	6	4	4	-1	7	13	13	-7	3	7	4	2	5-12		8	6	7	4	-6	8	6	6
-5	-3	7	8	7	5	-1	7	5	5	-6	3	7	7	7	5-11		8	6	7	-6	-5	8	6	5
-3	-3	7	17	17	6	-1	7	6	6	-5	3	7	9	10	-3-10		8	4	4	-5	-5	8	7	7
-2	-3	7	16	16	-9	0	7	9	10	-3	3	7	4	4	2-10		8	4	4	-4	-5	8	7	5
-1	-3	7	7	7	-8	0	7	6	7	-2	3	7	4	4	4-10		8	10	9	-3	-5	8	8	7
0	-3	7	6	6	-7	0	7	9	9	-1	3	7	11	11	5-10		8	4	3	-2	-5	8	6	7
2	-3	7	8	8	-6	0	7	4	3	0	3	7	9	9	-2	-9	8	6	6	-1	-5	8	4	4
3	-3	7	13	12	-4	0	7	5	4	-11	4	7	6	8	1	-9	8	8	7	0	-5	8	5	4
4	-3	7	9	9	-2	0	7	6	5	-10	4	7	5	5	2	-9	8	5	5	1	-5	8	11	11
5	-3	7	5	6	-1	0	7	22	21	-8	4	7	8	8	4	-9	8	7	7	2	-5	8	11	11
-8	-2	7	4	5	2	0	7	4	4	-6	4	7	8	8	5	-9	8	6	6	3	-5	8	7	7
-7	-2	7	4	4	3	0	7	4	5	-5	4	7	10	11	-4	-8	8	6	6	5	-5	8	6	4
-6	-2	7	7	7	5	0	7	7	6	-4	4	7	5	5	-3	-8	8	7	6	-6	-4	8	16	15
-5	-2	7	6	6	-8	1	7	6	4	-3	4	7	7	6	-2	-8	8	6	5	-5	-4	8	12	12
-4	-2	7	10	10	-7	1	7	10	10	1	4	7	4	5	-1	-8	8	4	4	-4	-4	8	9	9
-3	-2	7	22	23	-3	1	7	5	4	2	4	7	4	4	1	-8	8	6	5	-3	-4	8	15	16
-2	-2	7	21	21	-2	1	7	10	10	-11	5	7	5	6	2	-8	8	7	8	-2	-4	8	9	10
-1	-2	7	11	11	-1	1	7	11	12	-6	5	7	8	8	3	-8	8	5	4	0	-4	8	6	6
1	-2	7	12	10	0	1	7	5	4	-5	5	7	12	12	4	-8	8	6	6	1	-4	8	14	13
2	-2	7	9	9	2	1	7	10	10	-3	5	7	5	4	5	-8	8	4	5	2	-4	8	6	6
5	-2	7	5	6	4	1	7	7	7	-1	5	7	12	12	6	-8	8	4	3	3	-4	8	5	6
6	-2	7	7	7	-9	2	7	6	6	0	5	7	11	11	-4	-7	8	5	3	5	-4	8	11	11
-10	-1	7	7	7	-8	2	7	6	6	-10	6	7	6	5	-2	-7	8	18	19	6	-4	8	5	4
-9	-1	7	4	5	-7	2	7	5	6	-8	6	7	4	5	-1	-7	8	7	7	-7	-3	8	14	12
-7	-1	7	13	13	-5	2	7	4	5	-7	6	7	5	6	0	-7	8	5	5	-6	-3	8	17	16
-6	-1	7	12	12	-4	2	7	7	7	-5	6	7	10	12	1	-7	8	8	7	-5	-3	8	7	7

continued..

APPENDIX C (continued)

OBSERVED AND CALCULATED STRUCTURE FACTORS FOR MG TPP PIPERIDINE

H	K	L	FO	FC	H	K	L	FO	FC	H	K	L	FO	FC	H	K	L	FO	FC	H	K	L	FO	FC
-4	-3	8	4	5	4	-1	8	5	4	2	2	8	6	5	2	-10	9	11	11	-3	-4	9	15	16
-3	-3	8	19	19	5	-1	8	4	5	-11	3	8	5	4	3	-10	9	5	3	-2	-4	9	7	6
-2	-3	8	13	12	6	-1	8	5	3	-9	3	8	6	7	1	-9	9	12	12	0	-4	9	12	12
-1	-3	8	10	11	-7	0	8	11	11	-8	3	8	6	5	2	-9	9	5	4	2	-4	9	7	8
0	-3	8	4	3	-6	0	8	7	7	-6	3	8	4	5	3	-9	9	7	7	-7	-3	9	8	8
1	-3	8	11	10	-5	0	8	12	12	-4	3	8	20	19	4	-9	9	5	5	-6	-3	9	10	10
2	-3	8	6	6	-4	0	8	24	23	-2	3	8	6	7	-4	-8	9	7	6	-5	-3	9	8	8
3	-3	8	12	12	-3	0	8	6	6	1	3	8	4	5	0	-8	9	5	4	-4	-3	9	16	16
5	-3	8	8	9	-2	0	8	7	7	3	3	8	4	2	1	-8	9	12	12	-3	-3	9	20	20
-7	-2	8	7	7	0	0	8	6	5	-9	4	8	4	1	2	-8	9	6	7	-2	-3	9	9	9
-6	-2	8	4	5	1	0	8	9	9	-8	4	8	6	6	3	-8	9	9	9	-1	-3	9	8	8
-5	-2	8	5	4	3	0	8	10	11	-6	4	8	4	4	4	-8	9	9	8	0	-3	9	10	11
-4	-2	8	11	11	4	0	8	10	9	-5	4	8	5	5	-4	-7	9	6	5	1	-3	9	5	6
-3	-2	8	21	21	5	0	8	7	6	-3	4	8	6	7	-3	-7	9	10	10	2	-3	9	5	5
-2	-2	8	7	7	-9	1	8	7	7	-9	5	8	5	5	0	-7	9	7	8	3	-3	9	9	9
0	-2	8	7	7	-8	1	8	11	12	-6	5	8	8	9	1	-7	9	5	4	4	-3	9	4	3
1	-2	8	8	7	-7	1	8	9	9	-5	5	8	4	5	2	-7	9	10	10	-7	-2	9	11	11
2	-2	8	12	12	-6	1	8	8	8	-4	5	8	4	4	3	-7	9	7	7	-6	-2	9	7	8
3	-2	8	18	18	-5	1	8	12	12	-3	5	8	4	5	4	-7	9	7	7	-4	-2	9	16	16
4	-2	8	10	9	-4	1	8	9	9	-2	5	8	8	8	6	-7	9	4	2	-3	-2	9	5	5
5	-2	8	5	5	-3	1	8	4	4	-1	5	8	5	5	-5	-6	9	8	8	-2	-2	9	5	4
-9	-1	8	4	3	-2	1	8	14	15	0	5	8	5	4	-1	-6	9	5	4	0	-2	9	10	9
-8	-1	8	5	3	1	1	8	7	7	-9	6	8	5	5	1	-6	9	11	10	1	-2	9	4	4
-7	-1	8	5	5	2	1	8	10	11	-7	6	8	6	7	2	-6	9	4	3	2	-2	9	6	5
-6	-1	8	4	1	3	1	8	5	5	-4	6	8	5	5	3	-6	9	11	11	4	-2	9	5	5
-5	-1	8	15	14	5	1	8	5	6	-2	6	8	6	6	4	-6	9	7	7	-7	-1	9	9	9
-4	-1	8	16	16	-10	2	8	5	6	-1	6	8	5	5	-3	-5	9	16	16	-6	-1	9	10	9
-3	-1	8	21	21	-9	2	8	5	5	-8	7	8	6	5	-1	-5	9	5	5	-3	-1	9	5	5
-2	-1	8	9	8	-8	2	8	7	7	-9	8	8	5	4	1	-5	9	6	6	-2	-1	9	14	14
-1	-1	8	4	5	-6	2	8	7	7	-4	8	8	4	5	2	-5	9	6	7	-1	-1	9	5	4
0	-1	8	5	6	-5	2	8	6	6	0	-11	9	7	5	3	-5	9	11	12	0	-1	9	9	9
1	-1	8	7	7	-4	2	8	6	6	2	-11	9	5	6	4	-5	9	10	10	1	-1	9	9	8
2	-1	8	18	19	-3	2	8	4	4	0	-10	9	6	6	-7	-4	9	4	4	2	-1	9	10	10
3	-1	8	6	6	-2	2	8	12	12	1	-10	9	5	5	-4	-4	9	8	9	4	-1	9	13	12

OBSERVED AND CALCULATED STRUCTURE FACTORS FOR MG TPP PIPERIDINE

H	K	L	FO	FC	H	K	L	FO	FC	H	K	L	FO	FC	H	K	L	FO	FC	H	K	L	FO	FC
-8	0	9	7	6	-9	4	9	4	4	0	-5	10	8	8	-1	-1	10	11	11	-1	4	10	9	10
-7	0	9	14	14	-6	4	9	4	4	2	-5	10	10	10	0	-1	10	6	7	-9	5	10	4	3
-5	0	9	7	5	-3	4	9	5	5	3	-5	10	8	7	1	-1	10	7	8	-7	5	10	5	2
-4	0	9	17	18	1	4	9	4	1	4	-5	10	7	7	4	-1	10	4	4	-6	5	10	11	9
-3	0	9	14	14	-5	5	9	7	8	-7	-4	10	5	5	-8	0	10	10	9	-7	6	10	6	6
-1	0	9	8	8	-4	5	9	6	5	-6	-4	10	10	10	-7	0	10	4	3	-1	-10	11	5	4
0	0	9	6	5	-3	5	9	5	6	-3	-4	10	6	5	-5	0	10	20	20	-3	-8	11	4	3
1	0	9	14	13	-1	5	9	6	6	-2	-4	10	4	3	-4	0	10	6	6	-1	-8	11	7	6
2	0	9	7	8	-8	6	9	4	4	-1	-4	10	6	7	-1	0	10	7	7	4	-8	11	6	5
3	0	9	8	8	-4	6	9	6	5	0	-4	10	12	11	0	0	10	5	5	-2	-7	11	7	7
4	0	9	5	5	-4	7	9	4	1	1	-4	10	10	10	3	0	10	6	6	-1	-7	11	4	3
-9	1	9	4	3	-2	7	9	4	3	2	-4	10	16	16	-8	1	10	9	10	0	-7	11	5	3
-8	1	9	11	11	-2	-10	10	7	5	3	-4	10	15	15	-7	1	10	8	8	4	-7	11	5	4
-5	1	9	18	18	4	-10	10	6	5	4	-4	10	5	5	-5	1	10	14	14	-6	-6	11	7	5
-4	1	9	16	16	5	-10	10	5	4	-6	-3	10	6	6	-4	1	10	8	8	-2	-6	11	5	5
-3	1	9	7	7	-1	-9	10	12	11	-4	-3	10	7	6	-2	1	10	5	4	0	-6	11	16	16
1	1	9	8	8	0	-9	10	5	5	-2	-3	10	14	15	-1	1	10	7	7	1	-6	11	5	4
2	1	9	5	5	1	-9	10	6	6	-1	-3	10	10	10	0	1	10	6	7	2	-6	11	11	12
3	1	9	5	4	1	-8	10	13	13	0	-3	10	19	19	1	1	10	7	7	3	-6	11	7	6
-10	2	9	4	5	2	-8	10	7	5	2	-3	10	7	7	2	1	10	6	5	-2	-5	11	5	6
-8	2	9	5	6	0	-7	10	9	10	3	-3	10	9	9	3	1	10	5	5	-1	-5	11	10	10
-7	2	9	7	7	1	-7	10	5	3	-5	-2	10	6	6	-9	2	10	5	5	0	-5	11	5	3
-6	2	9	8	8	3	-7	10	5	5	-4	-2	10	15	15	-8	2	10	9	9	1	-5	11	5	4
-5	2	9	24	24	6	-7	10	5	3	-2	-2	10	7	6	-6	2	10	5	4	2	-5	11	9	9
-1	2	9	5	6	-5	-6	10	6	6	-1	-2	10	14	14	-5	2	10	5	5	3	-5	11	4	5
0	2	9	11	11	-3	-6	10	7	6	0	-2	10	5	6	-2	2	10	10	9	-6	-4	11	8	8
1	2	9	4	3	-1	-6	10	10	10	1	-2	10	10	10	0	2	10	4	4	-5	-4	11	5	4
3	2	9	8	7	0	-6	10	15	15	-8	-1	10	7	8	2	2	10	7	6	-4	-4	11	5	5
-10	3	9	7	7	2	-6	10	11	10	-7	-1	10	5	4	-9	3	10	4	4	-2	-4	11	6	5
-9	3	9	5	8	3	-6	10	4	3	-6	-1	10	11	11	-4	3	10	6	5	-1	-4	11	10	10
-8	3	9	4	6	4	-6	10	4	6	-5	-1	10	13	12	-2	3	10	4	3	0	-4	11	5	5
-5	3	9	8	8	-5	-5	10	6	5	-4	-1	10	14	15	-6	4	10	15	14	1	-4	11	9	9
-1	3	9	8	8	-4	-5	10	5	5	-3	-1	10	9	10	-5	4	10	8	8	2	-4	11	8	8
0	3	9	5	4	-1	-5	10	12	13	-2	-1	10	7	8	-2	4	10	4	5	3	-4	11	4	4

continued..

APPENDIX C (continued)

OBSERVED AND CALCULATED STRUCTURE FACTORS FOR MG TPP PIPERIDINE PAGE 13

H	K	L	FO	FC	H	K	L	FO	FC	H	K	L	FO	FC	H	K	L	FO	FC	H	K	L	FO	FC
-6	-3	11	7	4	-5	0	11	13	13	-1	4	11	5	5	1	-3	12	4	6	-2	2	12	6	5
-4	-3	11	4	1	-4	0	11	5	4	-7	5	11	5	5	-7	-2	12	5	5	-2	-7	13	6	6
-3	-3	11	11	11	-2	0	11	6	6	-7	6	11	5	4	-2	-2	12	13	12	1	-7	13	6	5
-2	-3	11	5	5	1	0	11	6	5	-1	-9	12	5	4	-1	-2	12	5	5	1	-6	13	5	4
-1	-3	11	11	11	-9	1	11	6	7	3	-7	12	5	5	0	-2	12	9	9	-5	-5	13	6	6
0	-3	11	5	6	-8	1	11	7	5	-2	-6	12	11	12	-7	-1	12	8	7	-3	-4	13	7	6
2	-3	11	4	4	-6	1	11	6	7	-1	-6	12	4	5	-3	-1	12	8	7	1	-4	13	5	7
-4	-2	11	9	9	-5	1	11	4	5	0	-6	12	5	5	-2	-1	12	9	8	-4	-3	13	6	5
-2	-2	11	14	14	-1	1	11	4	3	2	-6	12	4	4	0	-1	12	6	4	-2	-3	13	8	8
-1	-2	11	6	8	-9	2	11	7	8	3	-6	12	9	8	1	-1	12	7	7	-4	-2	13	6	6
0	-2	11	7	8	-7	2	11	5	5	-3	-5	12	6	5	2	-1	12	5	4	-3	-2	13	6	6
1	-2	11	12	12	-6	2	11	9	10	-1	-5	12	9	9	-6	0	12	5	5	-2	-2	13	10	10
2	-2	11	13	14	-3	2	11	6	7	-3	-4	12	5	5	-5	0	12	4	4	-3	-1	13	9	9
-6	-1	11	4	5	-1	2	11	8	8	-1	-4	12	10	9	-3	0	12	8	7	0	-1	13	4	4
-5	-1	11	6	5	-9	3	11	8	7	0	-4	12	4	5	-2	0	12	6	5	-4	0	13	6	4
-3	-1	11	10	11	-6	3	11	12	11	1	-4	12	8	9	1	0	12	4	3	-3	0	13	12	11
-1	-1	11	12	12	-4	3	11	6	4	2	-4	12	7	6	-6	1	12	9	10	-7	1	13	4	4
1	-1	11	8	7	-2	3	11	5	3	3	-4	12	5	5	-4	1	12	4	1	-4	1	13	6	5
2	-1	11	9	8	-7	4	11	4	4	-3	-3	12	6	6	-2	1	12	7	7	-3	1	13	5	2
-8	0	11	7	7	-6	4	11	6	5	-2	-3	12	7	5	0	1	12	6	4	-4	-2	14	5	5
-6	0	11	8	9	-3	4	11	7	7	0	-3	12	6	6	-5	2	12	5	5					

REFERENCES

1. Miller, K.R. (1979) Scient. Am., 241, 102.
2. Katz, J.J. and Norris, J.R. in "Current Topics in Bioenergetics" Vol.5, Sanadi, D.R. and Packer, L. Eds., Academic Press, New York, (1973) pp41-75.
3. Matthews, B.W. and Fenna, R.E. (1980) Acc. Chem. Res. 13, 309.
4. Fenna, R.E., Matthews, B.W., Olson, J.M. and Shaw, E.K. (1974) J. Mol. Biol. 84, 231.
5. Fenna, R.E. and Matthews, B.W. (1975) Nature 258, 573.
6. Fenna, R.E. and Matthews, B.W. (1976) Brookhaven Symp. Biol. 28, 170.
7. Matthews, B.W., Fenna, R.E., Bolognesi, M.C., Schmid, M.L.F. and Olson, J.M. (1979) J. Mol. Biol. 131, 259.
8. Brackett, F.S., Olson, R.A. and Crickard, R.G. in "Research in Photosynthesis". Gaffron, H., Brown, A.H., French, C.S., Livingston, R., Rabinowitch, E.I., Strehler, B.L. and Tolbert, N.E., Eds., Interscience, New York, (1957) pp412-418.
9. Cohen, M.H. and Robertson, A. (1971) J. Theor. Biol. 31, 101.
10. Robertson, A., in "Some Mathematical Questions in Biology" Vol. 4, Cowan, J.D., Ed., Providence, Rhode Island, (1972) pp47-73.
11. Jordan, P.C., "Chemical Kinetics and Transport". Plenum Press, New York (1979) pp201-232.
12. Boxer, S.G. and Wright, K.A. (1979) J. Am. Chem. Soc. 101, 6791.
13. Wright, K.A. and Boxer, S.G. (1981) Biochem. 20, 7546.
14. Clarke, R.H., Hanlon, E.B. and Boxer, S.G. (1982) Chem. Phys. Lett. 89, 41.

15. Boxer, S.G., Kuki, A., Wright, K.A., Katz, B.A. and Xuong, N.H. (1982) Proc. Natl. Acad. Sci. 79, 1121.

16. Davis, R.C. and Pearlstein, R.M. (1979) Nature 280, 413.

17. Pearlstein, R.M., Davis, R.C. and Ditson, S.L. (1982) Proc. Natl. Acad. Sci. 79, 400.

18. Katz, J.J. and Hindman, J.C. in "Photochemical Conversion and Storage of Solar Energy". Connolly, J.S. Ed., Academic Press, New York, (1981) pp27-78.

19. Mahler, H.R. and Cordes, E.H. "Biological Chemistry", Harper and Row, New York, (1966) pp475-507.

20. Cotton, T.M. and Van Duyne, R.P. (1981) J. Am. Chem. Soc. 103, 6020.

21. Murata, T., Toda, F., Uchino, K. and Yakushiji, E. (1971) Biochim. Biophys. Acta 245, 208.

22. Thornber, J.P., Trosper, T.L., Strouse, C.E. in "Photosynthetic Bacteria", Clayton, R.K. and Sistrom, W.R. Eds., Plenum Press, New York, (1978) pp133-160.

23. Ballschmiter, K. and Katz, J.J. (1969) J. Am. Chem. Soc. 91, 2661.

24. Chow, H.C., Serlin, R. and Strouse, C.E. (1975) J. Am. Chem. Soc. 97, 7230.

25. Evans, T.A. and Katz, J.J. (1975) Biochim. Biophys. Acta 396, 414.

26. Shipman, L.L., Cotton, T.M., Norris, J.R. and Katz, J.J. (1976) J. Am. Chem. Soc. 98, 8222.

27. Field, R.J. and Noyes, R.M. (1974) J. Am. Chem. Soc. 96, 2001.

28. Field, R.J. and Noyes, R.M. (1974) J. Chem. Phys. 60, 1877.

29. Nicolis, G. and Prigogine, I. "Self-Organization in Nonequilibrium Systems", Wiley-Interscience, New York, (1977).

30. Marek, M. and Stuchl, I. (1975) Biophys. Chem. 3, 241.

31. Tyson, J. (1973) J. Chem. Phys. 58, 3919.

32. Pavlidis, T. "Biological Oscillators; Their Mathematical Analysis", Academic Press, New York, (1973).

33. Field, R.J., Koros, E. and Noyes, R.M. (1972) J. Am. Chem. Soc. 94, 8649.

34. Field, R.J. and Noyes, R.M. (1972) Nature 237, 390.

35. Noyes, R.M., Field, R.J. and Koros, E. (1972) J. Am. Chem. Soc. 94, 1394.

36. Noyes, R.M. and Field, R.J. (1977) Acc. Chem. Res. 10, 273.

37. Noyes, R.M., Field, R.J. and Thompson, R.C. (1971) J. Am. Chem. Soc. 93, 7315.

38. Tyson, J.J. "Lecture Notes in Biomathematics", Vol. 10, Springer-Verlag, New York, (1976).

39. Noszticzius, Z.J. (1977) J. Phys. Chem. 81, 185.

40. Lefever, R. and Horsthemke, W. (1979) Proc. Natl. Acad. Sci. 76, 2490.

41. Kitahara, K., Horsthemke, W. and Lefever, R. (1979) Phys. Lett. 70A, 377.

42. Evans, W.H. (1980) Nature 283, 521.

43. Unwin, P.N.T. and Zampighi, G. (1980) Nature 283, 545.

44. Fujii, H. and Sawada, Y. (1978) J. Chem. Phys. 69, 3830.

45. Cairns, J. (1975) Scient. Am. 233, 64.

46. Swan, G.W. "Lecture Notes in Biomathematics", Vol. 42, Springer-Verlag, New York, (1981).

47. Marek, M. and Svobodeva, E. (1975) Biophys. Chem. 3, 263.

48. Daan, S. and Berde, C.J. (1978) J. Theor. Biol. 70, 297.

49. Koehler, W.K. and Fleissner, G. (1978) Nature 274, 708.

50. Kawato, M. and Suzuki, R. (1980) J. Theor. Biol. 86, 547.

51. Yamanishi, J., Kawato, M. and Suzuki, R. (1980) Biol. Cybernetics 37, 219.

52. Ypey, D.L., Van Meerwijk, P.M. Ince, C. and Groos, G. (1980) J. Theor. Biol. 86, 731.

53. Nakajima, K. and Sawada, Y. (1981) J. Phys. Soc. Japan, 50, 687.

54. Nakajima, K. and Sawada, Y. (1980) J. Chem. Phys. 72, 2231.

55. Rodley, G.A. and Ong, C.C. (1983) Inorg. Chim. Acta 78, 171.

56. Rodley, G.A. and Ong, C.C. (1984) Inorg. Chim. Acta 92, in press.

57. Ong, C.C. and Rodley, G.A. (1983) J. Inorg. Biochem. 19, 189.

58. Ong, C.C. and Rodley, G.A. (1983) Inorg. Chim. Acta 79, 166.

59. Ong, C.C. and Rodley, G.A. (1983) Inorg. Chim. Acta 80, 177.

60. Timkovich, R. and Tulinsky, A. (1969) J. Am. Chem. Soc. 91, 4430.

61. Katz, J.J., Oettmeier, W. and Norris, N.R. (1976) Phil. Trans. Roy. Soc. Lond. B 273, 227.

62. Katz, J.J., Closs, G.L., Pennington, F.C., Thomas, M.R. and Strain, H.H. (1963) J. Am. Chem. Soc. 85, 3801.

63. Anderson, A.F.H. and Calvin, M., (1964) Arch. Biochem. Biophys. 107, 251.

64. Katz, J.J., Dougherty, R.C. and Boucher, L.J. in "The Chlorophylls", Vernon, L.P. and Seely, G.R., Eds., Academic Press, New York, (1966) pp185-251.

65. Henry, M. and Leicknam, J.P. (1970) Colloq. Int. C.N.R.S. 191, 317.

66. Boxer, S.G., Closs, G.L. and Katz, J.J. (1974) J. Am. Chem. Soc. 96, 7058.

67. Katz, J.J., Janson, T.R., Kostka, A.G., Uphaus, R.A. and Closs, G.L. (1972) J. Am. Chem. Soc. 94, 2883.

68. Katz, J.J., Strain, H.H., Leussing, D.L. and Dougherty, R.C. (1968) J. Am. Chem. Soc. 90, 784.

69. Katz, J.J. and Crespi, H.L. (1972) Pure Appl. Chem. 32, 221.

70. Closs, G.L., Katz, J.J.,Pennington, F.C., Thomas, M.R. and Strain, H.H. (1963) J. Am. Chem. Soc. 85, 3809.

71. Freed, S. and Sancier, K.M. (1954) J. Am. Chem. Soc. 76, 198.

72. Seely, G.R. and Folkmanis, A. (1964) J. Am. Chem. Soc. 86, 2763.

73. Seely, G.R. (1965) Spectrochim. Acta 21, 1847.

74. Livingston, R. and Weil, S. (1952) Nature 170, 750.

75. Livingstone, R., Watson, W.F. and McArdle, J. (1949) J. Am. Chem. Soc. 71, 1542.

76. Wei, P.E., Corwin, A.H. and Arellano, R. (1962) J. Org. Chem. 27, 3344.

77. Hambright, P. (1971) Coord. Chem. Rev. 6, 247.

78. Miller, J.R. and Dorough, G.D. (1952) J. Am. Chem. Soc. 74, 3977.

79. Smith, K.M. (1979) Acc. Chem. Res., 12, 374.

80. Abraham, R.J., Eivazi, F., Pearson, H. and Smith, K.M. (1976) J. Chem. Soc., Chem. Commun., 698.

81. Storm, C.B., Corwin, A.H., Arellano, R.R., Martz, M. and Weintraub, R. (1966) J. Am. Chem. Soc. 88, 2525.

82. Kadish, K.M. and Shiue, L.R. (1982) Inorg. Chem. 21, 1112.

83. Mehdi, S.H., Brisbin, D.A. and McBryde, W.A.E. (1976) Biochim. Biophys. Acta 444, 407.

84. Rossotti, F.J.C. and Rossotti, H. "The Determination of Stability Constants", McGraw-Hill, New York, (1961) pp270-298.

85. Wang, J.H., Nakahara, A., Fleischner, E.B. (1958) J. Am. Chem. Soc. 80, 1109.

86. Wang, J.H. (1967) Proc. Natl. Acad. Sci. 58, 37.

87. Wang, J.H. (1970) Science 167, 25.

88. Dickerson, R.E. and Geis, I. "The Structure and Action of Proteins", Harper and Row, New York, (1969).

89. Antonini, E. and Brunori, M. (1970) Ann. Rev. Biochem. 39, 977.

90. Huheey, J.E. "Inorganic Chemistry, principles of structure and reactivity" 2nd edition, Harper and Row, New York, (1978) pp731-795.

91. Grinstein, M. (1947) J. Biol. Chem. 167, 515.

92. Falk, J.E. "Porphyrins and Metalloporphyrins", Elsevier, Amsterdam (1964).

93. Baum, S.J., Burnham, B.F. and Plane, R.A. (1964) Proc. Natl. Acad. Sci. 52, 1439.

94. Baum, S.J. and Plane, R.A. (1966) J. Am. Chem. Soc. 88, 910.

95. Sauer, K. in "Bioenergetics of Photosynthesis" Govindjee, Ed., Academic Press, New York (1975) ppl15-181.

96. Seely, G.R. and Jensen, R.G. (1965) Spectrochim. Acta 21, 1835.

97. Baker, E.W., Brookhart, M.S. and Corwin, A.H. (1964) J. Am. Chem. Soc. 86, 4587.

98. Datta-Gupta, N. Malakar, D. and Ramcharan, R.G. (1981) J. Inorg. Nucl. Chem. 43, 2079.

99. Kirksey, C.H., Hambright, P. and Storm, C.B. (1969) Inorg. Chem. 8, 2141.

100. Vogel, G.C. and Beckman, B.A. (1976) Inorg. Chem. 15, 483.

101. Vogel, G.C. and Searby, L.A. (1973) Inorg. Chem. 12, 936.

102. Nappa, M. and Valentine, J.S. (1978) J. Am. Chem. Soc. 100, 5075.

103. Hambright, P. (1967) J. Chem. Soc. Chem. Commun. 470.

104. Cole, S.J., Curthoys, G.C., Magnusson, E.A. and Phillips, J.N. (1972) Inorg. Chem. 11, 1025.

105. McLees, B.D. and Caughey, W.S. (1968) Biochem. 7, 642.

106. Erdman, J.G., Ramsey, V.G., Kalenda, N.W. and Hanson, W.E. (1956) J. Am. Chem. Soc. 78, 5844.

107. Pratt, J.M. in "Techniques and Topics in Bioinorganic Chemistry", McAulifee, C.A. Ed., MacMillan Press, London (1975) pp113-153.

108. Cole, S.J., Curthoys, G.C. and Magnusson, E.A. (1970) J. Am. Chem. Soc. 92, 2991.

109. Cole, S.J., Curthoys, G.C. and Magnusson, E.A. (1971) J. Am. Chem. Soc. 93, 2153.

110. Phillips, J.N. (1960) Rev. Pure Appl. Chem. 10, 35.

111. Falk, J.E. and Phillips, J.N. in "Chelating Agents and Metal Chelates", Dwyer, F.P. and Mellor, D.P. Eds., Academic Press, New York, (1964) pp441-490.

112. Hilinski, E.F. and Rentzepis, P.M. (1983) Nature 302, 481.

113. Boucher, L.J. and Katz, J.J. (1967) J. Am. Chem. Soc. 89, 4703.

114. Katz, J.J. in "Bioinorganic Chemistry" Vol. 2, Eichhorn, G.L. Ed., Elsevier, Amsterdam, (1973) pp1022-1066.

115. Weast, R.C. and Astle, M.J. "CRC Handbook of Chemistry and Physics", 60th edition, (1979-1980).

116. Collins, D.M. and Hoard, J.L. (1970) J. Am. Chem. Soc. 92, 3761.

117. Kenner, G.W., Rimmer, J., Smith, K.M. and Unsworth, J.F. (1976) Phil. Trans. Roy. Soc. Lond. B. 273, 255.

118. Mauzerall, D. (1976) Phil. Trans. Roy. Soc. Lond. B. 273, 287.

119. Marks, G.S. "Hemes and Chlorphyll", D. Van Nostrand Company, London, (1969) pp121-162.

120. Wang, J.H. (1970) Acc. Chem. Res. 3, 90.

121. Reed, C.A. in "Metal ions in biological systems', Vol. 7, Sigel, H. Ed., Marcel Dekker, New York, (1978) pp277-310.

122. Nakahara, A. and Wang, J.H. (1958) J. Am. Chem. Soc. 80, 6526.

123. Brault, D. and Rougee, M. (1974) Biochem. 13, 4591.

124. Rossotti, F.J.C. in "Modern Coordination Chemistry", Lewis, J. and Wilkins, R.G. Eds., Interscience, New York, (1960) pp1-77.

125. Makinen, M.W. in "Techniques and Topics in Bioinorganic Chemistry", McAulifee, C.A. Ed., MacMillan Press, London, (1975) pp21-59.

126. Martin, R.L. and White, A.H. in "Transition Metal Chemistry" Vol. 4, Carlin, R.L. Ed., Dekker, New York, (1968) pp113-198.

127. Allen, M.B., Murchio, J.C., Jeffrey, S.W. and Bendix, S.A. in "Studies on Microalgae and Photosynthetic Bacteria", Japan Soc. Plant Physiol. Ed., Uni. of Tokyo, (1963) pp407-412.

128. Goedheer, J.C. in "The Chlorophylls", Vernon, L.P. and Seely, G.R., Eds., Academic Press, New York, (1966) pp399-411.

129. Yakushiji, E., Uchino, K., Sigimura, Y., Shiratori, I. and Takamiya, A. (1963) Biochim. Biophys. Acta 75, 293

130. Olson, J.M. in "The Chlorophylls", Vernon, L.P. and Seely, G.R., Eds., Academic Press, New York, (1966) pp413-425

131. Thornber, J.P., Markwell, J.P. and Reinman, S. (1979) Photochem. Photobiol. 29, 1205.

132. Takamiya, A., Kamimura, Y. and Kira, A. in "Comparative Biochemistry and Biophysics of Photosynthesis", Shibata, K., Takamiya, A., Jagendorf, A.T. and Fuller, R.C. Eds., University of Tokyo Press, Tokyo, (1968) pp229-239.

133. Thornber, J.P., Alberte, R.S., Hunter, F.A., Shiozawa, J.A. and Kan, K.S. (1977) Brookhaven Symp. Biol. 28, 132.

134. Clayton, R.K. and Clayton, B.J. (1972) Biochim. Biophys. Acta 283, 492.

135. Davis, D.J. and Gross, E.L. (1976) Biochim. Biophys. Acta 449, 554.

136. Thornber, J.P. and Olson, J.M. (1968) Biochem. 7, 2242.

137. Takahashi, M. and Gross, E.L. (1978) Biochem. 17, 806.

138. Thornber, J.P. (1975) Ann. Rev. Plant Physiol. 26, 127.

139. Sauer, K. and Austin, L.A. (1978) Biochem. 17, 2011.

140. Okamura, M.Y., Steiner, L.A. and Feher, G. (1974) Biochem. 13, 1394.

141. Steiner, L.A., Okamura, M.Y., Lopes, A.D., Moskowitz, E. and Feher, G. (1974) Biochem. 13, 1403.

142. Williams, W.R., Sen, A. and Quinn, P.J. (1982) Biochem. Soc. Trans. 10, 335.

143. Sauer, K. (1978) Acc. Chem. Res. 11, 257.

144. Kendrew, J.C. (1962) Brookhaven Symp. Biol. 15, 216.

145. Perutz, M.F., Muirhead, H., Cox, J.M., Goaman, L.C.G. (1968) Nature 219, 131.

146. Katz, J.J., Shipman, L.L., Cotton, T.M. and Janson, T.R. in "The Porphyrins", Vol. 5, Dolphin, D. Ed., Academic Press, New York, (1978) pp401-458.

147. Cotton, T.M., Trifunac, A.D., Ballschmiter, K. and Katz, J.J. (1974) Biochim. Biophys. Acta 386, 181.

148. Philipson, K.D. and Sauer, K. (1972) Biochem. 11, 1880.

149. Beddard, G. in "Photochemistry Part VI. Chemical Aspects of Photobiology",Vol. 10, Specialist Periodic Reports, The Chemical Society, Burlington House, London, (1979) pp633-670.

150. Callahan, P.M. and Babcock, G.T. (1983) Biochem. 22, 452.

151. Ward, B., Callahan, P.M., Young, R., Babcock, G.T. and Chang, C.K. (1983) J. Am. Chem. Soc. 105, 634.

152. La Mar, G.N., Burns, P.D., Jackson, J.T., Smith K.M. and Langry, K.C. (1981) J. Biol. Chem. 256, 6075.

153. Warshel, A. and Weiss, R.M. (1981) J. Am. Chem. Soc. 103, 446.

154. Wasielewski, M.R., Norris, J.R., Shipman, L., Lin, C.P. and Svec, W.A. (1981) Proc. Natl. Acad. Sci. 78, 2957.

155. Davis, R.C., Ditson, S.L., Fentiman, A.F. and Pearlstein, R.M. (1981) J. Am. Chem. Soc. 103, 6823.

156. Seybert, D.W., Moffat, K. and Gibson, Q.H. (1976) J. Biol. Chem. 251, 45.

157. Yamamoto, H. and Yonetani, T. (1974) J. Biol. Chem. 249, 7964.

158. Falk, J.E., Phillips, J.N. and Magnusson, E.A. (1966) Nature 212, 1531.

159. Caughey, W.S. (1967) Ann. Rev. Biochem. 36, 611.

160. Asakura, T. and Sono, M. (1974) J. Biol. Chem. 249, 7087.

161. Tsubaki, M., Nagai, K. and Kitagawa, T. (1980) Biochem. 19, 379.

162. Gelin, B.R. and Karplus, M. (1977) Proc. Natl. Acad. Sci. 74, 801.

163. Keilin, J. in "Hemes and Hemoproteins", Chance, B., Estabrook, R. and Yonetani, T., Eds., Academic Press, New York, (1966) pp173-191.

164. Srivastava, T.S. (1981) Inorg. Chim. Acta 55, 161.

165. Srivastava, T.S. (1977) Biochim. Biophys. Acta 491, 599.

166. Antonini, E. and Brunori, M. "Hemoglobin and Myoglobin in their Reactions with Ligands", North-Holland, Amsterdam, (1971).

167. Granick, S. (1948) J. Biol. Chem. 172, 717.

168. Labbe, R.F. and Nishida, G. (1957) Biochim. Biophys. Acta 26, 437.

169. Chu, T.C. and Chu, E.J. (1955) J. Biol. Chem. 212, 1.

170. Walter, R.I. (1952) J. Biol. Chem. 196, 151.

171. Chu, T.C. and Chu, E.J. (1952) J. Am. Chem. Soc. 74, 6276.

172. Corwin, A.H. and Krieble, R.H. (1941) J. Am. Chem. Soc. 63, 1829.

173. Janson, T.R. and Katz, J.J. (1972) J. Magn. Reson. 6, 209.

174. Fuhrhop, J.H. and Granick, S. (1971) Biochem. Preparations 13, 55.

175. Breslow, E. (1964) J. Biol. Chem. 239, 486.

176. Teale, F.W.J. (1959) Biochim. Biophys. Acta 35, 543.

177. Rossi-Fanelli, A., Antonini, E. and Caputo, E.C. (1958) Biochim. Biophys. Acta 30, 608.

178. Alston, K. and Storm, C.B. (1979) Biochem. 18, 4292.

179. Bucci, E. and Fronticelli, C. (1965) J. Biol. Chem. 240, 551.

180. Waterman, M.R. and Yonetani, T. (1970) J. Biol. Chem. 245, 5857.

181. Whitmore, F.C. and Woodward, G.E. in "Organic Synthesis", Gilman, H. and Blatt, A.H. Eds., John Wiley, New York, (1941) pp159-160.

182. Boyer, P.D. (1954) J. Am. Chem. Soc. 76, 4331.

183. Lee, T.C.K. (1978) Anal. Biochem. 91, 646.

184. Creighton, T.E. (1979) J. Mol. Biol. 129, 235.

185. Stryer, L.J. (1965) J. Mol. Biol. 13, 482.

186. Yonetani, T., Yamamoto, H. and Woodrow, G.V. (1974) J. Biol. Chem. 249, 682.

187. Fluka Catalogue, Chemicals and Biochemicals, Switzerland, (1980-1981).

188. Ozols, J. and Strittmatter, P. (1964) J. Biol. Chem. 239, 1018.

189. Banerjee, R., Alpert, Y., Leterrier, F. and Williams, R.J.P. (1969) Biochem. 8, 2862.

190. Murata, T., Toda, F., Uchino, K., Yakushiji, E. (1971) Biochim. Biophys. Acta 245, 208.

191. Murata, T., Odaka, Y., Uchino, K. and Yakushiji, E. in "Comparative Biochemistry and Biophysics of Photosynthesis", Shibata, K., Takamiya, A., Jagendorf, A.T., Fuller, R.C. Eds., University of Tokyo Press, Tokyo, 1968 pp222-228.

192. Schumm, O. (1925) Hoppe-Seyler's Z. Physiol. Chem. 149, 111

193. La Mar, G.N., Budd, D.L., Viscio, D.B., Smith, K.M. and Langry, K.C. (1978) Proc. Natl. Acad. Sci, 75, 5755.

194. Rossi-Fanelli, A., Antonini, E. and Caputo, A. (1959) Biochim. Biophys. Acta 35, 93.

195. Hsu, M.C. and Woody, R.W. (1969) J. Am. Chem. Soc. 91, 3679.

196. Hsu, M.C. and Woody, R.W. (1971) J. Am. Chem. Soc. 93, 3515.

197. Chien, J.C.W. and Synder, F.W. Jr. (1976) J. Biol. Chem. 251, 1670.

198. Norvell, J.C., Nunes, A.C. and Schoenborn, B.P. (1975) Science 190, 568.

199. Phillips, S.E.V. and Schoenborn, B.P. (1981) Nature 292, 81.

200. Shaanan, B. (1982) Nature 296, 683.

201. Doster, W., Beece, D., Bowne, S.F., Dilorio, E.E., Eisenstein, L., Frauenfelder, H., Reinisch, L., Shyamsunder, E., Winterhalter, K.H., and Yue, K.T. (1982) Biochem. 21, 4831.

202. Caughey, W.S., Shimada, H., Choc, M.G., and Tucker, M.P. (1981) Proc. Natl. Acad. Sci. 78, 2903.

203. Choc, M.G. and Caughey, W.S. (1976) Biochem. 15, 388.

204. Choc, M.G. and Caughey, W.S. (1981) J. Biol. Chem. 256, 1831.

205. Bolard, J. and Garnier, A. (1972) Biochim. Biophys. Acta 263, 535.

206. Li, T.K. and Johnson, B.P. (1969) Biochem. 8, 3638.

207. Maxwell, J.C. and Caughey, W.S. (1976) Biochem. 15, 388.

208. Makinen, M.W., Houtchens, R.A. and Caughey, W.S. (1979) Proc. Natl. Acad. Sci. 76, 6042.

209. Maxwell, J.C., Volpe, J.A., Barlow, C.H. and Caughey, W.S. (1974) Biochem. Biophys. Res. Commun. 58, 166.

210. Maxwell, J.C. and Caughey, W.S. (1974) Biochem. Biophys. Res. Commun. 60, 1309.

211. Leonard, J.J., Yonetani, T. and Callis, J.B. (1974) Biochem. 13, 1460.

212. Atassi, M.Z. (1967) Biochem. J. 103, 29.

213. Hoffman, B.M. (1975) J. Am. Chem. Soc. 97, 1688.

214. Romberg, R.W. and Kassner, R.J. (1982) Biochem. 21, 880.

215. Muhoberac, B.B. and Brill, A.S. (1980) Biochem. 19, 5157.

216. Tamura, M., Woodrow III, G.V. and Yonetani, T. (1973) Biochim. Biophys. Acta 317, 34.

217. Sugita, Y. and Yoneyama, Y. (1971) J. Biol. Chem. 246, 389.

218. Smith, M.H. and Gibson, Q.H. (1959) Biochem. J. 73, 101.

219. Sono, M. and Asakura, T. (1975) J. Biol. Chem. 250, 5227.

220. Chang, C.K. (1977) J. Heterocyclic Chem. 14, 1285.

221. Mincey, T. and Traylor, T.G. (1979) J. Am. Chem. Soc. 101, 765.

222. Nicola, N.A. and Leach, S.J. (1977) Biochem. 16, 50.

223. Tamura, M., Asakura, T. and Yonetani, T. (1973) Biochim. Biophys. Acta 295, 467.

224. Perutz, M.F., Kilmartin, J.V., Nagai, K., Szabo, A. and Simon, S.R. (1976) Biochem. 15, 378.

225. Ollis, D.L., Wright, P.E., Pope, J.M. and Appleby, C.A. (1981) Biochem. 20, 587.

226. Ollis, D.L., Appleby, C.A., Colman, P.M., Cutten, A.E., Guss, J.M., Venkatappa, M.P. and Freeman, H.C. (1983) Aust. J. Chem. 36, 451.

227. Hamor,T.A., Caughey, W.S. and Hoard, J.L. (1965) J. Am. Chem. Soc. 87, 2305.

228. Hoard, J.L., Hamor, M.J. Hamor, T.A. and Caughey, W.S. (1965) J. Am. Chem. Soc. 87, 2312.

229. Moon, R.B., Dill, K. and Richards, J.H. (1977) Biochem. 16, 221.

230. Shelnutt, J.A., Rousseau, D.L., Friedman, J.M. and Simon, S.R. (1979) Proc. Natl.Acad. Sci. 76, 4409.

231. Deardorff, E.A., Carr, P.A.G. and Hurst, J.K. (1981) J. Am. Chem. Soc. 103, 6611.

232. Srivastava, T.S. (1980) Curr. Sci. 49, 900.

233. Srivastava, T.S. (1979) Curr. Sci. 48, 391.

234. Fiechtner, M.D., McLendon, G. and Bailey, M.W. (1980) Biochem. Biophys. Res. Commun. 92, 277.

235. Yonetani, T., Drott, H.R., Leigh, J.S.(Jr.), Reed, G.H., Waterman, M.R. and Asakura, T. (1970) J. Biol. Chem. 245, 2998.

236. Blough, N.V. and Hoffman, B.M. (1982) J. Am. Chem. Soc. 104, 4247.

237. Fabry, T.L., Simo, C. and Javaherian, K. (1968) Biochim. Biophys. Acta 160, 118.

238. Thiele, H.J., Behlke, J. and Scheler, W. (1964) Acta Biol. Med. Ger. 12, 19.

239. Moffat, K., Loe, R.S. and Hoffman, B.M. (1974) J. Am. Chem. Soc. 96, 5259.

240. Moffat, K., Loe, R.S. and Hoffman, B.M. (1976) J. Mol. Biol. 104, 669.

241. Bull, C., Fischer, R.G. and Hoffman, B.M. (1974) Biochem. Biophys. Res. Commun. 59, 140.

242. Gibson, Q.H., Hoffman, B.M., Crépeau, R.H., Edelstein, S.J. and Bull, C. (1974) Biochem. Biophys. Res. Commun. 59, 146

243. Hoffman, B.M. in "The Porphyrins", Vol. 7, Dolphin, D. Ed., Academic Press, New York, (1978) pp403-444.

244. Ikeda-Saito, M., Waldman, J.A., Yonetani, T. in "Porphyrin Chem. Adv. Pap. Porphyrin Symp", Ann Arbor, Michigan, (1979) pp179-188.

245. Fermi, G., Perutz, M.F., Dickinson, L.C. and Chien, J.C.W. (1982) J. Mol. Biol. 155, 495.

246. Hoffman, B.M. and Petering, D.H. (1970) Proc. Natl. Acad. Sci. 67, 637.

247. Hoffman, B.M., Spilburg, C.A. and Petering, D.H. (1971) Cold Spring Harbor Symp. Quart. Biol. 36, 343.

248. Hoffman, B.M. and Gibson, Q.H. (1978) Proc. Natl. Acad. Sci. 75, 21.

249. Chien, J.C. and Dickinson, L.C. (1972) Proc. Natl. Acad. Sci. 69, 2783.

250. Andres, S.F. and Atassi, M.Z. (1970) Biochem. 9, 2268.

251. O'Hagan, J.E. in "Hematin Enzymes", Vol. 19, Falk, J.E., Lemberg, R. and Morong, R.K. Eds., Pergamon, London, (1961) pp173-193.

252. Paulson, D.R., Addison, A.W., Dolphin, D. and James, B.R. (1979) J. Biol. Chem. 254, 7002.

253. Marshall, A.G., Lee, K.M. and Martin, P.W. (1980) J. Am. Chem. Soc. 102, 1460.

254. Horrocks, W. Dew (Jr.), Venteicher, R.F., Spilburg, C.A. and Vallee, B.L. (1975) Biochem. Biophys. Res. Commun. 64, 317.

255. Myer, Y.P. and Pande, A. in "The Porphyrins", Vol. 3, Dolphin, D. Ed., Academic Press, New York, (1978) pp271-322.

256. Blauer, G. in "Structure and Bonding", Vol. 18. Dunitz, J.D. Hemmerich, P., Holm, R.H., Ibers, J.A., Jorgensen, C.K., Neilands, J.B., Reinen, D. and Williams, R.J.P. Eds., Springer-Verlag, New York, (1974) pp69-129.

257. Jirgensons, B. "Optical Rotatory Dispersion of Proteins and Other Macromolecules", Molecular Biology 5, Springer-Verlag, New York (1969).

258. Harrison, S.C. and Blout, E.R. (1965) J. Biol. Chem. 240, 299.

259. Breslow, E., Beychock, S., Hardman, K.D. and Gurd, F.R.N. (1965). J. Biol. Chem. 240, 304.

260. Przywarska-Boniecka, H. and Trynda, L. (1978) Eur. J. Biochem. 87, 569.

261. Trynda, L. (1983) Inorg. Chim. Acta 78, 229.

262. Moscowitz, A. (1961) Tetrahedron 13, 48.

263. Day, P. (1967) Theor. Chim. Acta 7, 328.

264. Eichhorn, G.L. (1961) Tetrahedron 13, 208.

265. Sugita, Y., Nagai, M. and Yoneyama, Y. (1971) J. Biol. Chem. 246, 383.

266. Ruckpaul, K., Rein, H. and Jung, F. (1970) Naturiwssenchaften 57, 131.

267. Volkenstein, M.V., Metlyaev, L.T. and Milevskaya, I.S. (1969) Mol. Biol. 3, 190.

268. Kirkwood, J.G. (1937) J. Chem. Phys. 5, 479.

269. Woody, R.W. and Tinoco, I. (1967) J. Chem. Phys. 46, 4927.

270. Schellman, J.A. (1968) Acc. Chem. Res. 1, 144.

271. Woody, R.W. (1975) in "Protein-Ligand Interactions", Sund, H. and Glauer, G. Eds., Walter de Gruyter, Berlin, (1975) pp60-77.

272. Nagai, M., Sugita, Y. and Yoneyama, Y. (1969) J. Biol. Chem. 244, 1651.

273. Geraci, G. and Li, T.K. (1969) Biochem. 8, 1848.

274. Houssier, C. and Sauer, K. (1970) J. Am. Chem. Soc. 92, 779.

275. Atassi, M.Z. (1970) Biochim. Biophys. Acta 221, 612.

276. Harrington, J.P., Pandolfelli, E.R., and Herskovits, T.T. (1973) Biochim. Biophys. Acta 328, 61.

277. Nicola, N.A., Minasian, E., Appleby, C.A. and Leach, S.J. (1975) Biochem. 14, 5141.

278. Appleby, C.A., Nicola, N.A., Hurrell, J.G.R. and Leach, S.J. (1975) Biochem. 14, 4444.

279. Hatano, M. and Nozawa, T. (1972) Asahi Garasu Kogyo Gijutsu Shoreikai Kenkyu Hokoku 20, 213.

280. Casella, L., Gullotti, M. and Pacchioni, G. (1982) J. Am. Chem. Soc. 104, 2386.

281. Martin, R.B. in "Metal ions in biological systems", Vol. I, Sigel, H. Ed., Marcel Dekker, New York, (1974) pp129-156.

282. Sundberg, R.J. and Martin, R.B. (1974) Chem. Rev. 74, 471.

283. Taylor, J.F. (1940) J. Biol. Chem. 135, 569.

284. Hoard, J.L. in "Porphyrins and metalloporphyrins", Smith, K.M. ed., Elsevier, Amsterdam, (1975) pp317-380.

285. Bosnich, B. (1966) J. Am. Chem. Soc. 88, 2606.

286. Blout, E.R. and Stryer, L. (1959) Proc. Natl. Acad. Sci. 45, 1591.

287. Hayward, L.D. and Totty, R.N. (1971) Can. J. Chem. 49, 624.

288. Craig, D.P., Power, E.A. and Thirunamachandran, T. (1974) Chem. Phys. Lett. 27, 149.

289. Mason, S.F. (1975) Chem. Phys. Lett. 32, 201.

290. Mason, S.F. and Peacock, R.D. (1973) J. Chem. Soc. Chem. Commun. 712.

291. Sargeson, A.M. in "Chelating Agents and Metal Chelates", Dwyer, F.P. and Mellor, D.P. Eds., Academic Press, New York, (1964) pp183-235.

292. Rhoads, D.E., Peterson, N.A. and Raghupathy, E. (1982) Biochem. 21, 4782.

293. Drauz, K., Kleeman, A. and Martens, J. (1982) Angew. Chem. Int. Ed. 21, 584.

294. Tsangaris, J.M. and Martin, R.B. (1970) J. Am. Chem. Soc. 92, 4255.

295. Davankov, V.A., Rogozhin, S.V. and Kurganov, A.A. (1974) Izv. Akad. Nauk. SSSR, Ser. Khim., 6, 1313.

296. Kurganov, A.A., Zhuchkova, L.Ya. and Davankov, V.A. (1977) Izv. Akad. Nauk. SSSR, Ser. Khim., 11, 2540.

297. Yasui, T., Hidaka, J. and Shimura, Y. (1965) J. Am. Chem. Soc. 87, 2762.

298. Yasui, T. (1965) Bull. Chem. Soc. Japan, 38, 1746.

299. Yasui, T., Hidaka, J. and Shimura, Y. (1965), Bull. Chem. Soc. Japan, 38, 2025.

300. Bunel, S., Ibarra, C., Rodriguez, M., Urbina, A. and Bunton, C.A. (1981) J. Inorg. Nucl. Chem. 43, 967.

301. Gaudemer, A., Gaudemer, F. and Merienne, C. (1983) Org. Magn. Reson. 21, 83.

302. Bryce, C.F., Roeske, R.W. and Gurd, F.R.N. (1966) J. Biol. Chem. 241, 1072.

303. Boxer, S.G. and Bucks, R.R. (1981) Israel J. Chem. 21, 259.

304. Whitten, G. (1978) Rev. Chem. Intermed. 2, 107.

305. Mauzerall, D. and Hong, F.T. in "Porphyrins and Metalloporphyrins", Smith, K.M. ed., Elsevier, Amsterdam, (1975) pp701-725.

306. Hopf, F.R. and Whitten, D.G. in "Porphyrins", Vol. 2, Dolphin, D. Ed., Academic Press, New York, (1978). pp161-195.

307. Hopf, F.R. and Whitten, D.G. in "Porphyrins and Metalloporphyrins", Smith, K.M. Ed., Elsevier, Amsterdam, (1975) pp667-700.

308. Fuhrhop, J.H. (1974) Angew. Chem. Int. Ed., 13, 321.

309. Whitten, D.G. (1979) Angew. Chem. Int. Ed., 18, 440.

310. Turro, N.J. Gratzel, M. and Braun, A.M. (1980) Angew. Chem. Int. Ed. 19, 675.

311. Koiso, T., Okuyama, M., Sakata, T. and Kawai, T. (1982) Bull. Chem. Soc. Japan, 55, 2659.

312. Krüger, W. and Fuhrhop, J.H. (1982) Angew. Chem. Int. Ed. 21, 131.

313. Lascelles, J. "Tetrapyrrole Biosynthesis and its Regulation", W.A. Benjamin, New York, (1964) pp67-83.

314. Barrett, J. (1967) Nature 215, 733.

315. Fuhrhop, J.H., Wasser, P.K.W., Subramaniam, J. and Schrader, U. (1974) Liebigs Ann. Chem. 9, 1450.

316. Wasser, P.K.W. and Fuhrhop, J.H. (1973) Ann. New York Acad. Sci. 206, 533.

317. Fuhrhop, J.H. and Mauzerall, D. (1971) Photochem. Photobiol. 13, 453.

318. Oster, G., Broyde, S.B. and Bellin, J.S. (1964) J. Am. Chem. Soc. 86, 1309.

319. Oster, G., Bellin, J.S. and Broyde, S.B. (1964) J. Am. Chem. Soc. 86, 1313.

320. Brody, S.S. and Brody, M. (1961) Nature 189, 547.

321. Rafferty, C.N., Bolt, J., Sauer, K. and Clayton, R.K. (1979) Proc. Natl. Acad. Sci. 76, 4429.

322. Jori, G., Galiazzo, G. and Scoffone, E. (1971) Experientia 27, 379.

323. Jori, G., Galiazzo, G. and Scoffone, E. (1969) Biochem. 8, 2868.

324. Jori, G., Galiazzo, G., Tamburro, A.M. and Scoffone, E. (1970) J. Biol. Chem. 245, 3375.

325. Mauk, M.R. and Girotti, A.W. (1973) Biochem. 12, 3187.

326. Mauk, M.R. and Girotti, A.W. (1974) Biochem. 13, 1757.

327. Hudson, M.F. and Smith, K.M. (1975) Chem. Soc. Rev. 4, 363

328. Scheer, H. (1981) Angew. Chem. Int. Ed. 20, 241.

329. Dauvillier, A. "The Photochemical Origin of Life", Academic Press, New York, (1965), pp15-43.

330. Norden, B. (1978) J. Mol. Evol. 11, 313.

331. Kizel, V.A. (1981) Sov. Phys. Usp. 23, 277.

332. Monod, J. "Chance and Necessity" Alfred A. Knopf, New York, (1971)

333. Miller, S.L. and Orgel, L.E. "The Origins of Life on Earth", Prentice-Hall, Englewood Cliffs, (1974), pp166-174.

334. Hochstim, A.R. (1975) J. Mol. Evol. 6, 145.

335. Ponnamperuma, C. "The Origins of Life", E.P. Dutton, New York, (1972)

336. Wald, G. (1957) Ann. New York Acad. Sci. 69, 352.

337. Thiemann, W. (1974) J. Mol. Evol. 4, 85.

338. Noyes, H.P. and Bonner, W.A. (1975) J. Mol. Evol. 6, 91.

339. Bonner, W.A. and Lemmon, R.M. (1978) J. Mol. Evol. 11, 95.

340. Garay, A.S. (1968) Nature 219, 338.

341. Norden, B. (1977) Nature 266, 567.

342. Buchardt, O. (1974) Angew. Chem. Int. Ed. 13, 121.

343. Kagan, H.B., Balavoine, G. and Moradpour, A. (1974) J. Mol. Evol. 4, 41.

344. Rhodes, W. and Dougherty, R.C. (1978) J. Am. Chem. Soc. 100, 6247.

345. Harrison, L.G. (1974) J. Mol. Evol. 4, 99.

346. Belokon, Yu. N., Zel'tzer, I.E., Bakhmutov, V.I., Saporovskaya, M.B., Ryzhov, M.G., Yanosky, A.I., Struchkov, Yu. T. and Belikov, V.M. (1983) J. Am. Chem. Soc. 105, 2010.

347. Beck, M.T. in "Metal Ions in Biological Systems", Vol. 7, Sigel, H. Ed., Marcel Dekker, New York, (1978), pp1-28

348. Decker, P. (1973) J. Mol. Evol. 2, 137.

349. Decker, P. (1974) J. Mol. Evol. 4, 49.

350. Nicolis, G. and Prigogine, I. (1981) Proc. Natl. Acad. Sci. 78, 659.

351. Van't Hoff, J.H. in "Die Lagerung der Atome in Raume". 2nd Ed., Vieweg, Braunschweig, (1894).

352. Tenney, L., Davis, D. and Ackerman, J. (1945) J. Am. Chem. Soc. 67, 486.

353. Bernstein, W.J., Calvin, M. and Buchardt, O. (1972) J. Am. Chem. Soc. 94, 494.

354. Moradpour, A., Nicoud, J.F., Balavoine, G., Kagan, H. and Tsoucaris, G. (1971) J. Am. Chem. Soc. 93, 2353.

355. Stevenson, K.L. and Verdieck, J.F. (1968) J. Am. Chem. Soc. 90, 2974.

356. Stevenson, K.L. and Verdieck, J.F. (1969) Mol. Photochem. 1, 271.

357. Nordén, B. (1979) Inorg. Nucl. Chem. Lett. 13,355.

358. Nelander, B. and Nordén, B. (1973) Chem. Phys. Lett. 28, 384.

359. Harada, K. in "Molecular Evolution", Vol. 1, Buvet, R. and Ponnamperuma, C. Ed., North-Holland, Amsterdam, (1971) pp71-79.

360. Fischer, E. (1980) J. Phys. Chem. 84, 403.

361. Haas, E., Fischer, G. and Fischer, E. (1978) J. Phys. Chem. 82, 638.

362. Mauzerall, D. (1973) Ann. New York Acad. Sci. 206, 483.

363. Scheidt, W.R. and Reed, C.A. (1981) Chem. Rev. 81, 543.

364. Hoard, J.L. in "Hemes and Hemoproteins", Chance, B., Estabrook, R. and Yonetani, T., Eds., Academic Press New York, (1966) pp9-24.

365. Scheidt, W.R. (1977) Acc. Chem. Res. 10, 339.

366. Barkigia, K.M., Spaulding, L.D. and Fajer, J. (1983) Inorg. Chem. 22, 349.

367. Fischer, M.D., Templeton, D.H., Zalkin, A. and Calvin, M. (1971) J. Am. Chem. Soc. 93, 2622.

368. Serlin, R., Chow, H.C. and Strouse, C.E. (1975) J. Am. Chem. Soc. 97, 7237.

369. Kratky, C. and Dunitz, J.D. (1977) Acta Crystallogr. B 33, 545.

370. Kratky, C., Isenring, H.P. and Dunitz, J.D. (1977) Acta Crystallogr. B 33, 547.

371. Hoard, J.L. (1971) Science 174, 1295.

372. Collins, D.M. and Hoard, J.L. (1970) J. Am. Chem. Soc. 92, 3761.

373. Bonnett, R., Hursthouse, M.B., Malik, K.M.A. and Mateen, B. (1977) J. Chem. Soc. Perkin II, 2072.

374. Radonovich, L.J., Bloom, A. and Hoard, J.L. (1972) J. Am. Chem. Soc. 94, 2073.

375. Steffen, W.L., Chun, H.K., Hoard, J.L. and Reed, C.A. "Abstracts of Papers", 175th National Meeting of The American Chemical Society, Anaheim, C.A., March 1978. American Chemical Society, Washington, D.C., (1978), INOR 15, and Hoard, J.L. (private communication).

376. Adler, A.D. (1967) J. Org. Chem. 32, 476.

377. Barnett, G.H., Hudson, M.F. and Smith, K.M. (1975) J. Chem. Soc. Perkin Trans I 9, 1401.

378. Adler, A.D., Longo, F.R., Kampas, F. and Kim, J.J. (1970) Inorg. Nucl. Chem. 32, 2443.

379. Sheldrick, G.M., SHELXTL User Manual, Revision 3, Nicolet XRD Corporation, Cupertino, California (1981).

380. Cromer, D.T. and Mann, J.B. (1968) Acta Crystallogr. A 24, 321.

381. Cromer, D.T. and Liberman, D. (1970) J. Chem. Phys. 53, 1891.

382. Lauher, J.W. and Ibers, J.A. (1974) J. Am. Chem. Soc. 96, 4447.

383. Toney, J. and Stucky, G.D. (1967) J. Chem. Soc. Chem. Commun. 1168.

384. Thoennes, D. and Weiss, E. (1978) Chem. Ber. 111, 3381.

385. Piero, G.D., Cesari, M., Cucinella, S. and Mazzei, A. (1977) J. Organometal. Chem. 137, 265.

386. Magnuson, V.R. and Stucky, G.D. (1969) Inorg. Chem. 8, 1427.

387. Schubert, B., Behrens, U. and Weiss, E. (1981) Chem. Ber. 111, 2640.

388. Schwalbe, C.H., Goody, R. and Saenger, W. (1973) Acta Crystallogr. B 29, 2264.

389. Deloume, J.P., Loiseleur, H. and Thomas G. (1973) Acta Crystallogr. B 29, 668.

390. Cingi, M.B., Villa, A.C., Guastini, C. and Viterbo, D. (1974) Gazz. Chim. Ital. 104, 1087.

391. Halut-desportes, P.S. (1977) Acta Crystallogr. B 33, 599.

392. Stezowski, J.J., Countryman, R. and Hoard, J.L. (1973) Inorg. Chem. 12, 1749.

393. Passer, E., White, J.G. and Cheng, K.L. (1977) Inorg. Chim. Acta 24, 13.

394. Owen, J.D. (1978) J. Chem. Soc. Dalton, 1418.

395. Drew, M.G.B., Othman, A.H., McFall, S.G. and Nelson, S.A. (1975) J. Chem. Soc. Chem. Commun. 818.

396. Schoefield, K.S. "Hetero-Aromatic Nitrogen Compounds" Plenum Press, New York, (1967).

397. Hoffman, A.B., Collins, D.M., Day, V.W., Fleischer, E.B., Srivastava, T.S. and Hoard, J.L. (1972) J. Am. Chem. Soc. 94, 3620.

398. Pauling, L. "The Nature of the Chemical Bond", Cornell University Press, Ithaca, New York, 3rd ed., (1960).

399. Weissbluth, M. in "Structure and Bonding", Vol. 2. Jorgensen, C.K., Neilands, J.B., Nyholm, R.S., Reinen, D. and Williams, R.J.P. Eds., Springer-Verlag, New York, (1967) pp1-25.

400. Ohno, K., Tanabe, Y. and Sasaki, F. (1963) Theor. Chim. Acta 1, 378.

401. Scheidt, W.R., Cunningham, J.A. and Hoard, J.L. (1973) J. Am. Chem. Soc. 95, 8289.

402. Reed, C.A., Mashiko, T., Scheidt, W.R., Spartalian, K. and Lang, G. (1980) J. Am. Chem. Soc. 102, 2302.

403. Collins, D.M., Countryman, R. and Hoard, J.L. (1972) J. Am. Chem. Soc. 94, 2066.

404. Adler, A.D., Longo, F.R. and Kampas, F. in "The Porphyrins", Vol. 5, Dolphin D. Ed., Academic Press, New York, (1978) pp483-492.

405. Hoffman, B.M. and Ibers, J.A. (1983) Acc. Chem. Res. 16, 15.

406. Edwards, W.D., Head, J.D. and Zerner, M.C. (1982) J. Am. Chem. Soc. 104, 5833.

407. Kastner, M.E., Scheidt, W.R., Mashiko, T. and Reed, C.A. (1978) J. Am. Chem. Soc. 100, 666.

408. Hill, H.A.O., Roder, A. and Williams, R.J.P. in "Structure and Bonding", Vol. 8, Hemmerich, P., Jorgensen, C.K., Neilands, J.B., Nyholm, R.S., Reinen, D., Williams, R.J.P. Eds., Heidelberg, (1970) pp123-151.

409. Takano, T., Kallai, O.B., Swanson, R. and Dickerson, R.E. (1973) J. Biol. Chem. 248, 5234.

410. Richardson, J.S., Thomas, K.A., Rubin, B.H. and Richardson, D.C. (1975) Proc. Natl.Acad. Sci. 72, 1349.

411. Salemme, F.R., Freer, S.T., Ng Huu Xuong, Alden, R.A., Kraut, J. (1973) J. Biol. Chem. 248, 3910.

412. Nagai, K., La Mar, G.N., Jue, T. and Bunn, H. F. (1982) Biochem. 21, 842.

413. Stanford, M.A., Swartz, J.C., Phillips, T.E. and Hoffman, B.M. (1980) J. Am. Chem. Soc. 102, 4492.

414. Valentine, J.S., Sheridan, R.P., Allen, L.C. and Kahn, P.C. (1979) Proc. Natl.Acad. Sci. 76, 1009.

415. Landrum, J.T., Hatano, K., Scheidt, W.R. and Reed, C.A. (1980) J. Am. Chem. Soc. 102, 6729.

416. Shipman, L.L., Cotton, T.M., Norris, J.R. and Katz, J.J. (1976) Proc. Natl. Acad. Sci. 73, 1791.

417. Brace, J.G., Fong, F.K., Karweik, D.H., Koester, V.J., Shepard, A. and Winograd, N. (1978) J. Am. Chem. Soc. 100, 5203.

418. Nicolis, G. and Portnow, J. (1973) Chem. Rev. 73, 365.

419. Rossler, O.E. and Wegmann, K. (1978) Nature 271, 89.

420. Epstein, I.R., Kustin, K., De Kepper, P. and Orban, M. (1983) Scient. Am. 248, 96.

421. Cohen, M.H. in "Some Mathematical Questions in Biology", Vol. 3, Cowan, J.D. Ed., Providence, Rhode Island, (1972) pp1-32.

422. Goodwin, B.C. and Cohen, M.H. (1969) J. Theor. Biol. 25, 49.

423. Haag, J. "Oscillatory Motions" (Translated by Rosenberg, R.M.) Wadsworth, Belmont, California, (1962) pp157-163.

424. Hayashi, C. "Nonlinear Oscillations in Physical Systems", McGraw-Hill, New York, (1964) pp285-338.

425. Minorsky, N. "Nonlinear Oscillator", D. Van Nostrand, New York, (1962) pp433-459.

426. Stanshine, J. (1975) Ph.D. dissertation, Massachusetts Institute of Technology, Cambridge.

427. Koehler, W.K. and Fleissner, G. (1978) Nature, 274, 708.

428. Page, T.L, Caldarola, P.C. and Pittendrigh, C.S. (1977) Proc. Natl.Acad. Sci. 74, 1277.

429. Oguztoreli, M.N. and Stein, R.B. (1979) J. Math. Biol. 7, 1

430. Ermentrout, G.B. and Cowan, J.D. (1979) J. Math. Biol. 7, 265.

431. Rand, R.H., Storti, D.W., Upadhyaya, S.K. and Cooke, J.R. (1982) J. Math. Biol. 15, 131.

432. Delwiche, M.J. and Cooke, J.R. (1977) J. Theor. Biol. 69, 113.

433. Gerisch, G., Hulser, D., Malchow, D. and Wick, U. (1975) Phil. Trans. Roy. Soc. Lond. B. 272, 181.

434. Cowan, J.D. in "Some Mathematical Questions in Biology", Vol. 2, Providence, Rhode Island, (1970) pp1-57.

435. Chay, T.R. (1981) Proc. Natl.Acad. Sci. 78, 2204.

436. Roeder, P.E., Sargent, M.L. and Brody, S. (1982) Biochem. 21, 4909.

437. Wolpert, L. (1969) J. Theor. Biol. 25, 1.

438. Palmer, J.D. in "Biological Clocks in Marine Organisms", Wiley-Interscience, New York, (1974), pp127-155.

439. Meinhardt, H. and Gierer, A. (1980) J. Theor. Biol. 85, 429.

440. Cooke, J. and Goodwin, B.C. in "Some Mathematical Questions in Biology", Vol. 3, Providence Rhode Island, (1972) pp35-60.

441. Pastan, I. and Perlman, R. (1970) Science 169, 339.

442. Sorensen, T.S. and Castillo, J.L. (1980) J. Colloid Interface Sci. 76, 399.

443. Revel, J.P. and Karnovsky, J.J. (1967) J. Cell Biol. 33, C7.

444. Robertson, J.D. (1963) J. Cell Biol. 19, 201.

445. Makowski, L., Caspar, D.L.D., Phillips, W.C. and Goodenough, D.A. (1977) J. Cell Biol. 74, 629.

446. Caspar, D.L.D., Goodenough, D.A., Makowski, L. and Phillips, W.C. (1977) J. Cell. Biol. 74, 605.

447. Benedetti, E.L. and Emmelot, P. (1968) J. Cell Biol. 38, 15

448. Korn, R.W. (1982) J. Theor. Biol. 95, 543.

449. Britton, N.F. and Murray, J.D. (1979) J. Theor. Biol. 77, 317.

450. Adler, A.D. (1973) Ann. New York Acad. Sci. 206, 7.

451. Losada, M. (1976) J. Mol. Catal. 1, 245.

452. Phipps, D.A. in "Metals and metabolism", Atkins, P.W., Holker, J.S.E. and Holliday, A.K. Ed., Clarendon Press, Oxford, (1976) pp80-129.

453. Hughes, M.N. in "Inorganic Biochemistry" Vol. 3, Hill, H.A.O. Ed., Royal Society of Chemistry, London, (1980) pp33-77.

454. Mortier, W.J., Pluth, J.J. and Smith, J.V. (1975) Nature 256, 718.

455. Reuter, B. and Riedel, E. (1969) Z. Anorg. Allg. Chem. 369, 306.

456. Brusset, H., Gillier-Pandraud, H. and Delcroix, S.M. (1966) Bull. Soc. Chim. France, 3364.

457. Bacon, G.E. (1952) Acta Crystallogr. 5, 684.

458. Vallino, M. (1969) J. Organomet. Chem. 20, 1.

459. Zemann, A. and Zemann, J. (1961) Acta Crystallogr. 14, 835.

460. Williams, R.J.P. (1980) Chem. Soc. Rev. 9, 281.

461. Sternberg, M.J.E. and Thornton, J.M. (1978) Nature 271, 15

462. Stryer, L. "Biochemistry", Freeman and Company, San Francisco, (1975) pp11-45.

463. Baldwin, J. and Chothia, C. (1979) J. Mol. Biol. 129, 175.

464. Perutz, M.F. (1979) Ann. Rev. Biochem. 48, 327.

465. De Kepper, P. and Epstein, I.R. (1982) J. Am. Chem. Soc. 104, 49.

466. Furrow, S.D. and Noyes, R.M. (1982) J. Am. Chem. Soc. 104,38.

467. De Kepper, P., Epstein, I.R. and Kustin, K. (1981) J. Am. Chem. Soc. 103, 2133.

468. De Kepper, P., Epstein, I.R. and Kustin, K. (1981) J. Am. Chem. Soc. 103, 6121.

469. Sauer, K. (1980) Acc. Chem. Res. 13, 249.

470. Anderson, L.L. and Tillman, D.A. "Synthetic Fuels from Coal", Wiley-Interscience, New York, (1979) pp1-11.

471. Cahn, R.W. (1978) Nature 276, 665.

472. Dickson, D. (1978) Nature 273, 2.

473. Harriman, A. (1978) Nature 276, 15.

474. Wilson, J.I.B. and Weaire, D. (1978) Nature 275, 93.

475. Lehn, J.M. in "Photochemical Conversion and Storage of Solar Energy", Connolly, J.S. Ed., Academic Press, New York, (1981) pp161-200.

476. Tributsch, H. (1979) Nature 281, 555.

477. Brinkworth, B.J. (1980) Phil. Trans. Roy. Soc. Lond. A 295,361.

478. Page, J.K., Rodgers, G.G. and Souster, C.G. (1980) Phil. Trans. Roy. Soc. Lond. A 295,379.

479. Landsberg, P.T. (1978) Nature 274, 116.

480. Kampas, F.J., Yamashita, K. and Fajer, J. (1980) Nature 284, 40.

481. Archer, M.D. and Ferreira, M.I.C. in "Photochemical Conversion and Storage of Solar Energy", Connolly, J.S. Ed., Academic Press, New York, (1981) pp201-228.

482. Nozik, A.J. in "Photochemical Conversion and Storage of Solar Energy", Connolly, J.S. Ed., Academic Press, New York, (1981) pp271-295.

483. Porter, G. in "Light, chemical change and life", Coyle, J.D., Hill, R.R. and Roberts, D.R. Eds., Open University Press, Dorset, (1982) pp1-9.

484. Eccles, J. and Honig, B. (1983) Proc. Natl. Acad. Sci. 80, 4959.

485. Wilkinson, G. (1979) New Scient. 81, 867.

486. Lewin, R. (1976) New Scient. 70, 651.

487. Williams, L.O. "Hydrogen Power", Pergamon Press, Oxford, (1980).

488. Takahashi, T. in "Solar-hydrogen energy systems", Ohta, T. Ed., Pergamon Press, Oxford, (1979) pp35-58.

489. Kawai, T. and Sakata, T. (1979) Nature 282, 283.

490. Ohta, T. in "Solar-hydrogen energy systems", Ohta, T. Ed., Pergamon Press, Oxford, (1979) pp1-23.

491. Hann, R.A. (1980) Chem. in Br. 16, 474.

492. Mitsui, A. in "Solar-hydrogen energy systems", Ohta, T, Ed., Pergamon Press, Oxford, (1979) pp171-191.

493. Henbest, N. (1980) New Scient. 87, 585.

494. Calvin, M. (1978) Acc. Chem. Res. 11, 369.

495. Calvin, M. in "Photochemical Conversion and Storage of Solar Energy", Connolly, J.S. Ed., Academic Press, New York, (1981) pp1-26.

496. Gratzel, M. in "Photochemical Conversion and Storage of Solar Energy", Connolly, J.S. Ed., Academic Press, New York, (1981) pp131-160.

497. Brugger, P.A., Cuendet, P. and Gratzel, M. (1981) J. Am. Chem. Soc. 103, 2923.

498. Humphry-Baker, R., Lilie, J. and Gratzel, M. (1982) J. Am. Chem. Soc. 104, 422.

499. Borgarello, E., Kiwi, J., Pelizzetti, E., Visca, M. and Gratzel, M. (1981) Nature 289, 158.

500. Sherwood, M. (1980) New Scient. 88, 504.

501. Porter G. (1980) Nature 288, 320.

502. Maggiora, G.M. and Ingraham, L.L. in "Structure and Bonding" Vol. 2, Jorgensen, C.K., Neilands, J.B., Nyholm, R.S., Reinen, D., Williams, R.J.P. Eds., Springer-Verlag, New York, (1968) pp126-159.

503. Tanno, T., Wohrle, D., Kaneko, M., Yamada, A. (1980) Ber. Bunsenges, Phys. Chem. 84, 1032.

504. Stellwagen, E. (1978) Nature 275, 73.

505. Kuki, A. and Boxer, S.G. (1983) Biochem. 22, 2923.

506. McGourty, J.L. Blough, N.V. and Hoffman, B.M. (1983) J. Am. Chem. Soc. 105, 4470.

507. Sadler, P.J. (1982) Chem. in Br. 182.

508. Rosenberg, B., Van Camp, L. and Krigas, T. (1965) Nature 205, 698.

509. Rosenberg, B., Van Camp, L., Trosko, J.E. and Mansour, V.H. (1969) Nature 222, 385.

510. McAuliffe, C.A. in "Inorganic Biochemistry" Vol. 2, Hill, H.A.O. Ed., Royal Society of Chemistry, London, (1979) pp1-42.

511. McAuliffe, C.A. in "Inorganic Biochemistry", Vol, 3, Hill, H.A.O. Ed., Royal Society of Chemistry, London, (1980) pp1-32.

512. Fiel, R.J., Howard, J.C., Mark, E.H. and Dattagupta, N. (1979) Nucleic Acid Res. 6, 3093.

513. Fiel, R.J. and Munson, B.R. (1980) Nucleic Acid Res. 8, 2835.

514. Musser, D.A., Datta-Gupta, N. and Fiel, R.J. (1980) Biochem. Biophys. Res. Commun. 97, 918.

515. Pasternack, R.F., Gibbs, E.J. and Villafranca, J.J. (1983) Biochem. 22, 2406.

516. Turek, F.W., Earnest, D.J. and Swann, J. in "Vertebrate Circadian Systems", Aschoff, J., Daan, S., Groos, G.A. Eds., Springer-Verlag, Berlin, (1982) pp203-214.

517. Hartwig, H.G. in "Vertebrate Circadian Systems", Aschoff, J., Daan, S., Groos, G.A. Eds., Springer-Verlag, Berlin, (1982) pp25-30.

518. Aschoff, J., Daan, S. and Honma, K.I. in "Vertebrate Circadian Systems", Aschoff, J., Daan, S., Groos, G.A. Eds., Springer-Verlag, Berlin, (1982) pp13-21.

519. Stephan, F.K. in "Vertebrate Circadian Systems", Aschoff, J., Daan, S., Groos, G.A. Eds., Springer-Verlag, Berlin, (1982) pp120-128.

520. Zulley, J. and Wever, R.A. in "Vertebrate Circadian Systems", Aschoff, J., Daan, S., Groos, G.A. Eds., Springer-Verlag, Berlin, (1982) pp253-261.

521. Eastman, C. in "Vertebrate Circadian Systems", Aschoff, J., Daan, S., Groos, G.A.Eds., Springer-Verlag, Berlin, (1982) pp262-267.

522. Fuller, C.A. and Sulzman, F.M. in "Vertebrate Circadian Systems", Aschoff, J., Daan, S., Groos, G.A. Eds., Springer-Verlag, Berlin, (1982) pp224-236.